63-4-1

WEB SUBTASK 13.009
THE RESPONSE OF SOILS
TO DYNAMIC LOADINGS, REPORT 12

STATIC TESTS UPON THIN DOMES BURIED IN SAND

Robert V. Whitman
Zvi Getzler
Kaare Hoeg

R62-41

December 1962

MIT

DEPARTMENT
OF
CIVIL
ENGINEERING

SCHOOL OF ENGINEERING
MASSACHUSETTS INSTITUTE OF TECHNOLOGY
Cambridge 39, Massachusetts

Department of Civil Engineering Research Project R62-41

THE RESPONSE OF SOILS TO DYNAMIC LOADINGS

Report No. 12: Static Tests upon Thin Domes Buried in Sand

Robert V. Whitman
Zvi Getzler
Kaare Hoeg

December 1962

Contract No. DA-22-079-eng-224
with

U. S. Army Engineers Waterways Experiment Station
Department of the Army, R and D Subproject 8-S12-95-002
under Weapons Effects Board Subtask No. 13.009

Appendix C

PRELIMINARY PLATE LOADING TESTS

CONTENTS

LIST OF TABLES

LIST OF FIGURES

Appendix C

PRELIMINARY PLATE LOADING TESTS

C.1 Purpose and Scope of Preliminary Tests

Fourteen tests involving a single concentrated load upon the sand were carried out as a preliminary to the main tests with a uniformly applied pressure. The principal objective of these preliminary tests was to test and progressively develop the methods of placing sand in the bin and the various instrumentation systems. A secondary objective was to obtain some idea as to the magnitude of load reaching a dome-shaped buried structure as compared to that reaching a more common and better understood flat-roofed structure. By using a concentrated loading for these preliminary tests, the considerable effort of moving the upper beams of the loading frame before and after each test was avoided.

Table C.1 summarizes the features of each of the fourteen tests.* The first six tests served to perfect the means for placing the sand in the bin, and perhaps the main conclusions from these tests was that a dense sand mass could best be obtained by straining the sand through a muzzled pipe. In Tests PB-5 through PB-8, the quantity of instrumentation utilized was gradually increased, and Test PB-8 was the first fully instrumented test. Tests PB-9 through PB-14 served to provide some preliminary data concerning the interaction between sand and a buried dome, using a flat plate as a datum, and further to provide additional information regarding the reproducibility and symmetry of the movements of the sand mass. The first six tests were performed during the winter and spring of 1961, and the last six tests during the fall of that year.

This appendix sets forth the results of these preliminary tests in some detail. While the settlement of a loaded plate and the movements of the sand under this plate have little direct importance to the problem of the interaction between soil and buried structure, such data provide some basis for judging the uniformity of the sand mass as placed in the test bin. Quite incidental to this

*The symbol PB denotes pressure bin.

general type of result, the preliminary tests perhaps provide some worthwhile data regarding bearing capacity failures.

C.2 Apparatus and Instrumentation

The general arrangement of the loading frame as used for these tests has already been shown in Figure A.2; the bin was supported on three beams, and one beam provided the reaction for the concentrated load. The bin was made up of three rings, each 10 inches high. The lowest ring was blocked up 2 inches above the bottom cover plate so as to expose for use the cable holes in the flange of the cover plate. Thus, the height of the bin, from bottom to the top of the upper ring, was about 32 inches. Rubber layers between the rings were not used during the preliminary test program.

Figure C.1 shows the various forms of instrumentation employed in these tests, and the manner of supporting the model.

C.2.1 Applied loading

The applied load was determined by recording the pressure applied to the hydraulic jack, and multiplying this pressure times the effective area of the jack. The load was applied in increments, with readings of the instrumentation systems taken after each increment. For small loads (up to about 3000 lbs., or 34 lb/in^2 over the area of the plate) there was no creep in the sand, and the applied load would hold itself constant once it had been raised to the desired level. For larger loads, however, the load would relax downwards for several minutes after it had been pumped up to the selected level. The difference between the final "stable" level and the initial "transient" level increased as the magnitude of the load increased. Figure C.20 gives an idea of this load relaxation, which generally caused from 10% to 15% of the transient level to be lost. The loading process was generally carried out to the peak in the curve of load (either transient or stable) vs. plate movement, at which point the plate movements would increase beyond the measuring range of the instrumentation system.

C.2.2 Structure and load cell

Two buried "structures" were used in these

tests: (1) a rigid hemispherical steel dome, 8.5 inches in diameter, with a polished surface; and (2) a flat circular plate 8.5 inches in diameter. These two "structures" are shown in Figure C.2, together with the load cell on which they were supported.

This load cell was made by connecting top and bottom steel plates to a steel proving ring. Four SR-4 strain gauges were mounted on the ring and connected via a Wheatstone's bridge circuit to a strain indicator. This load cell could be used up to 2500 lbs, and had a sensitivity of 3 pounds.

The load cell was housed inside a steel cylinder 8 inches high: see Figure C.3(a). A rubber membrane covered the gap between the top of the cylinder and the bottom of the structure, thus keeping sand from entering the load cell chamber and ensuring that all force reaching the structure was transmitted to the load cell.

The load cell itself either rested upon the bottom cover plate, or was supported on a steel pipe at the desired elevation. The entire structure, load cell, blocking, and cover plate system obviously was not rigid. Imperfect seating of the load cell against the blocking and of the blocking against the cover plate contributed to the flexibility of this system. The amount of the overall flexibility was not determined in this preliminary test program; based upon calculations presented in section C.6 and upon later experiences from the tests with a uniform loading, it is thought that the system was considerably less rigid than the sand it replaced.

C.2.3 Movement measurements

Measurements were made of the vertical movement of the loading plate and of various points on the surface of and within the sand mass. Ames dials, with smallest dial division of 0.001 inch, were used to record these movements. In the earlier tests where just a few movement measurements were involved, the Ames dials were supported on rods which were in turn held by a magnetic clamp to the upper beam of the loading frame. As more measurement points were added, a light frame for holding the dials was constructed of channel sections and clamped to the upper beam: see Figure C.1 and C.4. Starting with Test PB-8, the deflection of the upper beam itself was measured, by means of an Ames dial attached to the ceiling.

The movement of the loading plate was measured at three points, spaced 120° apart, near the periphery of the plate. The stems of the Ames dials rested directly on the plate. For measuring the movement of the surface of the sand, metal disks 1 inch in diameter and 1/16 inch thick were placed on the surface. Again the stems of the Ames dials rested directly on the disks. "Anchor" disks of the same size were embedded within the sand mass, and rods 1/16 inch in diameter extended from these disks up through the sand. The tops of these rods were attached to the stems of the Ames dials. The method of placing the anchor disks within the sand is shown in Figure C.3(b); the horizontal clamping bar was removed after several inches of sand were placed over the disks.* The exact location of the sand movement measurement points varied from test to test, and the locations of these points are given in connection with the results presented later in this appendix.

In one test, the rods from the anchor plates were encased by a pipe, so as to prevent friction between sand and rod. Since this test yielded results substantially identical with those obtained using bare rods, it was felt that friction between sand and rod was not important.

C.2.4 Stress gages

Stress gages, oriented to measure vertical stress, were embedded within the sand mass during tests PB-7 through PB-10. These were the standard 6 inch diameter gage developed by the Waterways Experiment Station, and loaned to M.I.T. for use in connection with the soil-structure interaction tests of the program. These gages employ wire strain gages upon a deflecting diaphragm, and are approximately 1 inch thick. The output of the gages is read with a SR-4 strain indicator. A total of four gages were made available for the program.

C.3 Results Concerning Sand Density

Study of methods for placing sand was the major objective of the earliest tests in the preliminary program. The first goal was to find the best scheme for obtaining a dense sand mass. As indicated in Table C.1, several

*The muzzled pipe used to spread the sand appears in Parts (b) and (c) of Figure C.3.

schemes were tried, and the penetrometer described in Appendix B was used to evaluate the resulting density. These tests led to adoption of the muzzled rubber pipe system. The proposed scheme for obtaining a loose sand was likewise evaluated in Test PB-6. The penetration test data from these early tests have already been presented in Appendix B.

Starting with Test PB-7, the muzzled rubber pipe system was used in all tests to provide a dense sand mass. Such was our confidence in this system that additional penetrometer readings were omitted in the later tests. Based upon the data from the penetrometer data from the earlier tests, the unit weight of the sand in Tests PB-7 through PB-14 was between 101 and 103 lb/ft^3.

Certain penetrometer data were taken expressly for the purpose of checking the changes in density as the result of a loading test. These results are shown in Figures C.5 through C.9. These figures compare the penetration resistance, as measured starting at the top surface of the sand mass, before and after loading.* In Test PB-6 (Figure C.7) with the initially loose sand, the sand immediately below the loading plate densified as the result of the loading. In all other tests, the sand in this location decreased in density to a marked degree. It is clear that the sand right under the bearing plate was sheared to a considerable extent, and did not simply move downward as a rigid mass, as is assumed in the formulation of many bearing capacity theories.** Measurements during Tests PB-7 and PB-8 indicated that penetration resistance might be used to define the lateral extent of the failure wedge spreading outward from under a bearing plate.

C.4 Results Concerning Load Bearing Capacity

Load settlement curves from the various tests are presented in Figures C.10 through C.18. In Figure

* In some cases, penetration data obtained part way through the filling process are included: see "before" curves in Figures C-7 and C-8. These data showed the resistance with distance below the surface as it existed at that stage of filling. As indicated in Appendix B, data of this type were statistically the same for all stages of filling.

**For example, see TAYLOR "Fundamentals of Soil Mechanics", p.572

C.10, the several settlement readings taken on a plate have been averaged, and all readings of both settlement and load are those immediately following an increment of load increase and before the load relaxed. The subsequent figures show the settlement readings at the three settlement points individually; and in all figures except Figure C.12, the data are for the stable conditions following the several relaxations of the load. The insets in Figures C.11 through 18 show the direction and magnitude (expressed in percent, as in a 3% grade for a highway) of the tilt developed by the loading plate.

For the present purposes, these results are mainly of interest as a basis for judging the uniformity and reproducibility of the sand mass. Table C.2 summarizes the data from this standpoint. The scattering in the data is quite small, especially considering that the location and type of buried structure varied from test to test.

The average settlement results indicate excellent reproducibility with regard to the properties of the sand mass. If magnitude of tilting is to be taken as a measure of uniformity, then the uniformity might be judged to be less than satisfactory. On the other hand, it is possible and indeed likely that the tilting magnitude was influeneced by eccentricities in the application of load to the plate.

C.5 Results Regarding Movements Within Sand Mass

The data have been plotted in Figures C.19 through C.29. In Figures C.19 through C.22, the recorded data are those for the peak load reached during each increment; in the remaining figures the data are for the final stable load condition. In Figures C.19 through C.22, the location of the disks is indicated by an inset sketch, with the depth of the disk shown by the number in parentheses. The coding system used in the remaining figures may be explained by the following example: AP 24" (17") 270° means the anchor plate (disk) at 24 inch depth, 17 inches from the center-line of the bin, and at 270° in plain view from an arbitrary reference direction. For easy reference, the locations of the measurement points have been tabulated by test number in Table C.3.

There is much to be learned from these data concerning sand movements near a loaded area as failure

approaches and develops. The extent of the failure wedge could be ascertained by such measurements. Many of the measurements in this table were made in and around the buried structures. Once again, however, the results are most valuable in the context of this report as a means for judging the usefulness of the measurement technique, and also for judging the uniformity and reproducibility of the sand mass.

The measured movements were of a direction and magnitude that would be expected. On the other hand, it is evident that the level of reproducibility of movement measurements was relatively low. Frequently the movements at analogous points differed by as much as 50% of the larger value. Note that such comparisons generally involve movements of less than 0.02 inches, and it seemed that the shortcomings in the data reflected deficiencies in technique rather than lack of reproducibility or uniformity in the sand mass. It was concluded that: (1) as accomplished in these tests, the measurements were primarily of qualitative value; but (2) that with further development, the technique could be used for measurements of quantitative value.

C.6 Results Regarding Forces on Buried Structures

The results of these measurements are shown in Figures C.30 through C.37. The load reaching the buried structure is shown as a function at the load applied through the plate, both in actual magnitude and as a percentage of the applied load. The results are summarized in Figures C.38 through C.40. The last of these figures, which compares the average vertical stress over the plan area of the structure with the average vertical stress applied through the plate, gives the clearest picture of the results.

It may be noted from any of these three figures that the load reaching the dome was less than that reaching the flat plate at comparable depth.* This result is also shown in Figure C.41, in which the ratio of received to applied stress is plotted as a function of buried depth. This finding, although still qualitative in nature, is one of the more important results of these preliminary tests.

*Burial depth quoted for dome is to the center of gravity of the horizontal projection of dome.

The theoretical curve in Figure C.41 was obtained with the charts in the report by Foster and Ahlvin,* but assuming a parabolic stress distribution over the area of the loading plate. It is seen that the stresses reaching the buried structures were markedly less than the theoretical value. Figure C.42 shows the results of a study made to determine the reasons for this discrepancy. The rigidity of the sand was obtained from measurements under a uniform surface loading, as reported in Appendix E. The rigidity of the load cell was measured directly. Even neglecting any additional loss of rigidity due to seating errors, etc., the structure-load cell system was evidently much less stiff than the surrounding sand.

Table C.4 summarizes the data obtained from the WES stress cells. In each case, the center of the cell lay 18 inches from the center-line of the bin. While two cells were used in Tests PB-8 and PB-9, only one cell yielded useful results; the output of the other cell would fluctuate wildly when its lead cable was touched with the hand. The data from Test PB-10 have not been reduced. It is, of course, not possible to make a direct comparison of the stress recorded by the stress cell and the average stress reaching the dome, since these two "gages" are at different radii from the concentrated load. However, the data from Tests PB-7 and PB-8 do substantiate the belief that the structure-load gauge-support system is more compressible than the surrounding sand.

C.7 Conclusions

These preliminary tests provided a proving ground for the various techniques and instrumentation systems to be used in the main series of tests with a uniform surface loading. Simple schemes were evaluated for placing the sand in both a dense and a loose condition. From the series of loading tests upon dense sand masses, it was concluded that the properties of these masses were reasonably uniform and that the properties could be reproduced from test to test. No corresponding body of experience was accumulated for the loose sand.

*"Stresses and Deflections Induced by a Uniform Circular Load," C. R. Foster and R. G. Ahlvin, paper prepared for presentation to the Highway Research Board, 1952.

Based upon the results of these preliminary tests, it was concluded that the load cell was much more flexible than the sand it replaced, and that a much stiffer cell should be designed for the main test series. Experience was gained with a scheme for measuring the displacements within the sand mass: by detecting the movement of small metal disks embedded within the mass. This scheme clearly provided results of qualitative usefulness, and it was felt that further development of the scheme would yield even more accurate results.

Finally, some preliminary information was obtained as to the relative magnitude of the load reaching buried domes vs. that reaching a buried flat-roofed structure. For the loading conditions used in these preliminary tests, the load against the rigid dome was about 2/3 of that reaching a flat plate with the same depth of burial.

As a sideline to the main objectives, these tests have also provided new and additional information regarding the phenomenon of bearing capaicty failure, but no attempt has been made to extract and develop this subsidiary information.

TABLE C-I
PROGRAM FOR PRELIMINARY TESTS

Test Number	Bin left or right	Density				WES Stress Cell	Settlement Measurements				Load Cell	Structure
		Filling method	Sand density	Penetration Tests			Load Plate	Loading Beam	Surface Plates	Anchor Plates		
				before	after							
PB-1	R	directly from bags	medium	–	–	–	3	–	–	–	–	–
PB-2	R	after PB-1	medium	–	–	–	3	–	–	–	–	–
PB-3	L	B	medium	7	–	–	3	–	–	–	–	–
PB-4	L	after PB-3	medium	–	2	–	3	–	–	–	–	–
PB-5	R	C	dense	7	4	–	3	–	1	1	–	–
PB-6	L	A	loose	5	3	–	3	–	2	2	–	–
PB-7	R	C	dense	1	3	2	3	–	2	4	1	dome
PB-8	R	C	dense	–	4	2	3	1	3	10	1	dome
PB-9	R	C	dense	–	-	2	3	1	–	10	1	dome
PB-10	R	C	dense	-	–	1	3	–	–	10	1	dome
PB-11	R	C	dense	–	–	–	3	-	–	8	1	dome
PB-12	R	C	dense	–	–	–	3	–	–	8	1	flat plate
PB-13	R	C	dense	–	–	–	3	–	–	4	1	flat plate
PB-14	R	C	dense	–	–	–	3	–	–	10	1	flat plate

Number of Measurements

Filling Methods :

A - Free pouring in center

B - Showering through "combined funnels"

C - Showering through muzzled pipe

Dense sand: γ = 101 to 103 lbs/c.f.

Medium sand: estimated

Loose sand: γ = (about) 90 lbs/c.f.

Table C.2

LOAD-SETTLEMENT DATA FROM PLATE LOADING TESTS

Test	Depth of Structure (inches)	Maximum Load (lbs.)	Settlement, at 3000 lbs. Average (inches)	Differential (inches)
PB-7	23.0	6100	0.10	0.04
PB-8	23.0	5700	0.12	0.03
PB-9	11.5	5800	0.12	0.01
PB-10	12.5	5650	0.12	0.03
PB-11	5.5	-	0.10	0.02
PB-12	12.0	6000	0.11	0.03
PB-13	22.0	6100	0.12	0.01
PB-14	13.0	6200	0.09	0.03
Average		5940	0.110	0.025
Standard deviation		220	0.012	0.011

Notes: Loads are the stable values following relaxation of stress. In tests PB-9 through PB-11, the buried structure was a dome, and the quoted depth is to the center of gravity of the horizontal projection of the surface (1.3 inches below crown). In the remaining tests, the buried structure was a flat plate.

TABLE C-3

LOCATION OF SAND MOVEMENT MEASUREMENT POINTS

Depth Inches	Radius - inches													
	9	10	11	12	13	14	15	16	17	18	19	20	21	23
0									7 (2) 8 (3)					
8			11 12		12									
9						10 (2)								
10									7 (2) 9	9				
12			12	12										
13		14				14			11		14		11	14
14									7					
15					9; 10			10	9				9	
16						12	12							
17	14				14					14				14
18				10	9 11				11	10			9 11	
19				13										
21				13			13							
23						12 (2)								
24			14		11 13			10	7 9 (2)		10	14		

Note : The numbers in this table indicate the tests in which the various measurement points were used. Numbers in parentheses indicate duplicate or duplicate measurements.

TABLE C.4

DATA FROM WES STRESS CELLS

Test	PB-7				PB-8			PB-9		
Depth of cell	*24 in		30 in.		*24 in.			*12.5 in.		
Average stress applied by plate	22.3	35.7	22.3	35.7	26.8	35.7	44.6	26.8	35.7	44.6
Stress on stress cell	6.6	9.9	6.3	7.3	6.8	8.5	11.2	4.3	7.3	10.0
Average vertical stress on dome	2.9	5.3	2.9	5.3	3.8	5.3	7.0	9.3	13.3	17.1

Stresses in lb./in.^{2} Cell depths marked * equal depth to bottom of dome.

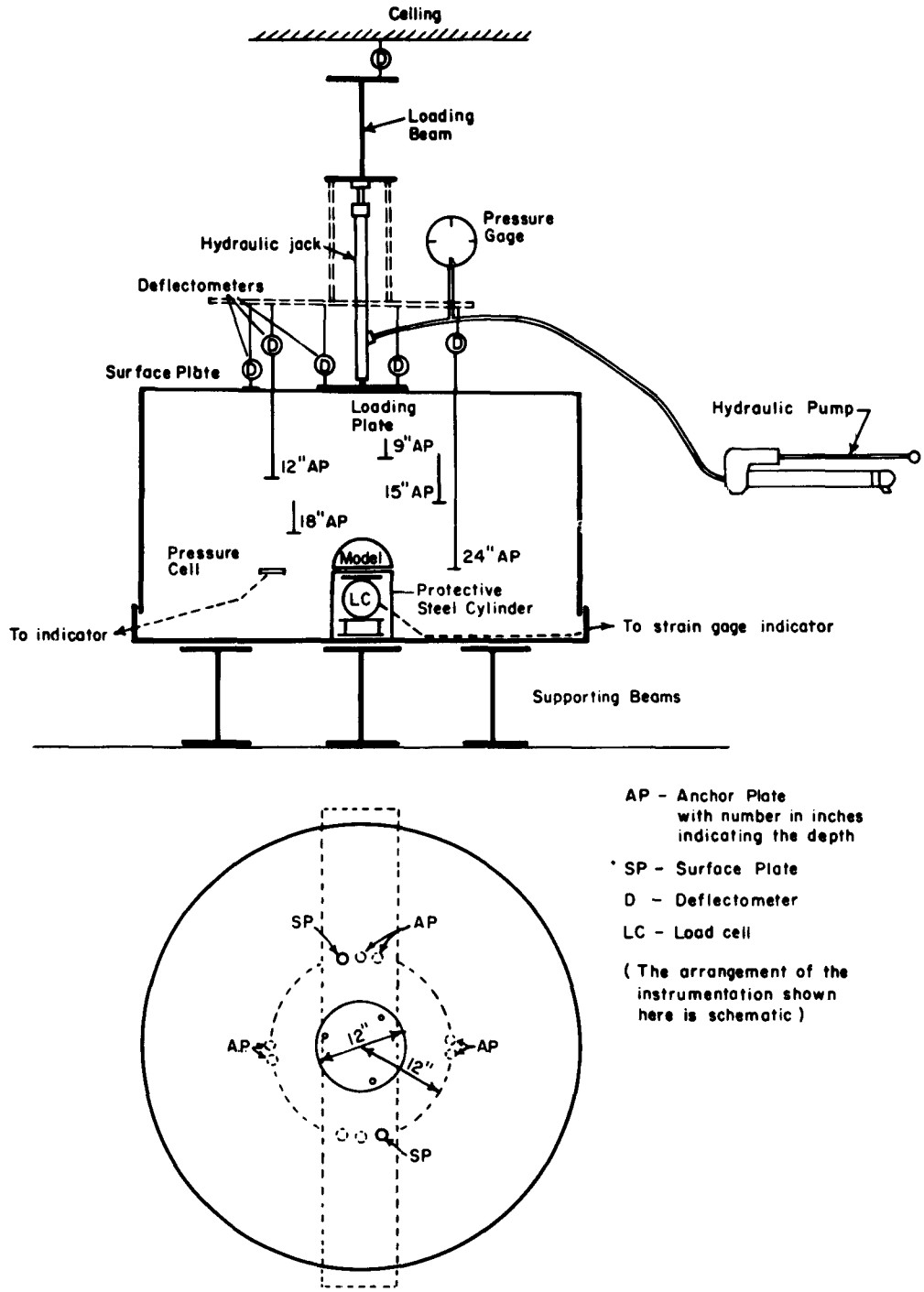

FIGURE C-1 LOADING TEST ARRANGEMENT: PB-7 to PB-14

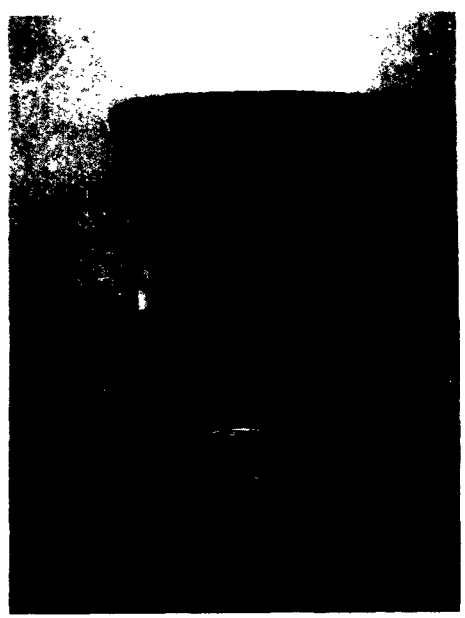

(a) Flat Plate

(b) Hemispherical Dome

FIGURE C-2 "STRUCTURE" ON LOAD CELL

(a)

Dome supported on load cell enclosed in steel cylinder

(b)

Placing anchor plates

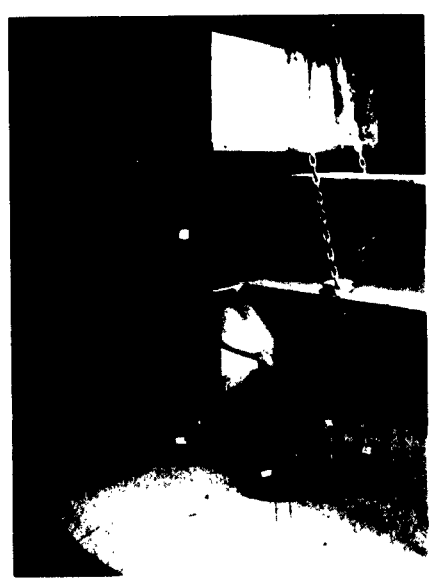

(c)

Transportation box, muzzled pipe, anchor plate rods, and loading plate

FIGURE C-3

PREPARATION OF SAND MASS

(a) Measuring Arrangement

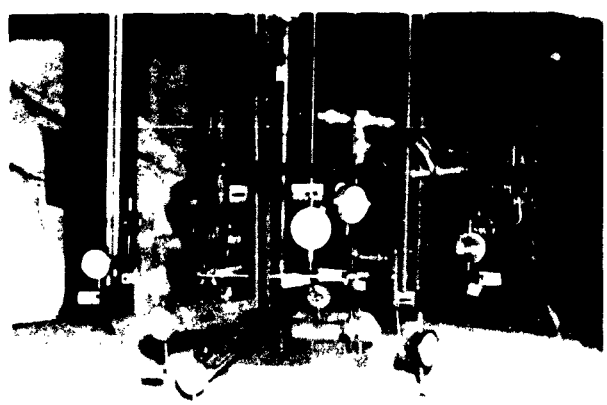

(b) Deflectometers Arrangement

FIGURE C-4 MOVEMENT MEASURING SYSTEMS

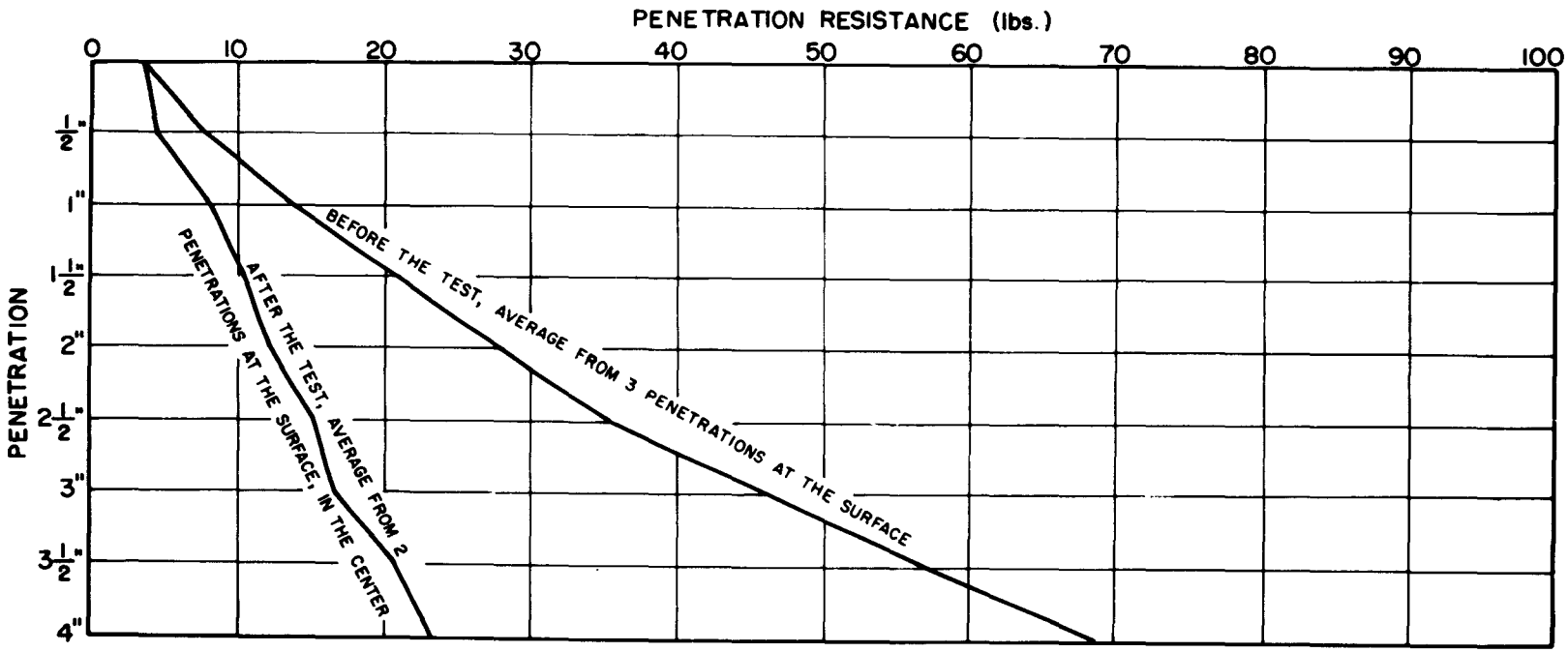

FIGURE C-5 PENETRATION TESTS: TESTS PB-3 & 4

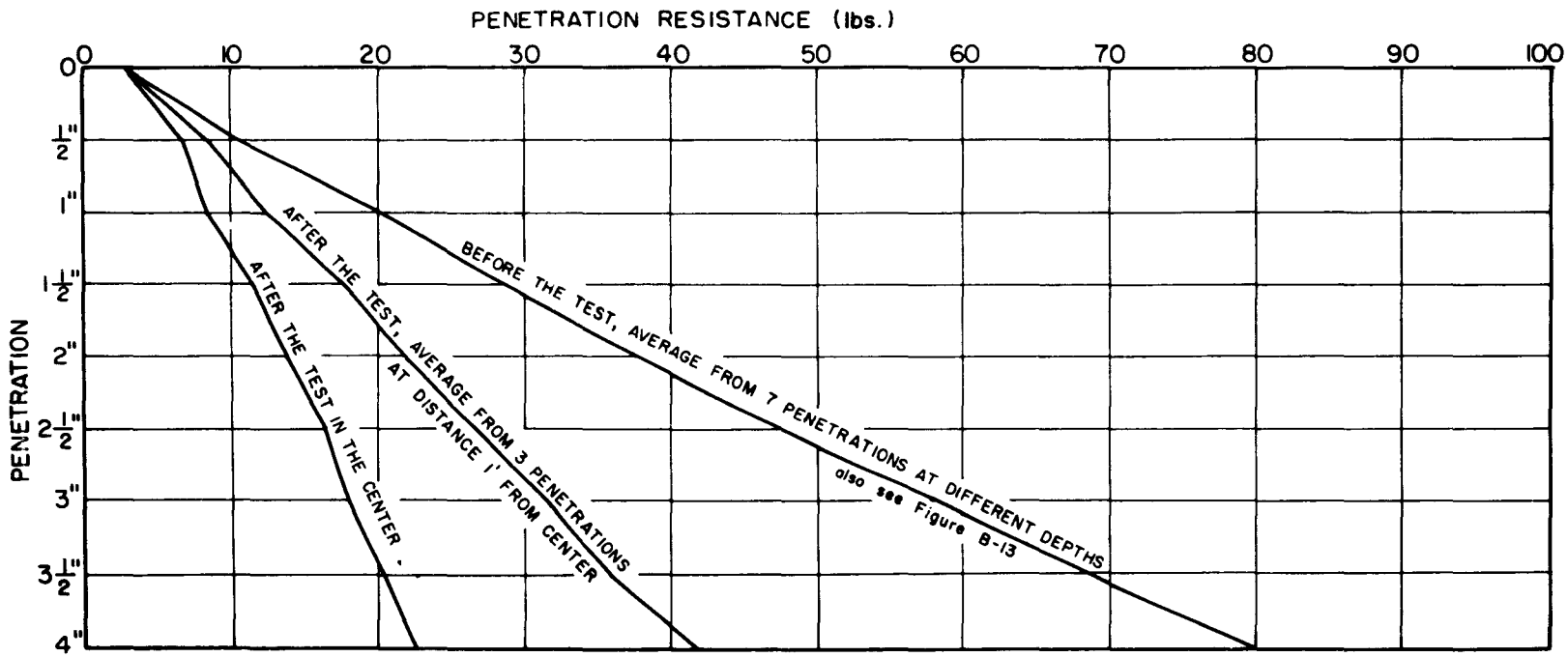

FIGURE C-6 PENETRATION TESTS: TEST PB-5

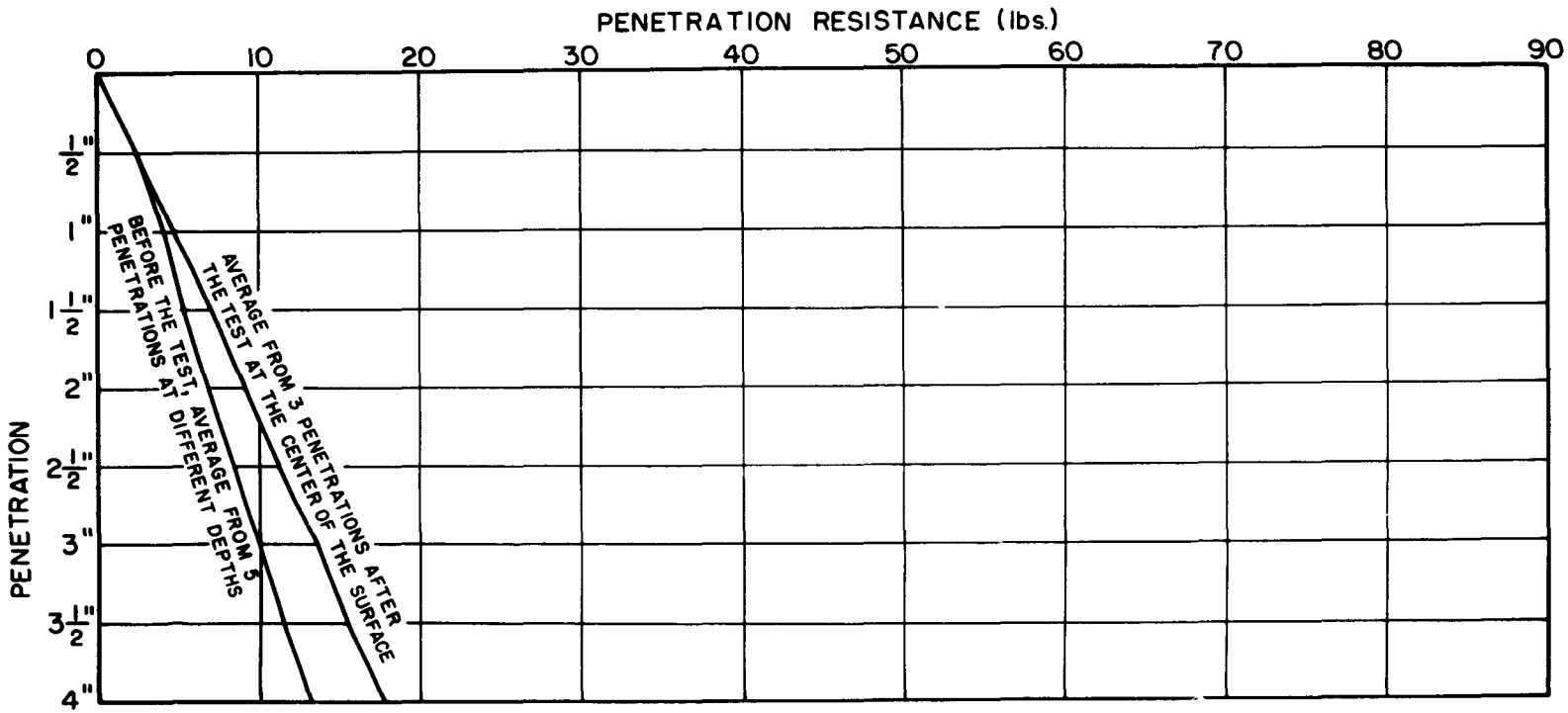

FIGURE C-7 PENETRATION TESTS: TEST PB-6

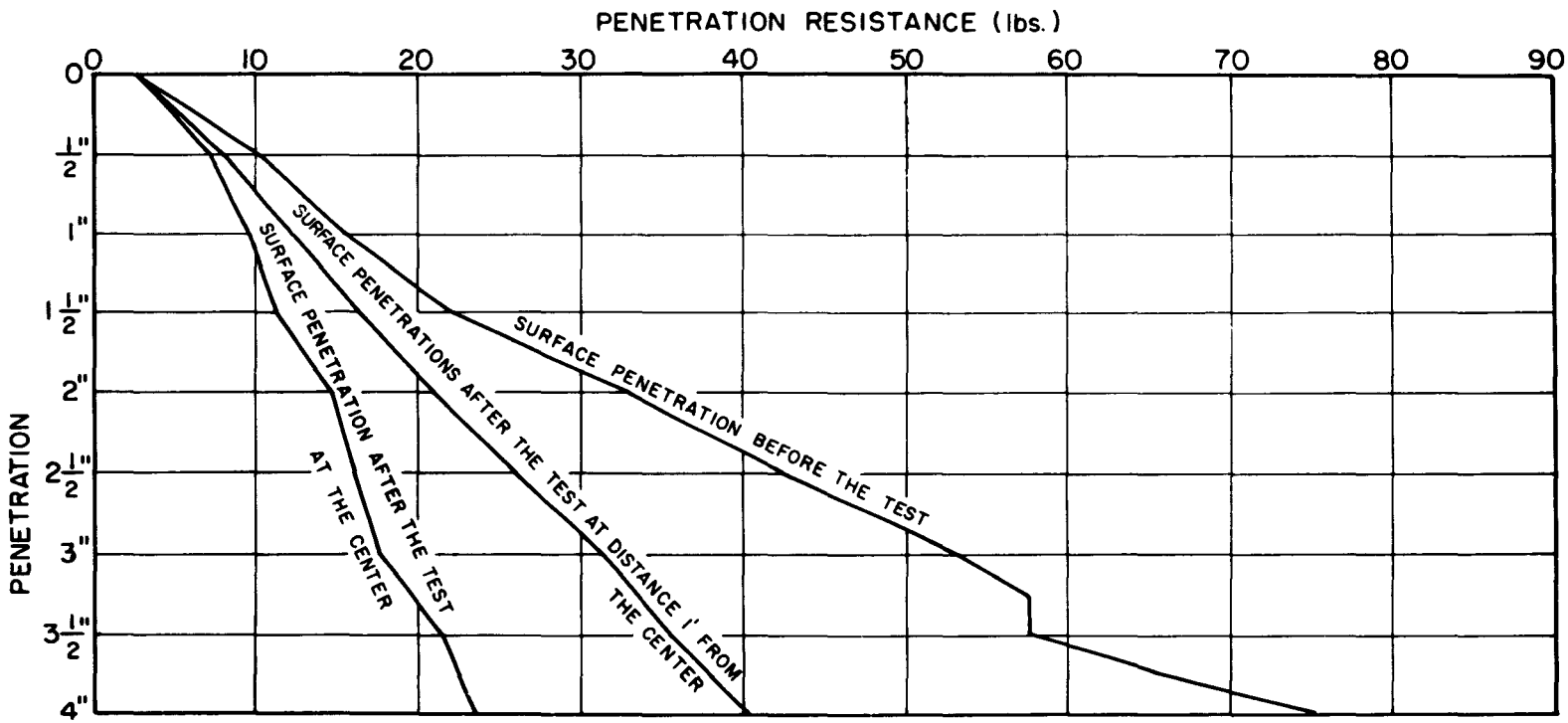

FIGURE C-8 PENETRATION TESTS: TEST PB-7

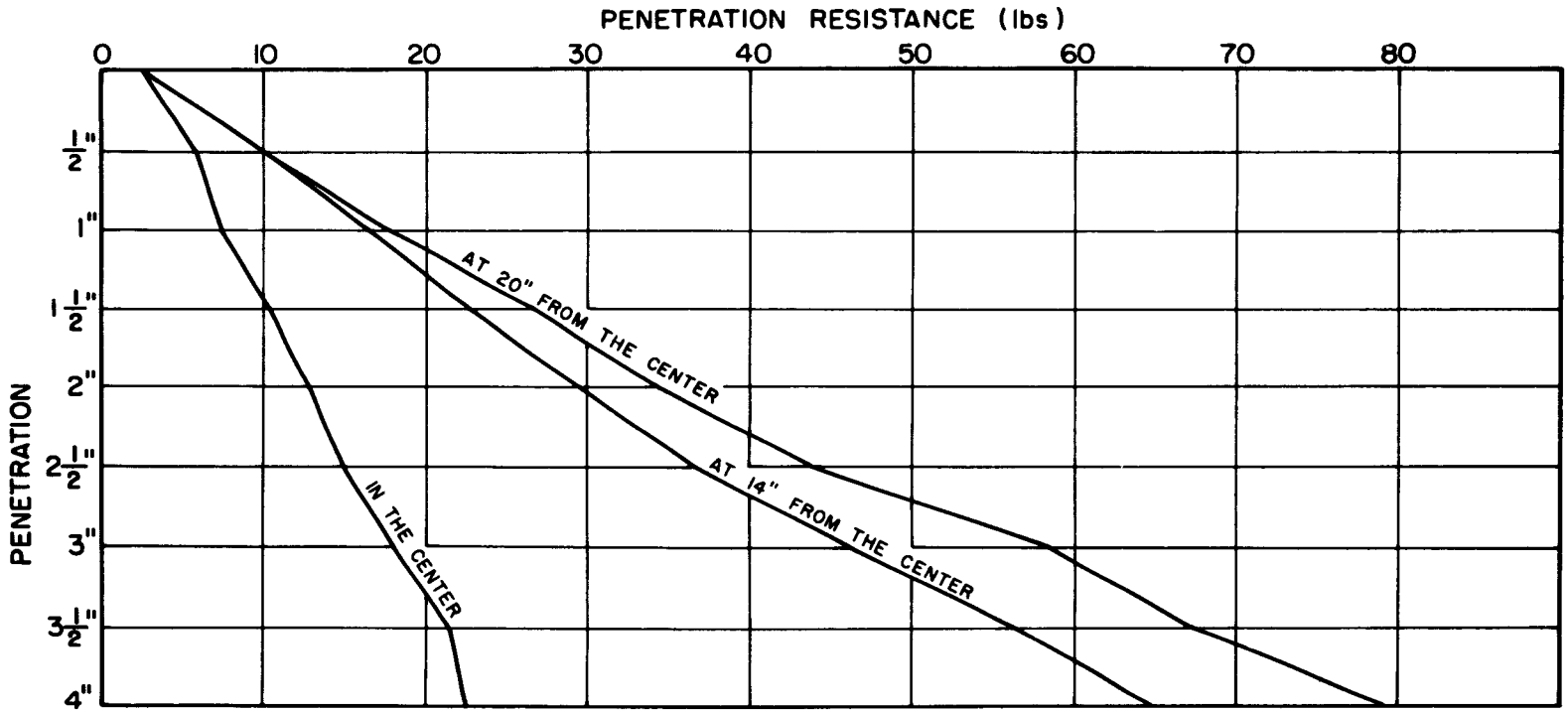

FIGURE C-9 PENETRATION TESTS AFTER TEST PB-8

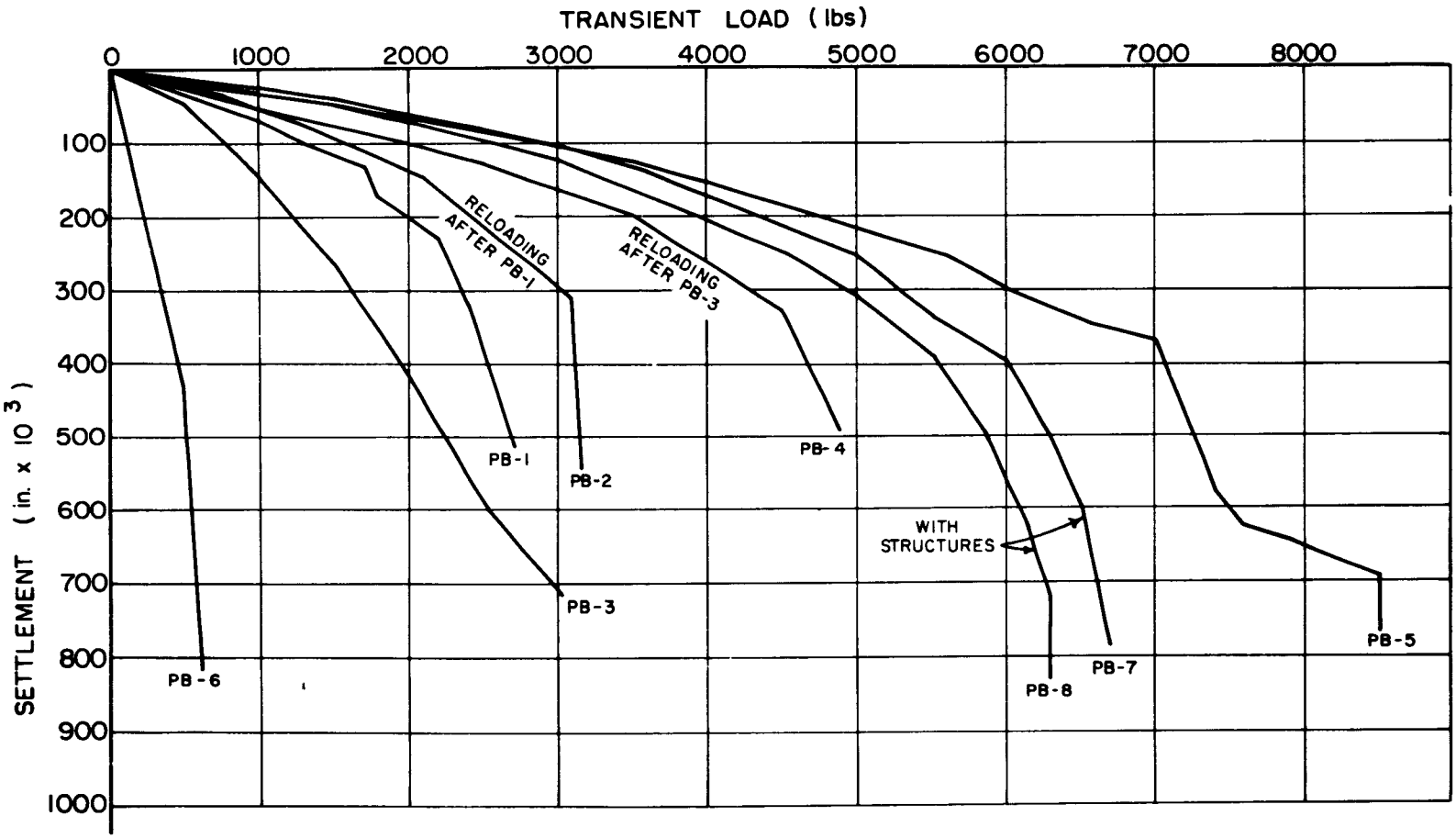

FIGURE C-10 LOAD-SETTLEMENT CURVES FROM PLATE LOADING TESTS

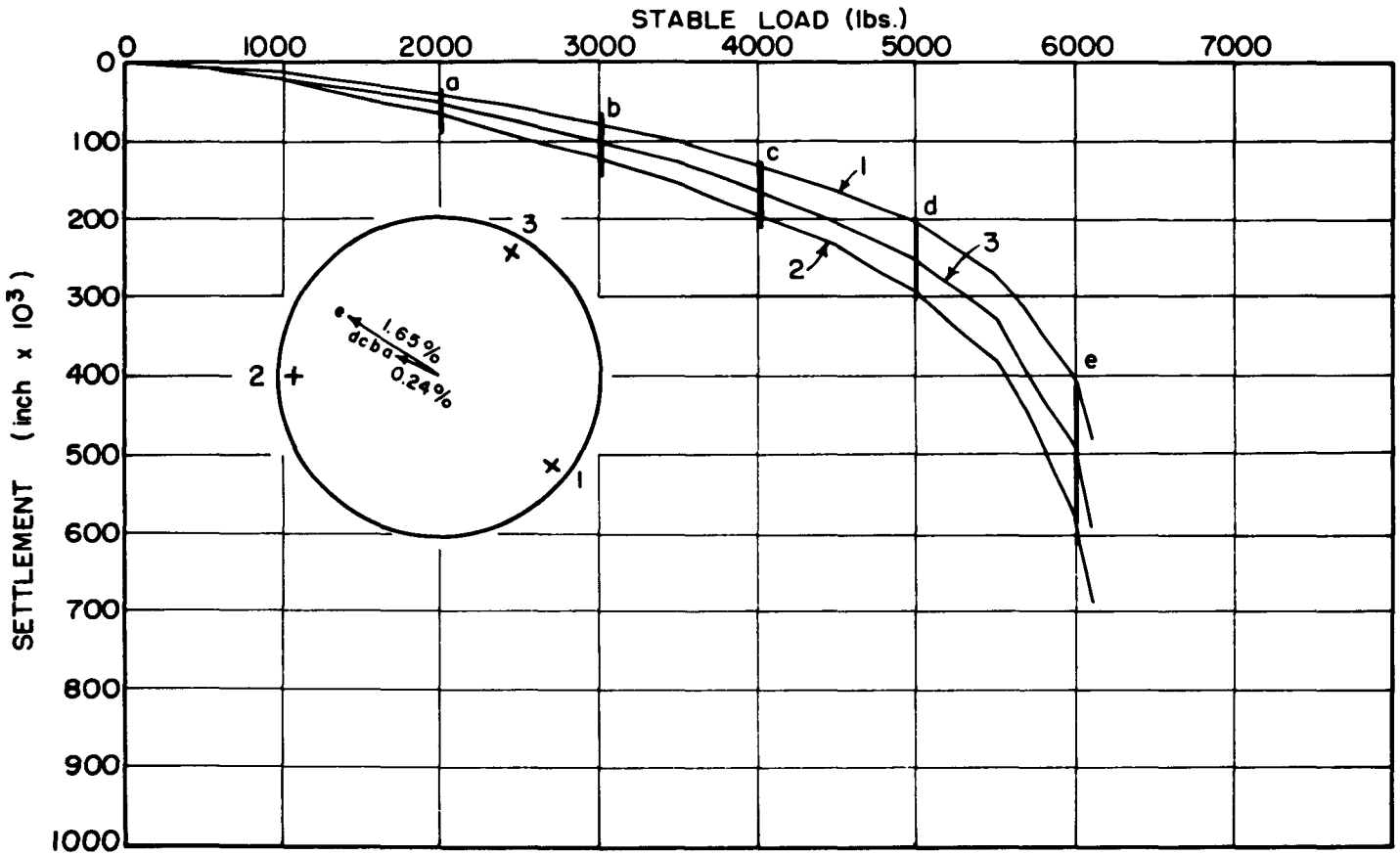

FIGURE C-11 SETTLEMENT OF LOADING PLATE: TEST PB-7

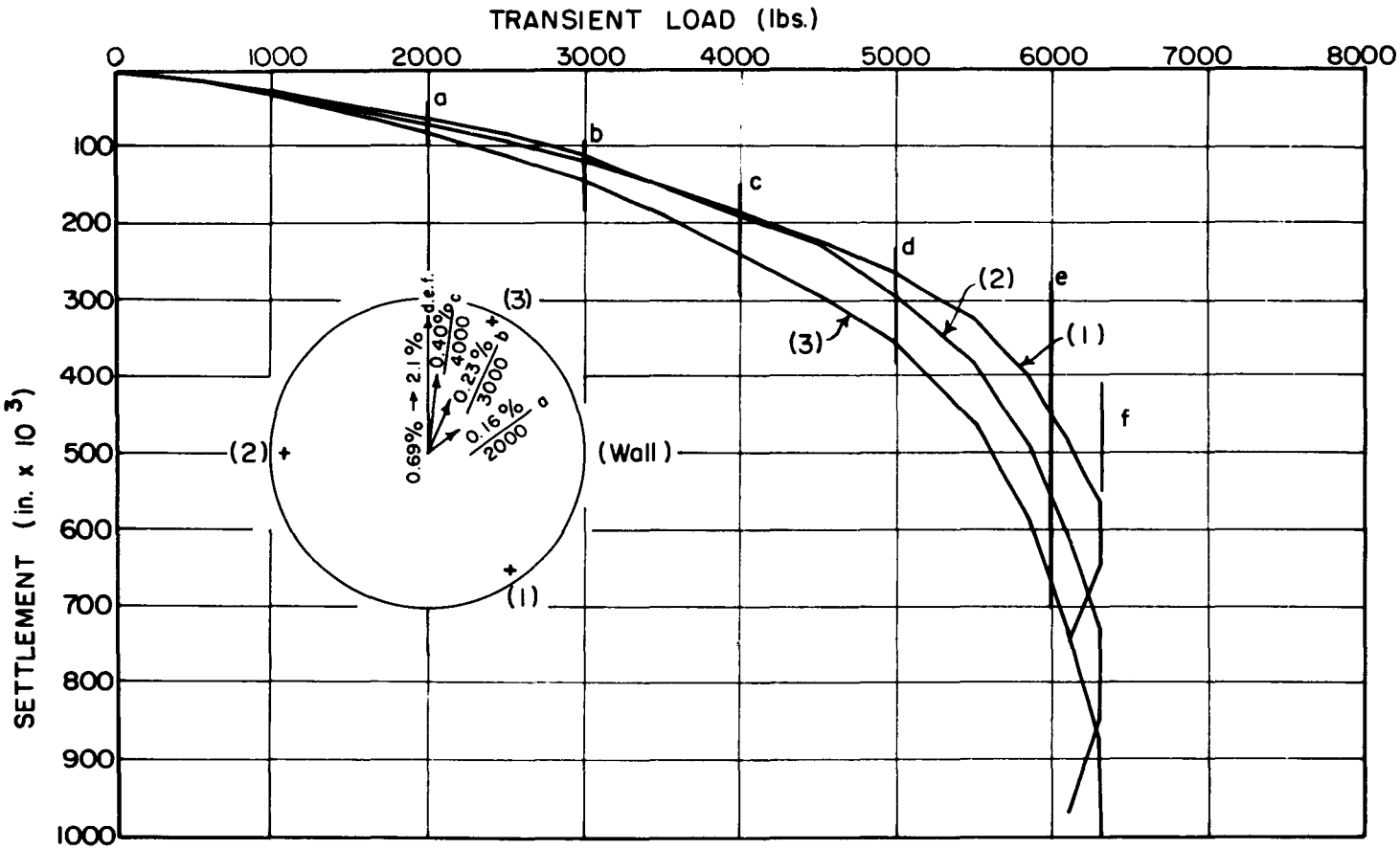

FIGURE C-12 SETTLEMENT OF LOADING PLATE: TEST PB-8

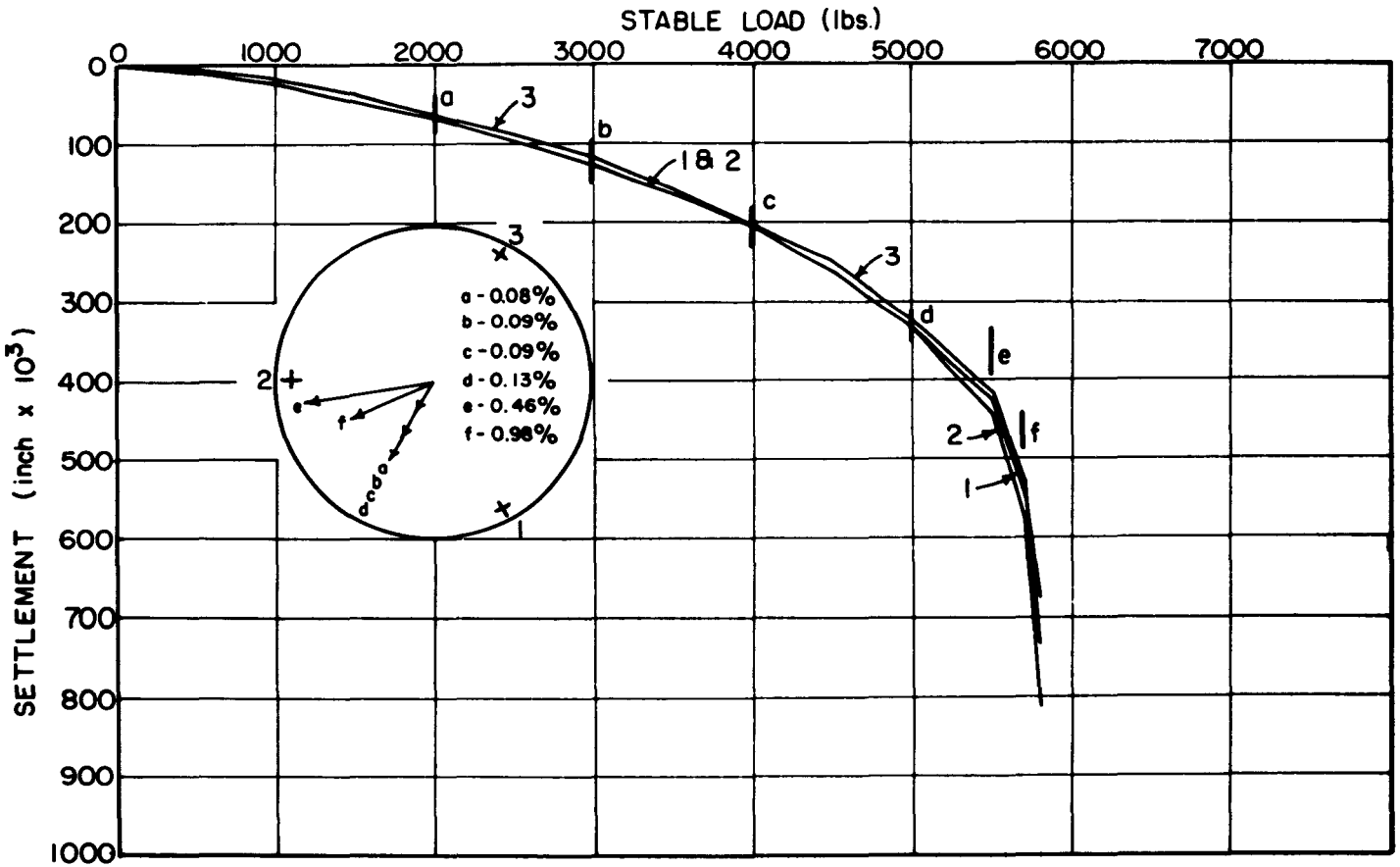

FIGURE C-13 SETTLEMENT OF LOADING PLATE : TEST PB-9

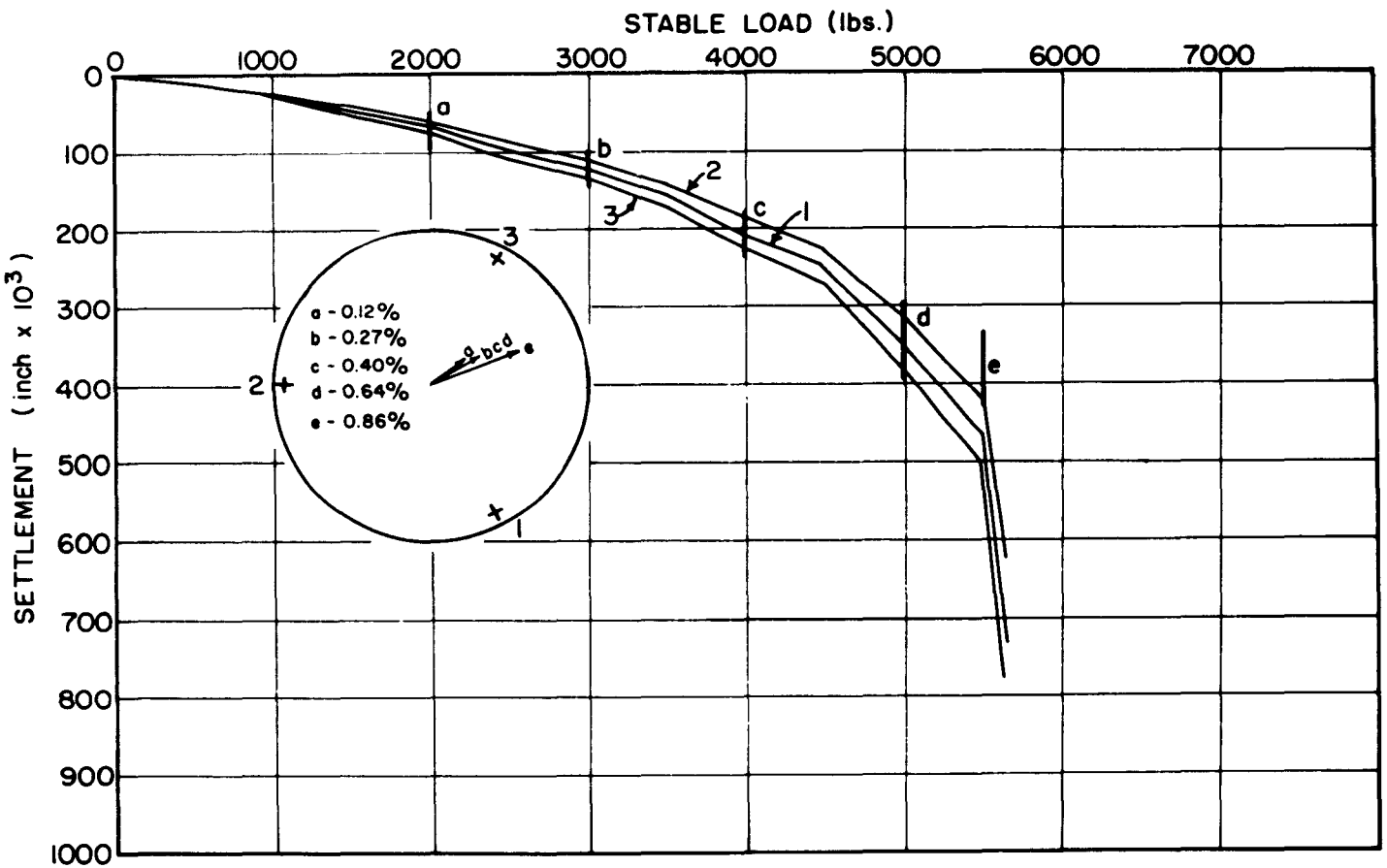

FIGURE C-14 SETTLEMENT OF LOADING PLATE: TEST PB-10

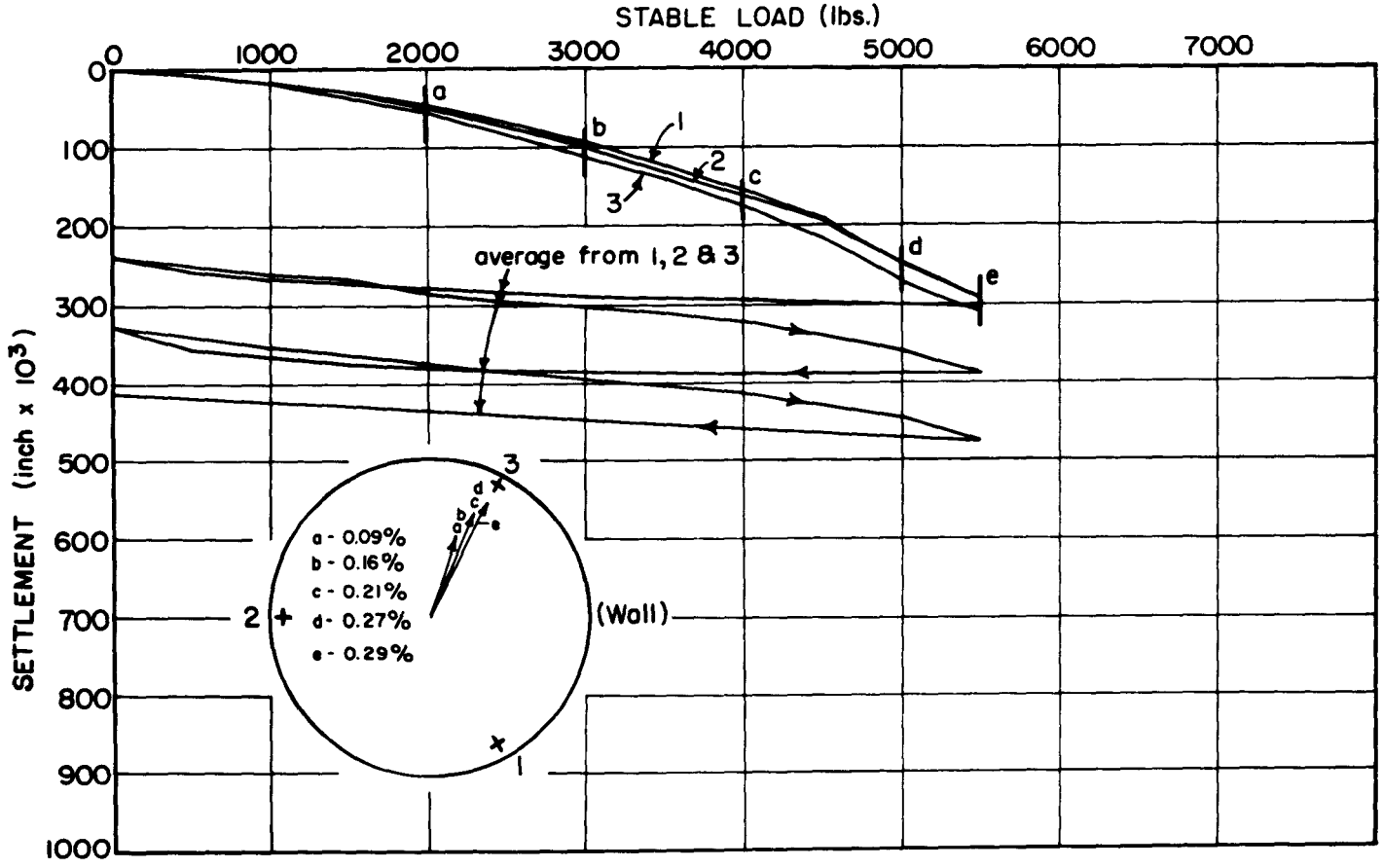

FIGURE C-15 SETTLEMENT OF LOADING PLATE: TEST PB-11

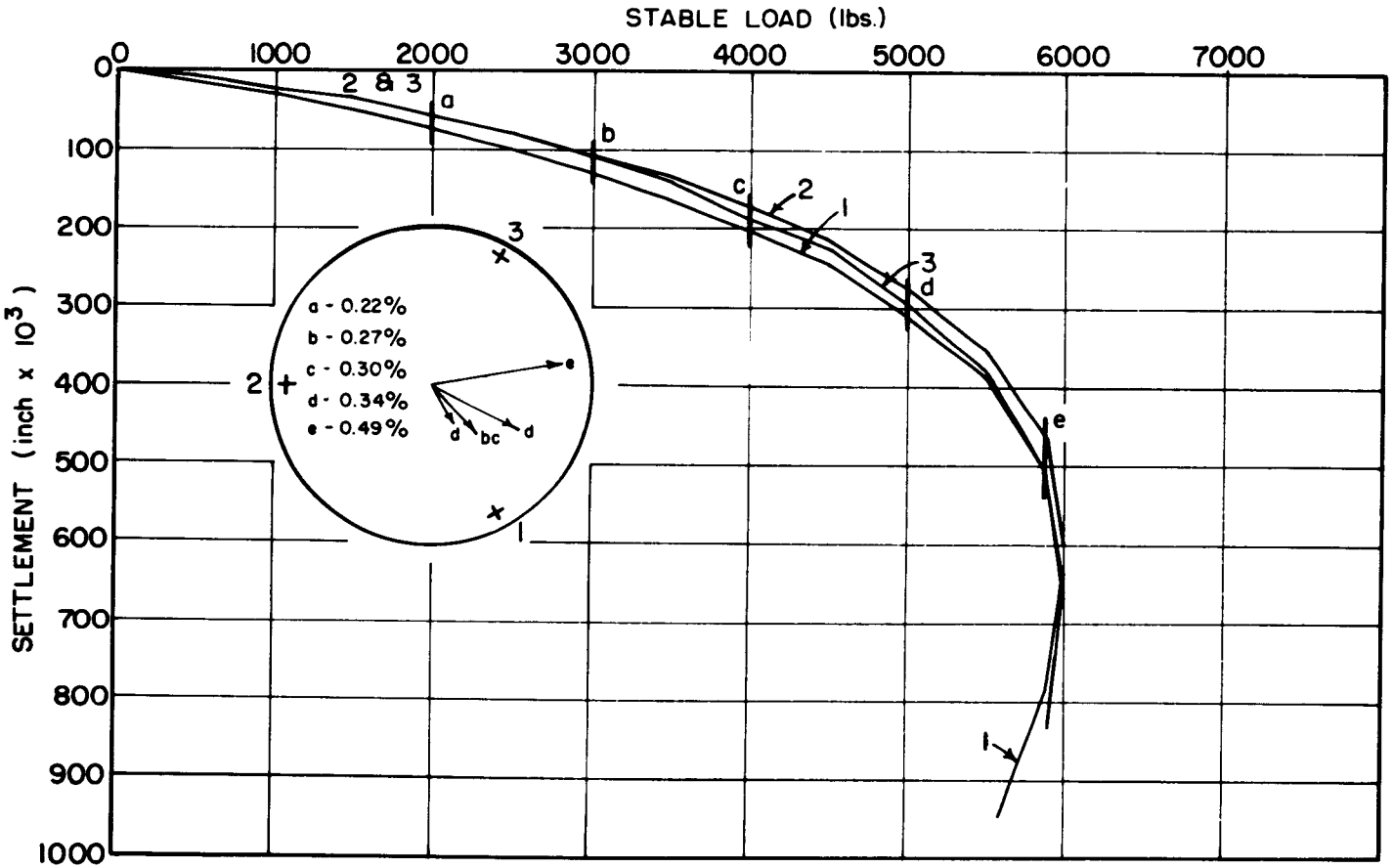

FIGURE C-16 SETTLEMENT OF LOADING PLATE: TEST PB-12

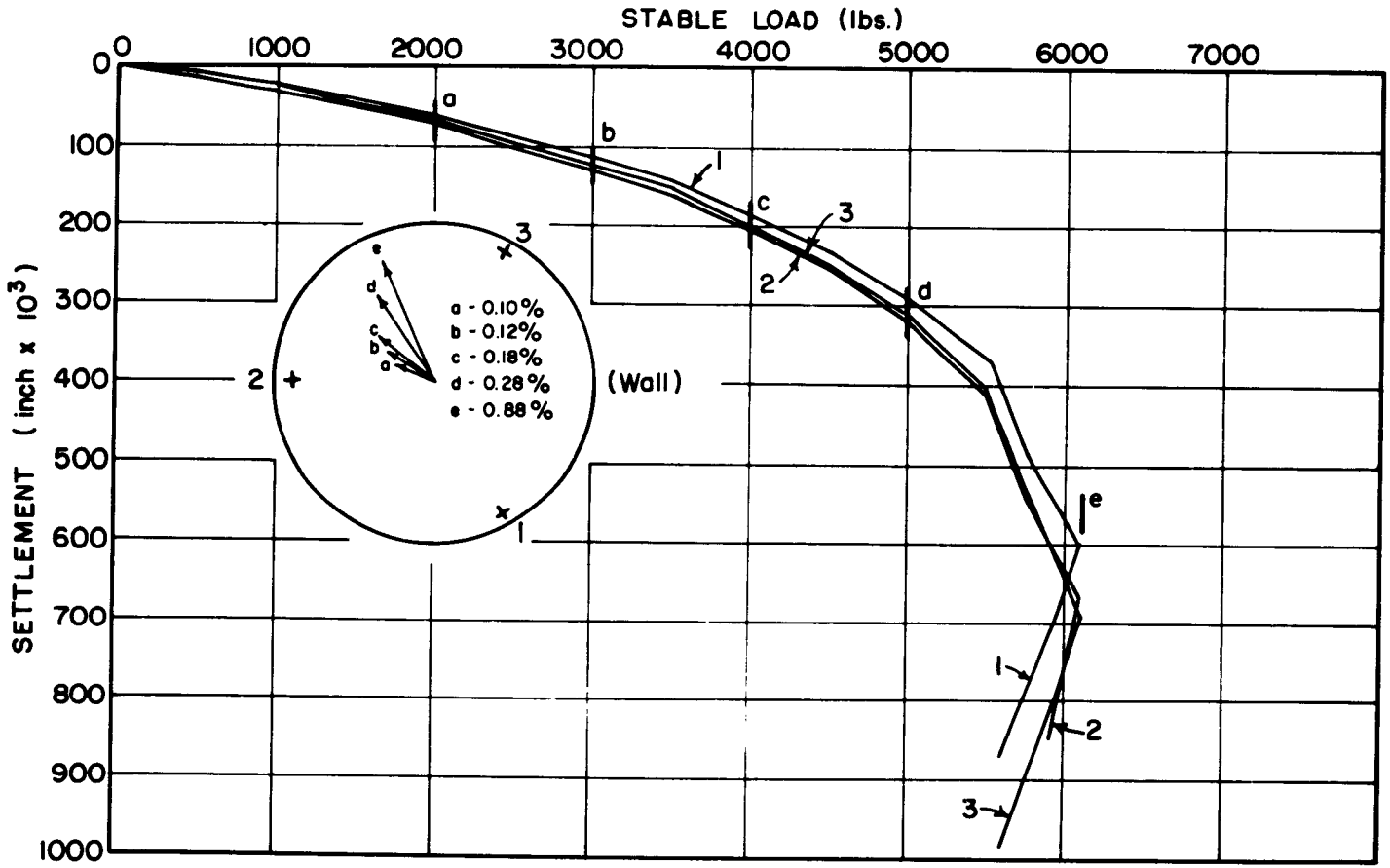

FIGURE C-17 SETTLEMENT OF LOADING PLATE: TEST PB-13

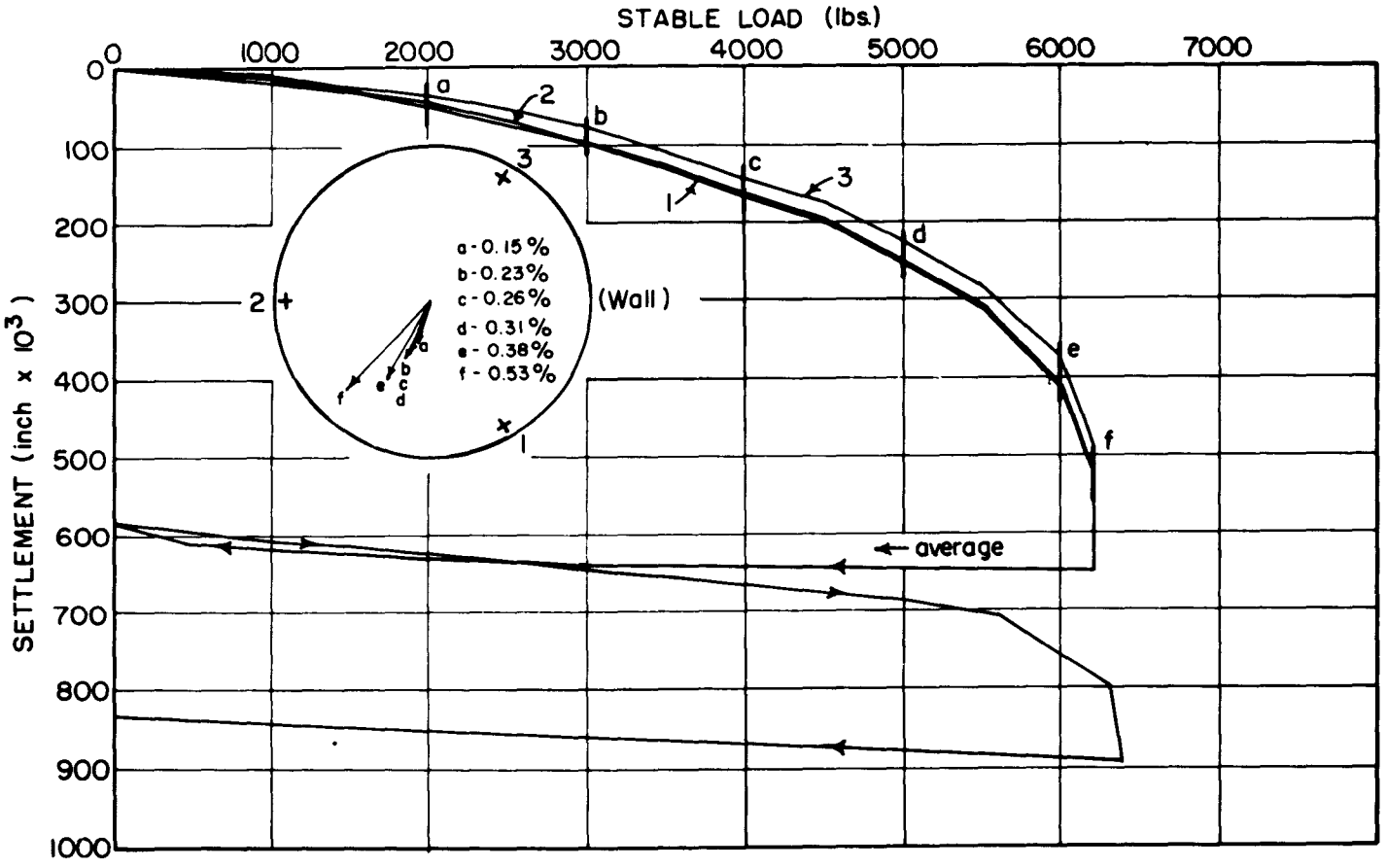

FIGURE C-18 SETTLEMENT OF LOADING PLATE: TEST PB-14

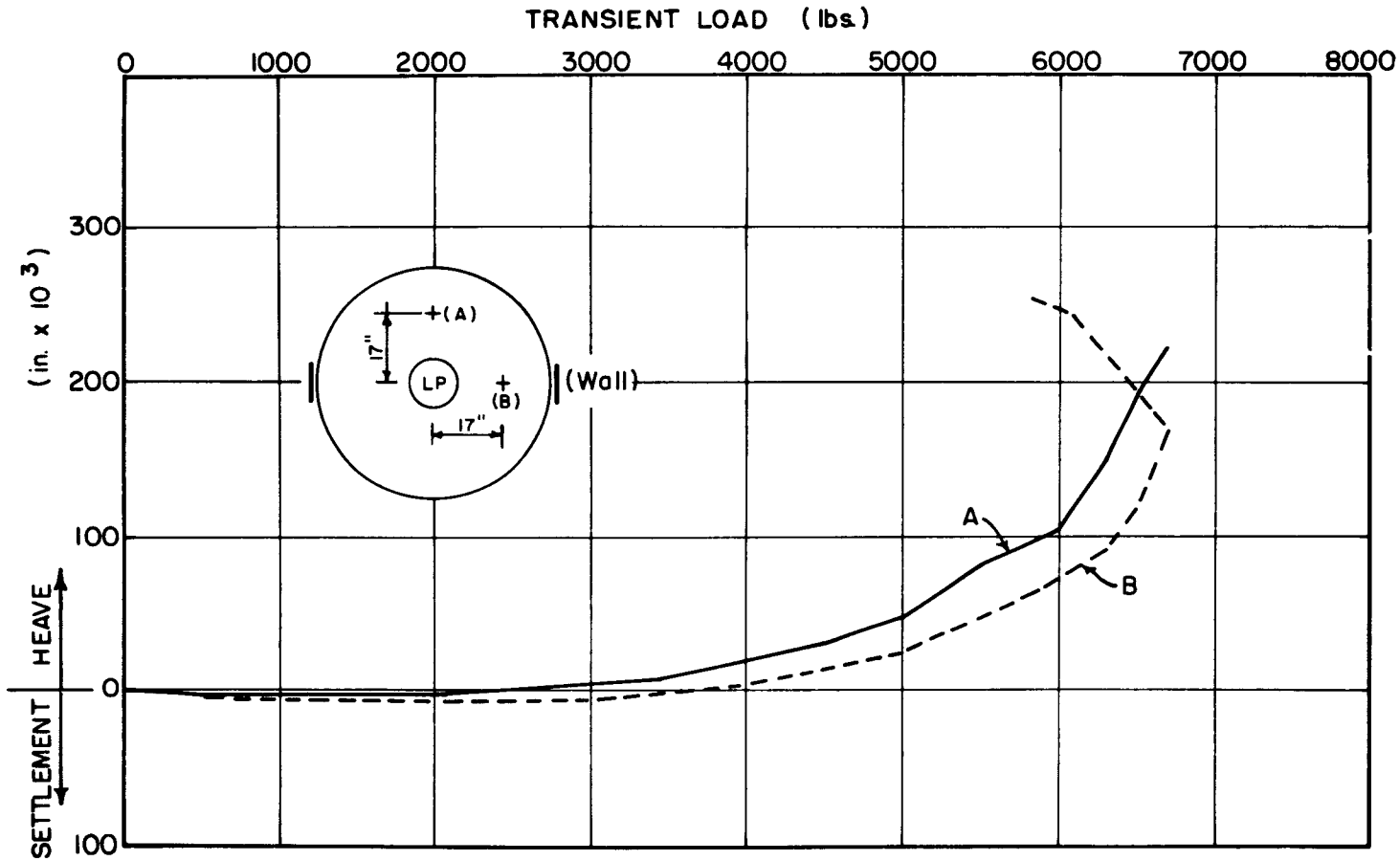

FIGURE C-19 MOVEMENT OF SURFACE PLATES: TEST PB-7

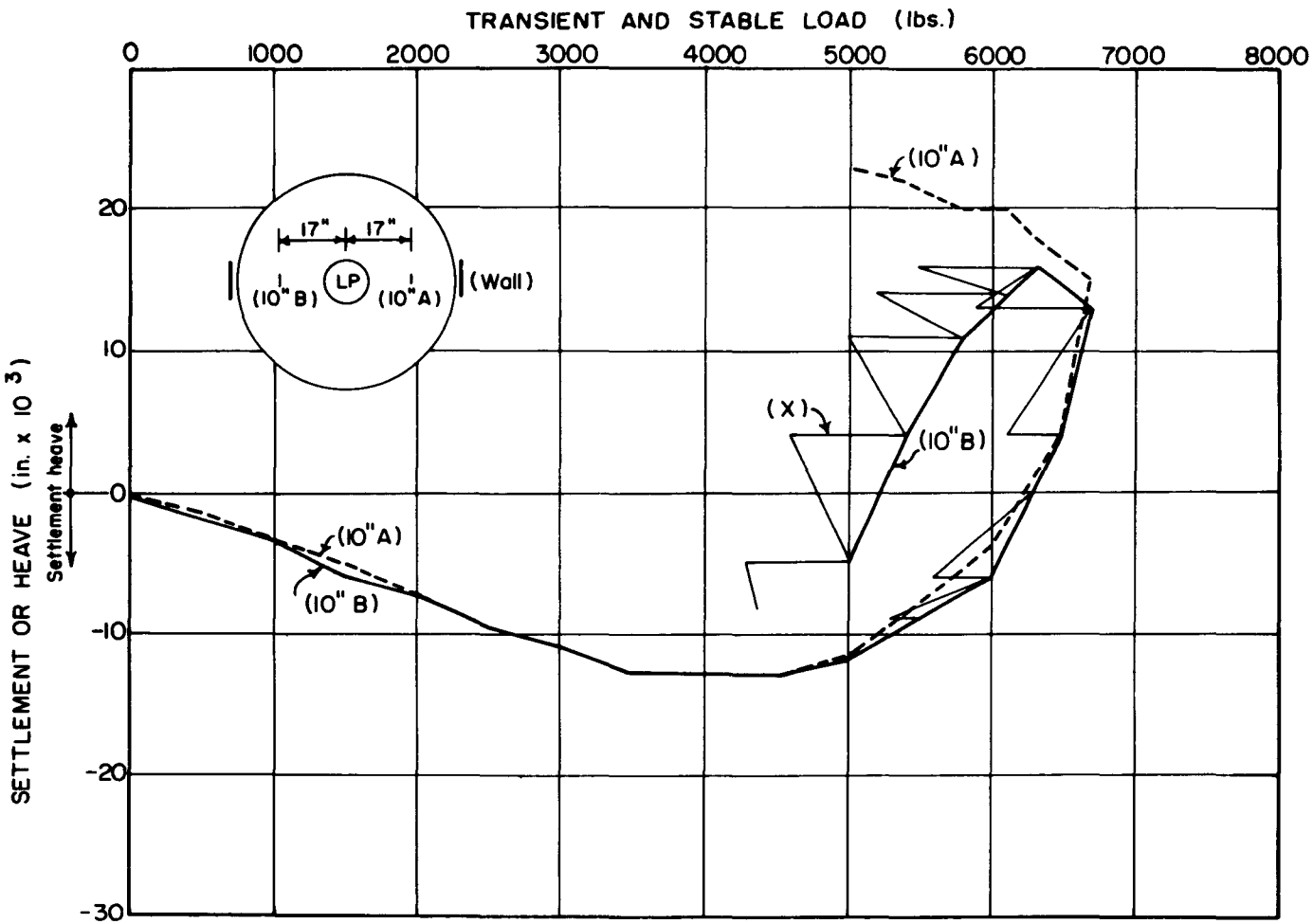

The heavy lines show the behavior for transient condition.

The light line shows the creep behavior (for 10" B only)

FIGURE C-20 MOVEMENT OF 10" DEEP ANCHOR PLATES: TEST PB-7

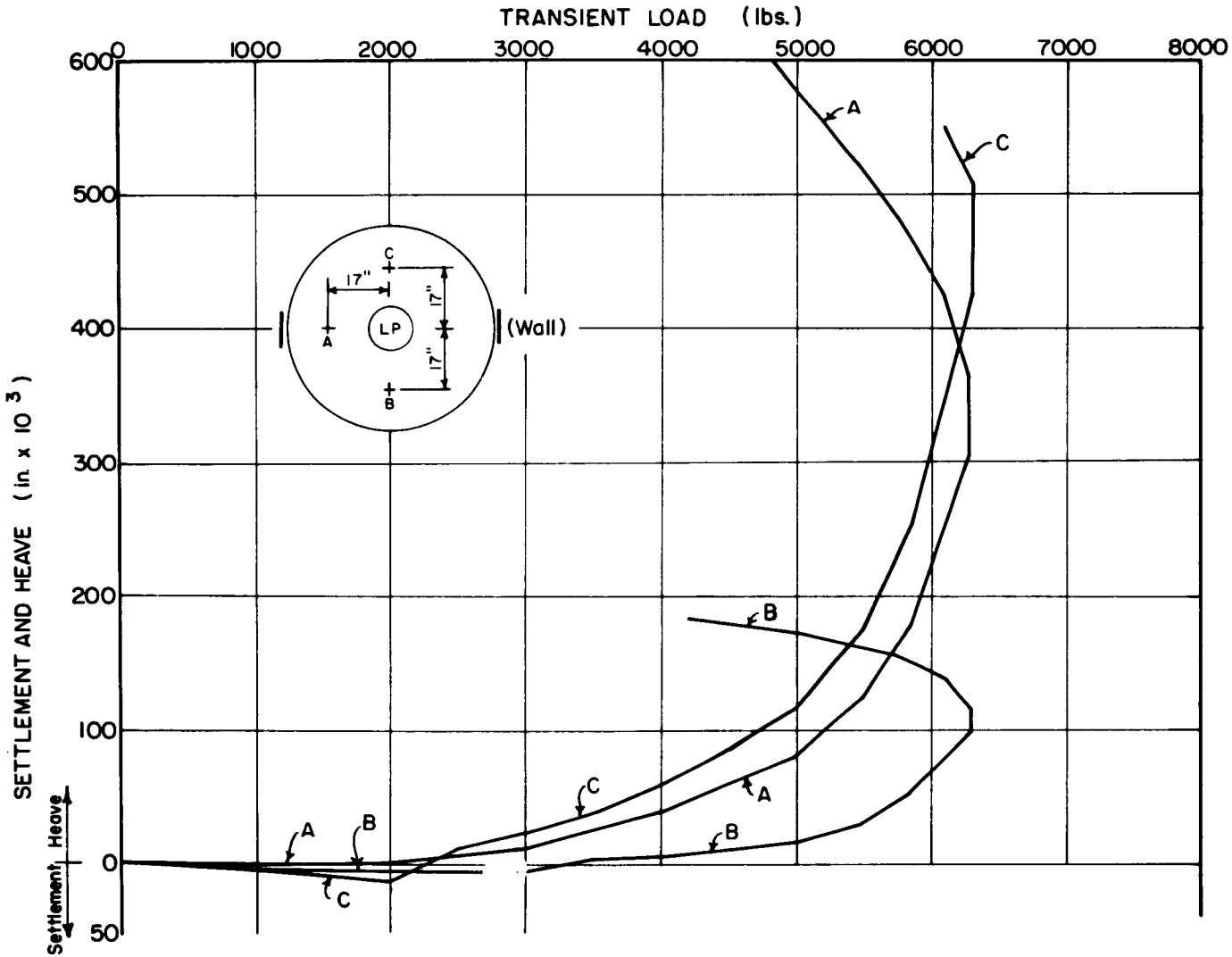

FIGURE C-21 MOVEMENT OF SURFACE PLATES: TEST PB-8

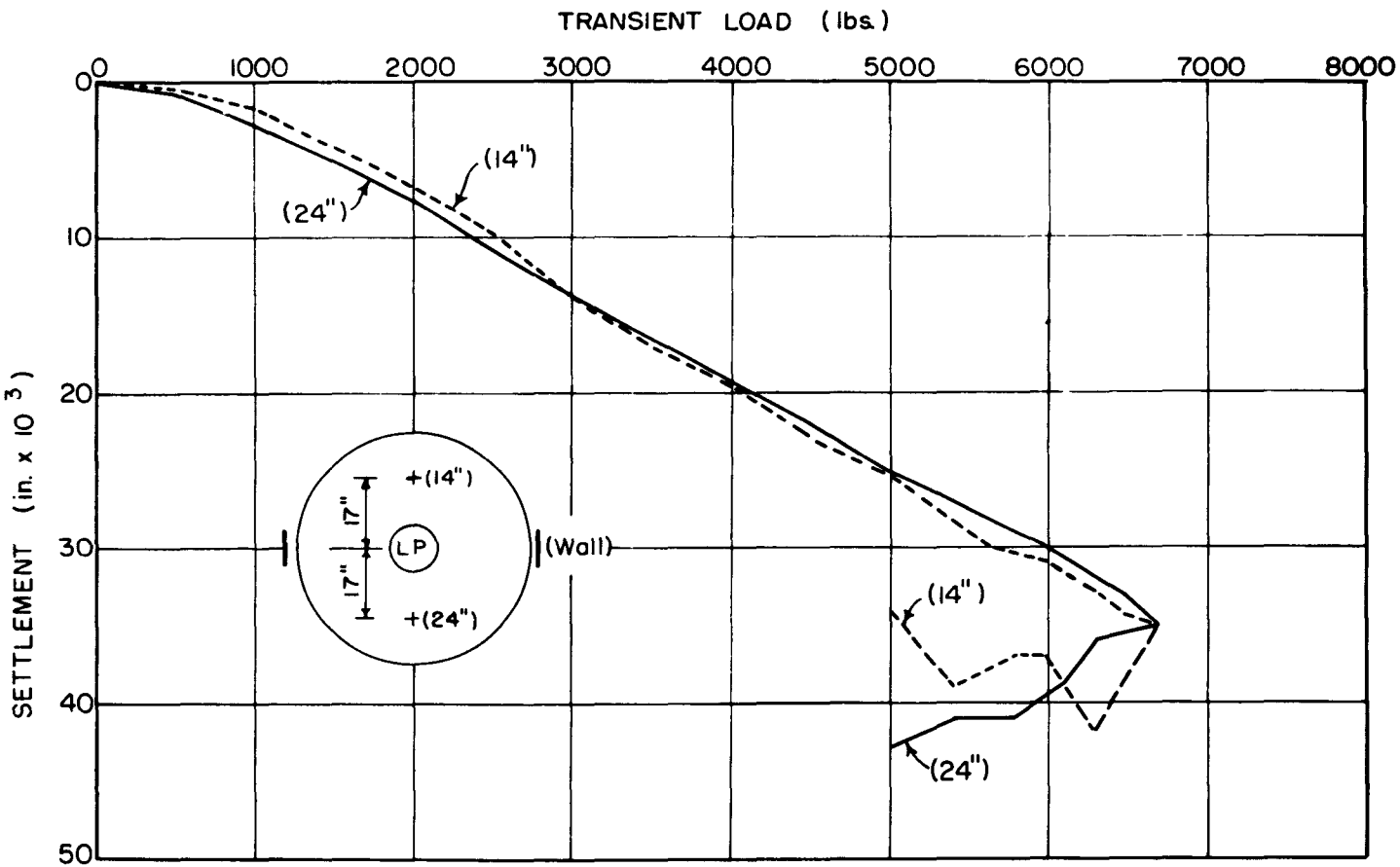

FIGURE C-22 MOVEMENT OF 14" & 24" DEEP ANCHOR PLATES: TEST PB-7

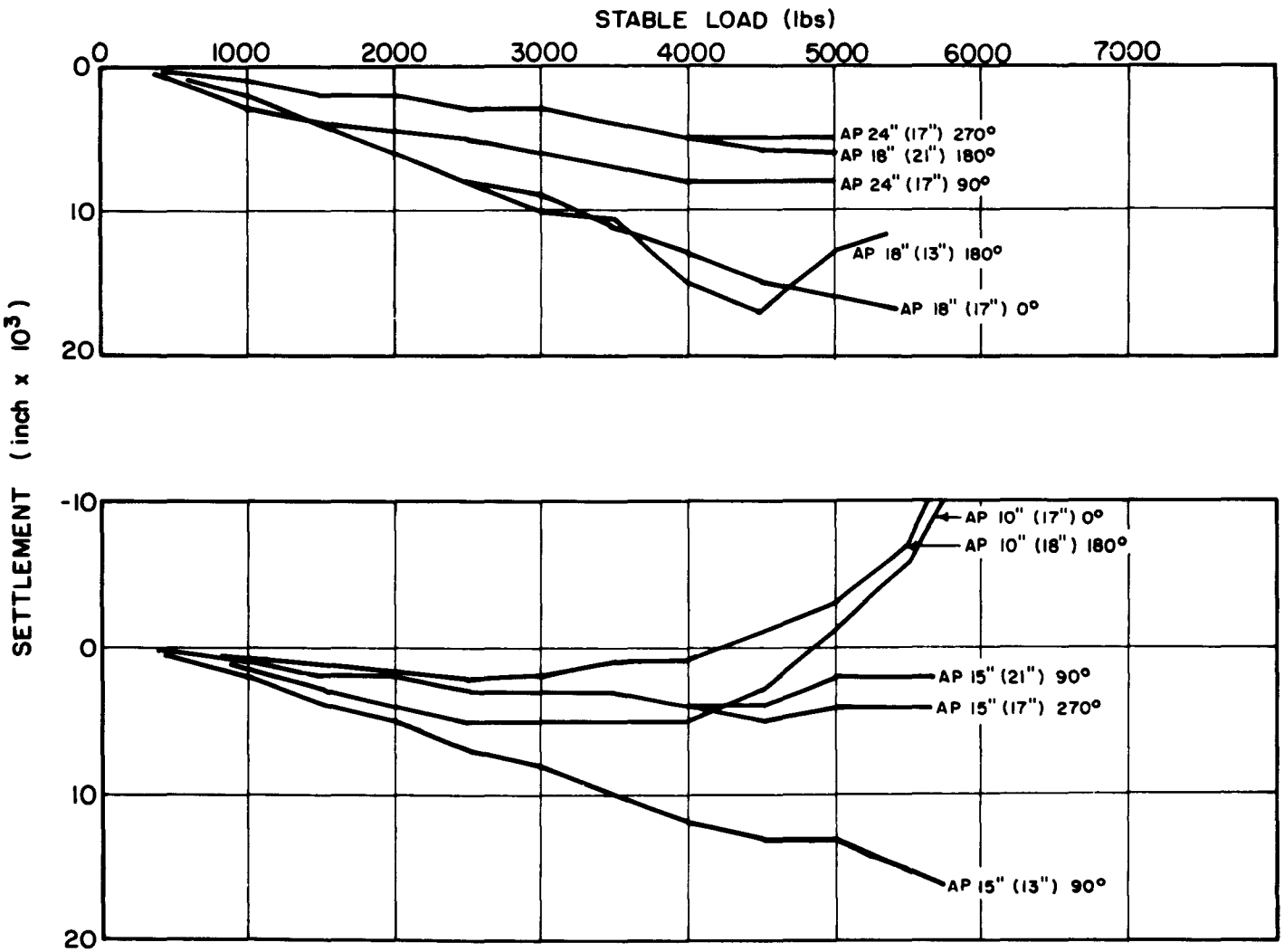

FIGURE C-23 ANCHOR PLATE MOVEMENT: TEST PB-9

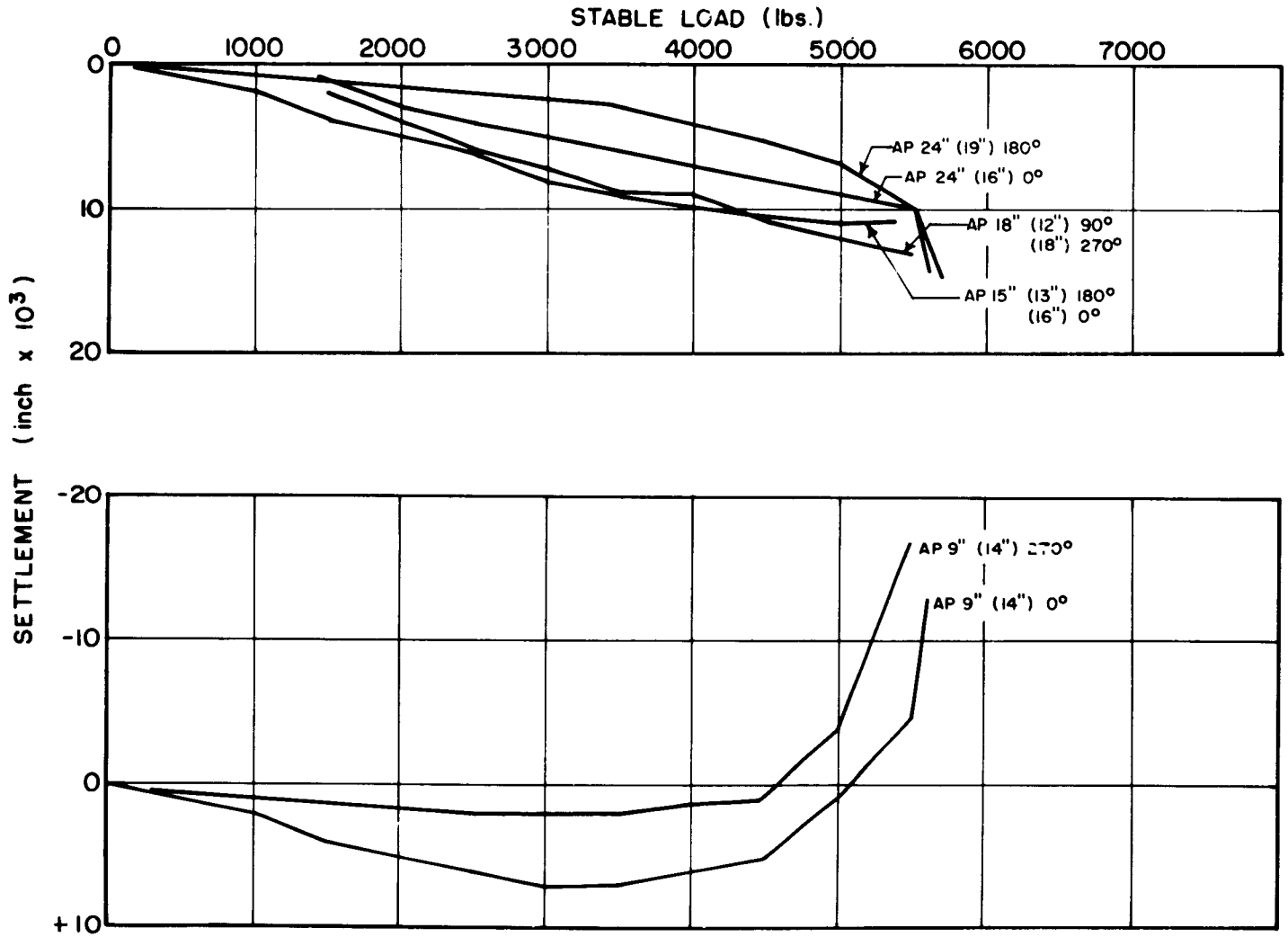

FIGURE C-24 ANCHOR PLATE MOVEMENT: TEST PB-10

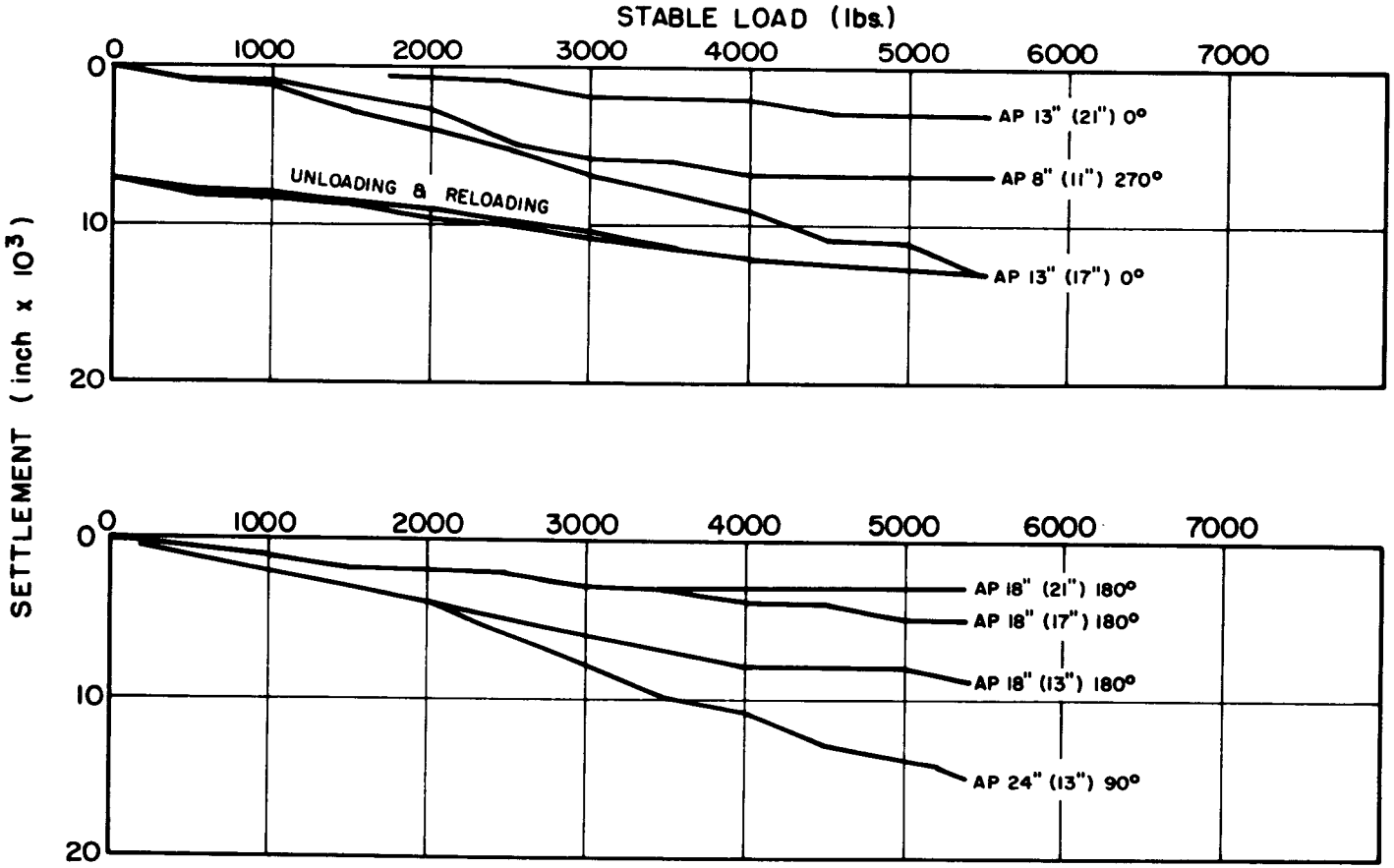

FIGURE C-25 ANCHOR PLATE MOVEMENT: TEST PB-11

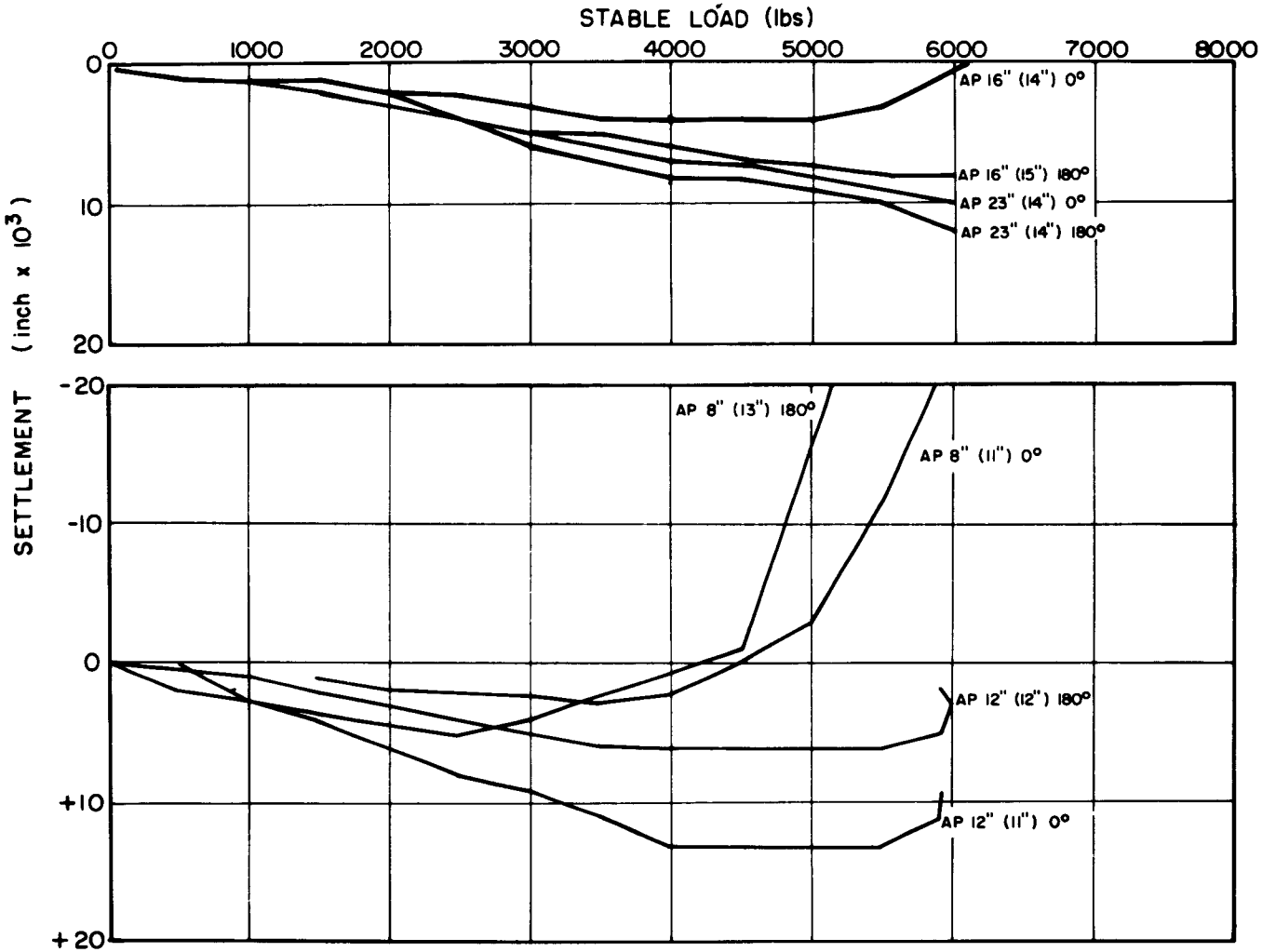

FIGURE C-26 ANCHOR PLATE MOVEMENT: TEST PB-12

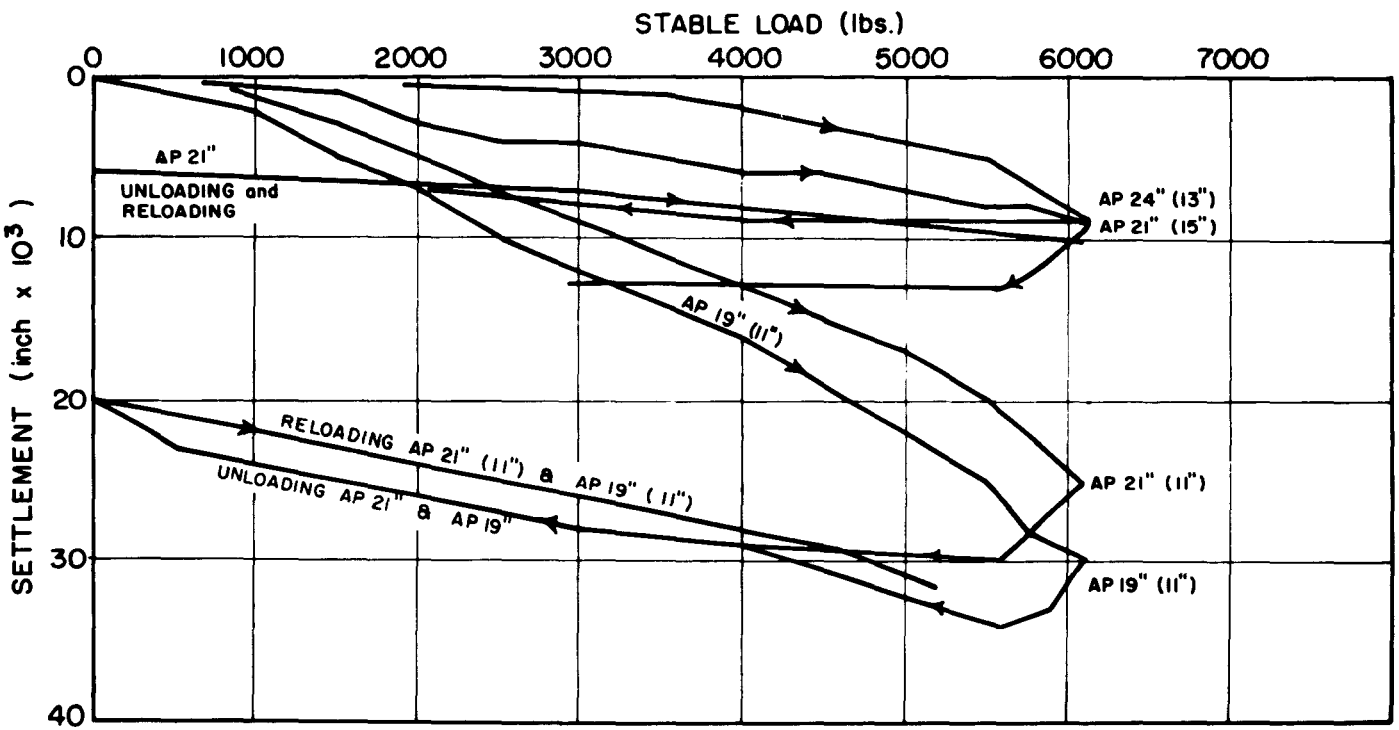

FIGURE C-27 ANCHOR PLATE MOVEMENT: TEST PB-13

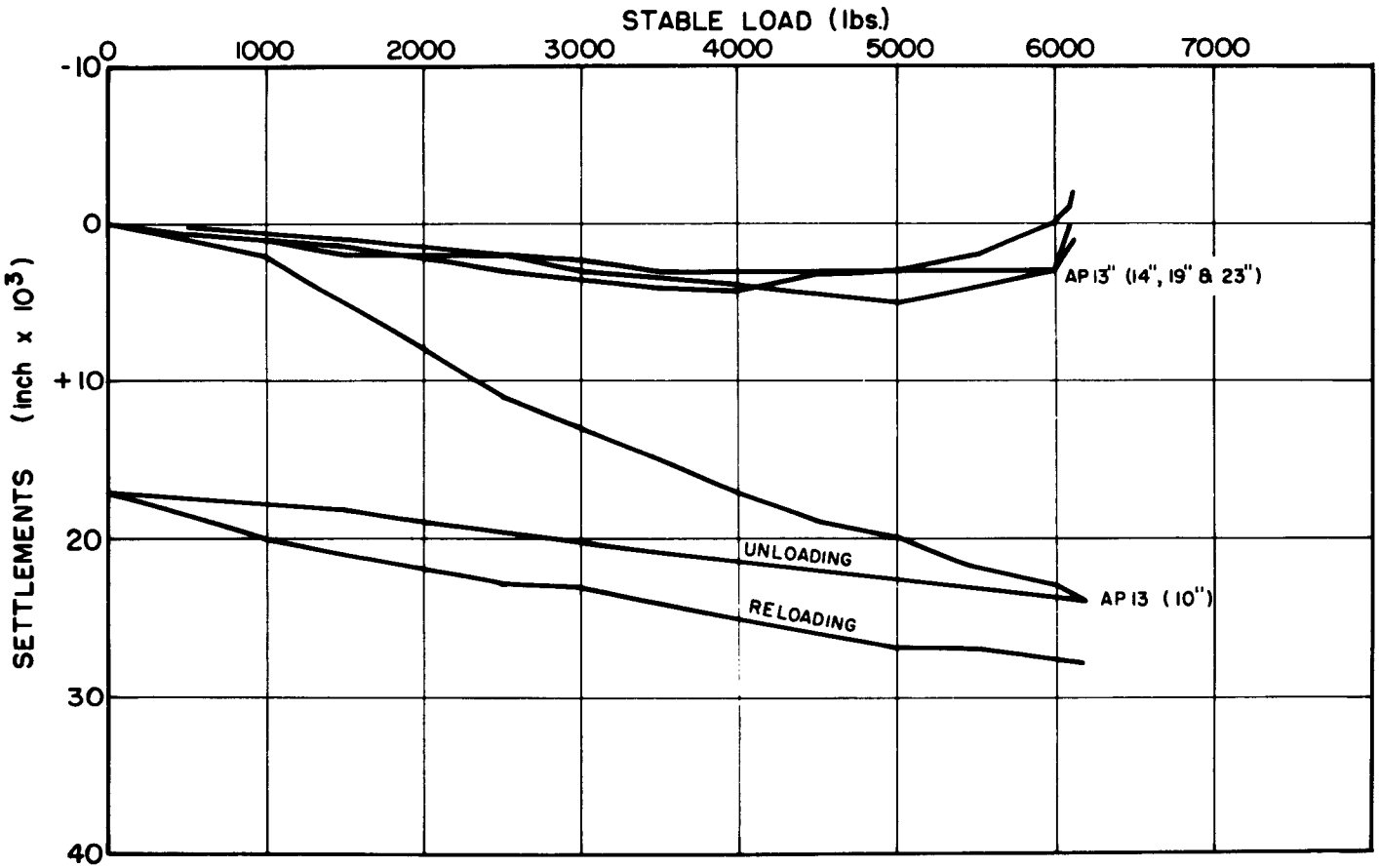

FIGURE C-28 ANCHOR PLATE MOVEMENT AT 13" DEPTH: TEST PB-14

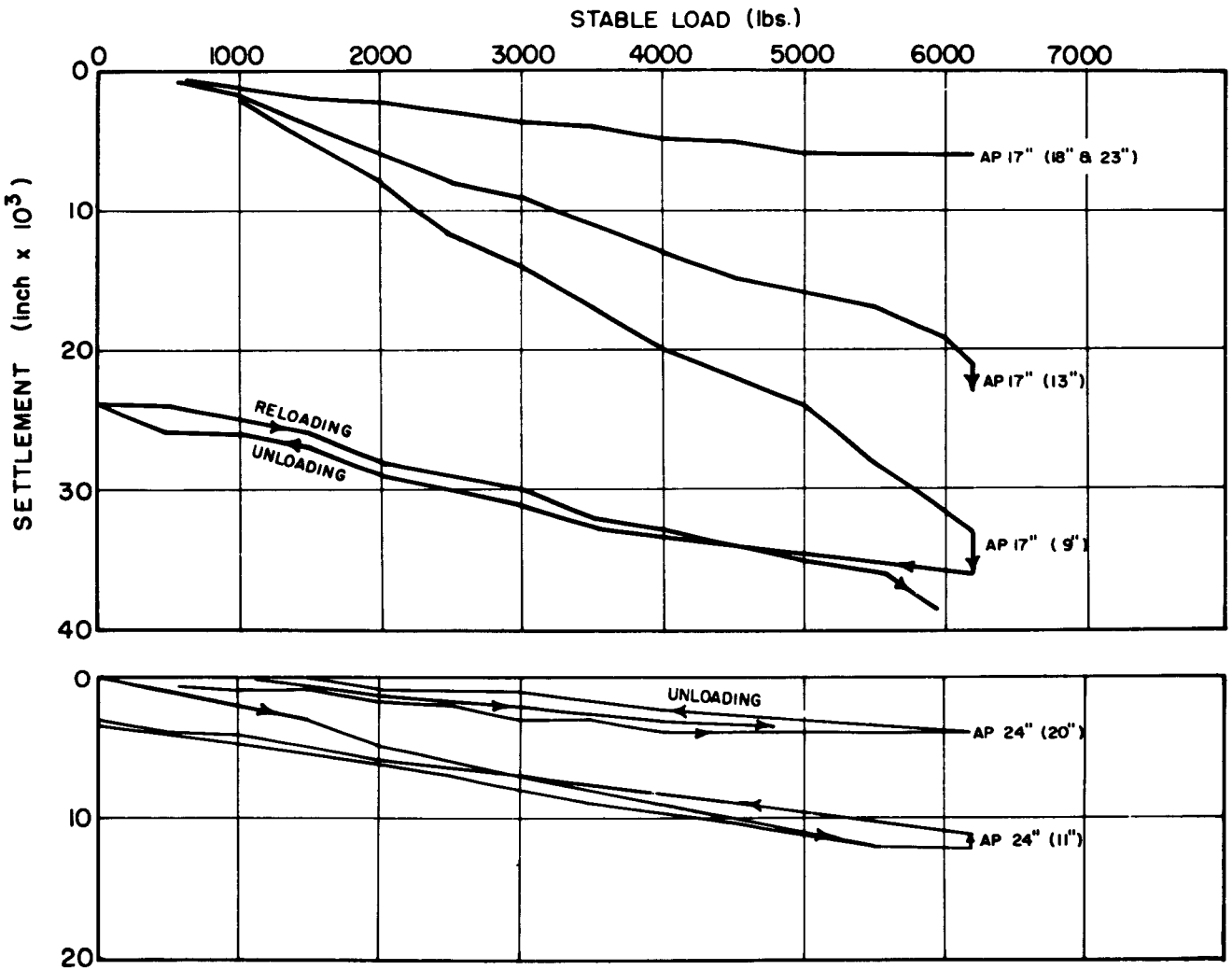

FIGURE C-29 ANCHOR PLATE MOVEMENT AT 17" & 24": TEST PB-14

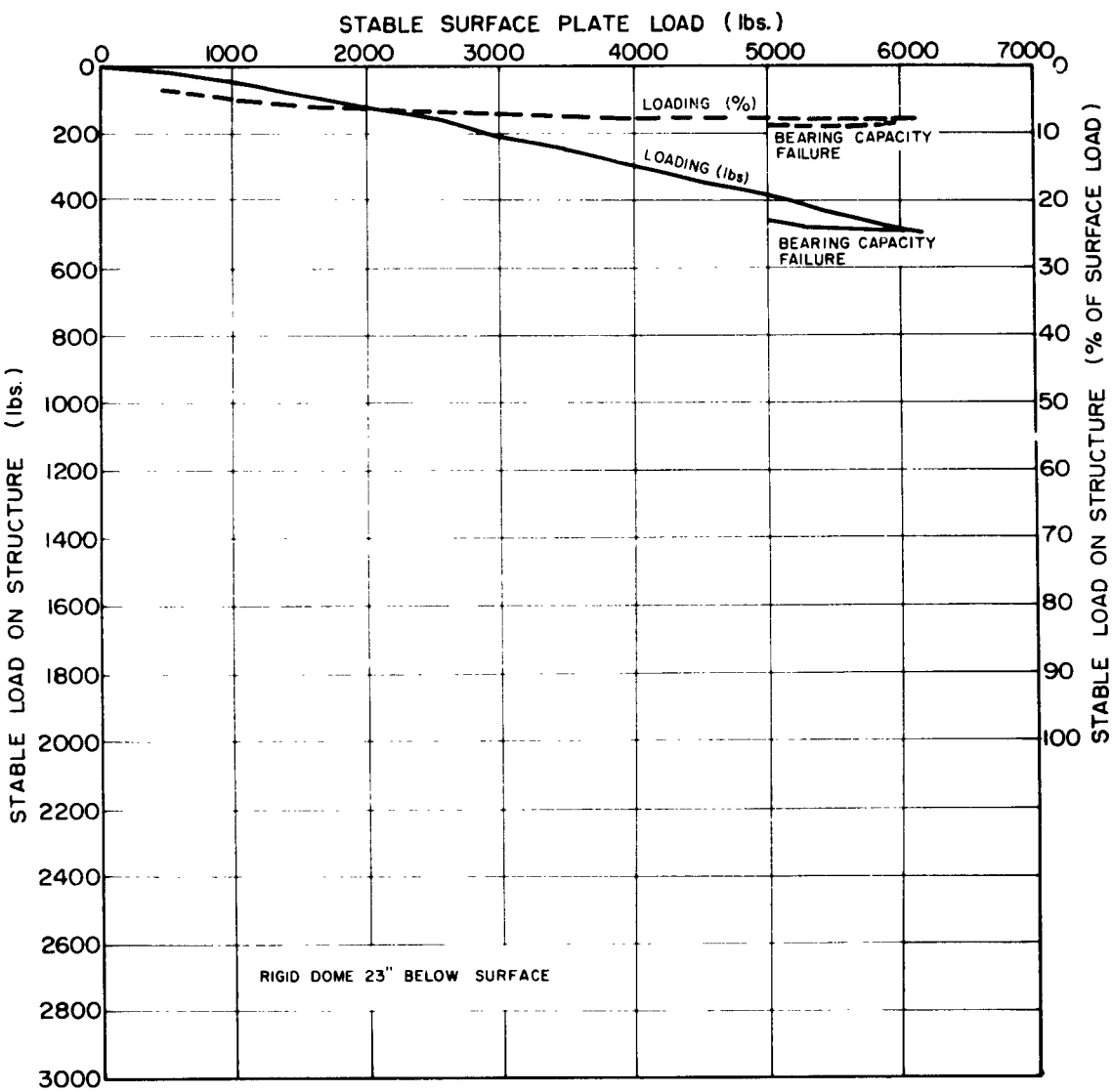

FIGURE C-30 LOAD ON STRUCTURE: TEST PB-7

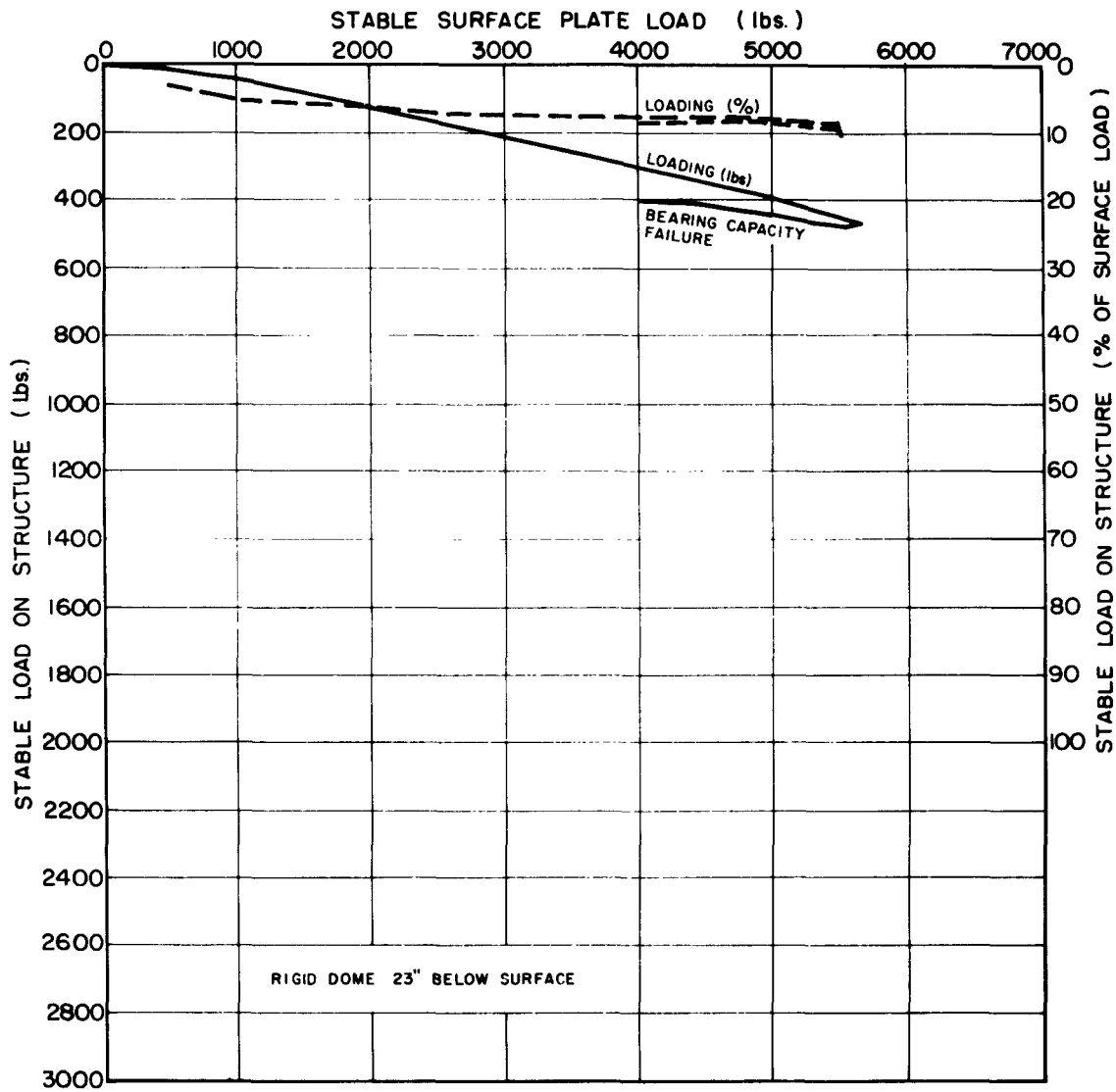

FIGURE C-31 LOAD ON STRUCTURE: TEST PB-8

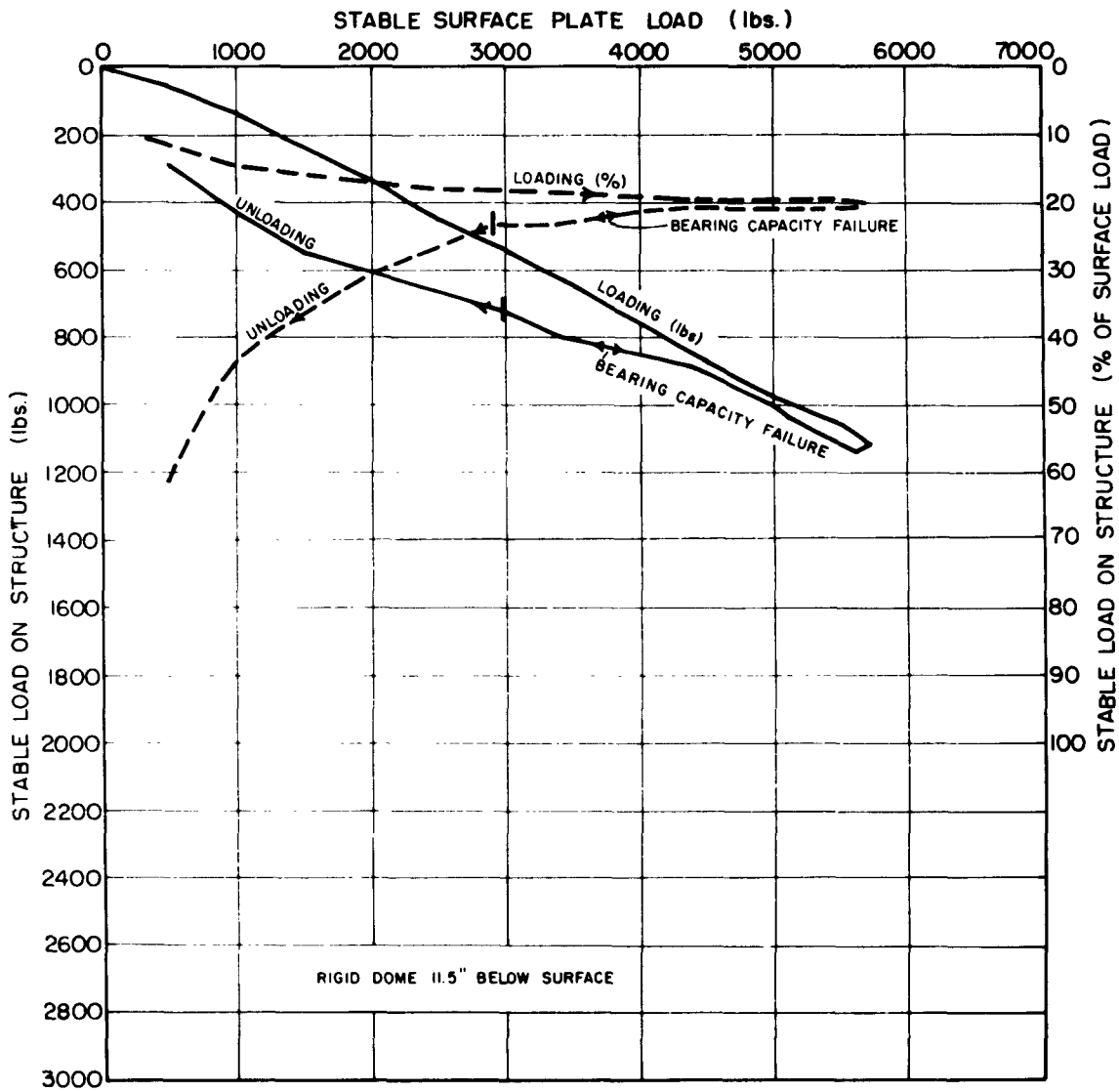

FIGURE C-32 LOAD ON STRUCTURE: TEST PB-9

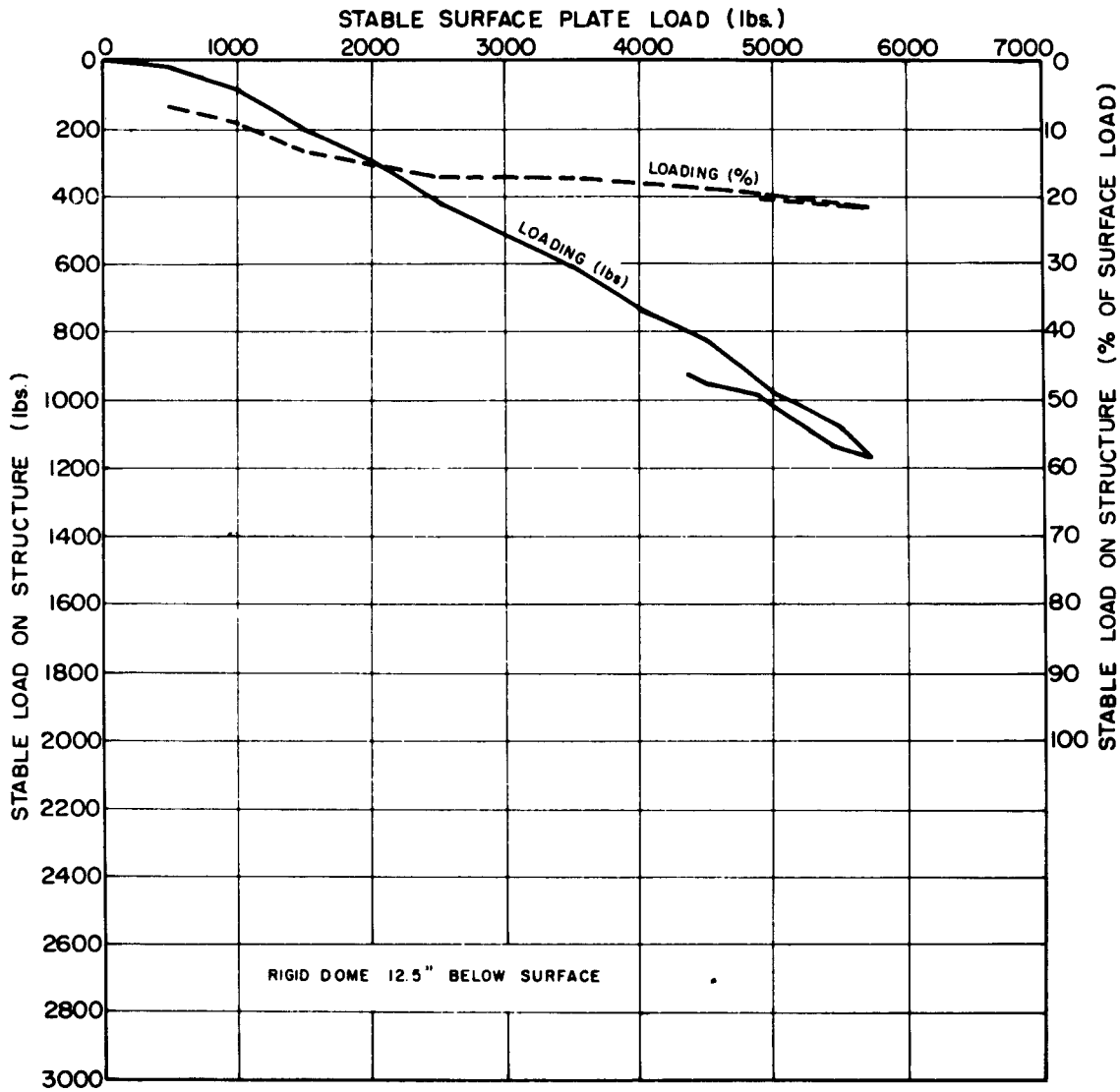

FIGURE C-33 LOAD ON STRUCTURE: TEST PB-10

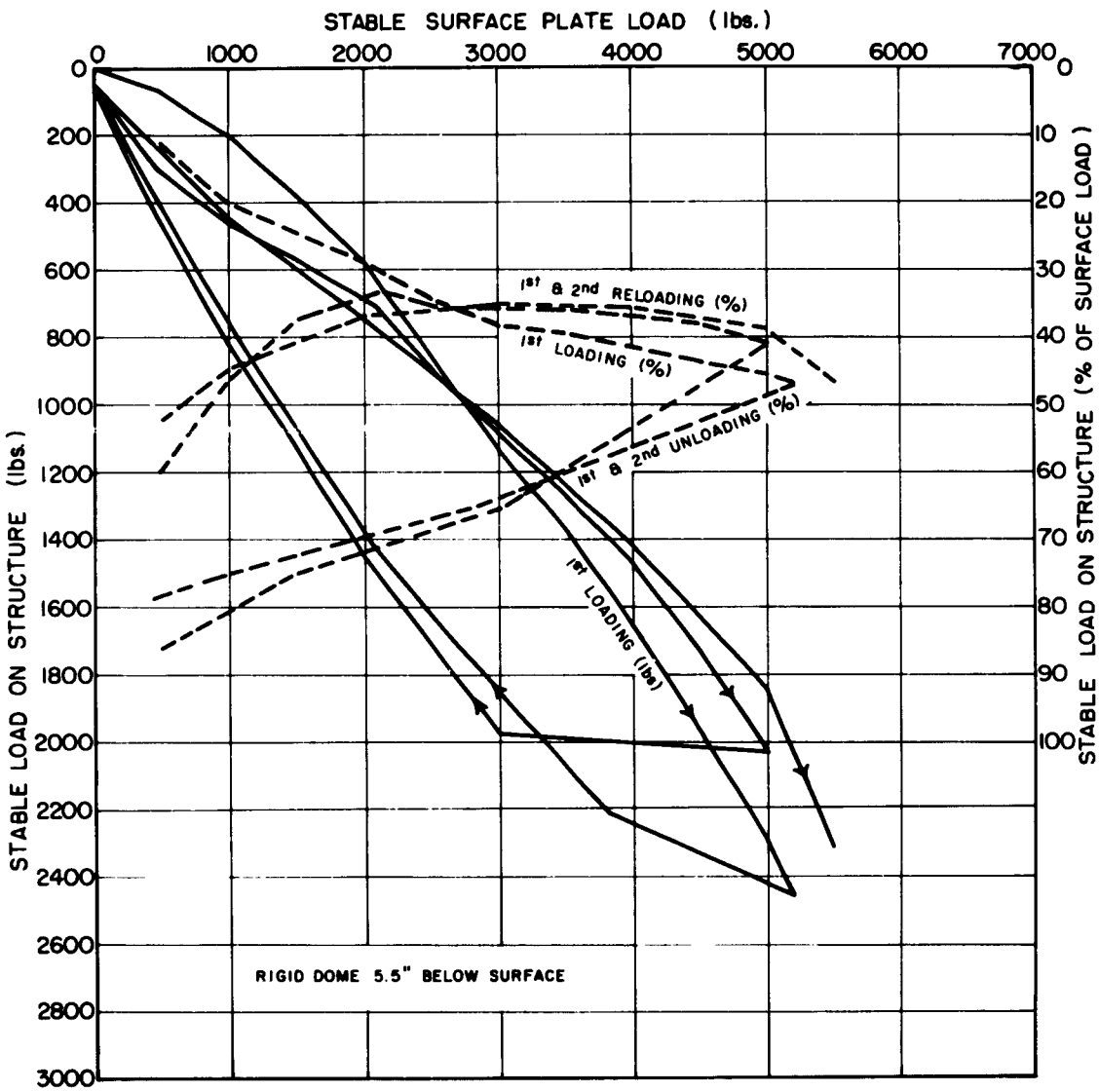

FIGURE C-34 LOAD ON STRUCTURE: TEST PB-II

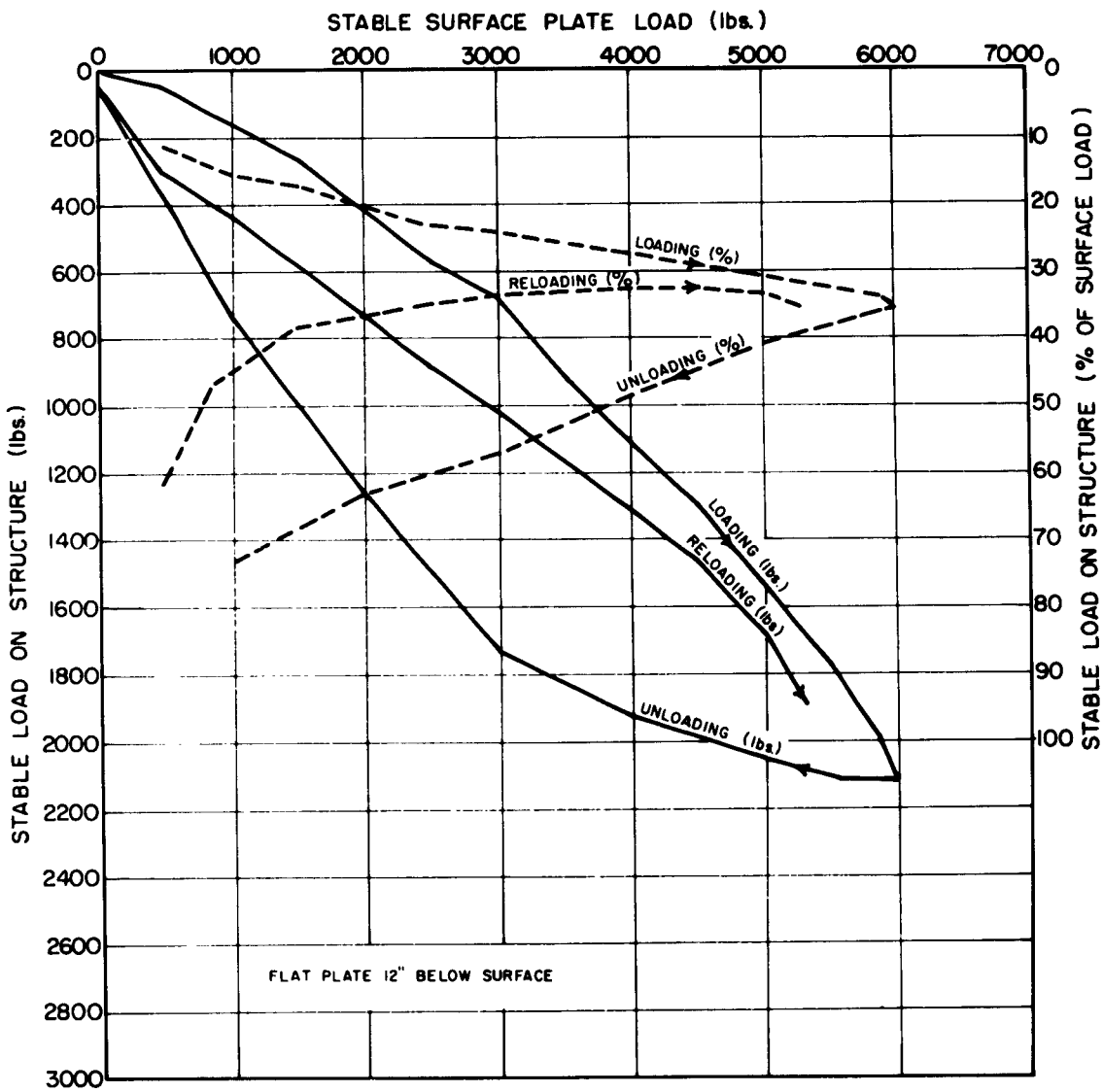

FIGURE C-35 LOAD ON STRUCTURE: TEST PB-12

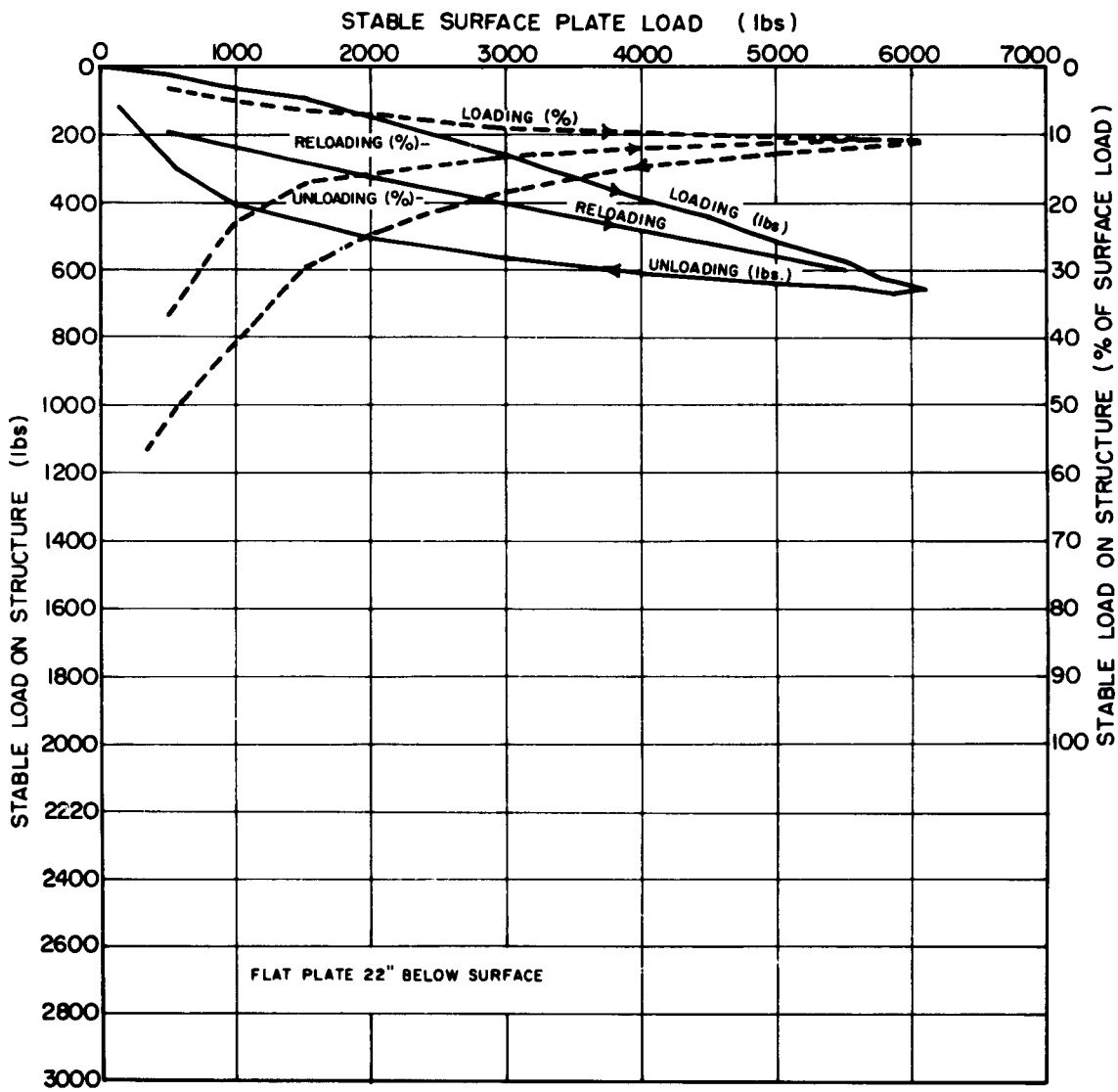

FIGURE C-36 LOAD ON STRUCTURE: TEST PB-13

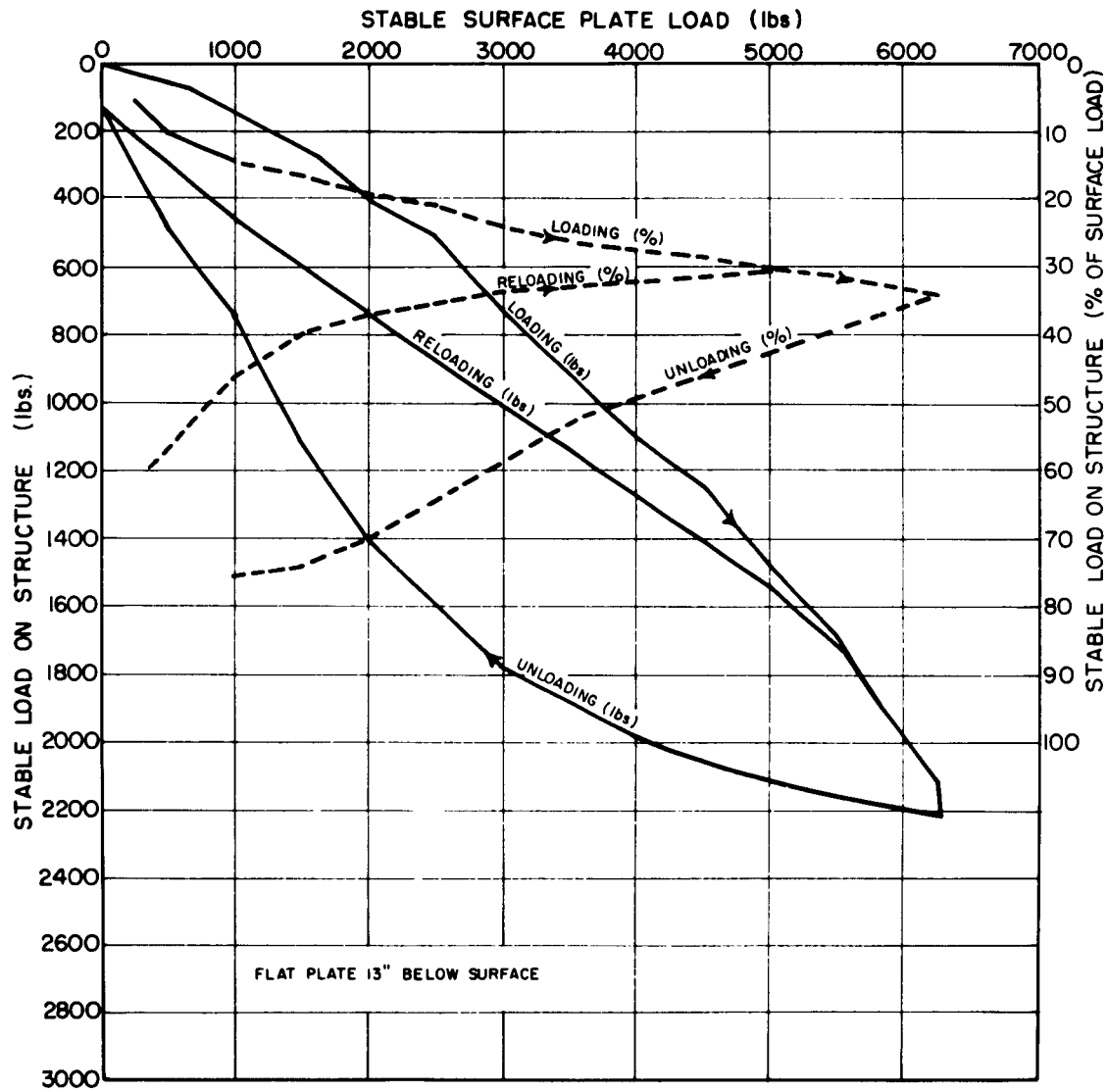

FIGURE C-37 LOAD ON STRUCTURE: TEST PB-14

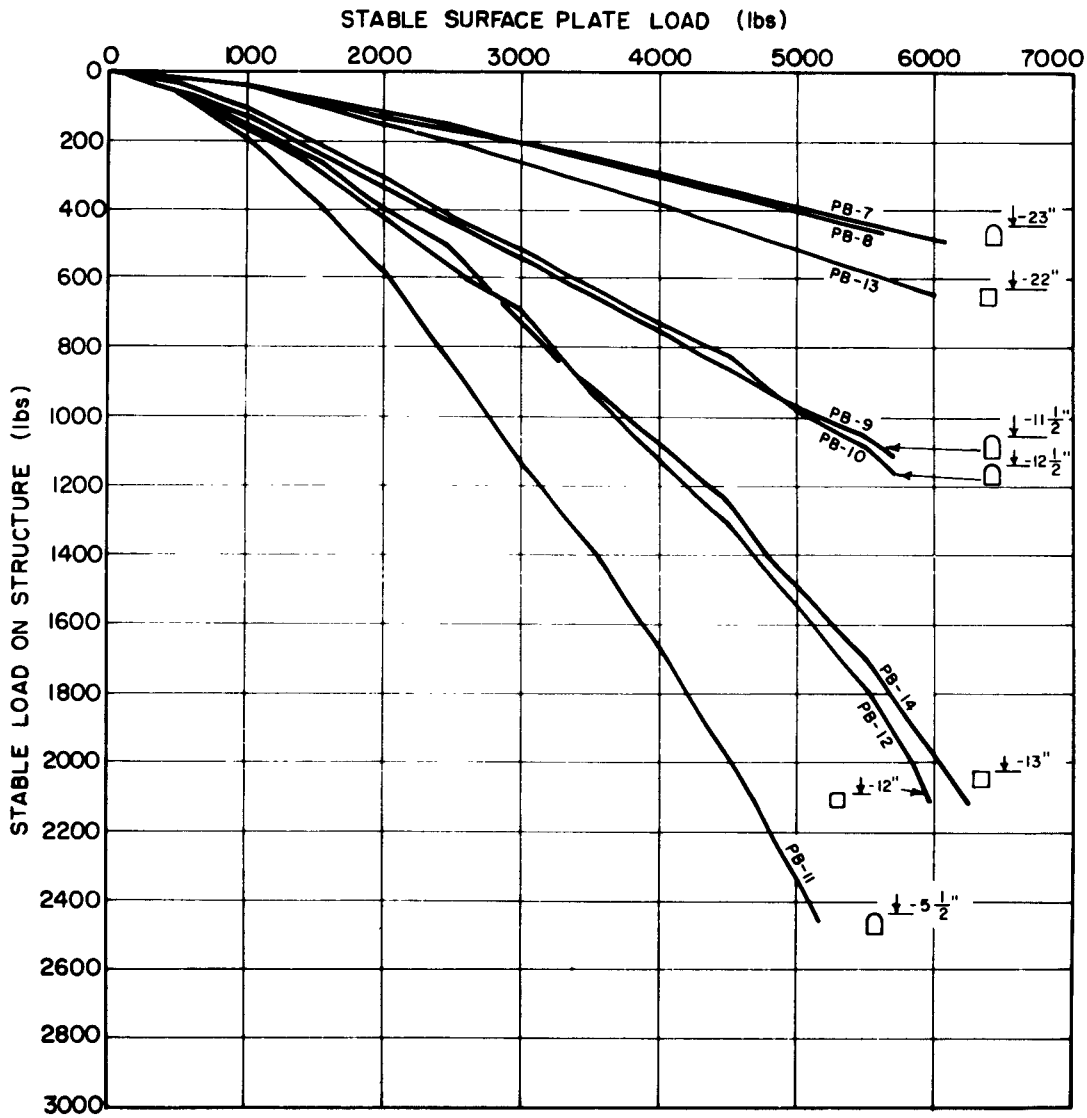

FIGURE C-38 COMPARISON OF LOADS ON STRUCTURES

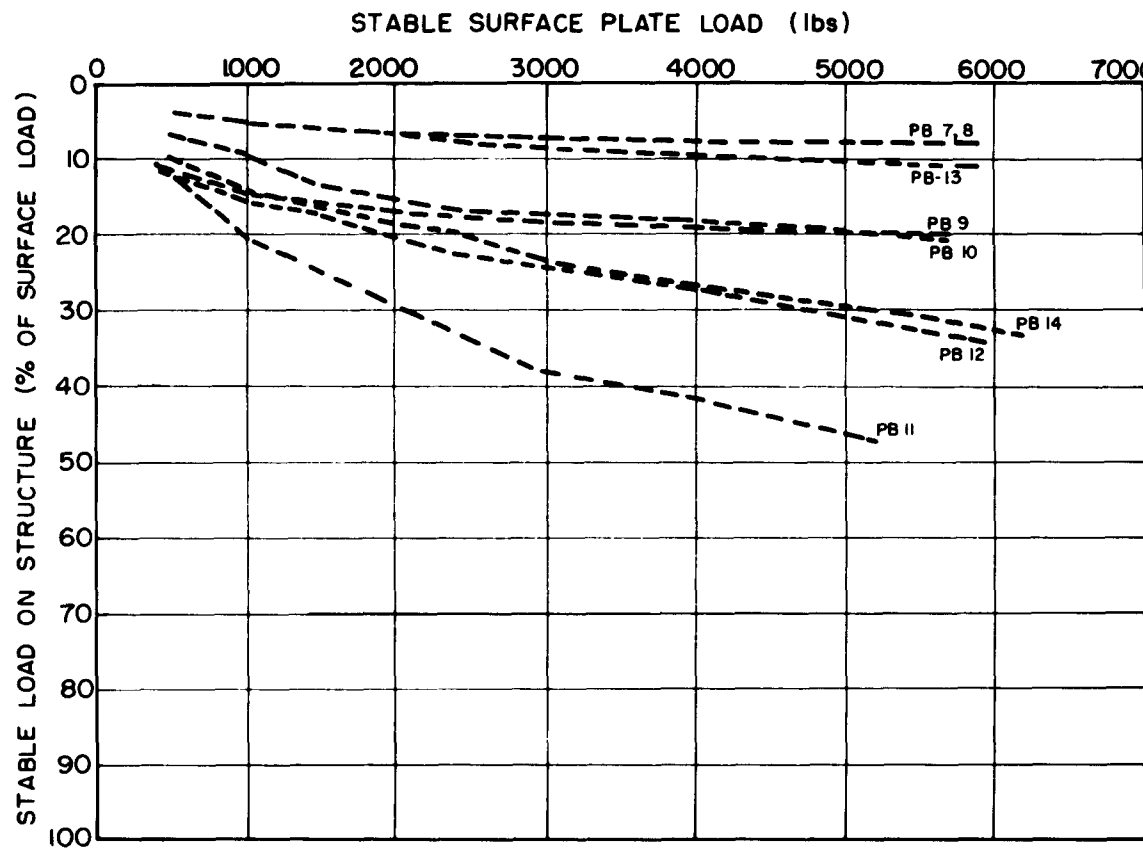

FIGURE C-39 COMPARISON OF PERCENTAGE LOADS ON STRUCTURES

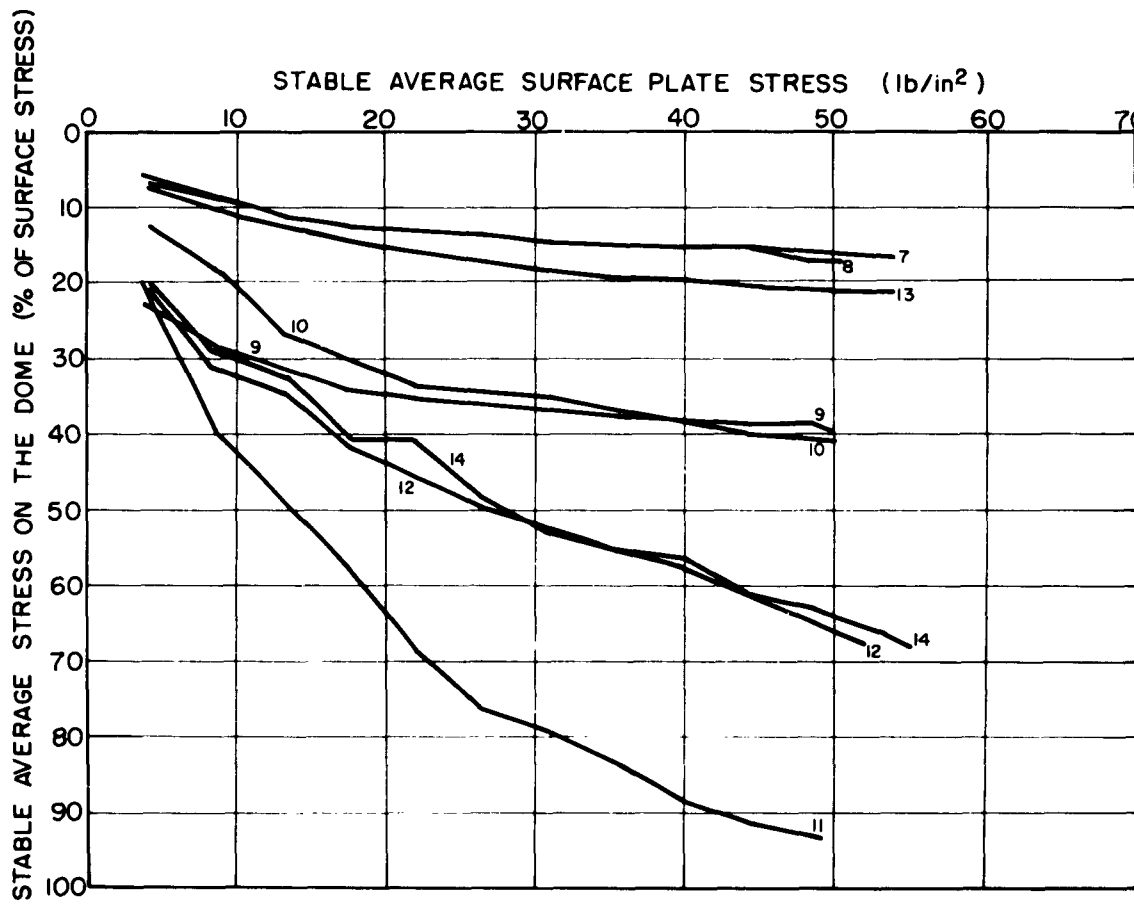

FIGURE C-40 COMPARISON OF LOADS ON STRUCTURES IN TERMS OF STRESSES

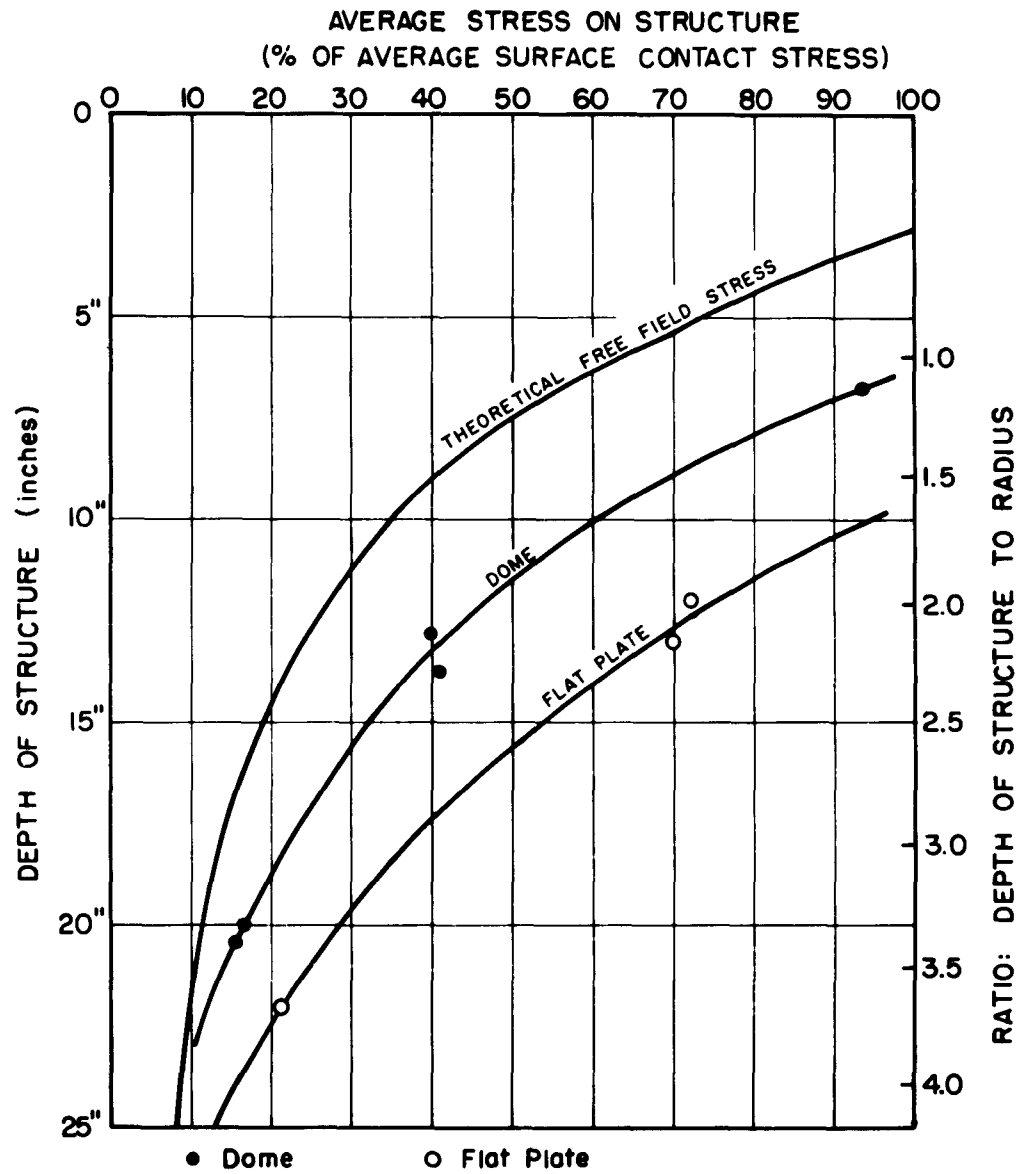

Depth: to the surface of the flat plate

Depth: to the center of gravity of the vertical projection of the dome surface (1.3" below the crown).

The theoretical curve is based on parabolic contact pressure distribution on the loading plate.

FIGURE C-41 STRESS ON STRUCTURE vs DEPTH

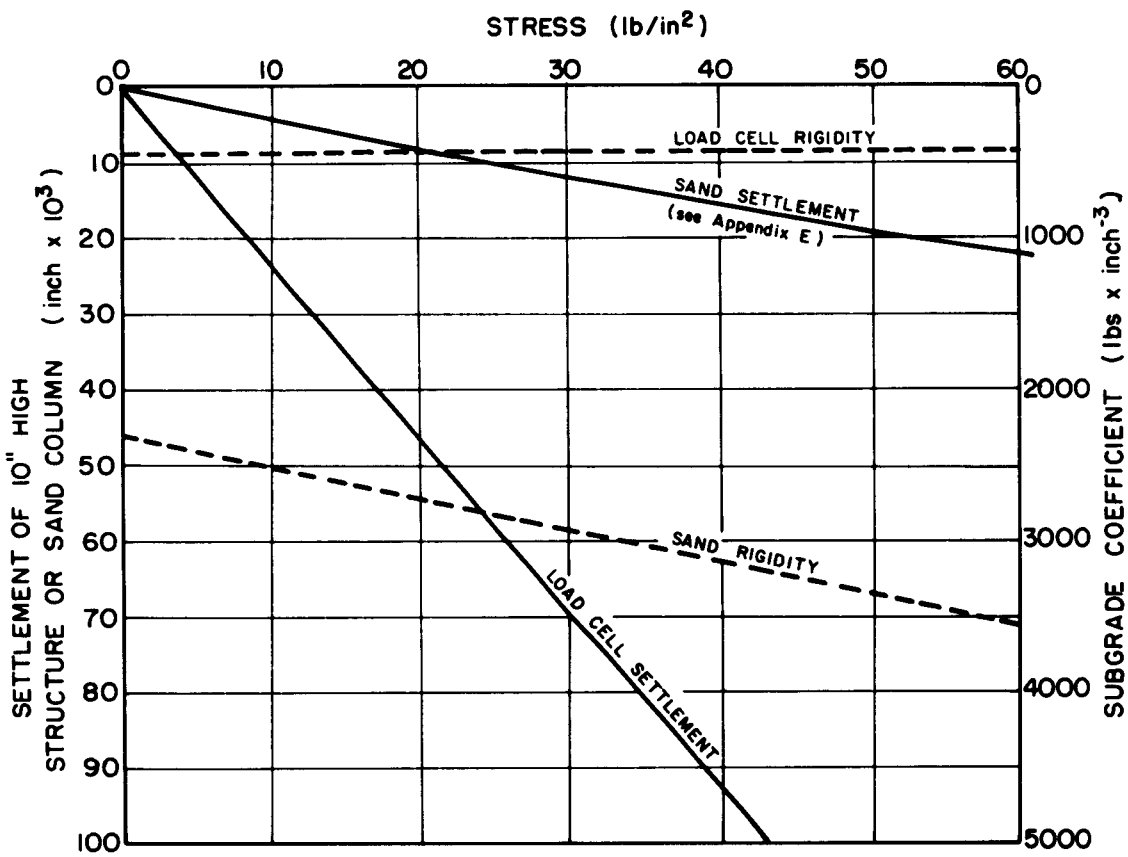

FIGURE C-42 SETTLEMENT AND RIGIDITY OF STRUCTURE AND EQUIVALENT SAND COLUMN

Appendix D

DOMES USED FOR BURIED STRUCTURE TESTS

CONTENTS

LIST OF FIGURES

Appendix D

DOMES USED FOR BURIED STRUCTURE TESTS

D.1 Introduction

This appendix describes the domes used for the buried structure tests, and describes the results of tests conducted to evaluate the behavior of the domes in the non-buried condition.

Selection of an appropriate small-scale structure was obviously a crucial step in the whole testing program. On one hand, it was essential that the structure could be fabricated in a reproducible way at reasonable cost; on the other hand, it was even more essential that the structure, when buried, fail under the action of surface pressures less than 300 lb/in^2. After some initial investigation, thin domes of aluminum were selected for this purpose.

D.2 Geometry and Properties of Aluminum Domes

Figure D.1 shows the dome in cross-section. These domes were segments of a 18 inch diameter full sphere, the central angle for the domes being $85^\circ \pm 2^\circ$. The domes had a base diameter of 12 inches and a rise of 2.5 inches. The wall thickness was 0.024 ± 0.001 inch. While it was possible to dent the domes by only moderate finger pressure, nonetheless the domes could easily be handled and transported with but a minimum of care.

The domes were made by a spinning process using aluminum 6061-0, and were afterwards heat-treated to relieve "worked-in" stresses. This aluminum has the following approximate properties:

$$f_y = 8{,}000 \text{ lb/in}^2 \text{ (defined at 0.2\% strain)}$$

$$f_{ult} = 18{,}000 \text{ lb/in}^2$$

$$E = 10 \times 10^6 \text{ lb/in}^2$$

The domes were supplied by a local machine shop.

D.3 Support Conditions

Two main requirements governed the design of the supporting detail: (1) it should be easily reproducible; and (2) the support preferably should not protrude on the outside of the circumference of the dome itself, since a protruding support would complicate the interpretation of the results.

As will be discussed later, it was hoped that valuable information concerning the soil-structure interaction could be obtained from measurement of strains in the domes. An attempt was therefore made to design a supporting detail which would allow only membrane stresses to exist. This was considered desirable because it would eliminate the necessity of attaching strain gages to both inside and outside surface of the dome. Gages on the outisde surface would create an irregular surface texture, which would further complicate the analysis. However, owing to practical difficulties, the idea of satisfying a "membrane-condition" along the support was abandoned, and the following supporting detail was chosen.

The dome was mounted on a 1 inch thick steel plate with a diameter of 12-5/16 inches: see Fig. D.1. The dome rested in a groove of 1/8 inch depth. The groove was filled with epoxy adhesive-sealant and the circumference of the dome was allowed to sink freely into the groove. Only very small stresses are believed to be built into the dome during this mounting procedure. The epoxy was strong enough to withstand the high contact stresses between the dome and the base plate without any crushing problem along the contact line.

This way of supporting the dome does give rise to local bending moments along the spring line. However, it may be shown that the attenuation of moments is very rapid: see for instance FLÜGGE (1962). Following a general bending theory for shells, it can be shown that these moments are insignificant above approximately 10° from the support of the domes used in this test program.

In the appendix of "Elementary Statics of Shells" PFLUGER (1961), the membrane stresses in a spherical dome are given for several different loading conditions. Fig. D.2 shows the distribution of membrane stresses in a spherical dome of constant wall thickness for three typical load distributions.

D.4 Buckling of Dome

D.4.1 Theory

According to the classical theory, the radial uniform, buckling pressure for a full sphere is equal to: (see TIMOSHENKO and GERE, 1961)

$$q_{CR} = \frac{2E}{\sqrt{3(1-\nu^2)}} \left(\frac{t}{R}\right)^2$$

where E = modulus of elasticity
ν = Poisson's ratio
t = wall thickness
r = radius of sphere

For a full sphere of the same material, radius and wall thickness as for the domes used in the described tests, q_{cr} is, according to this formula, 90 lb/in^2.* The fact that the domes were not full spheres, but only segments thereof, will not have any significant influence on this computed value: see TIMOSHENKO and GERE (1961). The critical buckling pressure is not very different if, instead of radial pressure, the dome experiences a loading of "snow-load" type distribution or a loading of a distribution as the "dead" weight of the structure itself: see FLUGGE (1962).

D.4.2 Previous experimental work

Experimental values do, however, not agree with the values obtained using the classical theory. Several investigators have studied this problem, and buckling pressures as low as 1/4 to 1/5 of the classic buckling theory value have been reported. The classic value quoted above is based on a linear, small-deflection thoery, and this may be the reason why experimental values are much lower than what the theory predicts. Imperfections of some kind (in geometry, etc.) will always be present. These give rise to "large" deflections, and a large-deflection approach should apparently be used in the analytical treatment of the buckling problem. Relatively little progress has been made in this area.

One of the most informative references on the subject of buckling of thin spherical domes is a paper by KLÖPPEL and JUNGBLUTH (1953). The authors proposed

*Computed for the hypothetical case that E remained constant equal to 10×10^6 lbs/in^2.

an empirical formula for the uniform, radial buckling pressure for a spherical dome. The formula gives satisfactory results for $400 < \frac{r}{t} < 2000$ and central angle bigger than 40° and less than 120°. This formula predicts a critical pressure for the domes used in this test program ($\frac{r}{t}$ = 374 and central angle 85°) of about 18 lb/in^2.

Before the domes were tested in a buried condition in the sand in the big pressure bin, it was essential to know their behavior unburied. Realizing how difficult it would be to predict this behavior accurately, it was decided that some simple experiments should be performed.

D.4.3 Testing apparatus

A cylindrical pressure chamber was designed, with a diameter of 14 inches and a height of 9.5 inches. The cylinder itself was made of plexi-glass with aluminum plates on top and bottom. The dome, glued to its baseplate as explained in Section D.3, was placed on the bottom of the pressure chamber. The chamber was filled with water; then the pressure was increased by compressed air until buckling occurred.

D.4.4 Results

Three domes were tested in the afore-mentioned way. Two of them buckled with a "dimple" startig to one side of the crown; one buckled symmetrically with a dimple starting at the crown. They all collapsed at about 25 lbs/in^2 ($\pm$2 lbs/in^2). This is in fair agreement with the value predicted by Klöppel and Jungbluth. Figure D.3(a) shows a picture of one of the collapsed domes.

One additional test was run in the pressure chamber. This time, sand of the same kind as was used in the big pressure bin was placed around the dome, until the sand surface was 2 inches above the crown of the dome: see Fig. D.4. On top of the sand was placed a 4.5 inch thick layer of steel punchings. Then the chamber was filled with water.

As in the other tests described in this section, the pressure was then applied to the dome through the

water by means of compressed air. Thus, the only difference between this test and the other tests in the chamber was that the dome now had some restrainment. The submerged weight of the sand and steel punchings caused an effective stress of approximately 1 lb/in^2 in the sand surrounding the dome. Under these conditions, the dome buckled when the pressure in the chamber was 37 lb/in^2; see Fig. 3(b).

With only a single such test, one must of course be very careful in drawing any conclusions, especially in view of the complexity of an instability problem. However, the test does indicate that even the small restrainment the sand provided under the described conditions was enough to increase the buckling resistance of these domes substantially.

References

FLUGGE, W., 1962: "Stresses in Shells," Springer-Verlag, Berlin, Gottingen, Heidelberg

KLÖPPEL, K. and JUNGBLUTH, O., 1953: "Beitrag zum Durchschlagproblem dünnwandiger Kugelschalen," der Stahlbau, June

PFLUGER, A., 1961: "Elementary Statics of Shells," English translation by Ervin Galantay, F. W. Dodge Corp., New York

TIMOSHENKO, S., and GERE, J., 1961: "Theory of Elastic Stability," McGraw-Hill Book Co., New York

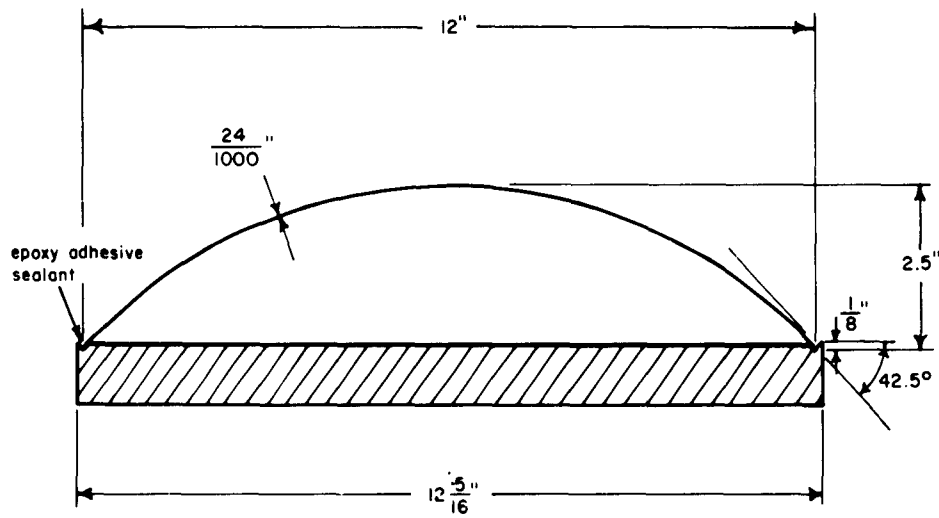

FIGURE D-1 THIN ALUMINUM DOME MOUNTED ON STEEL BASE PLATE

A: Uniform, radial pressure, intensity p

B: "Snow-load" type pressure distribution, intensity p (per unit area of horizontal projection)

C: Distribution like the dead weight of dome itself, unit weight p

$N\phi$ = meridional stress-resultant; $\sigma_\phi = \frac{N\phi}{t}$

$N\theta$ = latitudinal stress-resultant; $\sigma_\theta = \frac{N\theta}{t}$

– = compression

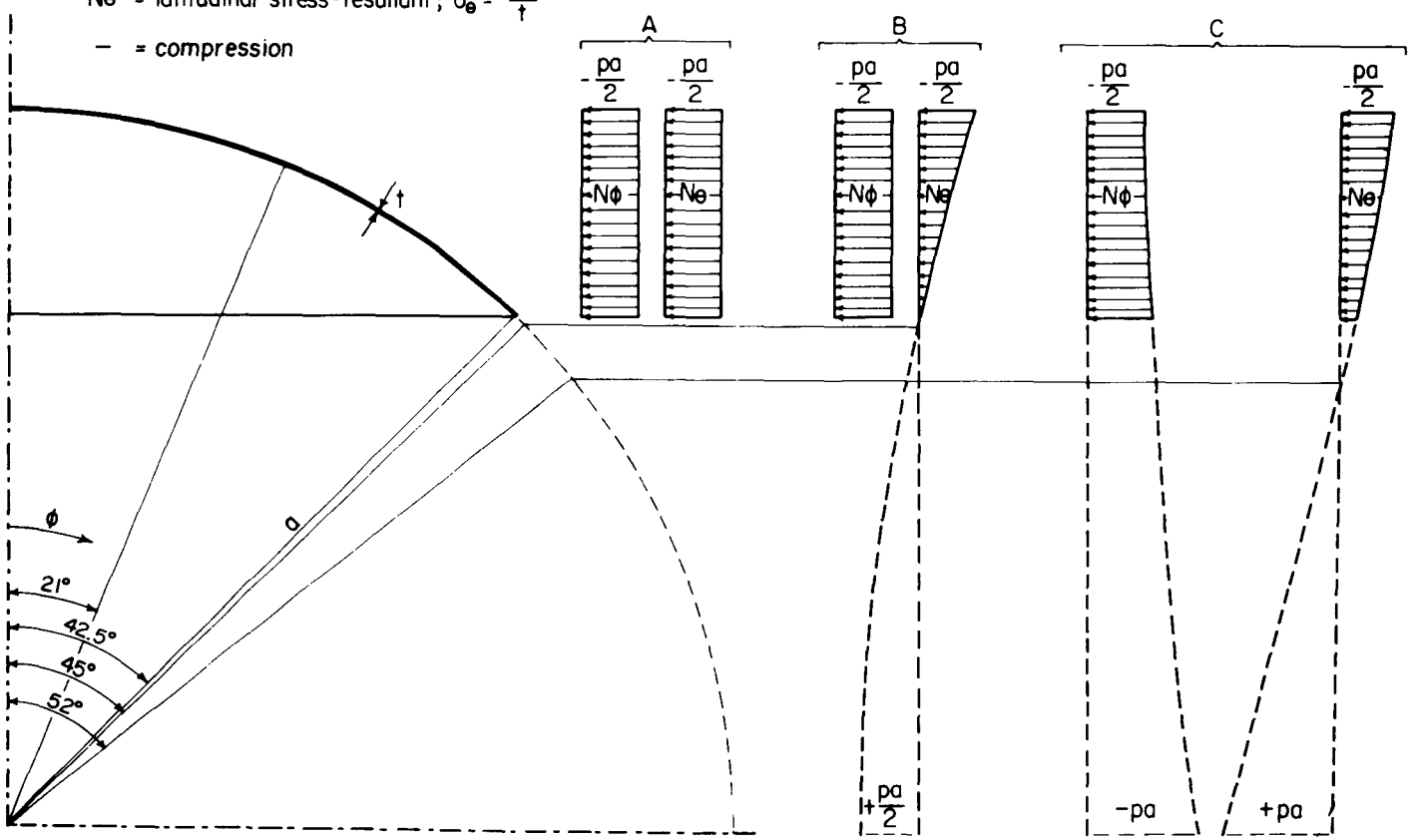

FIGURE D-2 MEMBRANE STRESSES IN A SPHERICAL DOME FOR 3 DIFFERENT LOAD DISTRIBUTIONS

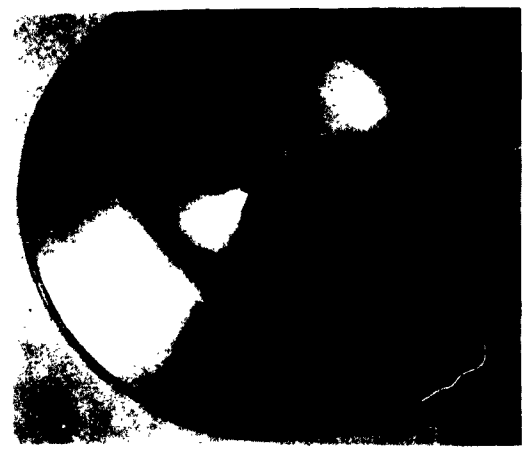

(a) Dome buckled under water pressure

(b) Partially restrained dome, after collapse at 37 lb/in^2

FIGURE D-3 PHOTOGRAPHS OF BUCKLED DOMES

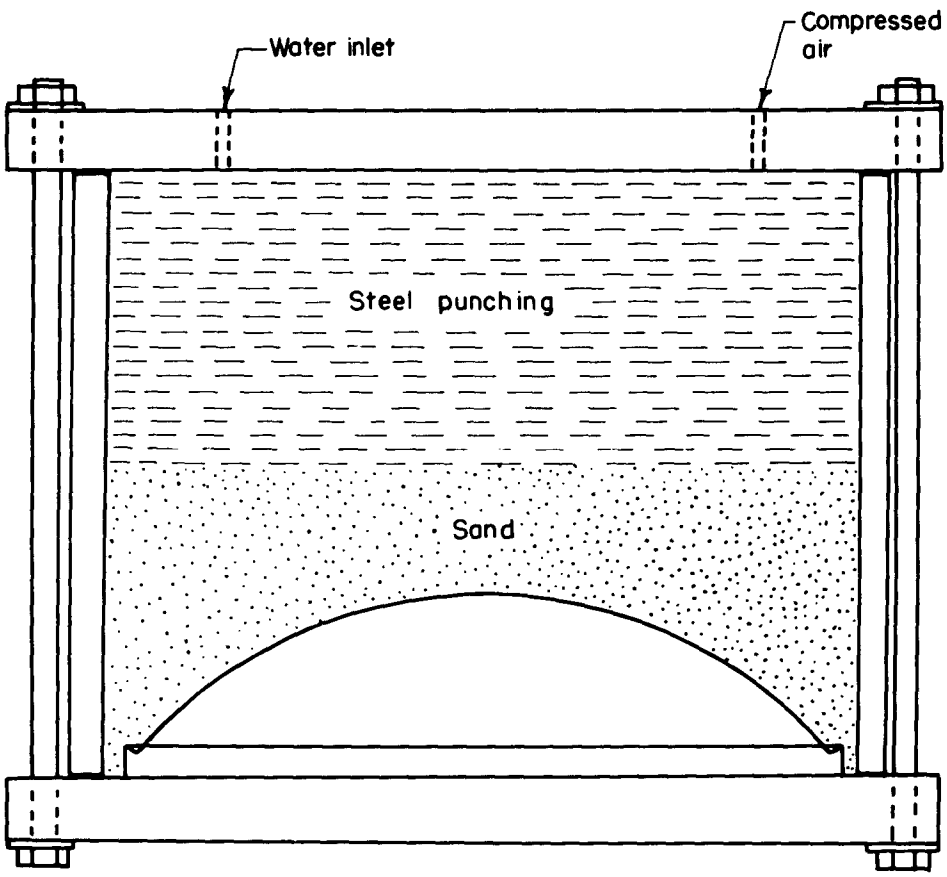

FIGURE D-4 TEST WITH SURROUNDING SAND

Appendix E

TESTS UPON BURIED DOMES

CONTENTS

LIST OF TABLES

LIST OF FIGURES

Appendix E

TESTS UPON BURIED DOMES

E.1 Test Program

The specific variables studied in the test series were: density of sand, flexibility of structure foundation, and depth of burial. The test program is summarized in Table E.1. Foundation flexibility was introduced by insertion of a cork layer beneath the dome.. Two preliminary tests served to indicate the magnitude of the vertical force reaching the dome and the load at which the dome would yield. Tests 3 and 4 were duplicates save for the detail of the load cell arrangement under the structure. Tests 6 and 10 were duplicate tests.

E.2 Apparatus and Instrumentation

The general arrangement of the buried dome and associated instrumentation is shown in Figure E.1.

E.2.1 Description of load cell

The load cell with its dimensions is shown in Figure E.2. The whole unit was made of aluminum 6061-T6. Eight SR-4 gages were attached to the wall of the thin, hollow cylinder at mid-height. Four of them were oriented vertically, 90^{o} apart, four of them horizontally, also 90^{o} apart. They were connected to form a complete bridge circuit. Thus, undesired bending effects (due to accidental eccentricity in loading on the load cell) and temperature effects were compensated. This closed external bridge circuit was connected to a Baldwin SR-4 strain indicator.

The load cell was calibrated up to 15000 lbs. It was recalibrated twice during the period of the test program; the readings were reproducible within 100 lbs. A load of 100 lbs. on the load cell corresponded to 18 micro-inches on the strain indicator.

Around the load cell was a 3/8 inch thick steel cyliner. This cylinder had two purposes; it protected the load cell, and it prevented sand from entering in under the base plate of the dome. For the first test, Test 3, the cylinder had an outside diameter of only 8-5/8 inches. However, this arrangement was not satisfactory, as it was impossible

to place sand properly in the zone under the edge of the dome. This detail influenced the test results, and data from Test 3 are generally omitted in the analyses which follow. For all the remaining tests a cylinder with an outside diameter of 12-5/16 inches was used.

E.2.2 Measurement of structure deformation and movement

Eight SR-4 strain gages were mounted on the inside surface of each dome. The location and orientation of the gages are shown in Figures E. 3 and E. 4. As may be observed, the location pattern of the gages changed somewhat during the course of the test series. However, most of the locations were kept the same so as to have a basis for comparison between the tests. In Tests 4 and 3 (not shown) three strain gages were purposely located very close to the spring line to detect the first signs of yielding in this critical region. However, such measurements were not necessary in later tests, because a sudden increase in the measured crown deflection clearly showed up when yield along the spring line occurred. Therefore, from Test 5 and on, these three gages were moved up from the support to get out of the region which was disturbed by the moments caused by the restrainment along the support (see Appendix D, Section D. 3). Still the gages closest to the spring line, Gages 7 and 8, were probably influenced somewhat by these moments.

The deflection of the crown of the dome was measured by a dial gage located on the concrete floor under the pressure bin. The stem of the gage was elongated up through the load cell (see Figure E. 5). In addition, one dial gage recorded the movement of the bottom flange of the load cell, in all tests except Tests 4 and 5.

One serious disadvantage in the equipment was encountered during the test program. The nature of the movement of the foundation of the dome (and as will be discussed, also the nature of the sand movements) was complicated by a nonuniform deformation of the bottom plate in the pressure bin. These deformation movements could unfortunately not be controlled without making major changes in the equipment; a step which was not feasible owing to time limitations. A further explanation of the problem is required, because it is important for the interpretation of some of the results which are given later.

A careful examination of the loading frame revealed that the I-beam grillage under the pressure bin did not have a perfect seating

on the concrete floor. As the I-beams were connected to the tension bars, some of the beams were apparently lifted up from the floor. This accidental clearance between the beams and the floor was small, but still significant. A consequence of this clearance was that when the tension bars were stressed, and the ends of the I-beams were deflected upward, the center portions of the beams would move downward. The deflection of an I-beam of this size for the pressures encountered is a small amount, but still very significant when one compares it with the total crown deflections of the domes as recorded in Section E. 4. 2.

In between the top flanges of the I-beams and the bottom plate of the pressure bin was a thin layer of gypsum to give the plate a good seating. The free distance between the flanges of the I-beams was 5. 5 inches (see Figure E. 5). This situation gave rise to small transverse deflections of the bottom plate. However, these deformations were not of as great concern as the longitudinal deflections mentioned in the preceding paragraph. As the free span of the bottom plate between the flanges of the I-beams is no more than 5. 5 inches, it is assumed that the sand above about 5-6 inches from the bottom plate would not be significantly influenced by these local bending deformations. In addition, arching action minimizes the transverse bending.

When the problem with the deflections of the bottom plate was realized, two additional dial gages were put in under the bin to record these deflections. The number of gages was limited to two because of practical difficulties involved (see Figure E. 5). The gages located under the bin were read by lying flat on the floor, observing the movements through holes in the templates connecting the tension bars.

Sections E.4.2 and E. 4. 3 present the results from the crown deflection measurements. Section E. 4. 3 contains a discussion of the significance of the problems described in the preceding paragraphs.

E. 2. 3 Measurement of movements within the sand

The movements within the sand were measured by settlement gages designed for this series of tests. A detailed sketch of the device is shown in Figure E. 6. The cylinder was filled with colored water. The movement of the settlement plate was transferred by the rod to the piston. The movement of the piston caused a change in

length of the water column in the plastic tube located outside the bin. A movement of 1/1000 inch of the piston, caused a change in length of the water column in the tube of 173/1000 inch. The metal pipe leading from the cylinder, along the bottom plate and out through the wall of the pressure bin, was rigid so its deformations under the pressure in the bin should be of no concern. (That this was the case, was proven by actually stepping on the tube.) The base plate of the device rested on the bottom plate of the pressure bin and could be leveled by three leveling screws.

Two, and in the beginning three, cylinders were connected to a common base plate. This was done to eliminate any differential movements of the settlement plates caused by local deformations of the bottom of the pressure bin; i. e. transverse bending of this plate.

The sand movements were measured at several different locations within the sand. Most of the settlement plates were located in the vicinity of the structure. In the early tests, some were also placed close to the wall of the pressure bin to investigate the influence of the presence of the wall on the sand movements in the bin. (Some comments on the problem of wall friction will be given in Section E. 4. 5.) The settlement plates were screwed on to the top of the rods as the bin was filled with sand. Thus, the formation of loose pockets of sand under the plates was prevented.

In Test 4, there were 14 settlement plates, in Test 5 only 7. All the other tests involved 12 plates. Figure E. 7 shows the location pattern with 12 settlement plates.

E. 3 Test Procedures

The time schedule for a typical test is given in Table E. 2. The surface pressure was applied in increments of 10 lbs/in^2. Readings were taken with shorter intervals in the neighborhood of the yielding pressure of the domes. For each increment the following data were collected: load on load cell, strains in the dome, crown deflection, and sand movements.

The tests were terminated when it was felt that nothing more of significance could be learned by increasing the surface pressure further. It was found desirable to have a visual inspection of the dome before it was deformed excessively. Unfortunately, in Test 7, the pressure bag punctuated. No permanent deformation of the

dome had as yet occurred, and the test was recycled. The problem with the recycling test was of course that the sand density had changed somewhat due to the first loading.

E. 4 Results

The main results are presented in the graphs and tables referred to in this section.

E. 4. 1 Loads upon domes

Figure E. 8 shows the average vertical pressure on the dome as a function of the applied surface pressure. Here the average pressure on the dome is computed as:

$$\frac{\text{Total thrust to the foundation of the dome.}}{\text{Area of base plate of dome.}}$$

Figure E. 9 shows the ratio between the average pressure on the dome and the applied surface pressure, plotted as a function of applied surface pressure. Figures E. 10, E. 11, E. 12 and E. 13 show the average pressure on the domes in Tests 4, 5, 7 and 9 respectively, when they were unloaded and reloaded again.

In unrestrained condition, the buckling pressure of the domes had been found to be about 25 lbs/in^2 (see Appendix D, Section D. 4). In none of the tests on the domes in buried condition did buckling occur, * even though the external pressure felt by the domes exceeded 25 lbs/in^2 by far. The sand provided sufficient restraint to prevent instability under all the different conditions investigated in this series of tests.

When the average pressure on the dome reached approximately 70 lbs/in^2, the dome failed along the support (see Figure E. 14(a); a discussion of this type of failure is given in Section E. 5. 3). A sudden increase in the crown deflection was recorded, and simultaneously the pressure felt by the dome decreased significantly (see Figure E. 8). After this support failure had occurred, the dome became much more flexible than before, and each increment in applied surface pressure gave from now on a considerably smaller pressure increment on the dome.

*See comments on plastic buckling in Section E. 5. 3.

E.4.2 Deformation of domes

Table E.3 gives the strains as they were recorded at different points on the dome as the surface pressure was increased.

Figure E.15 presents a comparison of meridional strains in the domes in the different tests. These are the strains 21^{o} up from the support (see Figures E.3 and E.4 for location of strain gages). The strains have been plotted as a function of applied surface pressure. Figure E.16 gives the same strains as Figure E.15, but they are plotted here as a function of average pressure on the dome. Figure E.17 compares the latitudinal strains in the domes, 21^{o} up from the support, in the different tests. In all these three figures, only strains within the approximately linear region of the stress-strain diagram for the aluminum are plotted.

Figure E.18 gives the crown deflections as a function of applied surface pressure. It should be remembered that these deflections are the total deflections due to deformation of the dome itself plus deformation of the foundation upon which it is resting. Figures E.19, E.20, E.21 and E.22 present the crown deflections of the domes in Tests 4, 5, 7 and 9, respectively, when the sand mass was unloaded and reloaded again.

Whereas there was no direct measurement of the deflection of the crown of the dome relative to its base plate, this deflection may be inferred from the test data. Up until the sudden jump in the load-movement curves of Figure E.17, the movements are primarily the result of seating errors in the structure-load cell stem. The elastic crown deflection can be computed according to theory (FLÜGGE, 1962) and is found to be approximately 4/1000 inch for an average vertical pressure on the dome of 30 lbs/in^2. As may be noted, this is a very small deflection compared to the total crown deflection. The magnitude of the sudden jump indicates the relative movement between crown and base plate as the result of yielding at the support. This magnitude varied widely between the different tests. In Test 4, this deflection only amounted to about 1.5% of the initial rise of the dome, while in Test 10 this number was considerably higher; about 9%. In Test 5, it was about 3.5%, in Test 8, about 5%. In Test 9 it was about 4% (but as may be seen from the deflection curve, the deflection increased also very rapdily after the sudden yielding had taken place). In Test 7 no yield occurred before the air bag punctured, while the dome in Test 6 collapsed completely (see

Figure E. 14(b)). The behavior in Test 6 will be discussed further in Section E. 5. 4.

E. 4. 3 Deflections of structural system

Section E. 2. 2 has mentioned the movements of the bottom in the pressure bin. Since crown movements were measured relative to the concrete floor, whereas the sand movements were measured relative to the bottom plate of the bin, the deflections of the structural system were the cause of considerable concern. Using the deflection measurements that were taken, this section will try to evaluate the influence of these deflections upon the other data obtained in the tests.

As shown in Figure E. 5, 2 dial gages were located very close to each other under the center of the bin. One gage recorded the movement of the bottom flange of the load cell, the other recorded the movement of the bottom plate in the pressure bin. The diameter of the flange of the load cell was 8 inches, and the distance between the flanges of the I-beams was 5. 5 inches. Therefore, if the bottom flange of the load cell rested directly on the bottom plate of the bin, the flange of the load cell should move the same amount as the flanges of the neighboring I-beams (neglecting any minute bending deformation of the load cell itself). In Tests 9 and 11, where the load cell was in direct contact with the bottom plate of the bin, the two dial gages recorded the same movements.

Therefore, as mentioned in Section E. 2. 2, the transverse bending-deformations of the bottom plate between the I-beams were apparently insignificant. This situation seemed at least to be true in the central region of the bin. A dial gage placed 17 inches from center (see location on Figure E. 5) did not record the same deflections from test to test. Compared to the gage under the center of the bottom plate, it gave higher values in two tests (about 40%) and lower values in three tests (about 30%).

To sum up: the deflection of the bottom plate of the pressure bin constituted a sizable part of the total crown deflection of the domes. The bottom deflections were not the same in all tests, and the magnitude varied over the bottom area. In the subsequent comparisons between the movements of the sand and of the crown deflection (see Section E. 5. 2), it will be assumed that the center region (say, diameter 1. 5 ft.) of the bottom plate moved like a "rigid plateau" (see Figure E. 23). The transverse deflections of the bottom plate between

the I-beams and the longitudinal bending deflections of the I-beams, were thus neglected. While the data are not sufficient to prove the validity of this assumption, they likewise do not indicate an alternate assumption. It should be noted that this assumption has only significance as far as the evaluation of the information given in Figures E. 34, E. 35 and E. 36 is concerned. All other results presented are based on direct measurements.

The total deflection of the crown of a dome consisted of four contributions (see Figure E. 24):

(1) Deformation of dome itself.

(2) Deformation of load cell plus any movement in the connection between base plate of dome and top flange of load cell. (This base plate was never disconnected from the load cell during the period of the test program.)

(3) Deformation of 1/8 inch cork layer (if present).

(4) Movement of the bottom plate of the pressure bin.

To give some idea of the relative magnitudes of these contributions, Figures E. 25 and E. 26 have been prepared.

E. 4. 4 Movements within the sand

Table E. 4 gives the sand movements at different depths and distances from the center line of the bin, as a function of applied surface pressure. Figures E. 27, E. 28, E. 29, E. 30 and E. 31 show the sand movements in Tests 4, 6, 8, 9 and 11 plotted as a function of applied surface pressure. It is interesting to note the "jumps" in the settlement curves. As the domes yielded along the support, a pressure increment was suddenly thrown over to the surrounding sand.

The discrepancies between the number of installed settlement plates and recorded points is due to leakage problems. However, as experience was gained in the use of the gages, they were found to work very satisfactorily.

E. 4. 5 Pressures within sand mass

Two tests were carried out with WES pressure cells (6 inch diameter) placed within the sand mass.

One objective of the first of the preliminary tests was to see if there was any effect upon pressure distribution from side friction at the walls of the bin. Two cells were placed 10 inches from the wall, and two other cells were located 22 inches from the wall. All of these cells rested directly on the bottom of the bin. The measured pressures were all less than the applied surface pressure, and the actual magnitude of the pressure bore no relation to the location of the gage. It seemed apparent that poor seating between cell and bin, plus bending deflections in the bottom plate of the bin, gave rise to arching around the pressure cells. Subsequently, it was concluded from the pattern of sand movements that there was indeed little effect of side friction.

A special test, with pressure cells embedded as shown in Figure E. 32, was carried out following the main program of tests. The sand mass was placed in a dense condition. The objective of this test was to get a feel for the uniformity of the pressure within the sand mass. The maximum scatter of the readings from the theoretical value was 25%. Some of this scatter of course comes from the problem of placing the cells, and the results shown were considered to be quite encouraging.

E. 5 Analysis of Results

E. 5. 1 Compressibility of sand

Based on the measured sand movements, one may compute the compressibility of the sand in the pressure bin. In doing this, one must realize that the sand movements in the immediate vicinity of the structure certainly are influenced directly by the deformation of the structure itself. Thus, for instance, one would get somewhat bigger movements in the sand for points close to the dome in tests with flexible foundation (see Section E. 1) than in tests with rigid foundation. To minimize this influence, the compressibility-computations are all based on sand movements recorded in points more than 12 inches out from the central axis of the bin. The strains given in Figure E. 33 are computed from the sand movements

in a zone between 12 inches and 20 inches from the central axis of the bin, and from a layer between 8 inches and 14 inches from the bottom of the bin (in Test 4 from a layer between 8 inches and 24 inches).

Figure E. 33 presents two curves, one showing the strains induced in the dense sand as a function of applied surface pressure, the other curve is for loose sand. In each case only an average curve is plotted. It is indicated on the diagram how much the results deviated from the average. Before one evaluates the results, it should be noted that even if the sand had been placed to the exact same density, there would have been differences in the strains induced in the different tests. This is due to the fact that the soil and structure interacts differently in the different tests, as has already been pointed out. Even if part of these differences have been eliminated by only considering strains in the sand in a region "far" from the structure, undoubtedly the behavior of the sand also in this region is affected by the presence of the structure. (Actually, of course, if one knew how big a region of the sand was affected, and to what extent it was affected, one would be much better prepared to attack the soil-structure interaction problem analytically.)

From the results presented in Figure E. 33, it may be fair to conclude that the compressibility of the sand in tests with dense sand agreed quite well from test to test. In the case of loose sand, the agreement between the two tests was also very good. The very big difference between the compressibilities of the loose and dense sand may easily be observed.

As mentioned under Section E. 3, it took 2 men 7 hours to place the sand (somewhat shorter time to place the loose sand than the dense sand). It would certainly have been possible to obtain even better uniformity than was the case in these tests by spending more time and controling the flow of sand into the bin more carefully. However, all together, the results from the penetration tests and also the sand movement measurements both in the dense and loose state indicated that the sand uniformity may be characterized as good.

The main use of sand movement data was to compare the compressibility of the sand with the flexibility of the structure. This is explained in Section E. 5. 2.

E. 5. 2 Arching prior to support failure

Figure E. 9 shows for each test the percentage of the applied surface pressure that was transferred down through the sand to the domes.

Except for the very early stages of the tests, all domes with rigid foundation experienced an average pressure which was from 90% to 120% of the applied surface pressure. This held true up to the pressures where the domes failed along the spring line. The dome in Test 11 experienced the highest pressures.

No satisfactory explanation can be given for the low percentages in the initial portion of the curves. It first seemed possible that this result was due to simply a misrecording of the applied surface pressure. As the pressure gage used for these experiments had to cover a range from 0 to 300 psi, a difference in the true and recorded pressure may have been as high as 2 psi. Of course a difference in 2 psi will greatly change the percentages computed for low surface pressures, while it has very little influence on the percentages computed for high surface pressures. However, by looking at the unloading and reloading curves for Tests 4 and 5 (Figures E. 10 and E. 11) one may observe that also the unloading produced much lower percentages for low surface pressure than for higher surface pressure. Therefore, simply a misrecording of the applied pressure is not believed to be the real explanation of this phenomenon.

The domes with flexible foundation imbedded in dense sand "felt" much lower pressures than the domes with rigid foundation. The curves for Tests 6, 7 and 10 in Figure E. 9 start out at approximately 50%. As the surface pressure was increased, the ratio decreased to about 30%. Notice that the dome in Test 8, which had a flexible foundation but was buried in loose sand, experienced pressures as high as 95% of the applied surface pressure.

Qualitatively, the trend shown by the results recorded in Figure E. 8 might have been predicted. However, quantitatively some of the information contained in this diagram was surprising, at least to the investigators. This will be made clearer by looking at Figures E. 34, E. 35 and E. 36. They were prepared to compare the compressibility of the sand with the flexibility of the structure which was buried in the sand. It should be emphasized that the

information given in these figures are not directly recorded results. The following paragraphs will explain how the curves were derived.

The crown deflection as recorded included the deflection of the bottom plate (see Figure E. 24). The sand movements as they were recorded were the movements of the settlement plates relative to the bottom plate of the pressure bin. In order to compare the crown deflection with the sand movements, the crown deflection was modified. From the recorded crown deflection was subtracted the deflection of the bottom plate at center of pressure bin. As explained in detail in Section E. 4. 3, the center portion of the bottom plate was assumed to deflect like a "rigid plateau" (see Figure E. 23). As has been pointed out, the exact magnitude of the correction is in doubt. The deflection of the bottom plate was not recorded in Tests 4. 5 and 6, and the deflections recorded in the later tests had to be used as a basis for correcting the results of these early tests.

Further, there were no measurements of sand movement at the level of the crown of the dome (11. 5 inches from bottom of pressure bin). The sand movements in Figures E. 34, 35 and 36 are based on the movements recorded 8 inches and 14 inches from the bottom of the pressure bin, and about 8 inches from the central axis of the bin.

Based on these comparisons it may be concluded that there apparently is no simple relationship between the degree of arching around a structure and the relative flexibility of the structure and the sand. By combining the information given in Figures E. 9, E. 34, E. 35 and E. 36, one may point out the following facts:

(a) A buried structure may be "quite a bit" more compressible than the sand it replaced, and still very little "positive arching" may occur (see Figure E. 34)

(b) By comparing the results from Tests 4 and 7, for instance, it may be stated that the flexibility of the structure in Test 7 was large "enough" compared to the compressibility of the sand to develop an appreciable arching effect, while in Test 4 it was not.

(c) Very little "negative arching" occurred when the structure was much more rigid than the sand

(see Figure E. 36).

(d) The ratio between the pressure felt by the dome and the applied surface pressure decreased as the compressibility of the sand decreased. This is particularly clear in Test 11. This phenomenon is counteracted in Tests 6, 7 and 10 by the fact that the cork foundation gets less compressible for higher strains. This is believed to be the reason why the curves from Tests 6, 7 and 10 in Figure E. 9 flatten at high surface pressures.

If one compares the movement of the crown of the dome relative to its base plate to the deformation of a sand column of length 2. 5 inches, (equal to the rise of the dome) one will find the following.

In the case of the dense sand the compressibility of the sand was smaller than the flexibility of the dome. The ratio between the two compressibilities will change rapidly as the surface pressure is increased, because the compressibility of the sand decreases and the modulus of elasticity of the aluminum in the dome decreases with increasing strain. The largest observed ratio of sand compressibility to dome "compressibility" was approximately one half.

In the case of the loose sand, the compressibility of the sand was much greater than the flexibility of the dome before yielding started along the support. The largest value of the compressibility was approximately 8; this ratio decreased as the surface pressure increased. The numbers quoted here are based on the measured compressibility of the sand (see Figure E. 33) and the computed deformations of the shell itself (FLUGGE, 1962).

E. 5. 3 Load required to cause support failure

The first two parts of this section contain a discussion of the way the domes might be expected to fail along the spring line and gives a prediction of the magnitude of pressure at which this might occur. Then, in the final two parts, the predictions are compared with the actual test results.

Assumed mode of failure: The combined stresses due to edge moments and meridional forces will cause the formation of a "plastic yield hinge" along the spring line. It is not truly a plastic hinge

because aluminum has no distinct yield point with a consequent yielding region where the stress stays constant, but for the following computations the stress-strain curve will be idealized and assumed to have a yielding region such as does mild steel. After this first plastic hinge has formed, the external pressure on the dome may be increased further with no (assumed) increase in the moment at this point. The pressure may be increased until a plastic hinge forms at the section experiencing the highest positive movements (approximately 4 degrees up from the spring line). Figure E. 37a gives a sketch of the situation along the support at this stage. This is still an over-all stable configuration as far as the whole dome is concerned. However, what may now occur is that the linkage between the spring line and up to the second plastic hinge (approximately a truncated cone) buckles, thus giving rise to a support failure similar to the one sketched in Figure E. 37a.

To compute the deformations of the dome as the pressure is increased, will necessarily be very difficult as soon as the strains in the aluminum increases beyond the point where the modulus of elasticity is constant. The local deformations along the support will constitute an increasingly greater part of the deflection of the crown of the dome.

Prediction of failure pressure: The following assumptions are made: (1) Full fixity along the spring line; and (2) Idealized stress strain diagram for the aluminum (see Figure E. 37b). The computations performed are for uniform, radial pressure on the dome. The nature of the calculations is sketched in the following paragraphs. Forces and moments are expressed in terms of the radial pressure p (p is in lbs/in^2).

By using a general bending theory (see TIMOSHENKO and WOINOWSKY-KRIEGER, 1959), one will find forces along the spring line of the dome of magnitude as given in Figure E. 38a. The moment in the meridional direction will "penetrate" into the dome as shown in Figure E. 38b. The plastic moment capacity of the wall cross-section of the dome in pure flexure is $M_p = Z\sigma_y$, where Z is the plastic modulus of a wall strip of unit width and σ_y is the yield strength of aluminum (assumed to be 12000 lbs/in^2). Thus M_p = 1.73 lbs. in.

The axial force to cause yield of section in pure compression is $N_y = A\sigma_y$, where A is the cross-sectional area of a strip of unit

width. Thus, N_y = 288 pounds.

The section is actually under a combination of axial force, moment and a neglible shear force. The interaction curves given by BEEDLE (1958) are used for the following computations. It is assumed that these curves may be used, even though the presence of the stresses in the latitudinal direction may have some influence on the capacity of the section.

For $p = 45$ lbs/in^2

$$\frac{M}{M_p} = \frac{0.022}{M_p} = 0.58 \qquad \frac{N}{N_y} = \frac{4.12}{N_y} = 0.65$$

This combination of moment and axial force will "exhaust" the capacity of the section, and it is therefore assumed that the first plastic hinge forms at this pressure, i.e. $p = 45$ lbs/in^2.

The second hinge will form when the combined effects of the positive bending moment (see Figure E.38b) and the meridional force reaches the ultimate capacity of the section. The additional pressure required to do this is $\Delta p = 20$ lbs/in^2, computed the same way as shown above. Therefore, the total pressure required to cause the formation of the second hinge is $(p + \Delta p) = 65$ lbs/in^2.

As mentioned in the introductory remarks concerning the assumed mode of failure, the section between the hinges may now buckle plastically. The strains in this region are high and the modulus of the aluminum has been greatly reduced. To predict at what pressure instability will occur is extremely difficult, and no attempt has been made to do this. The assumption concerning the idealized stress-strain diagram is far from realized, and any accuracy in predicting the failure pressure cannot be expected without approximating the stress-strain behavior more closely.

Based on these very approximate calculations, one might predict that the dome would fail along the spring line at a pressure somewhere around 65 lbs/in^2. As the ultimate strength of the aluminum is considerably higher than 12000 lbs/in^2, which was assumed for the idealized stress-strain curve, one would be inclined to think that the pressure may exceed this value somewhat, at the expense of big deformations, before the dome "gives in" along the support.

If one went through similar computations with a snow load type loading (see Figure D. 2), one would end up with a prediction of failure pressure close to the one computed above. The differences that arise due to these two different load distributions are small compared to the uncertainties in the analysis.

Observed yield pressures: The average pressure on the base plate of the dome required to cause failure along the support, varied between the different tests. In Tests 6 (see further comments on this test later in the section) and 10 the average pressure required was 60 psi. In Test 5 the pressure was as high as 82 psi, while the domes in Tests 4, 8 and 9 failed along the spring line for pressures in between these two extremes. The dome in Test 7, during reloading, "felt" an average pressure as high as 77 psi, and no support failure had occurred when the test was terminated.

It is hard to evaluate how significant these differences in failure pressure are. The variation may partly be due to properties of the domes themselves as they were produced. Also, the way in which the contact pressures between the sand and the domes were distributed, was not the same in the different tests (see later). This observation may explain some of the variation. However, if the failure took place the way it was described in the beginning of this section, a variation in pressure distribution should not significantly influence this type of failure.

The comparison between the predicted and actual failure pressure is very good. What is perhaps more important than this close (fortuitous) agreement is that the type of support failure that actually occurred agrees quite well with the assumed mode of failure. The instantaneous increase in crown deflection indicates that it was an instability type of failure. Based on the calculations which have been shown on the preceding pages, it may be concluded that it was no surprise that the domes failed along the edge when the average pressure was in the vicinity of 70 lb/in^2.

Backfigured pressure distribution: Having the information as to total load on the dome and strains in various locations on the dome, an attempt has been made to backfigure the distribution and magnitude of the contact pressures between the sand and the domes in the various tests. Figure D. 2 has given the stress distribution in a spherical dome of constant wall thickness for three different load distributions. Notice that the figure gives the membrane

stresses only. As has been already discussed in Appendix D, a membrane solution is valid for the major part of the dome. It is not an easy task to backfigure what the contact pressures may have been; many different load distributions give rise to similar strains in the dome. The discussion presented here suffers from the limitation of having data from only 8 strain gages. Practical difficulties in the instrumentation prohibited the use of any larger number. All the computations of stresses have been based on the strains given in Table E.3.

The contact pressures in Tests 6, 7 and 10 seem to have had a distribution which resembles quite well the distribution "B" in Figure D.2 (snow load type distribution). The meridional stresses were fairly constant over the height of the dome. The latitudinal stresses 21° up from the spring line were equal to about 0.7 times the meridional stresses at the same point. Assuming a snow load type distribution, the magnitude of the pressures were backfigured from the strains (see Figure E.39); the agreement between measured and computed values is quite good. Notice that all the tests (6, 7 and 10) had flexible foundations.

From Figure E.16, one may observe that the meridional strains 21° up from the spring line were considerably lower in Tests 4, 5, 8 and 9 than in Tests 6, 7 and 10 for the same average pressure on the dome. By comparing all the test results (Table E.3), one will find that a support failure did not take place until the strains had reached a value of something like 1500-2000 microinches per inch. The strains in the domes in Tests 4, 5, 8 and 9 were well below this level in the upper part of the dome at the time of failure. The conclusion is that while the contact pressures in Tests 6, 7 and 10 may have been uniformly distributed over the horizontally projected area, the pressure in the other tests had a marked concentration towards the spring line of the dome. All the tests (4, 5 and 9) had rigid foundations. The dome in Test 8 had a flexible foundation but it was buried in loose sand, and its behavior was much more similar (in all respects) to the domes with rigid, rather than flexible foundation.

A consequence of the concentration of contact pressures towards the spring line, was that the support of the dome failed long before the stresses in the remaining part of the dome were "excessive". As described earlier, (Section E.4.1) a relief of pressures on the dome took place when it "gave in" along the support; thus the upper

region of the dome never experienced excessive stresses. This was brought out most clearly in Test 4 (see Table E.3). The almost uniform stress distribution (in the meridional direction) which resulted from the contact pressures in the tests with flexible foundation (except Test 8), may have been the reason for the dramatic failure of the dome in Test 6. What happened in this test was that when the support finally failed, the stresses also in the upper region of the dome had reached very high values. The result was a complete collapse (see Figure E.14b). This may be characterized as a plastic buckling failure. Whereas it has been stated earlier (Section E.4.1) that buckling of the domes did not occur in a buried condition, it was here meant that instability did in no case prevent the mobilization of the strength of the material in the structure (as may be recalled, the domes buckled in unrestrained condition at a pressure of about 25 lbs/in^2, see Appendix D). The sand restrained the domes from buckling until the strains in the aluminum were so high as to decrease the modulus of elasticity significantly, and a plastic buckling occurred in Test 6.

The collapse of the dome in Test 6 was the main reason for performing a test under "identical" conditions, Test 10. The dome in Test 10 did not collapse, but the crown deflections caused by support failure was larger than in any other test..

E.5.4 Behavior following support failure

The instant the dome "gave in" along the spring line, the pressure carried by the dome decreased sharply. The magnitude of the deformation of the dome, as a percentage of the initial rise, has been given in Section E.4.2. Simultaneous with this relief of pressure on the dome, the strain in the surrounding sand suddenly increased. The strain increment was a result of the "pressure transfer" from the dome over to the surrounding sand. To satisfy static equilibrium, the sand had to carry the pressure of which the dome had relieved itself.

When the surface pressure was increased after the support failure had taken place, the rate of increase in pressure carried by the domes in Tests 4 and 9 was significantly smaller than before (see Figure E.8). Test 5 showed a similar behavior but not to that extent, while the dome in Test 10 "picked up" pressure faster after rather than before the support failed. It should be noted in this connection that Tests 4 and 9 both had much deeper cover of burial

than tests 5 and 10. The surface pressure was not increased after support failure in Test 8, and the dome in Test 7 behaved "elastically" until the end of the test. As was described in the previous section, the dome in Test 6 collapsed completely. It may be observed from Figure E. 8 that a small relief in pressure took place when this happened and was followed by a fairly rapid increase again. A few comments will be made to try to explain this behavior. Similar reasoning may be applicable to explain the behavior of the domes in Test 5 and 9 during reloading.

In Test 6 the deformations of the dome may have been so large as to impair the "arching action" of the sand. If the dome had given the sand above it some support (as in Test 4 for instance) the sand would have been more efficient in transferring the pressure from the projected area of the structure over to the surrounding sand. The result might have been a much lower pressure on the foundation of the dome than was the case when the dome deformed (buckled) to the extent it did. In Test 6, the sand structure above the dome partly collapsed; an inspection of the surface indicated that the sand had caved in somewhat, thus, it would seem, leaving regions of the sand unable to promote any "arching action". These observations point in the same direction as the results obtained by Terzaghi (1936) in his well known trap door experiments. It was shown that the pressure on the trap door was a minimum for a certain small downward movement of the trap door. If the movement was increased beyond this optimum amount, the pressure on the trap door increased again. It should be kept in mind that Terzaghi's experiments were performed with no overpressure on the sand surface.

Figures E. 10, E. 11, E. 12 and E. 13 show the results from the tests which were unloaded and reloaded. Except for the dome in Test 7, the domes in Tests 4, 5 and 9 had already failed along the support. In Test 4 one may observe that the curves showing crown deflection during "virgin" loading and reloading respectively, are very close (see Figure E. 19). (When reloading started, each dome had a residual deflection as shown on the figure. The deflection curve for the reloading test only shows the crown deflections in excess of this residual deflection.) However, to cause these deflections during the reloading required only a fraction of the virgin average pressure on the dome (see Figure E. 10). The reason for this was that in the reloading test the dome in itself was much more flexible than during virgin loading. This was a consequence of the bend along the spring line. The bend gave rise to bending deformations in addition to the deformations

occurring during virgin loading (i. e. deformations caused by membrane stresses plus deformations caused by the moments arising from retrainment at the spring line).

By looking at the unloading and reloading curves for Test 5 (Figure E. 11), one will find that both these curves lie above the virgin loading curve after support fialure. Comparing the behavior of the domes in Tests 4 and 5, this seems to be the main difference between the two tests. The fact that the average pressure on the dome was higher during relaoding in Test 5 than in Test 4, may have been a consequence of the big deformation of the dome in Test 5 at failure. Figure E. 8 shows that the instantaneous pressure relief at failure in Test 5 was considerably higher than in Test 4, but at the same time, the pressure transferred to the dome in Test 5 increased much faster after failure. One reason for this may be the difference in depth of burial for the two domes (that was the only difference between the two tests). However, this may not be a satisfactory explanation, and one is inclined to use the same line of reasoning as was given during the discussion of Test 6.

In Test 9, with loose sand, the reloading curve lies considerably above the unloading curve from virgin loading (see Figure E. 13). This pattern did not occur in either Test 4 or 5. It appears the "arch", which was "built up" when the dome failed along the support, partly broke down during the unloading.

In Test 7 (see Figure E. 12) the average pressure on the dome during relaoding was higher than during virgin loading. This occurred in spite of the fact that the sand was densified somewhat during virgin loading and was approximately 10% less compressible in the reloading test. However, by looking at Figure E. 21 one may observe that also the crown deflection during reloading was smaller than during virgin loading. This may be explained by the nonelastic properties of the cork foundation. The stress-strain properties of the cork will be different in the two load cycles. This is believed to be the reason for the higher pressures on the dome during the reloading.

E. 6 Summary and Conclusions

(a) Domes in buried condition could be subjected to pressures which reached several times their buckling capacity without surrounding sand. Under all the conditions of burial of the domes in this test series, the sand provided sufficient restrainment to eliminate elastic

buckling as the mode of failure.

(b) Initial failure of the domes consisted of the formation of "plastic yield hinges" in the vicinity of the spring line due to flexure. As a result of this local support failure, the pressure transferred to the structure was greatly reduced.

(c) The maximum overpressure on the sand surface to cause initial failure of the dome was about the same for burial depths of 1.5 and 0.5 times the diameter of the dome, respectively.

(d) Increased flexibility of the foundation of the structure led to a substantial reduction of the pressures transferred to the structure.

(e) If additional flexibility is introduced in a buried structure to decrease the total load transferred to the structure, one should consider how the distribution of pressures on the structure may be affected.

(f) Relative density of the sand was a significant influence on the amount of the applied surface pressure transferred to the dome.

(g) Comparison of structure flexibility with compressibility of surrounding sand did not indicate any simple relationship between these parameters and the amount of surface pressure transferred to the dome.

Table E. 1

SUMMARY OF TEST PROGRAM

Test Number	Sand Density	Depth Burial (in.)	Foundation Flexibility	Flexibility of Dome
3 & 4	dense	17. 5	rigid	flexible
5	dense	5	rigid	flexible
7	dense	17. 5	flexible	flexible
6 & 10	dense	5	flexible	flexible
9	loose	17. 5	rigid	flexible
8	loose	17. 5	flexible	flexible
11	dense	5	rigid	rigid

Note: The depth of burial is measured to the crown of the dome.

Table E.2

TIME SCHEDULE FOR TYPICAL TEST

Process	Time Required
Mounting of strain gages	3 hours for 1 man
Placing the model and its instrumentation in the bin (this item includes gluing of the dome to the base plate).	4 hours for 1 man
Placing and adjustment of settlement gages	3 hours for 1 man
Filling the sand in the bin	7 hours for 2 men
Assembling the loading system	4 hours for 2 men
Performing the test	4 hours for 3 men
Disassembling the loading system	2 hours for 2 men
Removing the sand from the bin	2 hours for 2 men
This gives a sum total of 52 man hours	

Table E. 3

STRAIN RECORDINGS

The pressures are given in lbs/in^2
The strains are given in microinches/inch

For location and orientation of strain gages see Figures E. 4 and E. 5. Notice that all strain gages were mounted on the inside surface of dome.

The strain readings seldom deviated more than 10% from the average, except where noted.

TEST 4

Applied surface pressure.	Ave. press. on dome	Ave. between strain gages:		
		4, 5 and 6	7 and 8	1, 2 and 3 *
0	0	0	0	0
8	3.9	25	30	43
14	11.6	84	92	125
24	23.8	197	194	261
34	33.7	280	276	365
44	43.8	359	361	458
56	53	440	500	483
66	61.1	552	640	470
74	67.4	664	747	453
86	73.5	781	840	480
100	52.5	460	600	beyond range of strain indicator.
116	51.8	450	585	
126	54.3	440	585	
137	56	420	585	
147	58.7	400	585	
158	60.5	385	580	
169	62.5	380	580	
183	64.5	370	570	
195	66.5	355	570	
216	70.3	340	565	
236	73.6	330	555	
249	75.8	320	545	

*The small compressive strains in gages 1, 2 and 3 are explained by the location of the gages. The purpose of the gages was to detect when the failure along the spring line occurred, and high bending stresses are present in this region.

TEST 5

Applied surface pressure.	Ave. press. on dome.	Ave. between strain gages:		
		1, 2 and 3	4 and 6	7 and 8
0	0	0	0	0
10	9.5	106	52	95
20	21.5	235	116	220
30	33	380	188	365
40	43	490	248	495
50	53	621	335	655
61	62	720	425	935
69	68	816	492	1300
80	76	991	566	1805
90	82	1100	616	2190
92	58	860	-130 329	beyond range
98	37.5	920	- 50 -56	of strain
112	45	1000	0 -99	indicator
121	49	1035	+10 -110	
132	55	1085	+25 -111	
141	60	1120	+40 -109	
152	67	1150	+ 50 - 111	
161	72	1150	+ 50 - 111	
171	76.5	1120	+40 -106	
181	81	1090	+25 -99	
191	85.5	1050	+ 15 - 99	

* Gage 5 did not function.

TEST 6

Applied surface pressure.	Ave. press. on dome.	Ave. between strain gages		
		1, 2 and 3	4, 5 and 6	7 and 8
0	0	0	0	0
8	3.5	50	45	60
19	10.5	150	100	200
30	15	240	133	300
40	18.5	315	160	390
50	21.5	380	190	545
61	25	450	215	610
71	27.5	510	250	680
80	31	580	290	750
89	32.5	660	335	865
102	36.5	830	415	915
110	38	930	440	1065
121	42	1150	520	1195
130	44.5	1300	570	1450
141	48.5	1520	645	1720
150	51.5	1660	700	1820
161	54	1860	750	1930
171	57	2000	795	2190
180	59	2130	840	2420
186	54			
196	56.5	complete collapse		
209	62.5	(Fig. 14 b)		

TEST 7

Applied surface pressure.	Ave. press. on dome.	Ave. between strain gages:		
		1, 2 and 3	4, 5 and 6	7 and 8
0	0	0	0	0
8	4	60	33	67
19	9.5	158	82	168
28	13	234	125	255
38	15.5	285	150	307
48	18	341	179	364
59	20	388	206	420
69	22.5	440	232	470
78	24.5	482	257	515
88	27	535	291	572
98	29	595	329	625
108	31	633	355	665
120	33.5	703	399	737
129	36	759	437	795
139	39	829	488	895
149	41	893	536	963
158	43	947	571	1020
169	46	1018	625	1115
179	48.5	1078	673	1207
188	51.5	1150	716	1305
199	54.5	1231	773	1430
210	57	1299	817	1485
220	59	1351	866	1670
229	62			

Test 8

Applied surface pressure	Ave. press. on dome	Ave. between strain gages:			
		1, 2 and 3	4 and 5	6	7 and 8
0	0	0	0	0	0
10	7	65	55	65	94
20	16	169	174	135	225
29	26	287	279	210	364
40	36	414	379	322	565
50	47	585	500	410	780
60	57	836	630	740	1310
69	65	1115	739	1245	1860
71	21	430	250	680	1800

Test 9

Applied surface pressure	Ave. press. on dome	Ave. between strain gages:				
		1 and 2	3 and 6	7	8	4 and 5
0	0	0	0	0		0
10	7.5	70	55	85	75	81
20	18	206	110	210	160	165
29	30.5	326	192	385	260	280
40	45	529	330	645	350	452
50	55.5	821	480	1050	505	625
55	63	1100	710	1460	630	765
60	66.5	1300	905	1685	765	860
64	71	1631	1278	2175	905	985
65	23.5	940	695	1780	240	600
72	21.5	934	707	1665	330	595
82	22	1015	712	1750	730	500
95	24.5	950	698	1570	1070	595

TEST 10

Applied surface pressure.	Ave. press. on dome	Ave. between strain gages:			
		1 and 2	3 and 6	7 and 8	4 and 5
0	0	0	0	0	0
10	6	105	77	100	50
21	10	210	157	195	87
30	12.5	290	215	265	110
40	15.5	365	280	337	132
50	17.5	432	332	397	152
60	19.5	492	392	452	170
70	22	570	460	515	190
81	24	645	540	580	220
92	27	735	617	645	253
102	29	812	697	707	282
112	31.5	887	777	752	320
124	34.5	987	897	852	370
136	38.5	1110	1065	960	432
151	43	1268	1312	1115	515
168	47	1402	1567	1285	595
181	51	1545	1752	1432	675
194	54.5	1682	1832	1612	731
210	59.5	1845	2140	1915	805
222	34	1500	1922	2762	30 430
234	38	1550	1952	2762	20 440
250	44	1625	2027	2745	5 460
269	49.5	1723	2127	2700	0 470

Table E. 4

SAND MOVEMENTS

Surface pressure is given in lbs/in^2
Sand movements are given in 1/1000 inch
d = distance from bottom of bin in inches
r = distance from central axis of bin in inches
= orientation of settlement gage (see Fig. E. 7)

TEST 4

Applied surface press. \ d	8	8	8	8	8	16	16	24	24	24	24	24	24
r	10	10	15	20	25	10	15	10	10	10	15	20	25
α	0°	180°	0°	0°	0°	0°	0°	0°	90°	180°	0°	0°	0°
0	0	0	0	0	0	0	0	0	0	0	0	0	0
8	—	0.2	—	—	0.3	0.5	0.1	1.4	2.3	2	2.1	1.6	1.3
14	1.1	1.1	0.8	0.9	1.4	2.7	2.5	6.2	6.5	6.6	6.5	6.7	5.6
24	2.5	2	2.4	2.7	3.2	5.4	6.6	12.4	13.3	12.4	12.8	15.3	13.5
34	3.8	2.9	3.5	3.3	4.3	7	9.5	18.5	18.3	16.4	17.8	20.9	19.1
44	5	3.6	4.7	4.7	5.9	10.8	12.8	23.7	24.4	21.4	22.9	26.5	24.3
56	6.1	4	5.8	5.8	7.3	13.7	15.7	28.8	30	26.3	27.7	31.7	29.1
66	7	4.7	6.9	6.8	8.3	16.5	18.3	33.2	34.7	30.1	32.1	36.1	33.9
74	7.9	5.4	7.6	7.4	9.3	19	20.6	36.6	39	33.8	36	40	37.9
86	9	5.9	8.5	8.3	10.6	21.6	23	41	43.7	37.8	40.2	44.2	42.3
100	11	7.9	10.1	9.4	11.3	29.3	27	49.5	52.2	47.1	46.9	50	48.1
116	12.8	8.8	11.2	10.3	13.1	34.4	28.5	56	58.2	53.3	53.1	55.5	53.6
126	13.7	9.4	11.8	10.8	14	38.5	33.2	60.5	62.2	57.3	56.6	58.8	57.4
137	14.8	9.9	12.5	11.7	14.9	42	35.5	65.5	67	61.8	60.1	62.5	60.4
147	15.8	10.6	13.2	12.1	15.8	44.8	37.5	69	70.2	66.3	63.8	66	64.8
158	16.7	11	13.9	12.6	16.4	47.5	39.7	73	74.2	70	66.9	69.1	68.1
169	17.3	11.5	14.3	13.2	17.3	50.5	41.7	76	77.7	73.3	69.6	71.4	71.3
183	18.2	12.2	15.2	13.9	18.2	53.8	43.8	80.5	82.2	77.3	74.1	74	75.6
195	19.1	12.6	15.9	14.4	19.1	57	46.	84	86.2	80.8	77.7	76.5	79.3
216	20.3	13.7	16.8	15	20.3	61.2	49.3	90	92.2	86.6	83.2	81.5	85.6
236	21.3	14.8	17.7	15.9	21.8	65	52.3	95.5	97.2	89.5	87.9	83.9	90.4
249	22.3	15.5	18.4	16.5	22.8	67.5	54.5	99	101.2	94.3	89.2	84.5	94.1

TEST 5

Applied surface press. \ d	8	8	14	14	14
r	15	25	10	15	20
α	0°	0°	0°	0°	0°
0	0	0	0	0	0
10	1.3	1.8	0.5	3.2	3.6
20	3.1	4.3	5.4	7.2	7.2
30	4.7	6.7	10.6	11.2	11.2
40	5.8	8.3	13.5	13.5	15.1
50	6.3	9.9	16.6	15.9	18.4
61	7.4	11.2	19.1	18	21.7
69	7.9	12.1	21.8	19.8	23.8
80	8.8	13	24.3	21.6	26.3
90	9.2	13.9	27.2	23.4	28.5
92	9.4	14.6	32.6	24.7	29.7
98	10.6	15	40.3	27.4	30.8
112	11.5	16.2	44.5	28.8	33.3
121	11.7	16.6	46.1	29.7	33.7
132	12.1	17.5	48.3	30.8	34.5
141	12.3	18.2	50.6	32	35
152	13	19.1	53.3	33.7	37
161	13.5	19.5	57.7	34.9	38

TEST 6

Applied surface press. \ d	8	8	8	14	14	14	14	14	14
r	8	8	16	8	8	8	12	16	18
α	0°	180°	90°	0°	90°	180°	150°	90°	0°
0	0	0	0	0	0	0	0	0	0
8	2.1	2.2	1.4	4.7	4.5	4.7	4.3	3.2	4.3
19	6.5	6.7	3.8	13.2	11.7	14.4	12.6	9.7	10.4
30	9	9.2	5.4	18.4	17.3	19.5	17.1	13.9	14.6
40	11	11.2	6.5	22.7	22.3	24	20.9	17.5	18
50	12.8	12.8	7.4	26.5	26.8	27.8	24	20.2	20.9
61	14.1	14.4	8.3	29.9	30.8	31.4	26.8	22.7	23.4
71	15.5	15.5	9	32.8	34	34.1	29.2	24.7	25.2
80	16.1	16.4	9.7	35	36.6	36.4	31.2	26.3	26.7
89	17.3	17.3	10.4	37.5	40	39	33.3	28.1	28.5
102	18.6	18.6	11	40.6	43.8	42	36	30.4	30.6
110	19.3	19.1	11.7	42	45.6	43.5	37.3	31.2	31.7
121	20.4	20.2	12.4	44.8	49.2	46.3	39.8	33.3	33.5
130	21.1	20.9	13	46.5	51.5	48.2	41.4	34.6	34.8
141	22.2	22	13.7	49.5	54.8	49.9	43.6	36.4	36.4
150	22.9	22.5	14.2	50.8	56.8	52.5	44.9	37.5	37.5
161	23.6	23.2	14.9	52.5	59.5	54.5	46.5	38.7	38.8
171	24.2	23.8	15.3	54.4	61.7	56.3	48.1	39.8	40
180	24.9	24.5	15.5	55.7	63.5	57.7	49.5	40.9	40.9
186	26	25.6	16.2	61.40	70.3	62	51	41.5	41.8
196	26.5	26.1	16.7	62.70	71.70	63.3	52.3	42.7	42.8
209	27.4	26.8	17.1	64	74	64.8	54.2	43.8	44

TEST 7

Applied surface press. \ d	8	8	8	14	14	14	14	14
r	8	12	16	8	8	12	16	18
α	180°	150°	90°	0°	90°	150°	90°	0°
0	0	0	0	0	0	0	0	0
8	1.4	0.9	0.9	4	4.1	3.2	2.2	2.7
19	4.5	2.9	2.9	11.3	11.2	7.9	7.2	7.4
28	6.5	5.4	4.5	16.9	16.8	15	11.9	11.5
38	8.4	7.2	5.6	20.7	22.2	18.6	14.8	14.4
48	10.2	9.0	7	24.8	27	22.5	17.8	16.8
59	11.7	10.8	8.3	28.1	31	25.8	20.4	19.1
69	13	12.4	9.2	31.2	34.8	28.8	22.7	20.9
78	14	13.5	9.7	33.7	37.8	31	24.5	22.7
88	15	14.8	10.8	36.4	41.1	33.9	26.5	24.5
98	16.2	16	11.7	38.9	44.2	36	28.5	26.3
108	16.8	16.9	12.4	40.7	46.5	37.5	29.6	27.4
120	17.8	18.7	13.3	43.3	50	40	31.6	29.2
129	18.6	19.8	14	45.6	52.5	41.8	33	30.6
139	19.4	21.1	14.9	47.8	55.5	44.3	34.8	32.2
149	20.4	22.2	15.3	49.7	57.7	46	36.2	33.2
158	20.8	23.1	15.8	51	60	47.6	37.5	34.6
169	21.5	24	16.4	53.2	62.3	49.5	38.8	35.7
179	22	25.2	16.9	55	64.5	51	40	37.1
188	22.8	26	17.4	56.4	66.3	52.3	41.1	38.2
199	23.3	27	18	58.5	68.5	54.5	42.5	39.3
210	23.8	28	18.5	60	70.7	55.7	43.8	40.6
220	24.5	28.8	18.9	61.1	72.4	57	44.6	41.5
229	24.8	29.6	19.7	62.6	74.1			

TEST 8

Applied surface press. \ d	8	8	8	14	14	14	14	14
r	8	8	12	8	8	12	16	18
α	180°	0°	150°	180°	90°	150°	90°	0°
0	0	0	0	0	0	0	0	0
10	27	26.3	29	57	51	60	54	56
20	51.3	51	54.5	108.5	98	112	103	107
30	68.5	69	72	144	133	148	135	135
40	80.3	81.5	85.5	170	160	175	161	161
50	90	91	96.5	190	180	195	182	182
60	96 8	99	105.5	206	197	214	201	200
69	101.5	105	112.5	218	210	225	213	211
71	113.5	115.5	120		242	240	228	233

TEST 9

Applied surface press. \ d	8	8	8	8	8	8	14	14	14	14	14	14
r	8	8	8	12	16	18	8	8	8	12	16	18
α	180°	90°	0°	150°	90°	0°	180°	90°	0°	150°	90°	0°
0	0	0	0	0	0	0	0	0	0	0	0	0
10	28	24	28	35.3	38.6	30.3	62.5	57.5	63	65	63	61
20	52	46.7	50.4	64	69	56	113.3	102	106	115	113	107
30	70	65	67	85	91	75	148.5	137	141	155	151	142
40	84	80	81	104	110	92	179	164	168	187	182	171
50	92.3	89	89	114	119	99	198	182	185	205	202	190
55	97.3	94	94	121	124	104	204	193.5	196	218	214	201
60	100	97	98	124	127	107	214	198	200	223	219	205
64	102.5	100	100	128	130	109	221	204.5	206	230	228	211
65	113	108	110	136	137	119	247	231	237	244	237	226
72	116	112	113	141	141	123	260	246	251	250	246	235
82	125	122	123	152	150	128	287	268	270	250	262	249
95	131	130	132	161	159	134	314	292	288	274	278	261

TEST 10

Applied surface press. \ d	8	8	8	14	14	14	14	14
r	8	8	18	8	8	8	12	18
α	180°	0°	0°	180°	90°	0°	150°	0°
0	0	0	0	0	0	0	0	0
10	2.2	2.9	2.2	5.6	7.4	7	5.8	9.2
21	5	5.8	4.6	10.5	14.4	13	11.9	16.2
30	6.8	7.2	6.8	14.4	19.3	17.1	16	21.2
40	8.6	9.2	8.6	18.4	24	20.8	20.4	25.6
50	9.7	10.8	10	21.7	28.1	23.8	24	29
60	11	11.9	11	24.5	31	26.5	26.6	31.6
70	12.1	13.3	12.2	27.2	35	29	29.5	34.4
81	13	14.1	13.3	30	36.8	31.5	32.4	37.2
92	14.1	15.3	14.5	32.7	41.2	34	35	39.5
102	15	16.2	15,3	34.7	44	36	37.3	41.6
112	15.7	16.7	16.2	36.4	46.2	37.9	39.4	43
124	16.6	17.7	17	39	48.9	40	41.5	45.5
136	17.3	18.9	18.2	41	51.8	41.8	44.4	47.6
151	18.4	20	19.5	44	55.5	44.7	47.6	50
168	19.3	20.6	20.6	46.4	58.7	46.7	50	52.5
181	20.2	21.6	21.5	49	61.8	49	51	54.7
194	21	22		51	64	51		

TEST 11

Applied surface press.	d	8	8	8	8	8	8	14	14	14	14	14	14
	r	8	8	8	12	16	18	8	8	8	12	16	18
	α	180°	90°	0°	150°	90°	0°	180°	90°	0°	150°	90°	0°
0		0	0	0	0	0	0	0	0	0	0	0	0
10		2	2.9	0.9	2.9	2.5	2.3	5	5.4	5.6	5.6	6.1	6.5
20		3.4	5.4	2.5	5.8	4.7	4.7	7.9	9.7	8.7	9.7	10.8	10.8
30		4.7	7.4	3.8	8.3	6.5	7	10.1	16	11.9	13.5	15.3	15.3
41		5.6	9.2	5.2	10.3	7.9	8.8	12.6	17.1	14.6	16.9	19.1	22
50		6.3	10.6	5.9	12	8.7	9.9	14.6	20	16.6	19.5	22	25
60		7	12.2	6.5	13.5	9.9	11.5	16.4	22.5	18.7	22	24.2	28
70		7.4	13.7	7.4	15.7	11	12.6	18	25.6	21	24.7	27.2	31
80		8.1	15	8.1	16.8	11.7	13.7	19.8	27.6	22.5	26.7	29.4	33
90		8.8	16.2	8.8	18.2	12.6	14.8	21	30	24	28.6	31.4	35.2
100		9.2	17.8	9.4	19.5	13.7	16	22.5	32.5	25.7	31	34	37.5
110		9.7	18.9	9.9	20.7	14.4	16.9	23.6	34.2	26.5	32.6	35.7	39.4
120		10.1	19.8	10.3	21.6	15	17.5	24.6	36.2	28.5	34.2	37.5	41
130		10.6	21.4	10.8	22.7	16.4	18.7	26	38.5	30	36	39.5	43
140		11	22.2	11.5	24	17.3	19.3	27	40.5	31.4	37.5	41.4	44.5
146		11.2	22.4	11.9	24.3	17.8	19.7	27.5	41.5	32	39	42	45

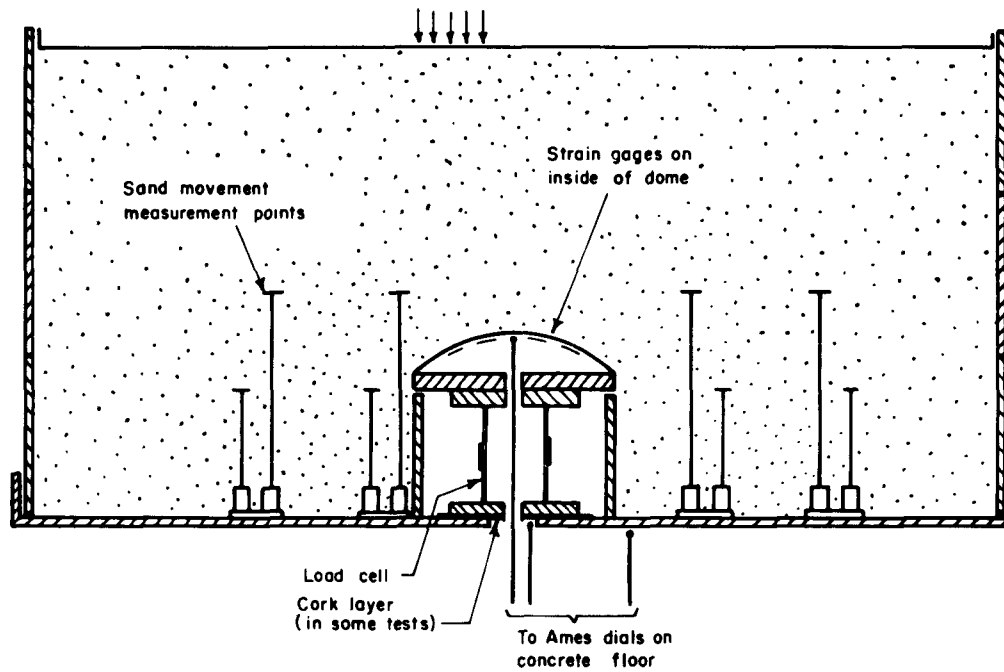

FIGURE E-1 GENERAL ARRANGEMENT OF APPARATUS

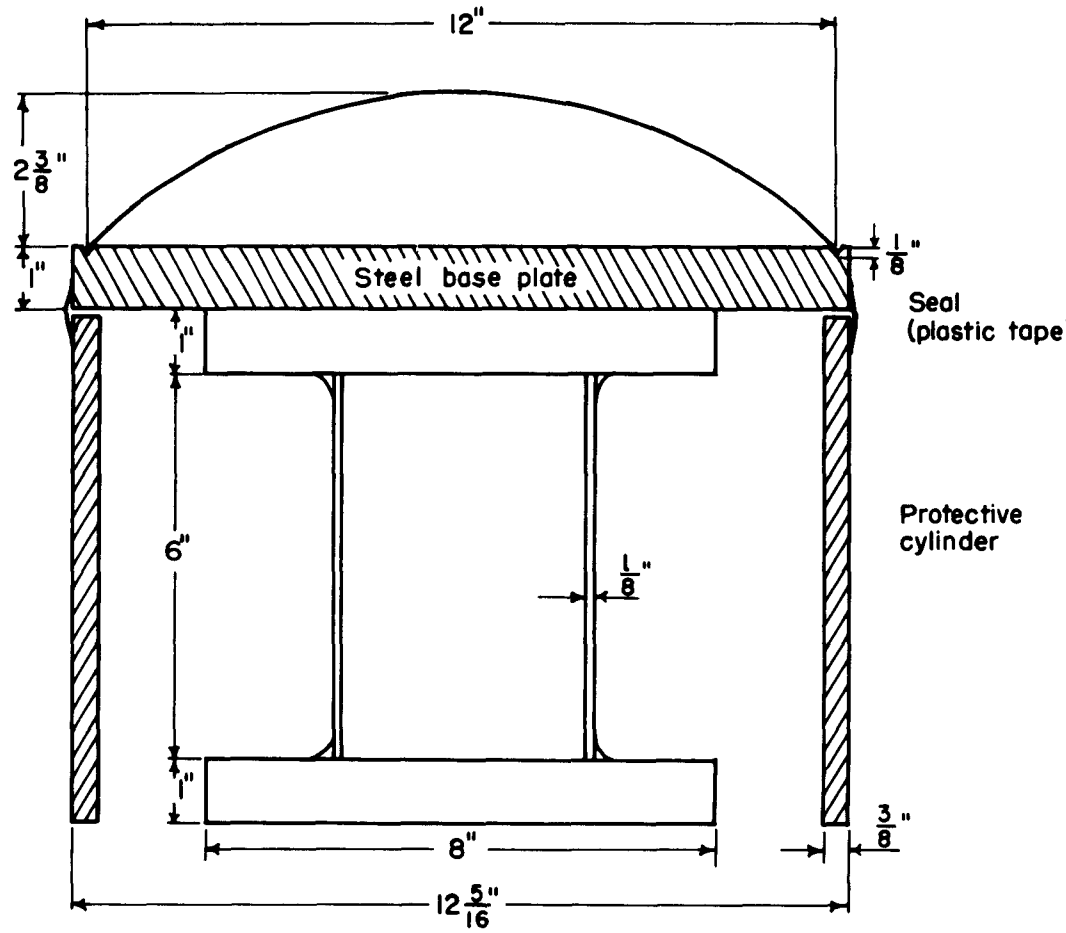

FIGURE E-2 DOME, LOAD CELL AND PROTECTIVE CYLINDER

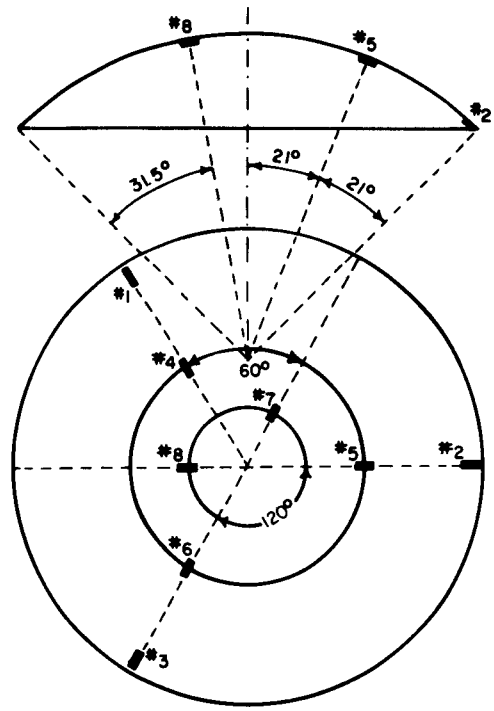

Location and orientation of strain gauges in test 4

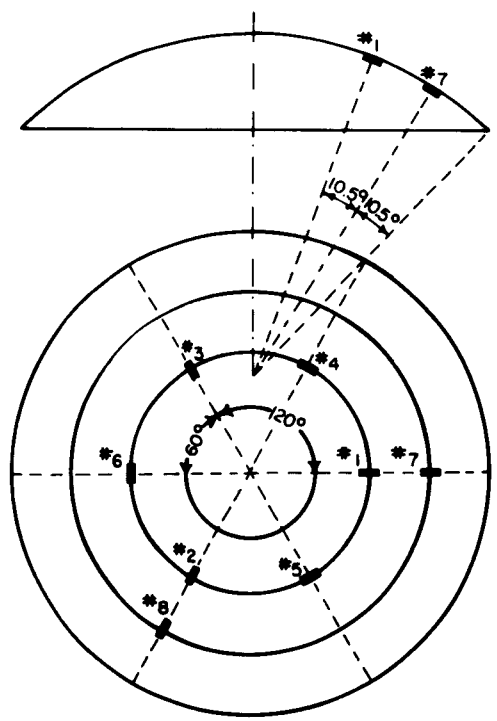

Location and orientation of strain gauges in tests 5, 6 and 7

FIGURE E-3 LOCATION OF STRAIN GAGES TESTS 4, 5, 6 and 7

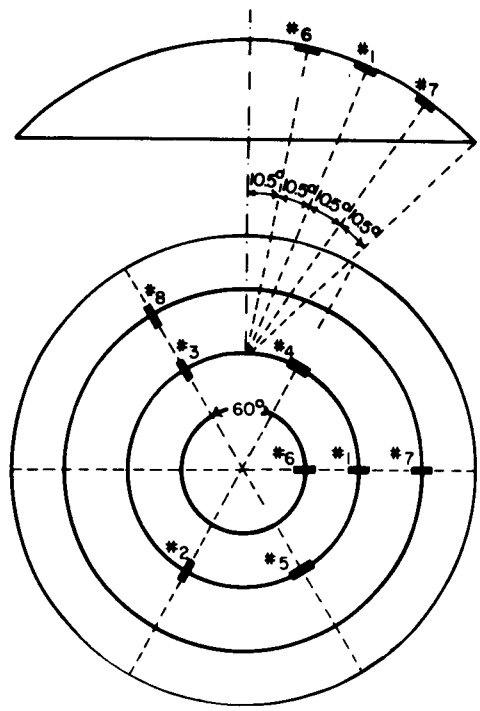

Location and orientation of strain gauges in test 8

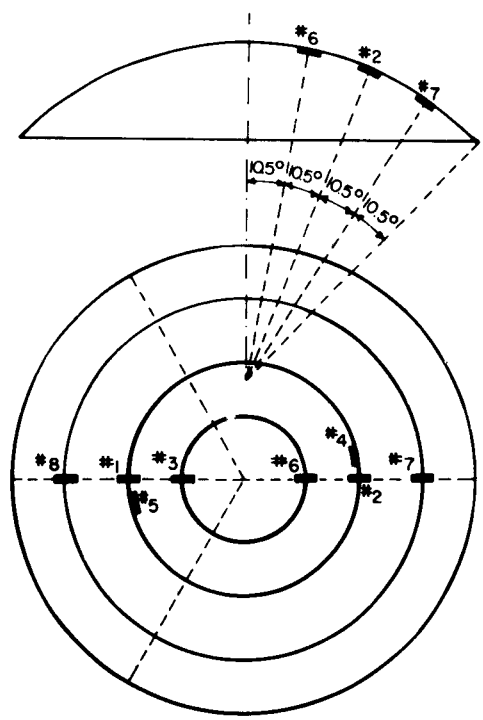

Location and orientation of strain gauges in tests 9 and 10

FIGURE E-4 LOCATION OF STRAIN GAGES TESTS 8, 9 AND 10

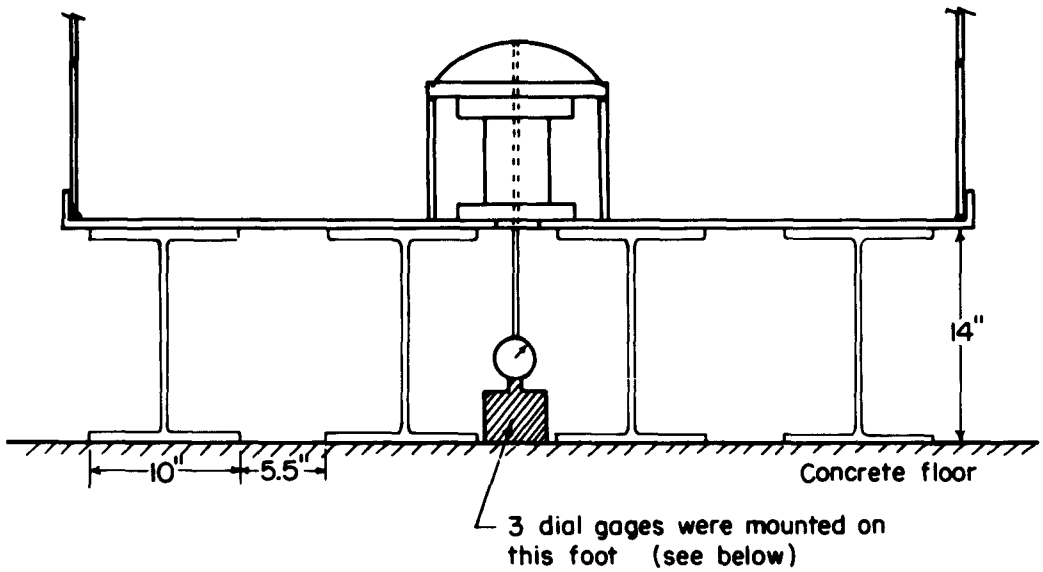

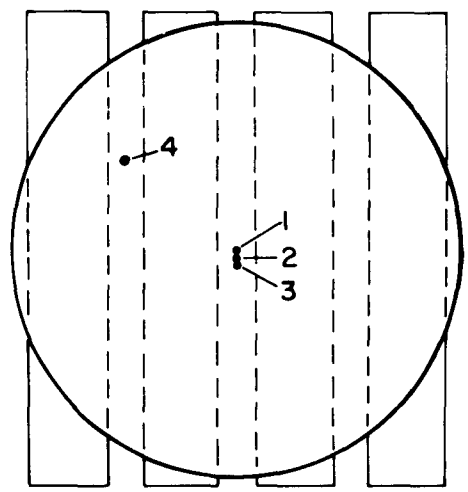

Gage 1 measured crown deflection

Gage 2 measured movement of bottom flange of load cell

Gages 3 & 4 measured movement of bottom plate of bin

FIGURE E-5 LOCATION OF DIAL GAGES

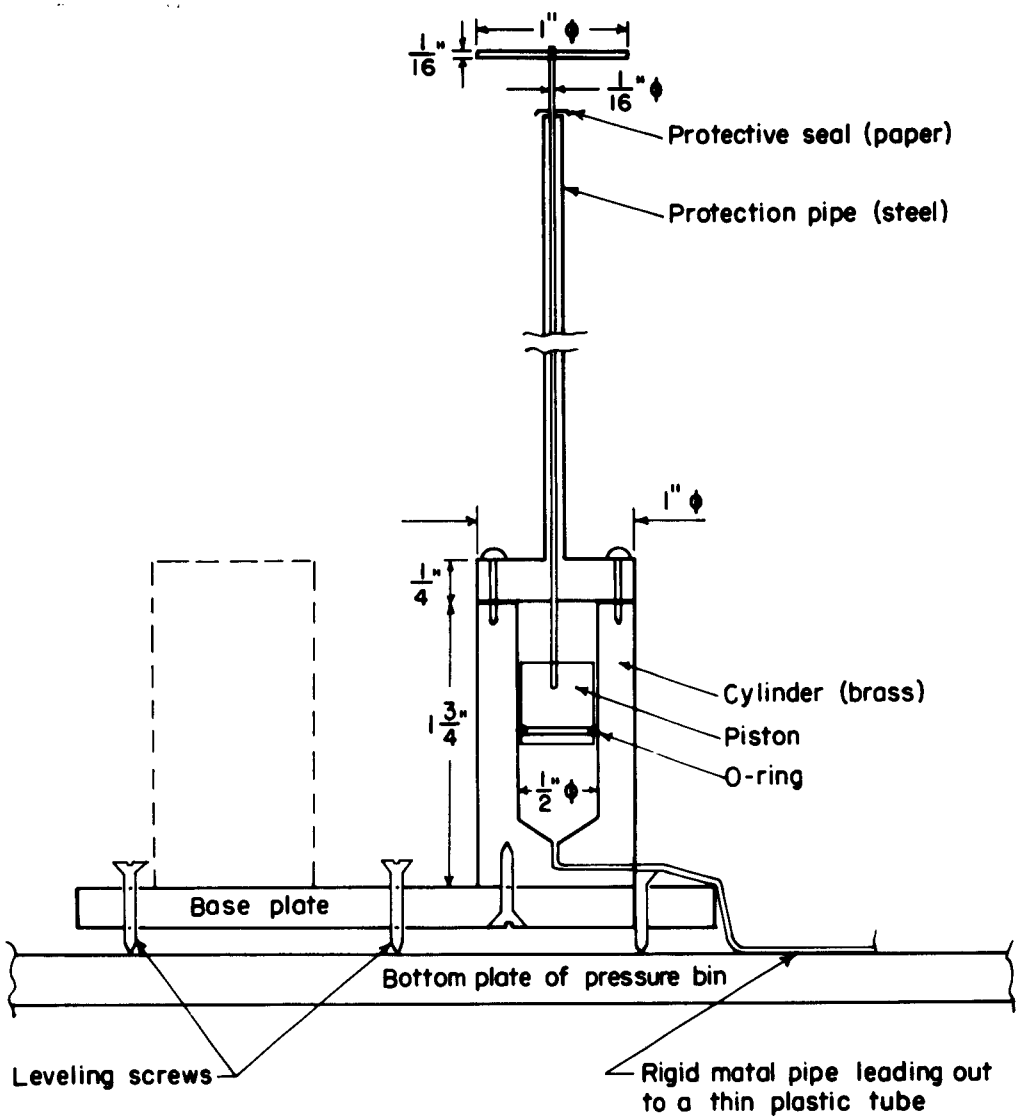

FIGURE E-6 SAND SETTLEMENT GAGE

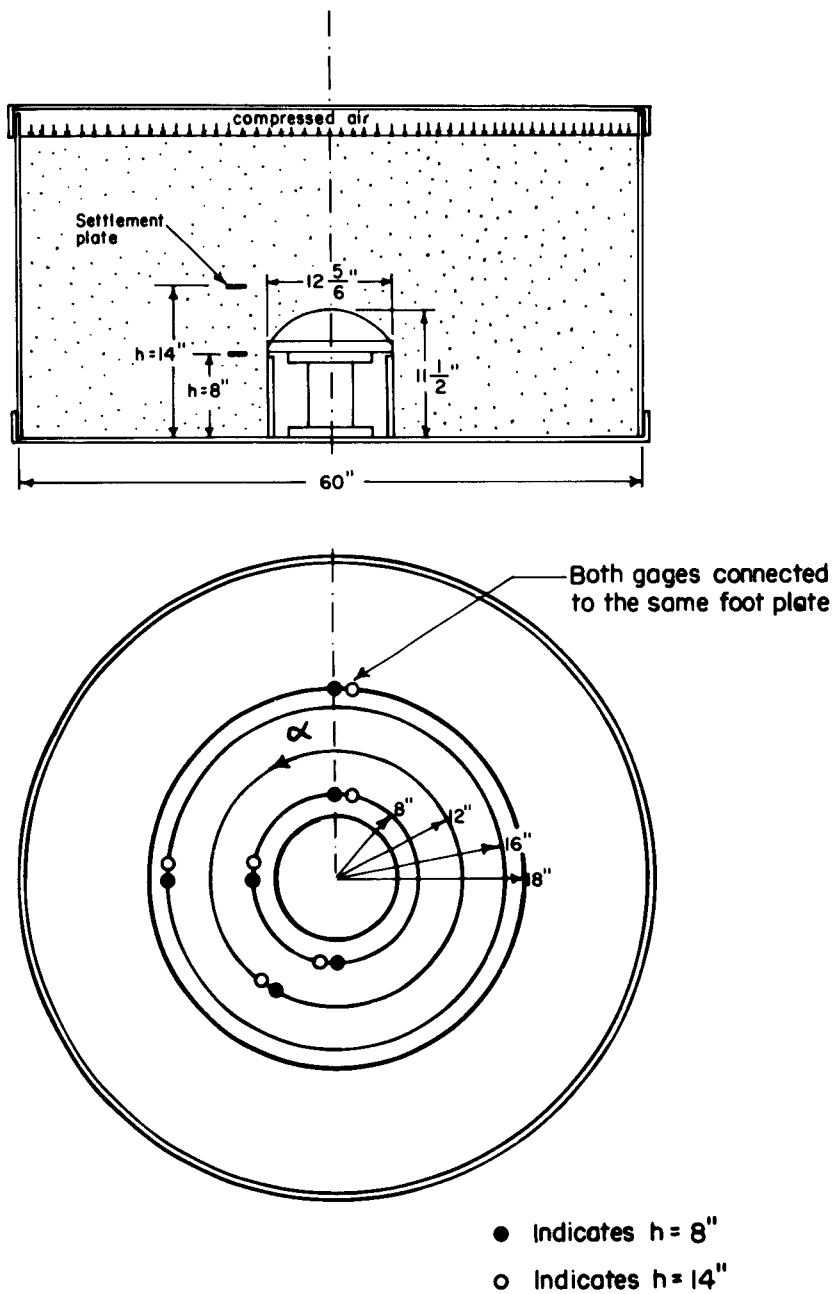

FIGURE E-7 LOCATION OF SETTLEMENT PLATES

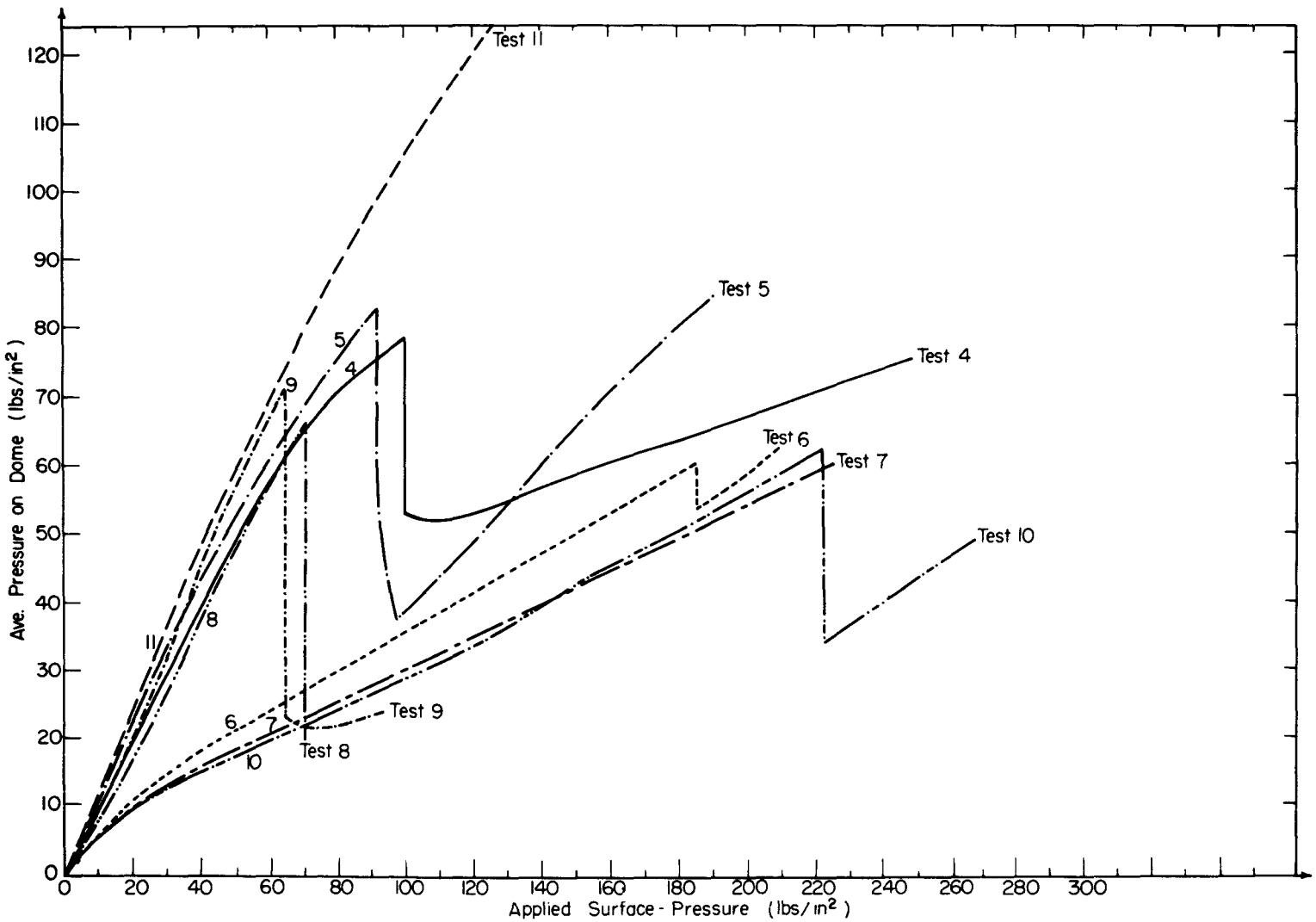

FIGURE E-8 AVERAGE PRESSURE ON DOME vs SURFACE PRESSURE - ALL TESTS

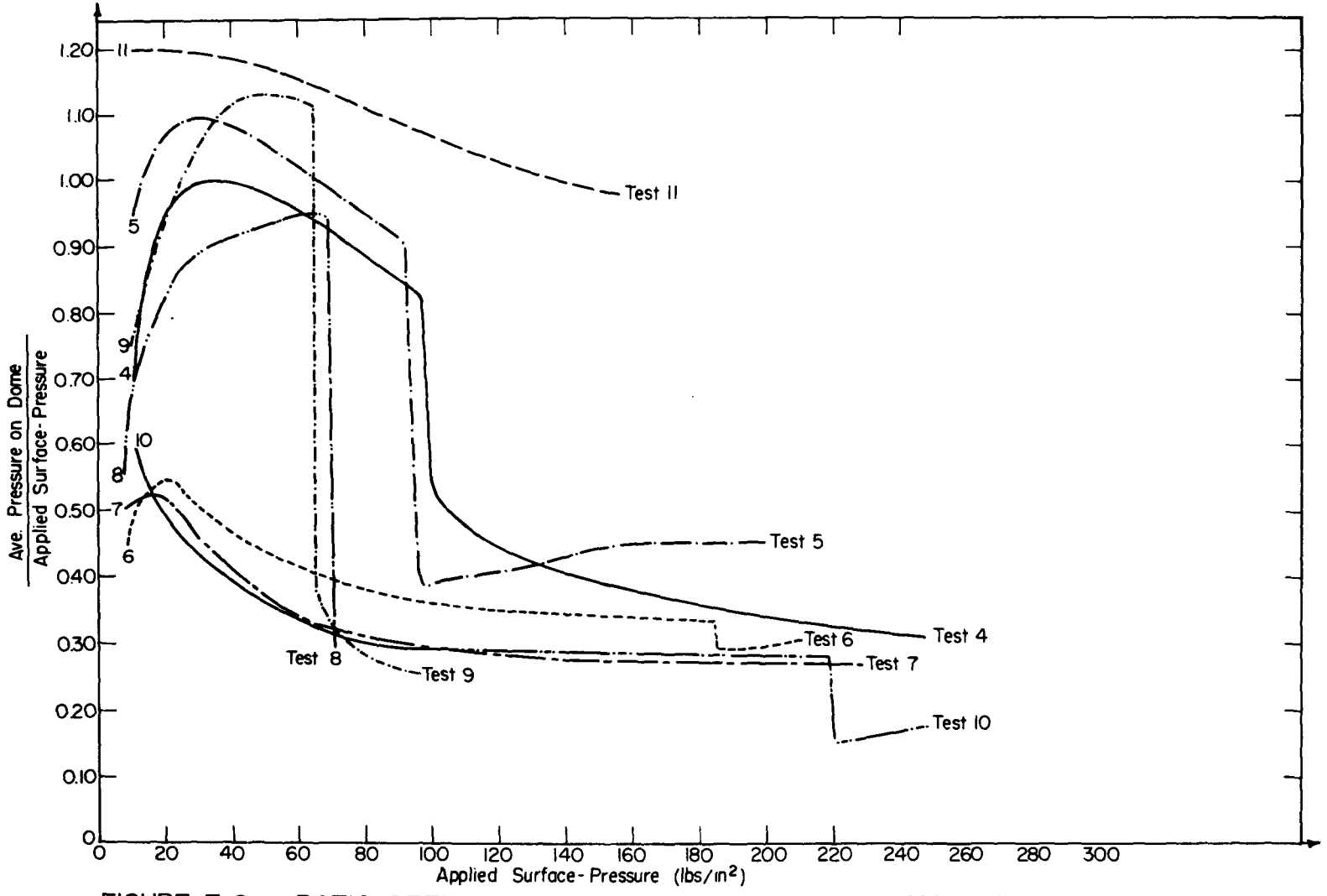

FIGURE E-9 RATIO BETWEEN AVERAGE PRESSURE ON DOME AND SURFACE PRESSURE ALL TESTS

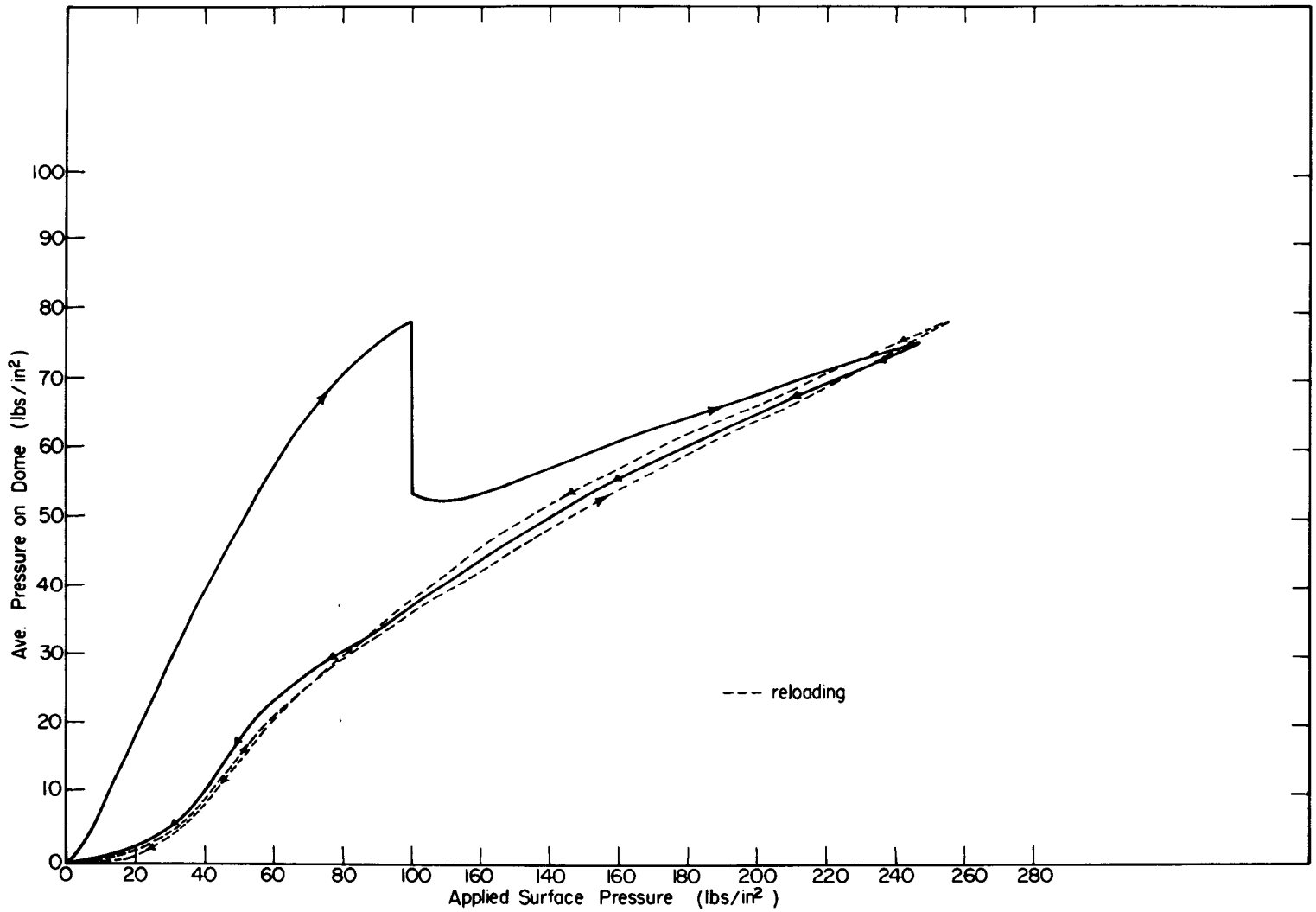

FIGURE E-10 AVERAGE PRESSURE ON DOME vs SURFACE PRESSURE - TEST 4

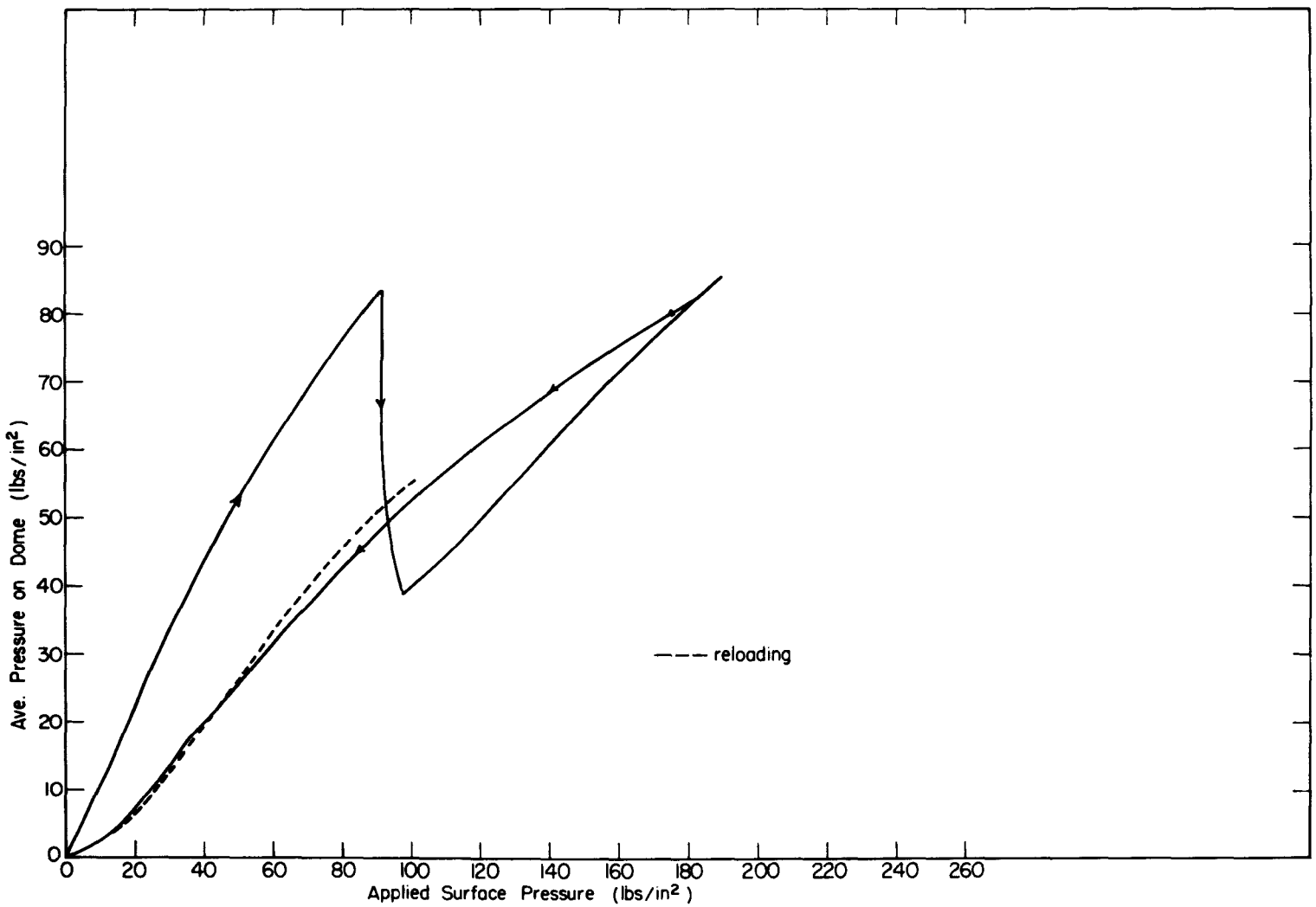

FIGURE E-11 AVERAGE PRESSURE ON DOME vs SURFACE PRESSURE - TEST 5

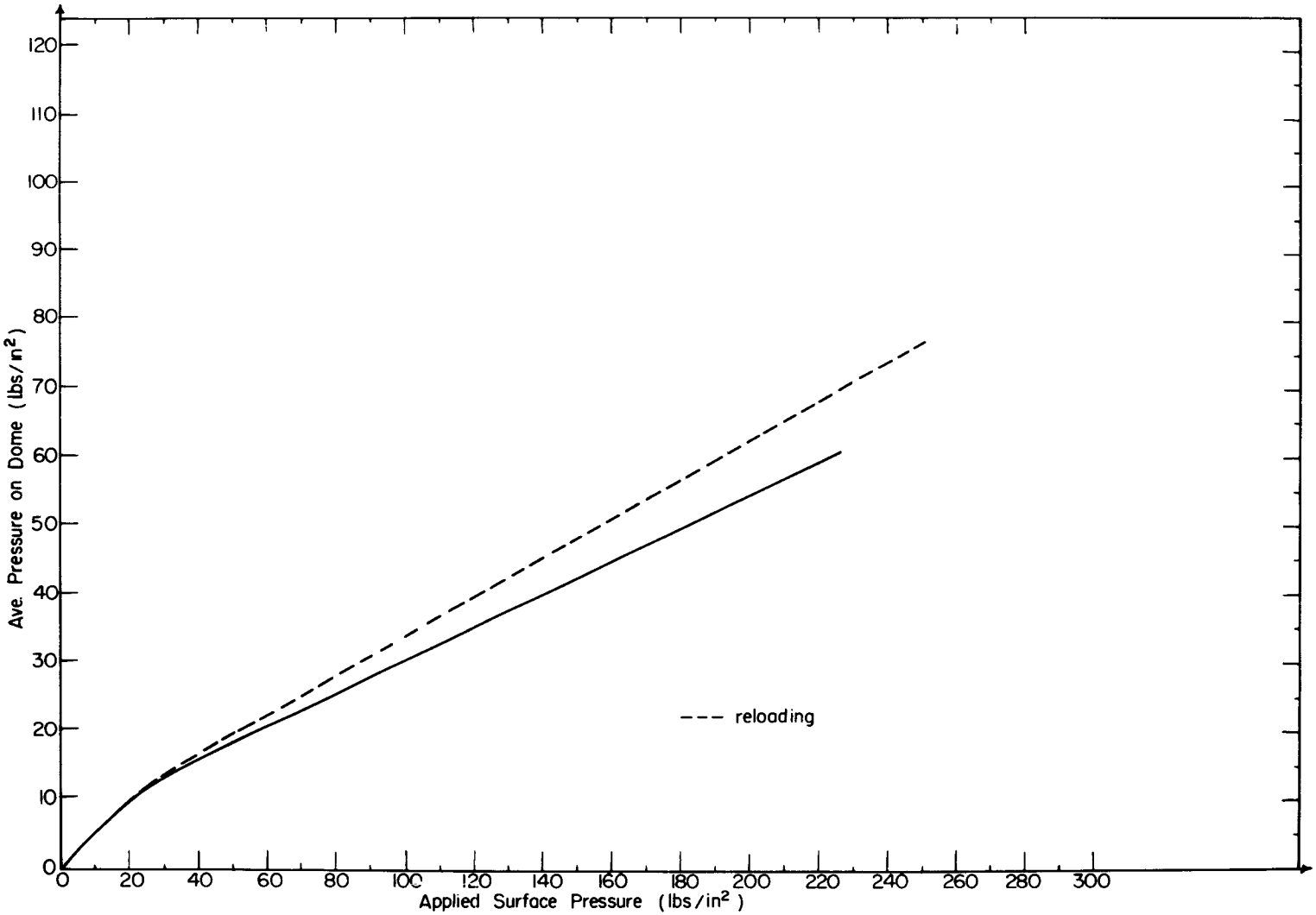

FIGURE E-12 AVERAGE PRESSURE ON DOME vs SURFACE PRESSURE - TEST 7

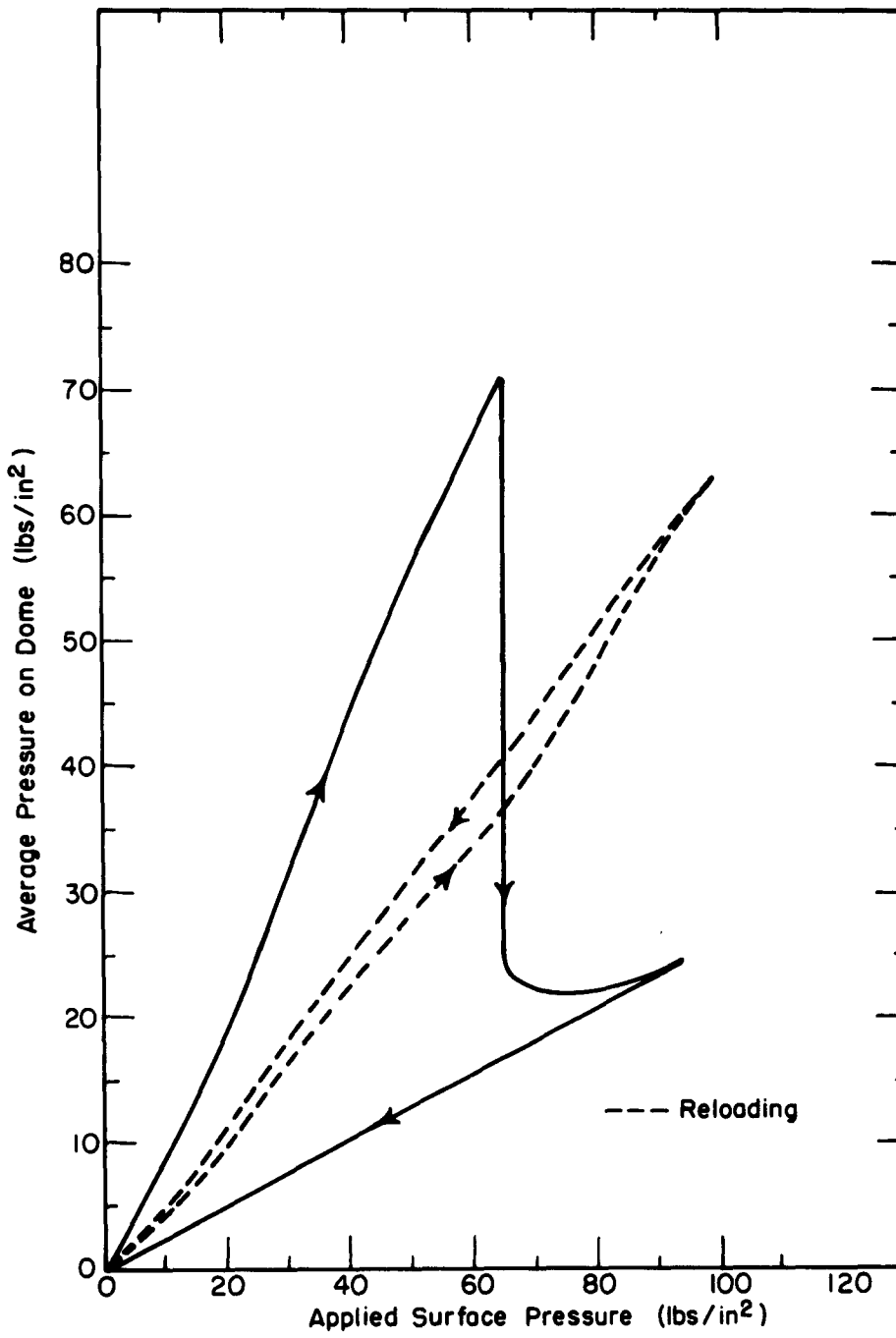

FIGURE E-13 AVERAGE PRESSURE ON DOME vs SURFACE PRESSURE - TEST 9

(a) Observe the local support failure (dome from test 4)

(b) The complete collapse of dome in test 6

FIGURE E-14 DOMES AFTER TEST - TEST 4 & 6

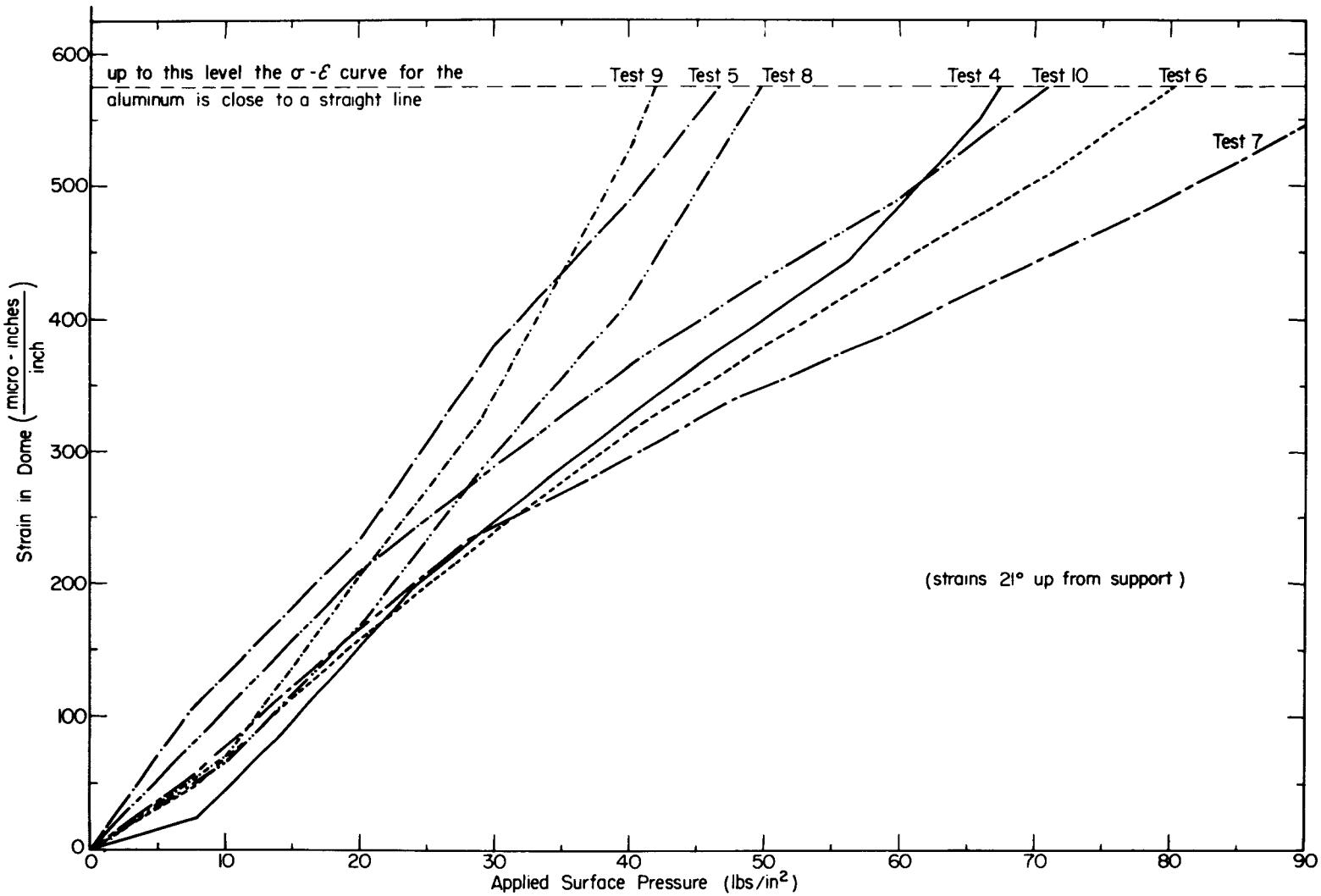

FIGURE E-15 MERIDIONAL STRAINS vs SURFACE PRESSURE - ALL TESTS

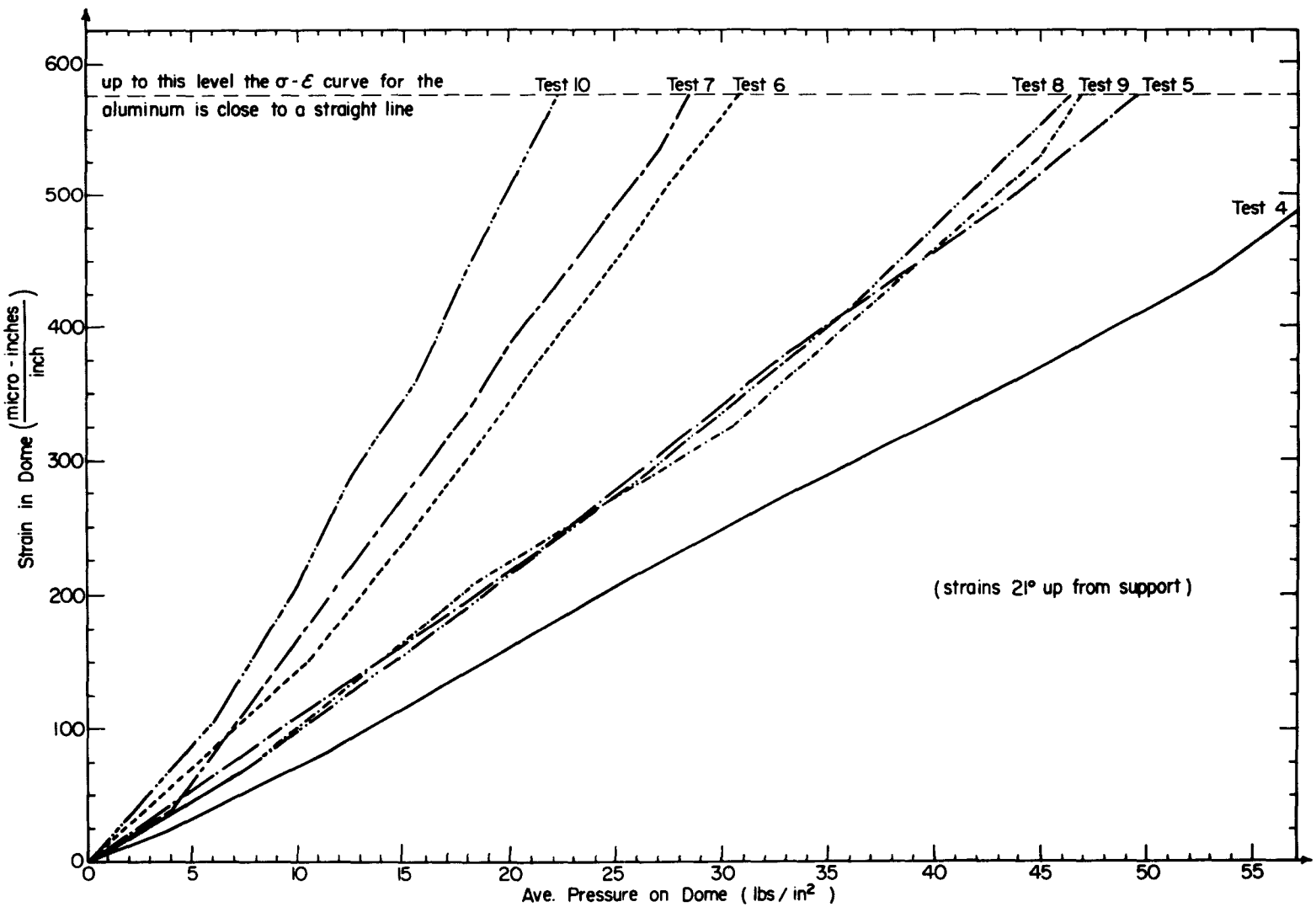

FIGURE E-16 MERIDIONAL STRAINS vs AVERAGE PRESSURE ON DOME - ALL TESTS

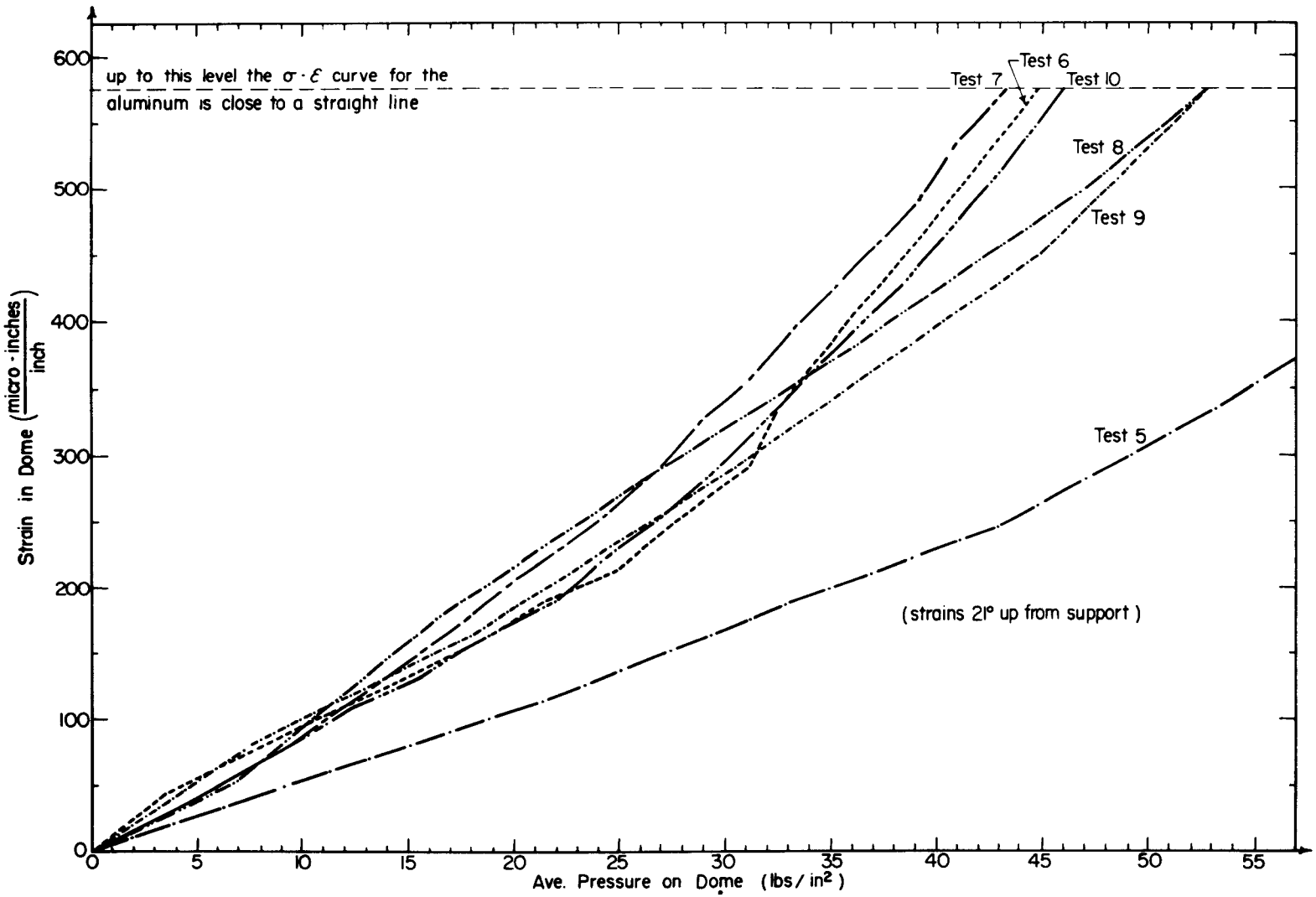

FIGURE E-17 LATITUDINAL STRAINS vs AVERAGE PRESSURE ON DOME

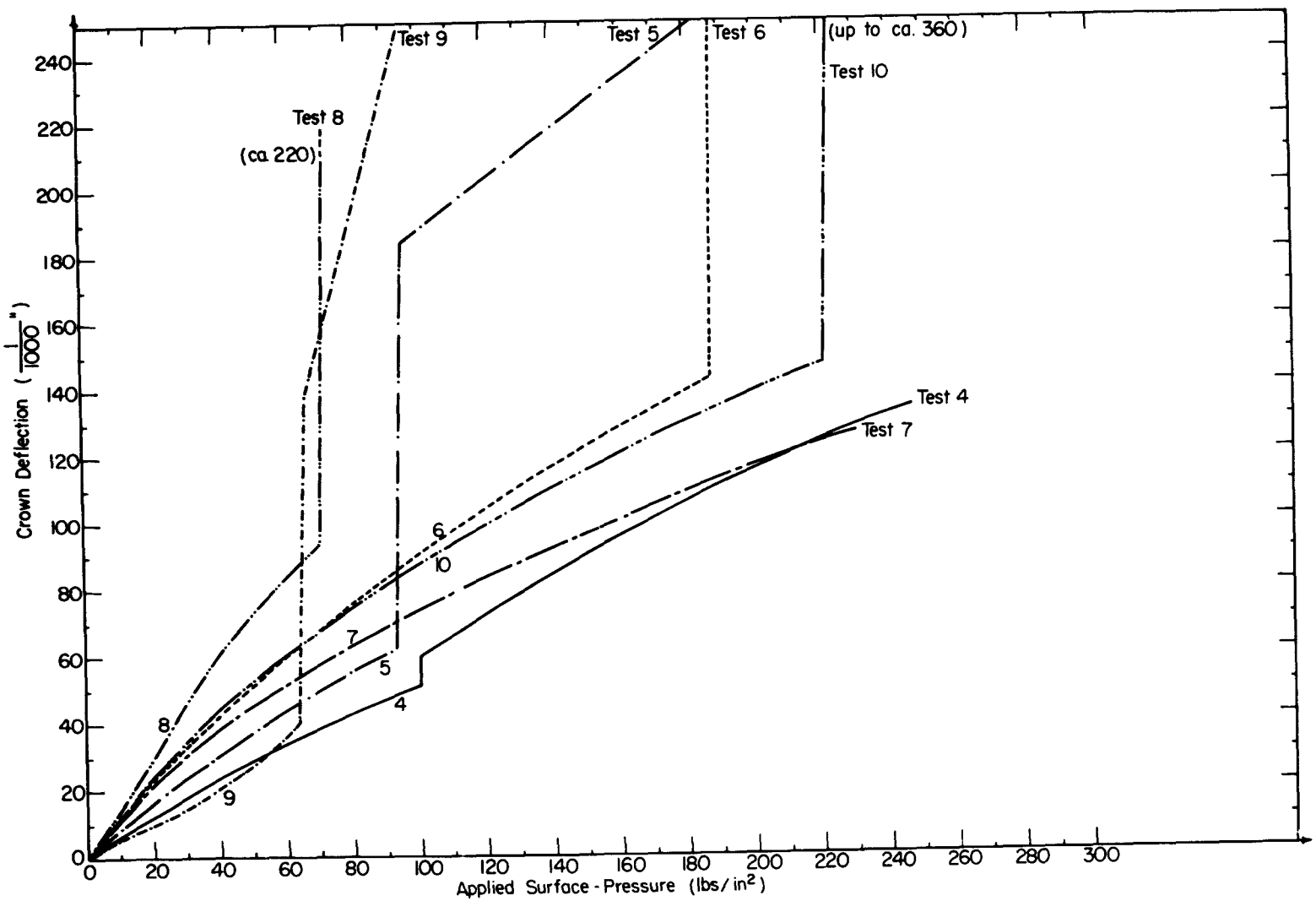

FIGURE E-18 CROWN DEFLECTION vs SURFACE PRESSURE - ALL TESTS

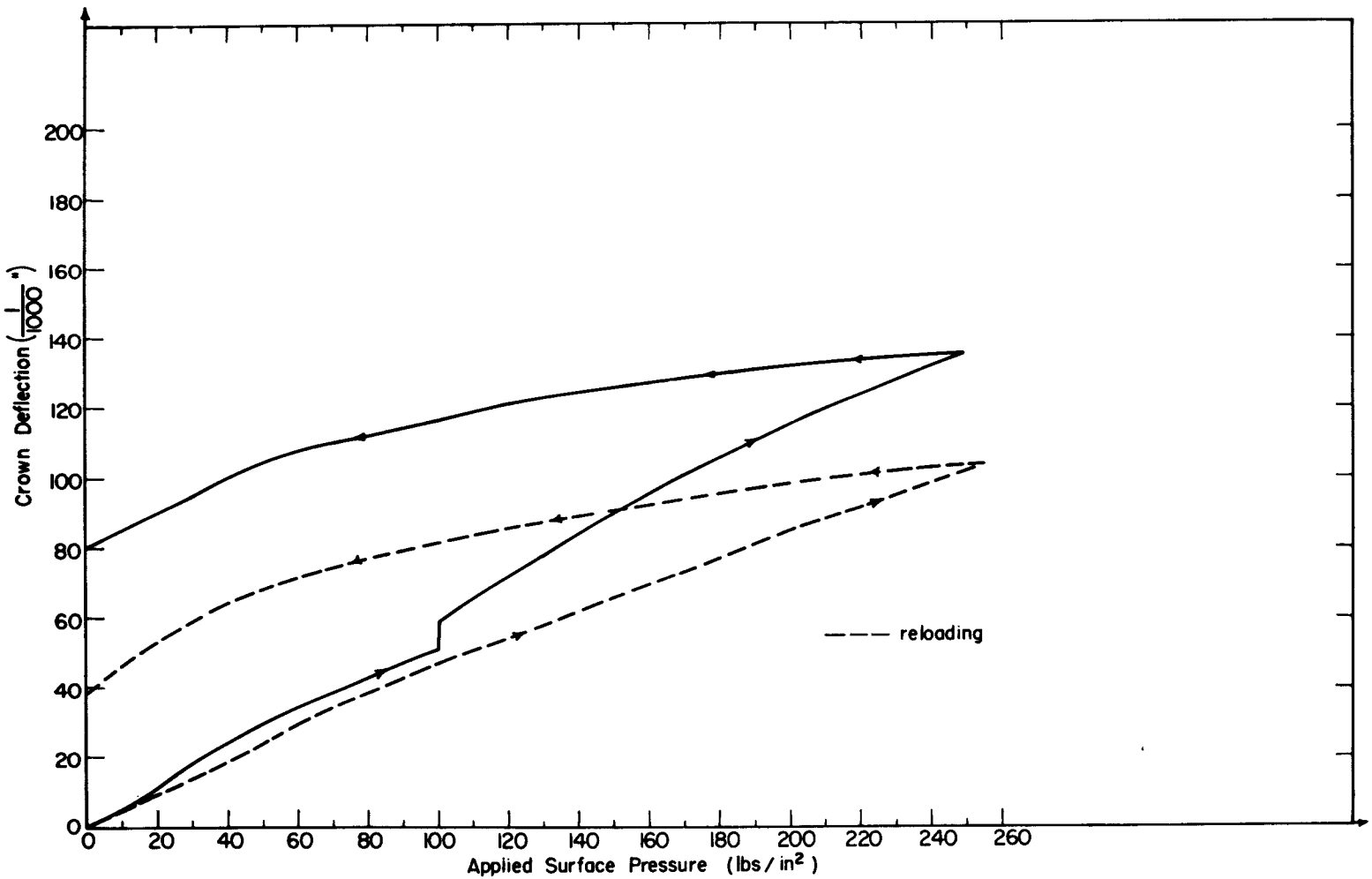

FIGURE E-19 CROWN DEFLECTION vs SURFACE PRESSURE - TEST 4

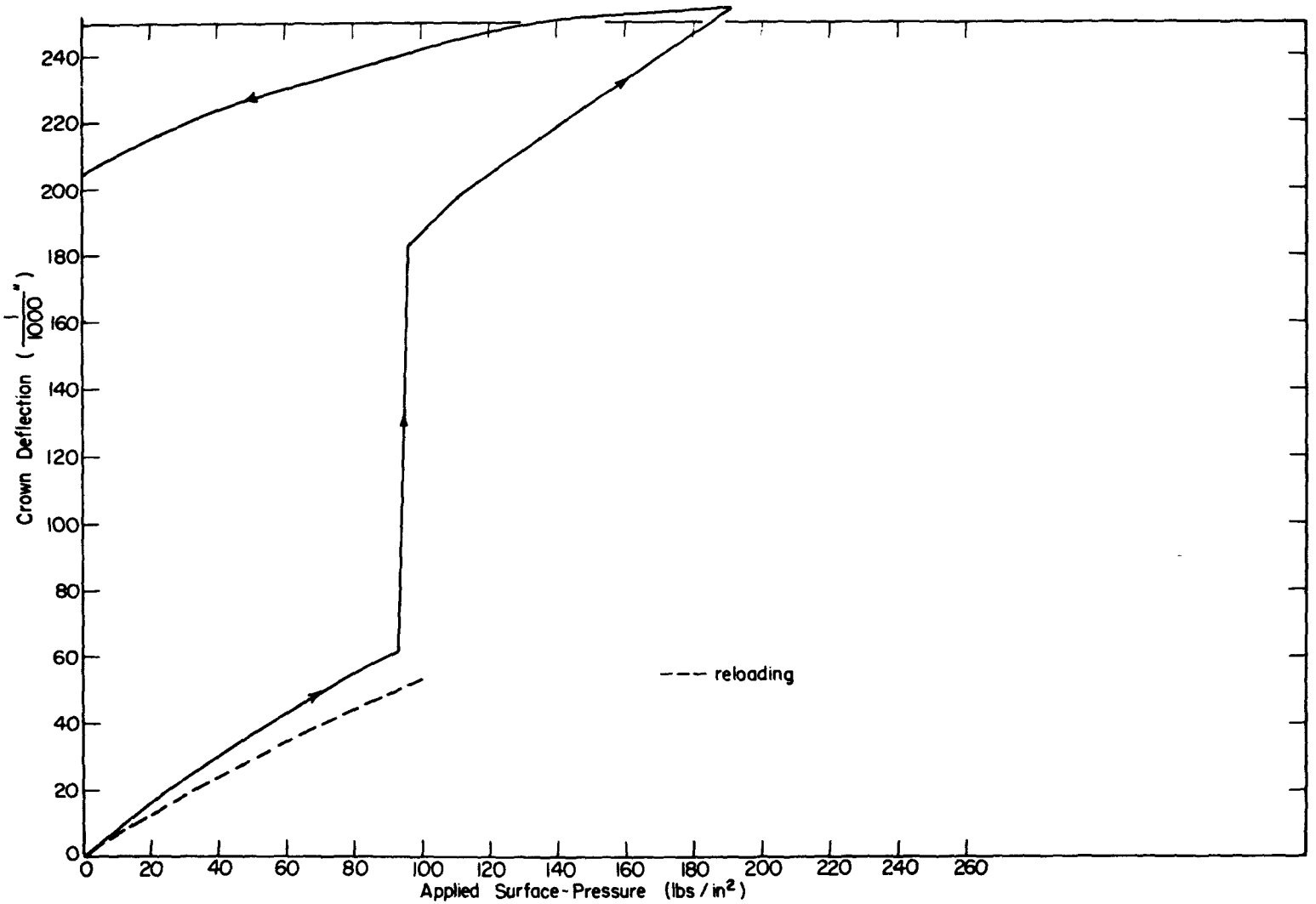

FIGURE E-20 CROWN DEFLECTION vs SURFACE PRESSURE - TEST 5

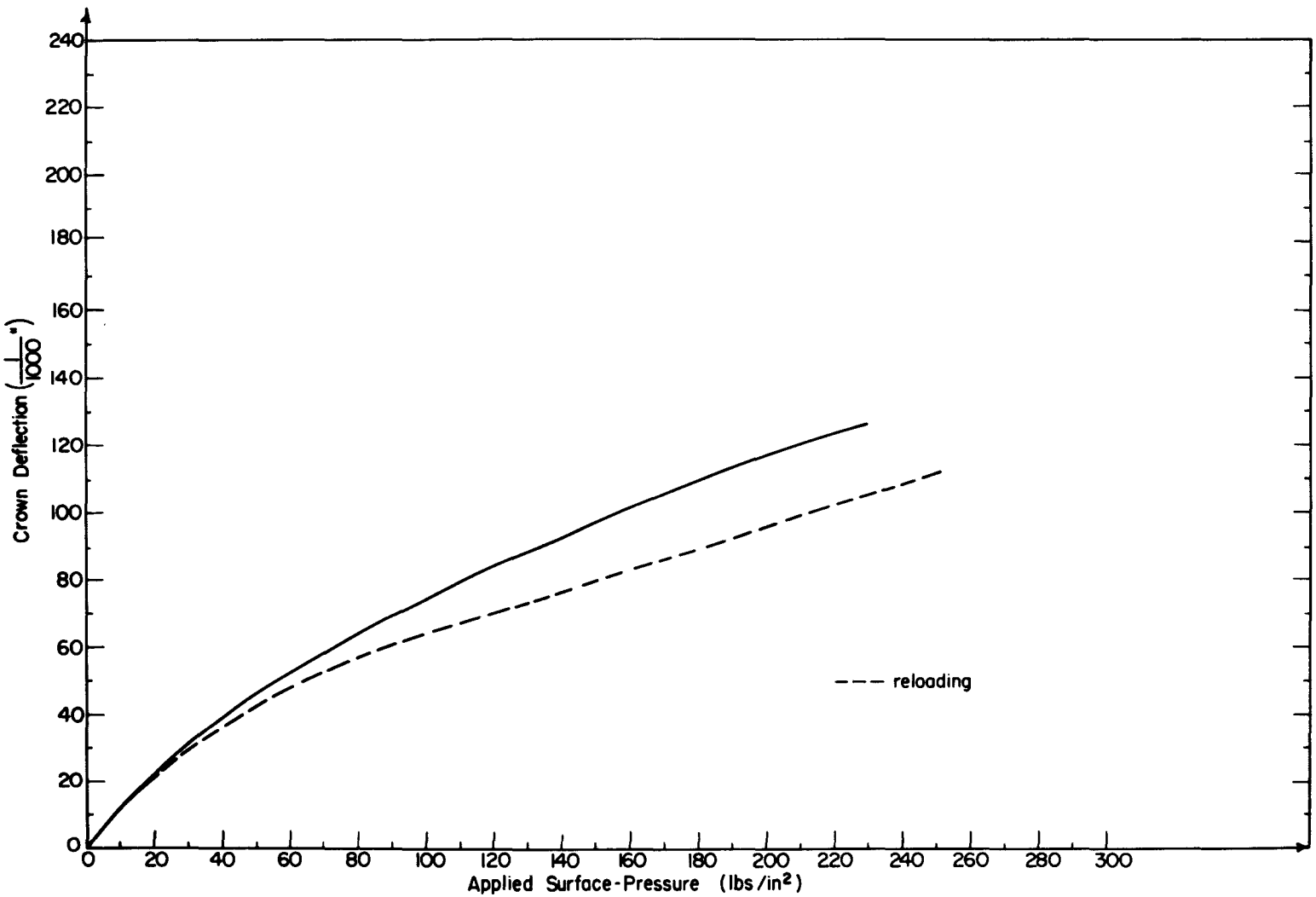

FIGURE E-21 CROWN DEFLECTION vs SURFACE PRESSURE - TEST 7

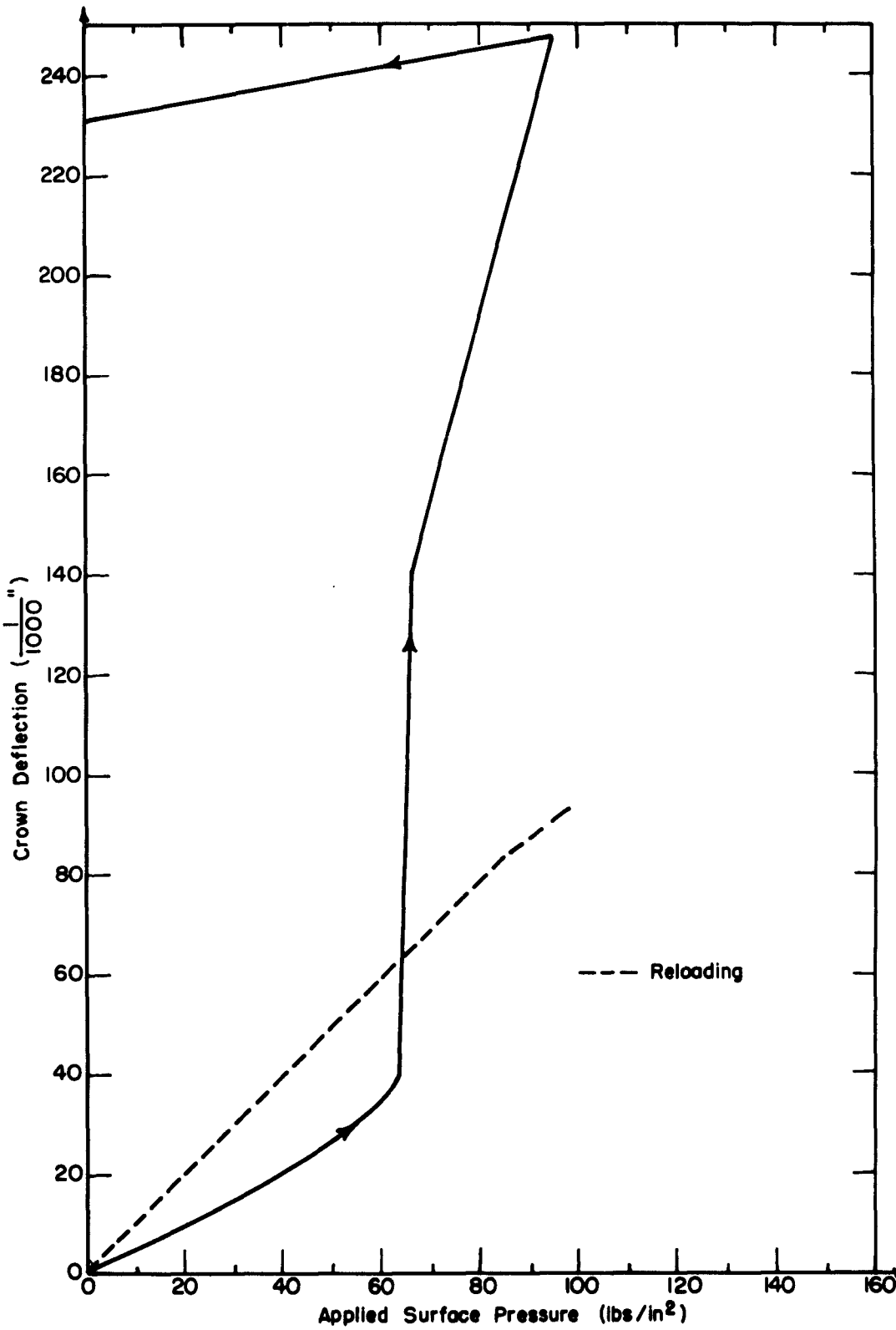

FIGURE E-22 CROWN DEFLECTION vs SURFACE PRESSURE - TEST 9

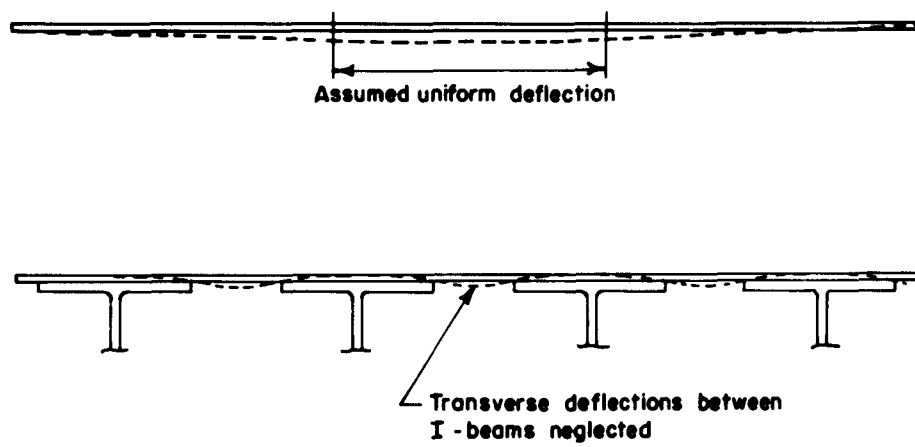

Assumptions described in Section E.4.3.

FIGURE E-23 DEFLECTION OF BOTTOM PLATE

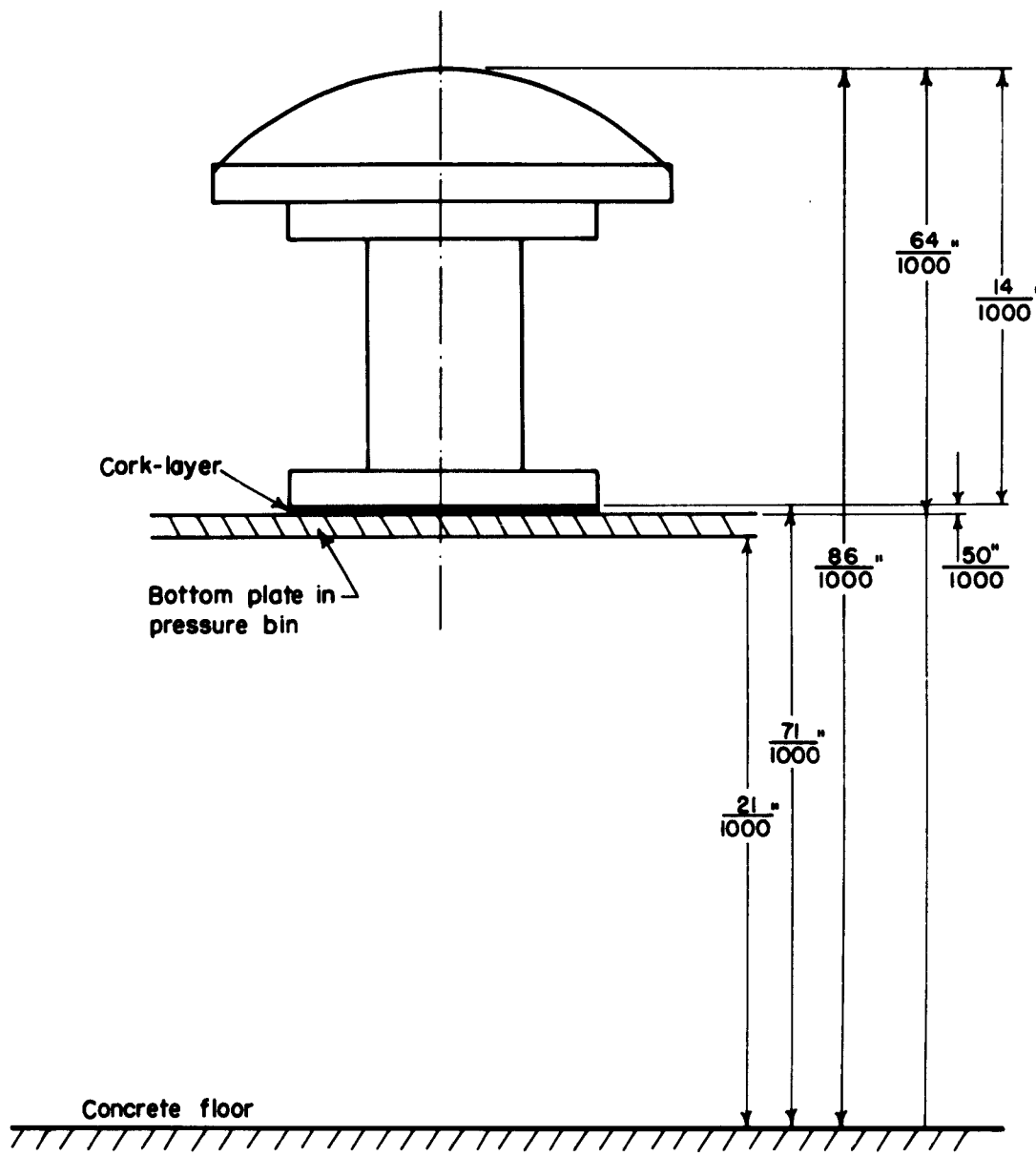

Results from test 7

Deflections and deformations when the average pressure on the dome was 35 lbs/in^2

FIGURE E-24 CONTRIBUTIONS TO CROWN DEFLECTION

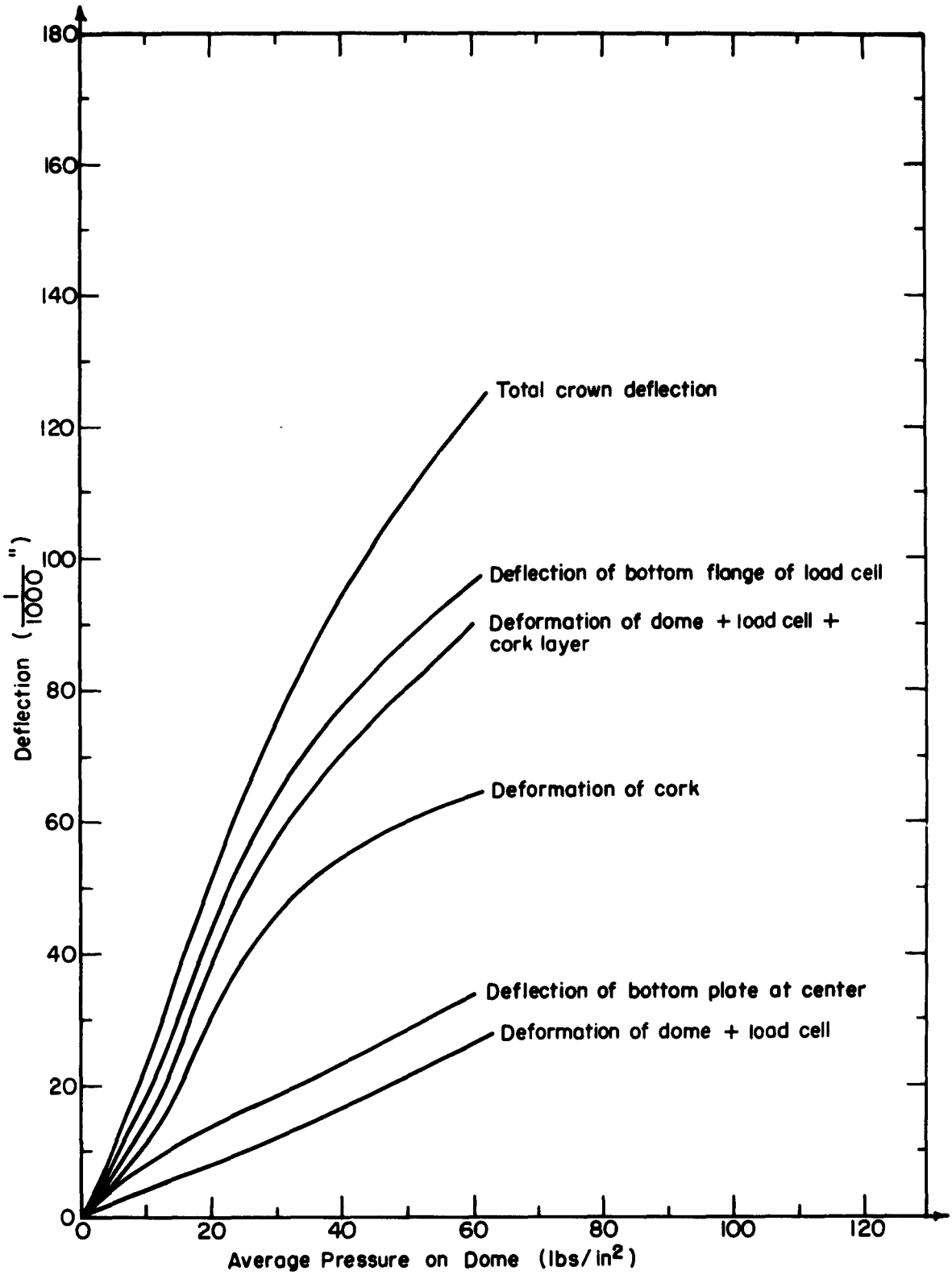

FIGURE E-25 CONTRIBUTIONS TO CROWN DEFLECTION - TEST 7

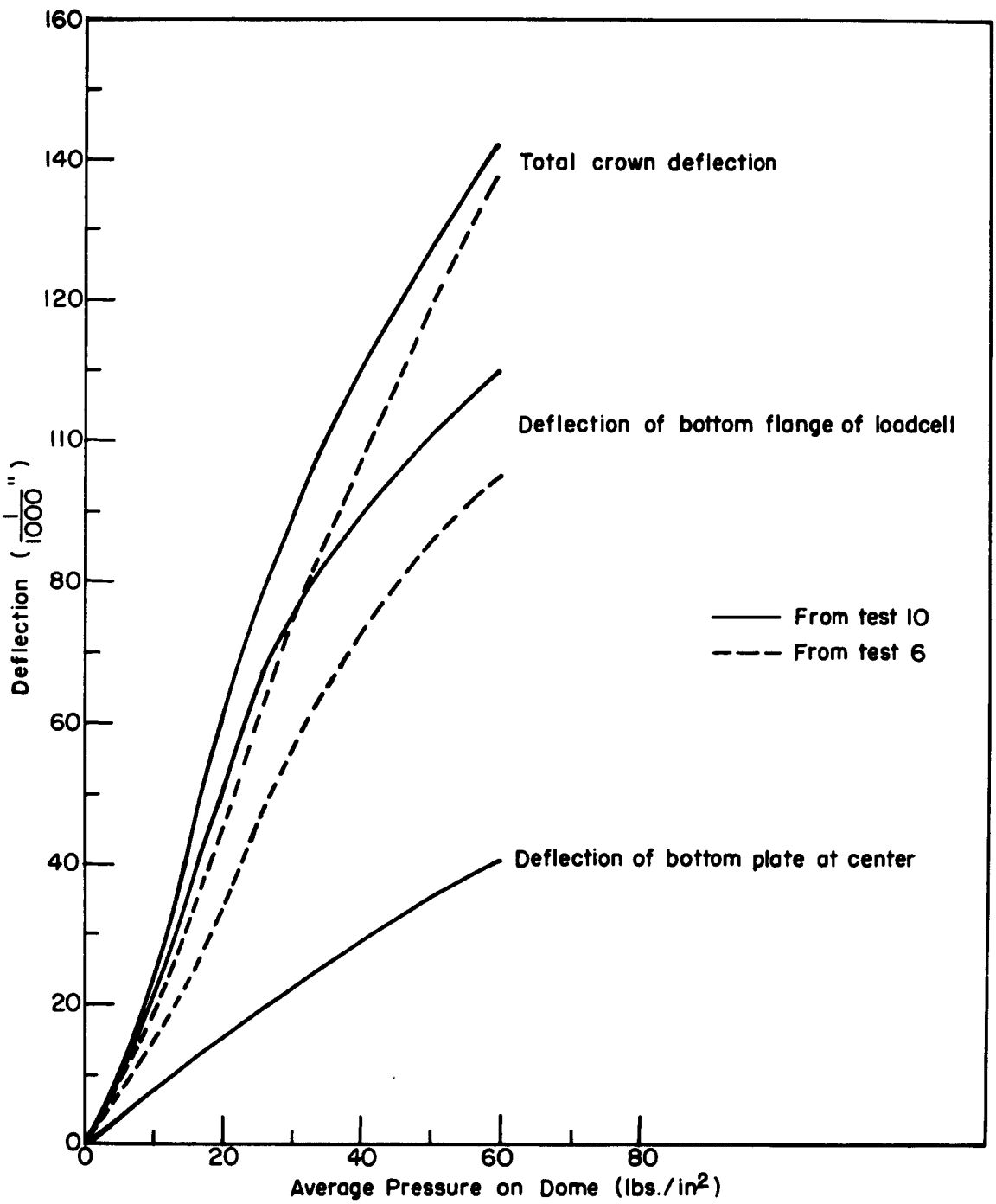

FIGURE E-26 CONTRIBUTIONS TO CROWN DEFLECTION TESTS 6 & 10

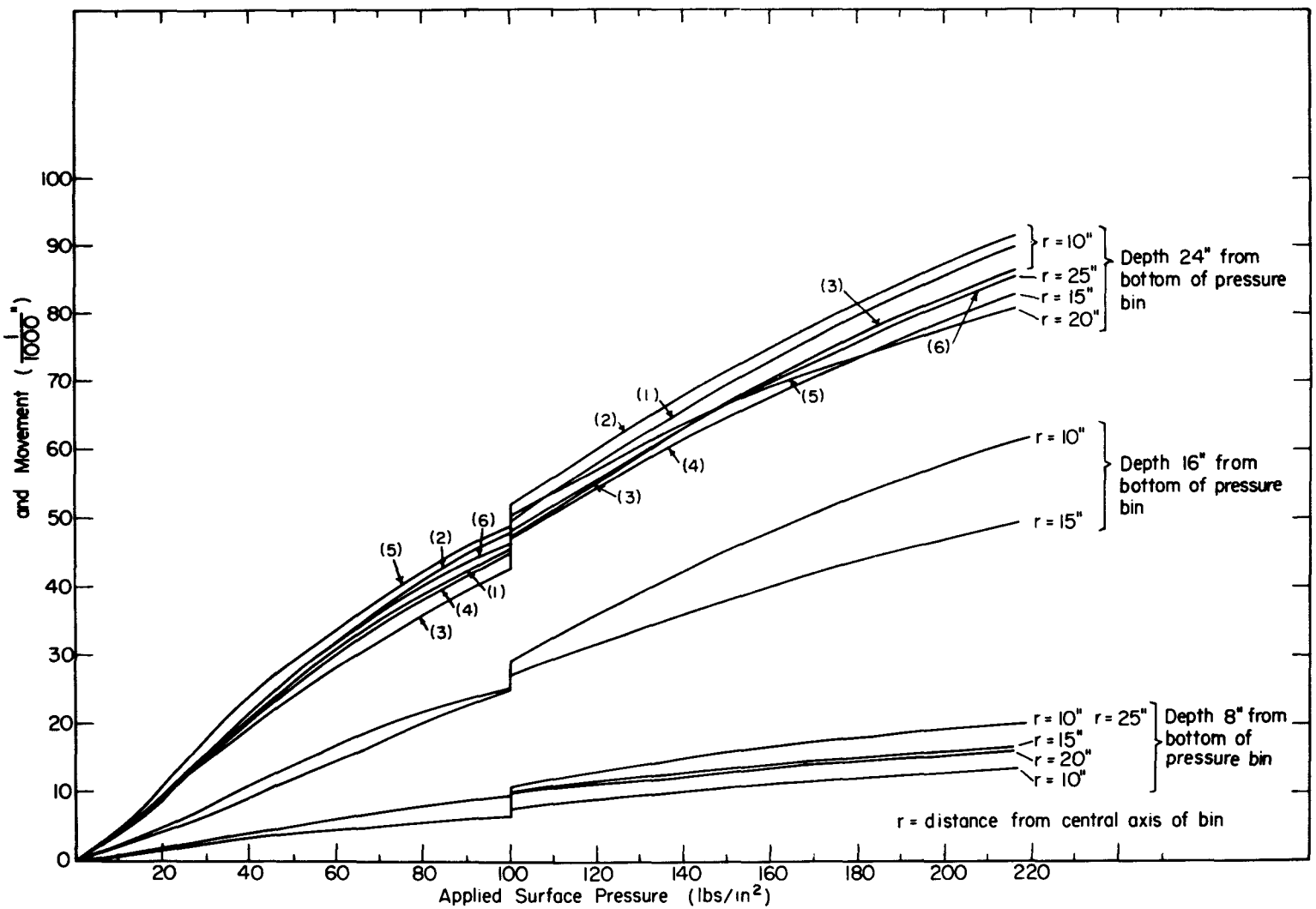

FIGURE E-27 SAND MOVEMENTS - TEST 4

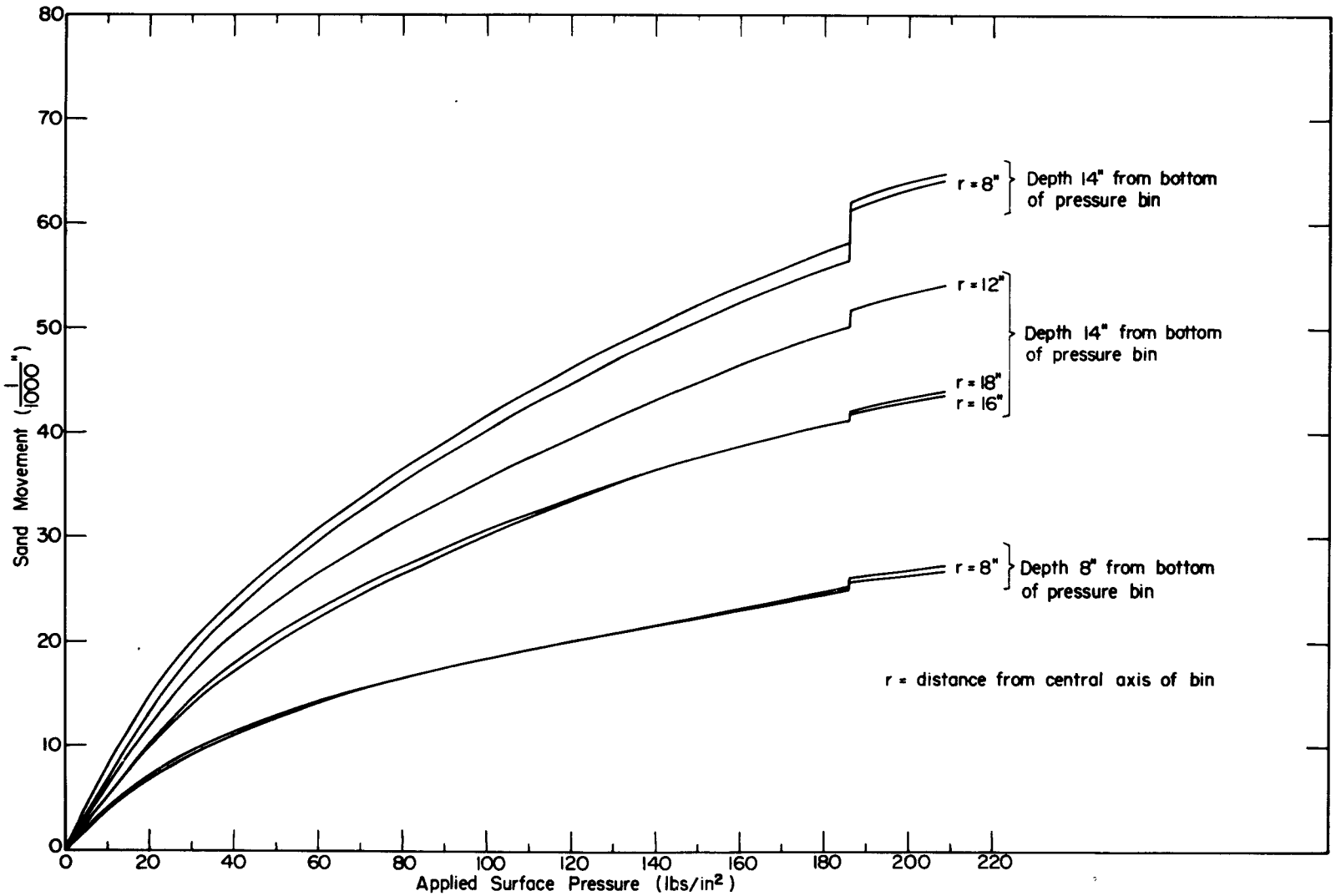

FIGURE E-28 SAND MOVEMENTS - TEST 6

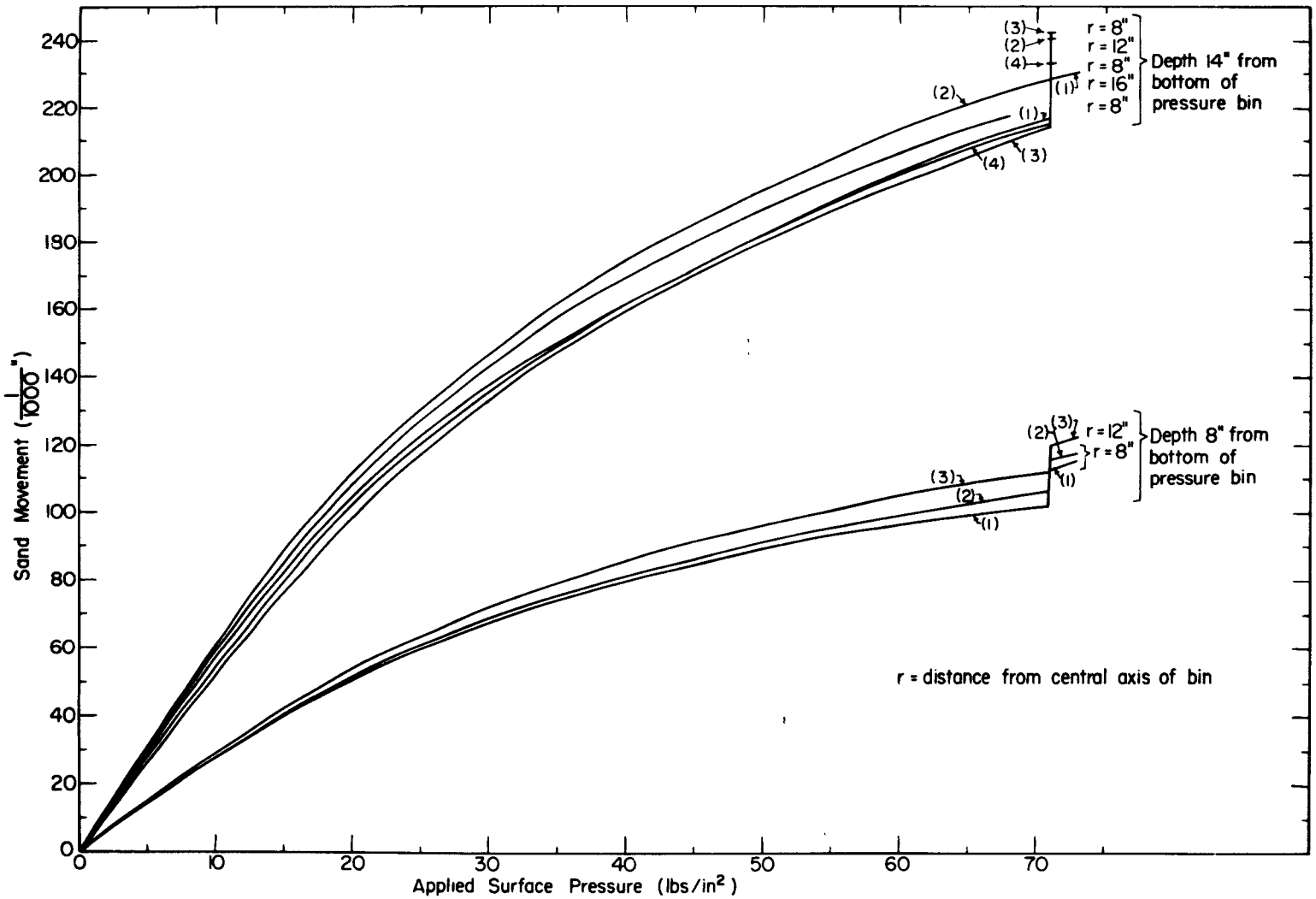

FIGURE E-29 SAND MOVEMENTS - TEST 8

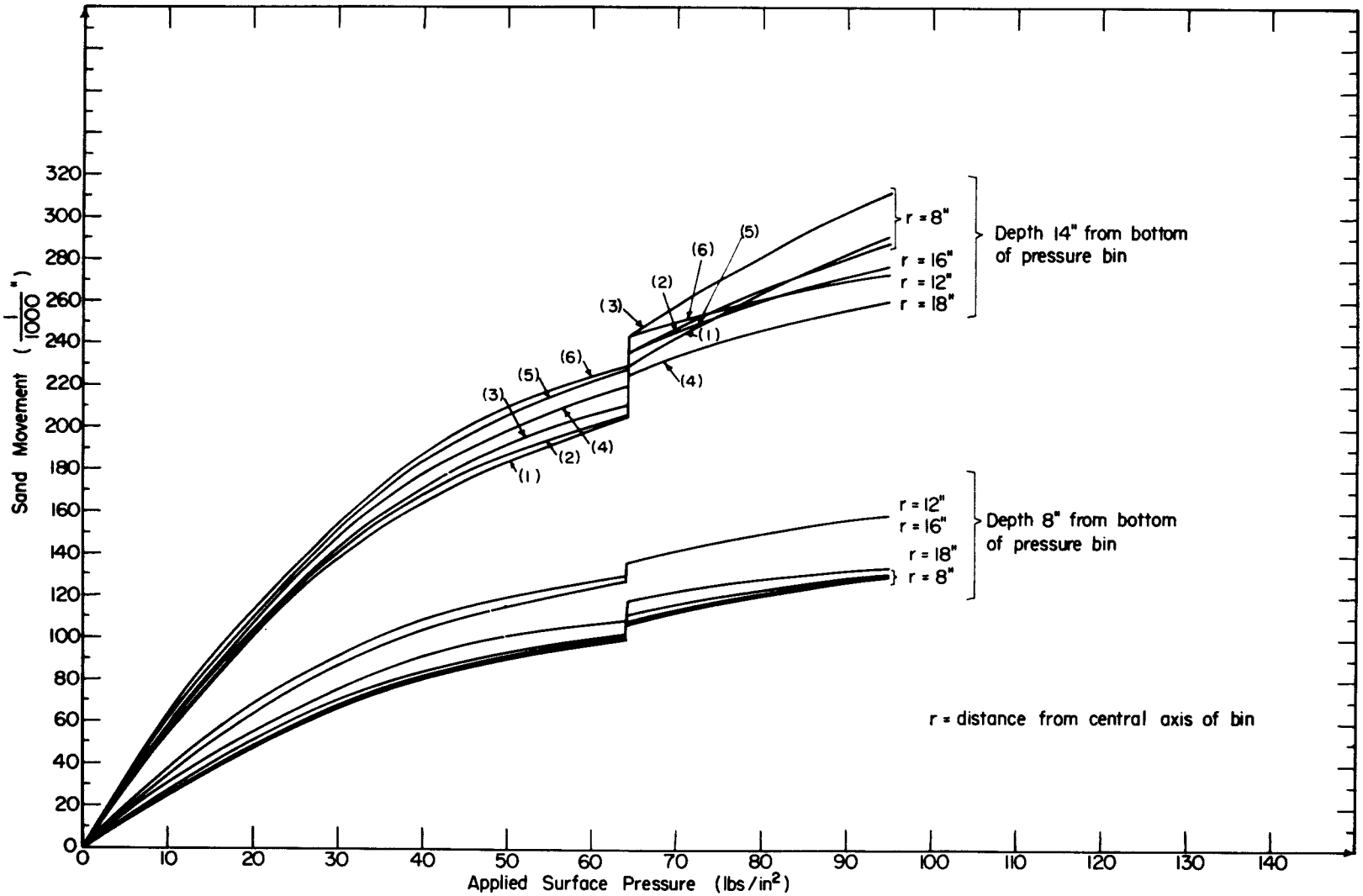

FIGURE E-30 SAND MOVEMENTS - TEST 9

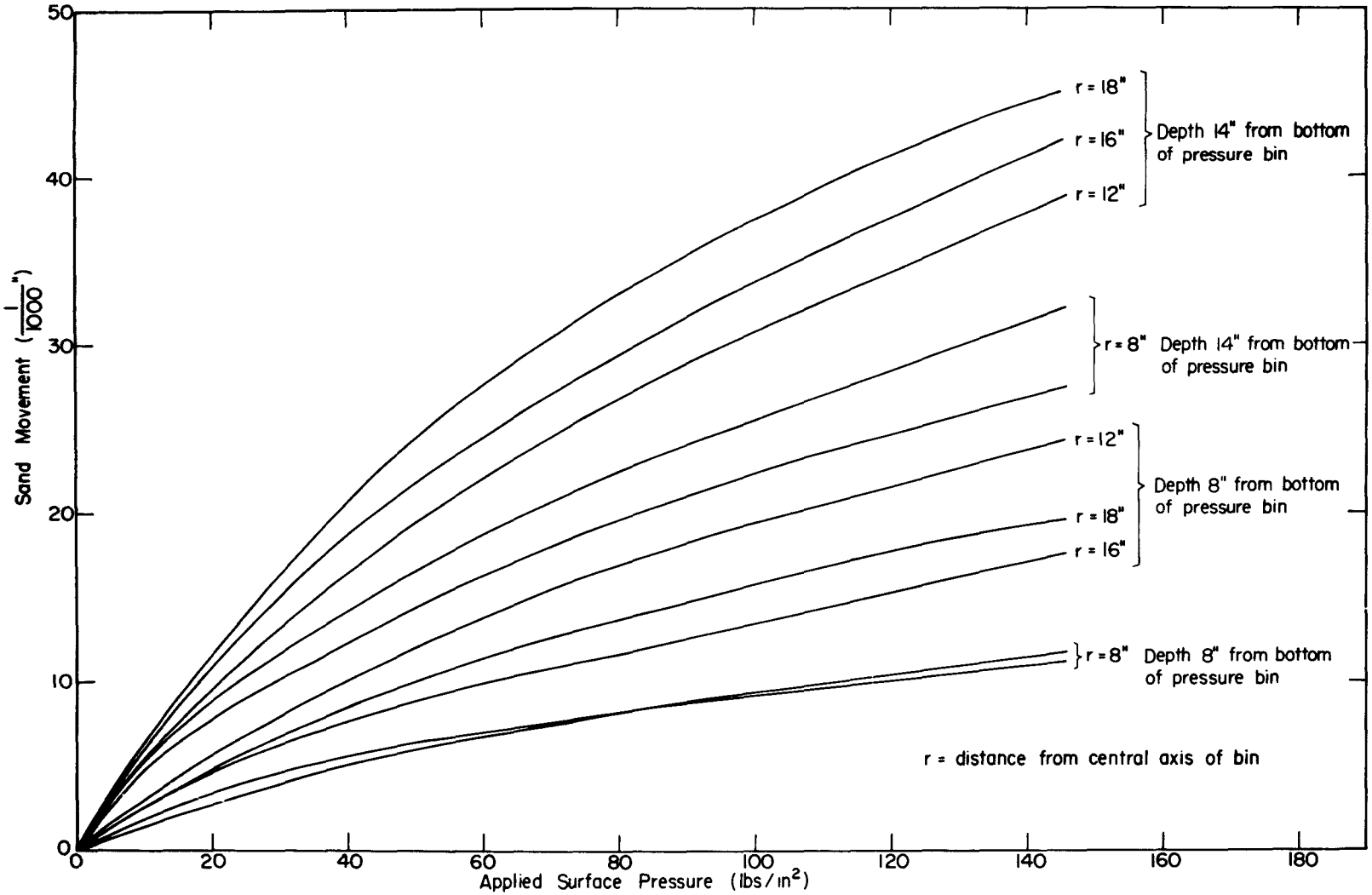

FIGURE E-31 SAND MOVEMENTS - TEST II

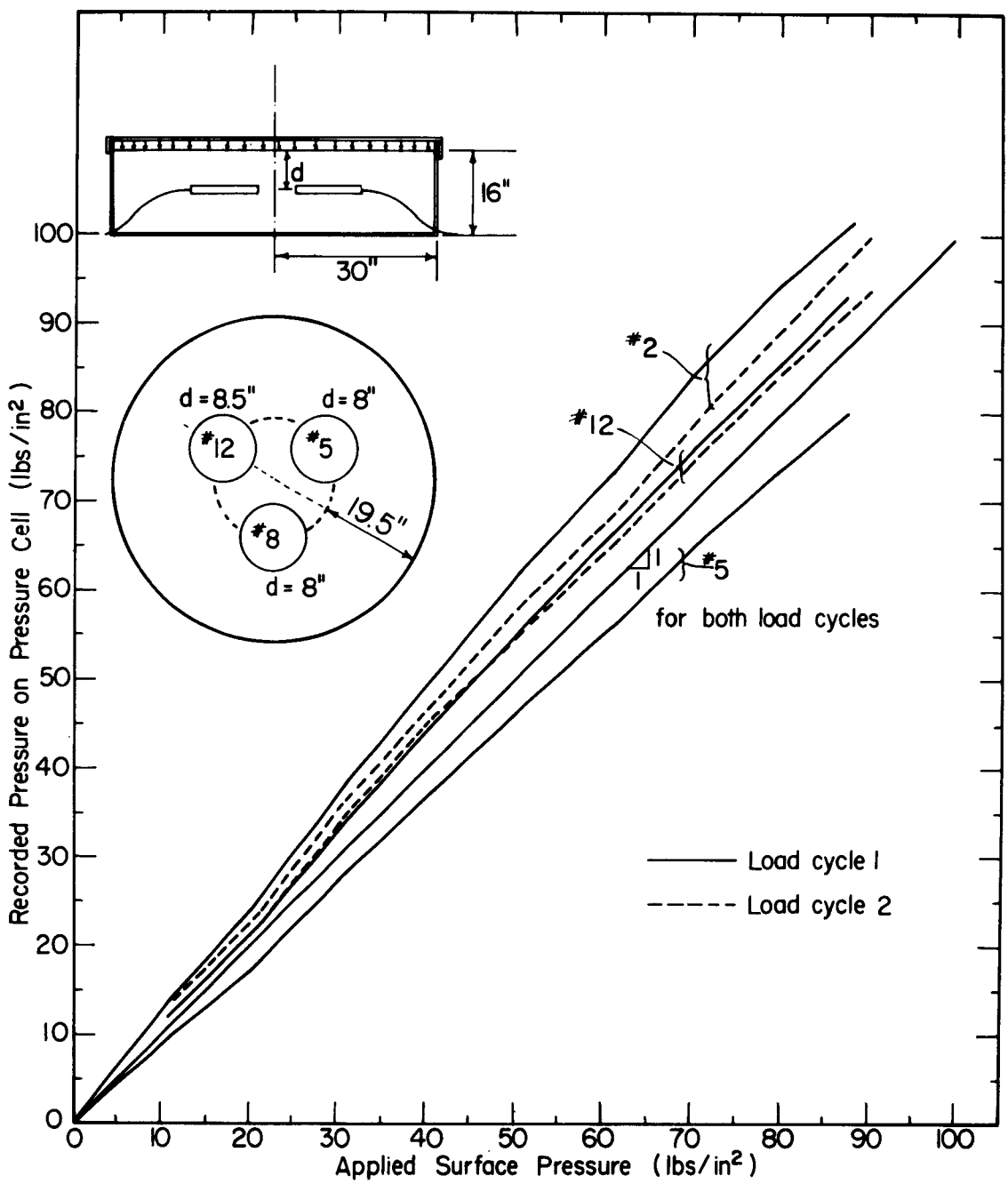

FIGURE E-32 TEST WITH W.E.S.-PRESSURE CELLS

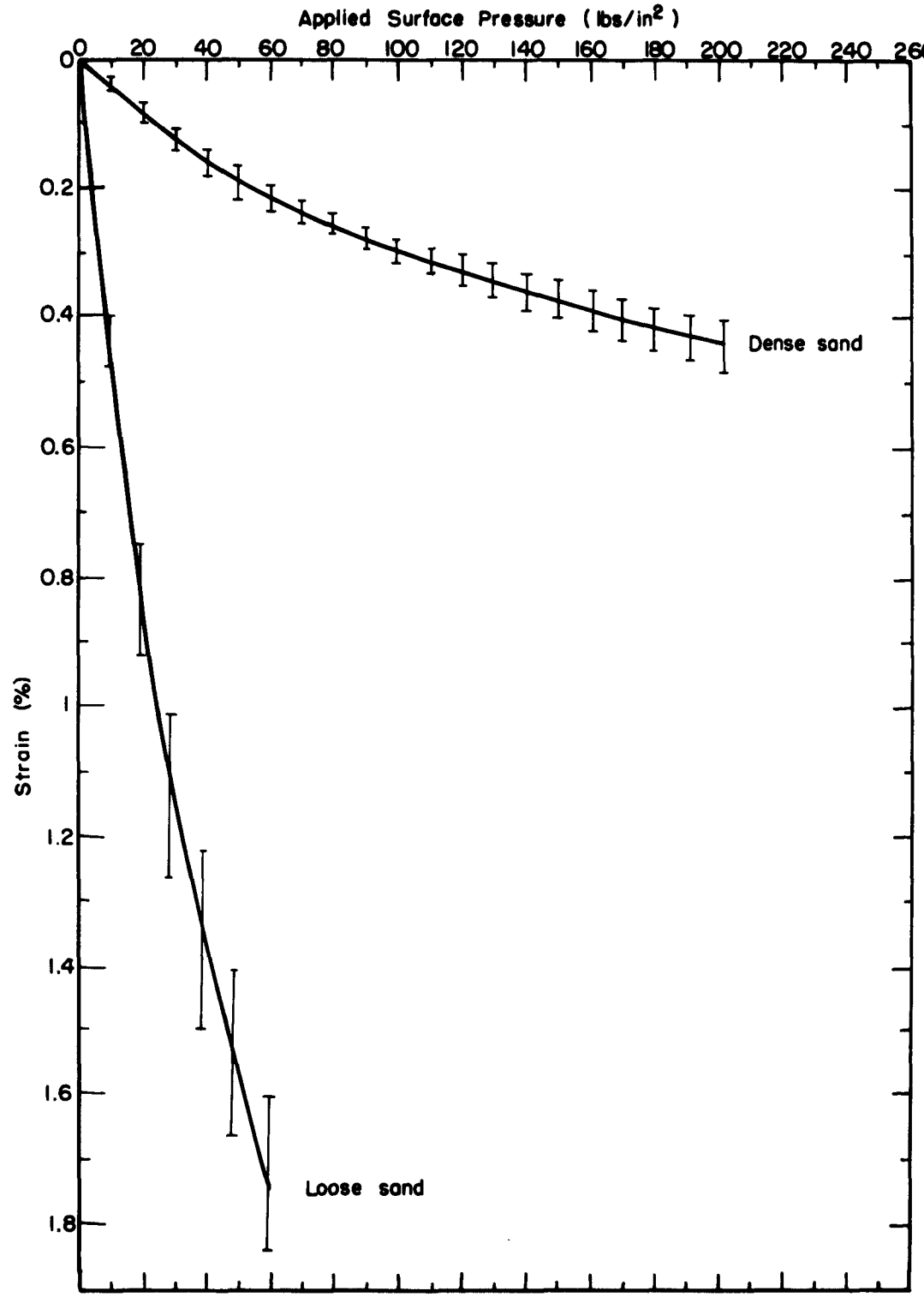

FIGURE E-33 COMPRESSIBILITY OF SAND

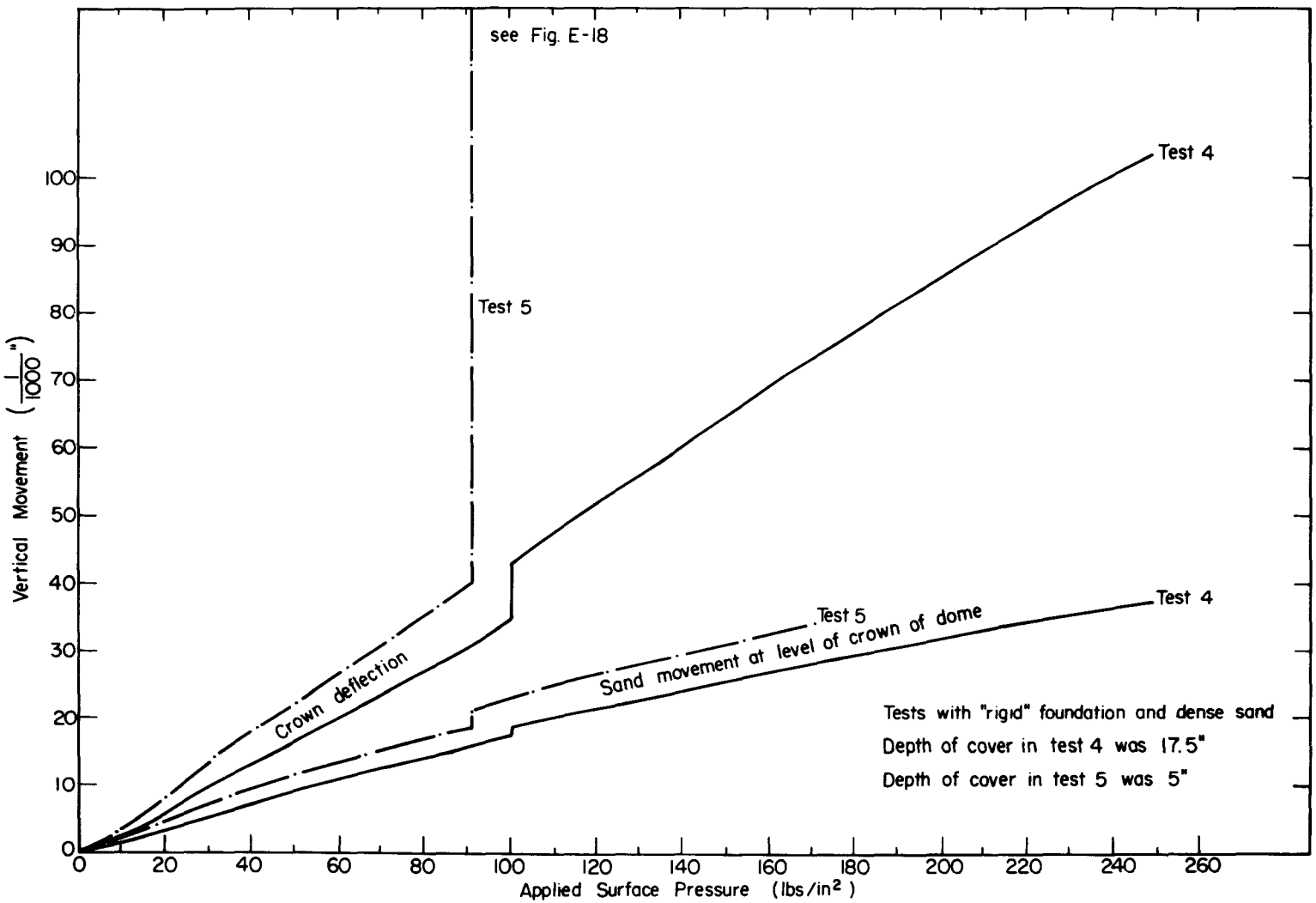

FIGURE E-34 COMPARISON BETWEEN CROWN DEFLECTION AND SAND MOVEMENT - TESTS 4 and 5

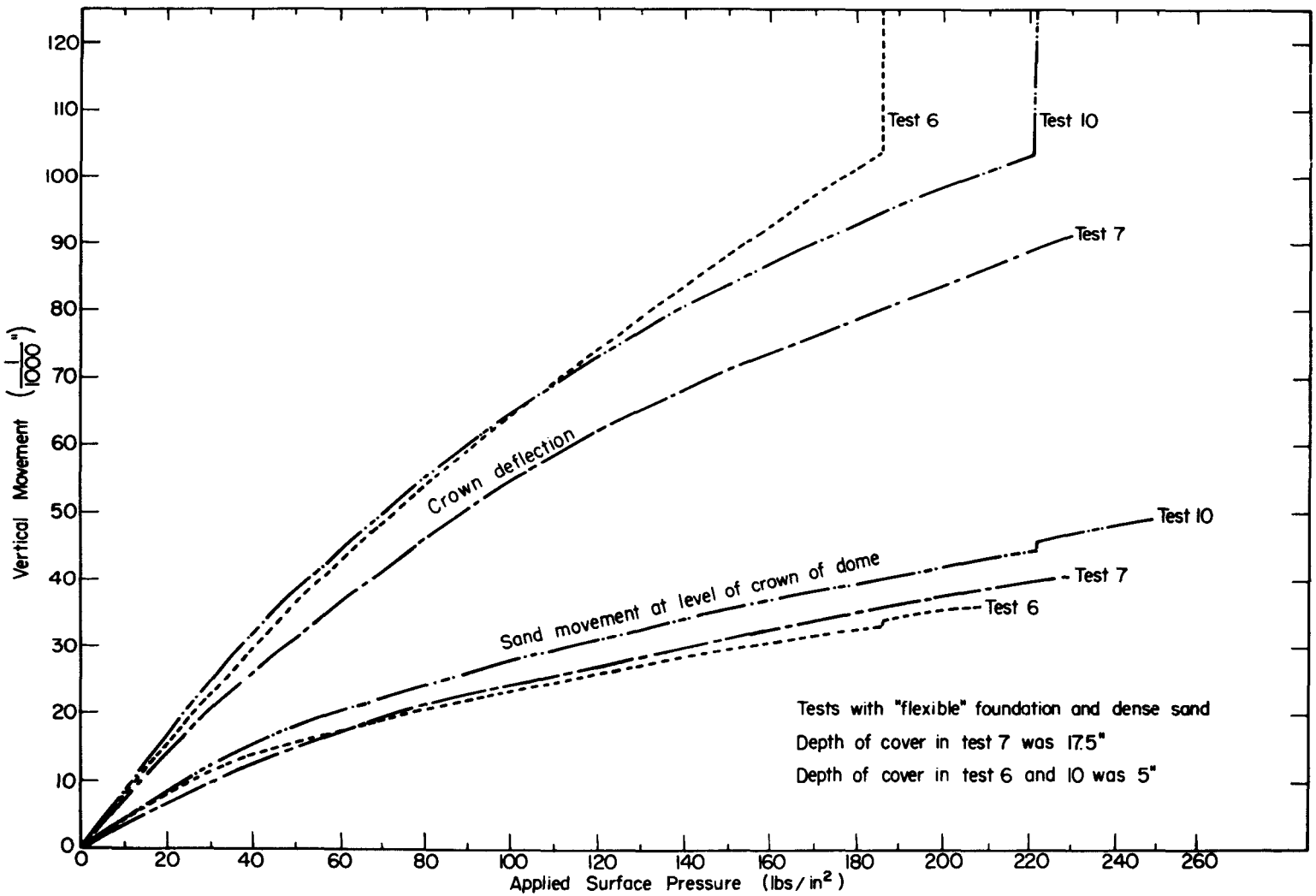

FIGURE E-35 COMPARISON BETWEEN CROWN DEFLECTION AND SAND MOVEMENT - TESTS 6, 7 and 10

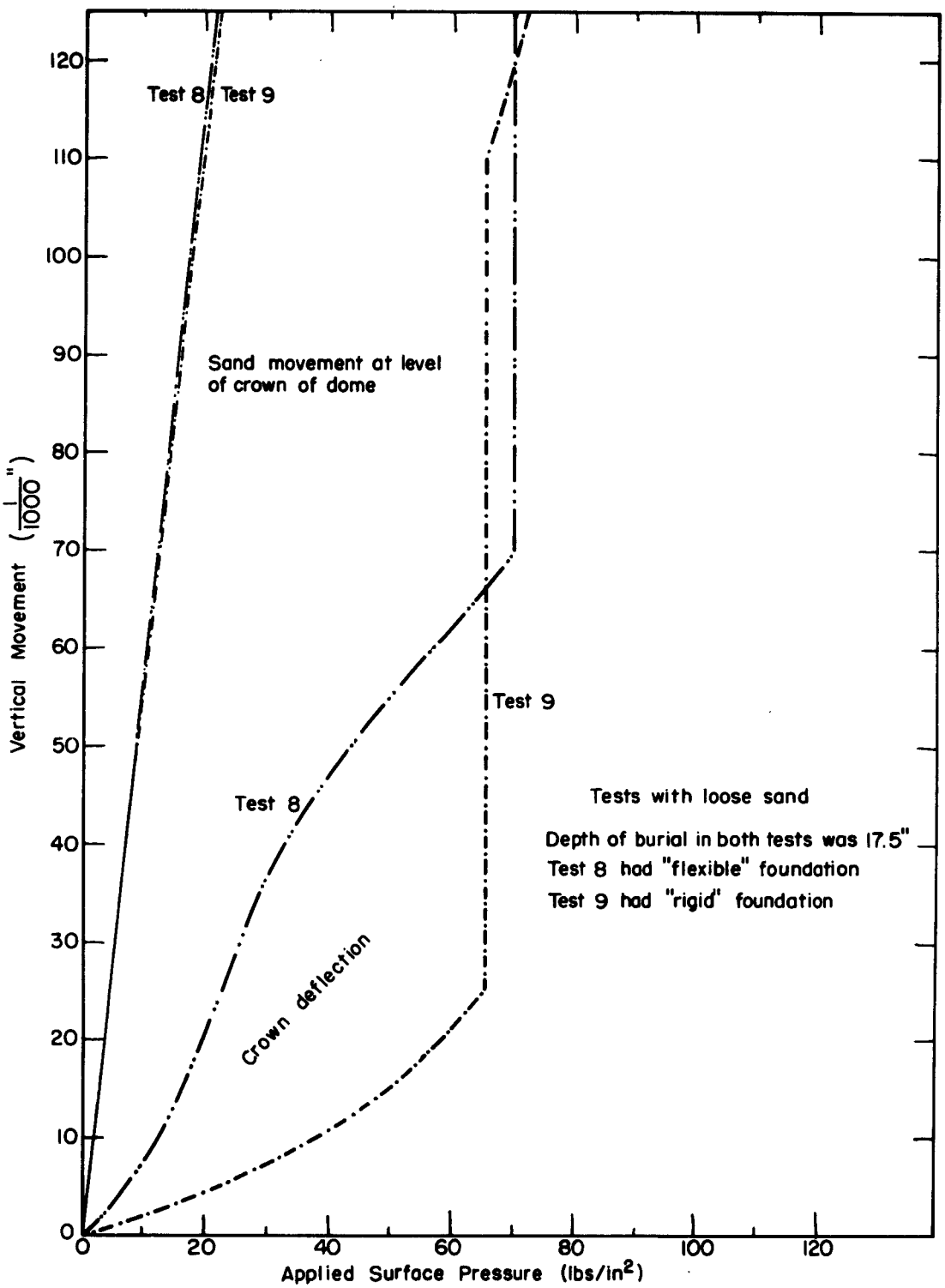

FIGURE E-36 COMPARISON BETWEEN CROWN DEFLECTION AND SAND MOVEMENT - TEST 8 & 9

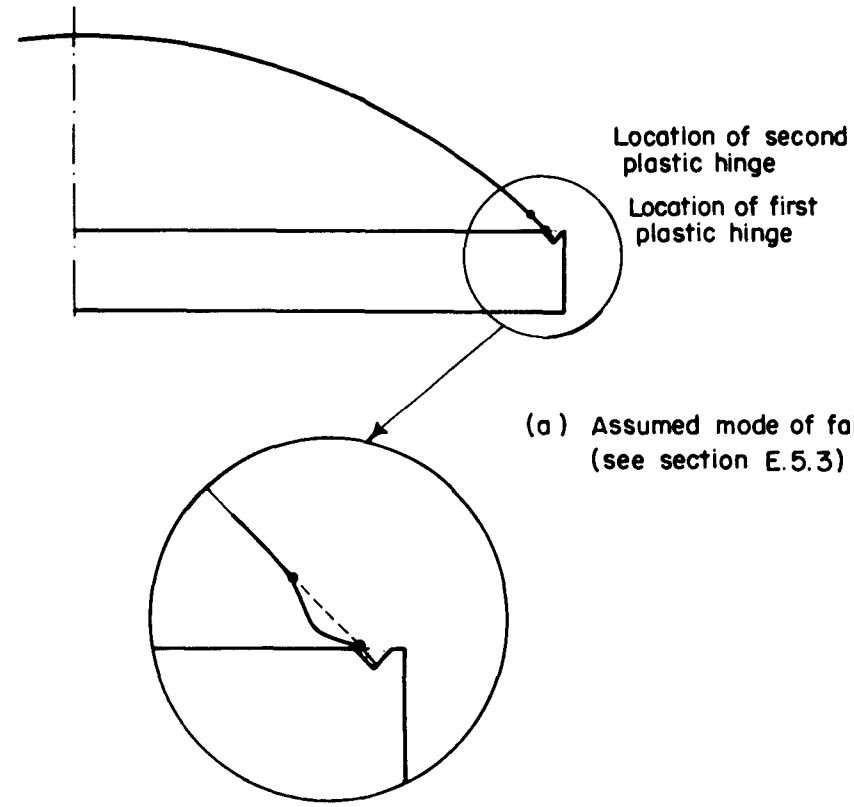

(a) Assumed mode of failure (see section E.5.3)

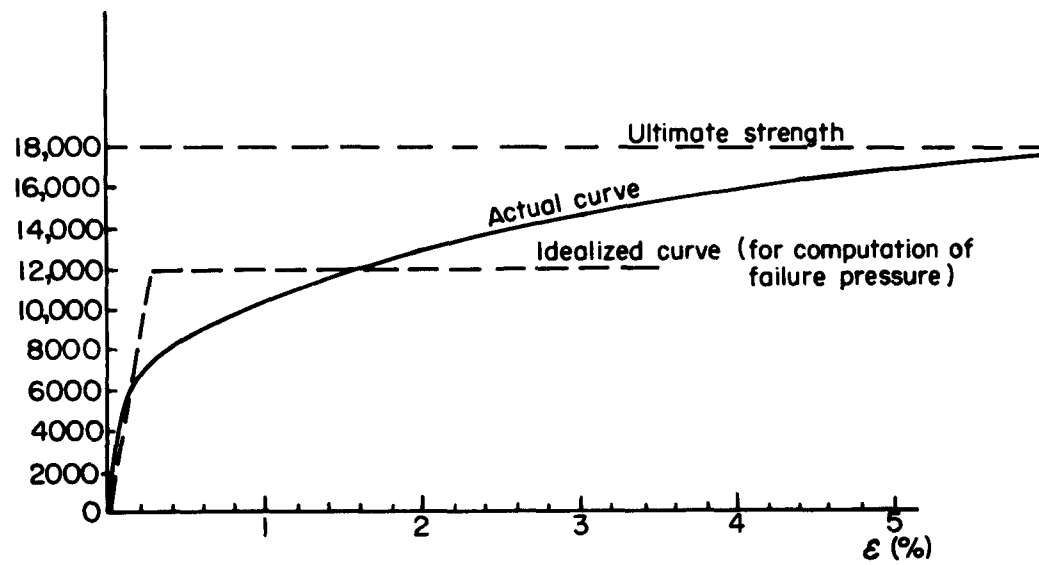

(b) Idealized stress-strain diagram for the aluminum

FIGURE E-37 ASSUMED FAILURE MODE

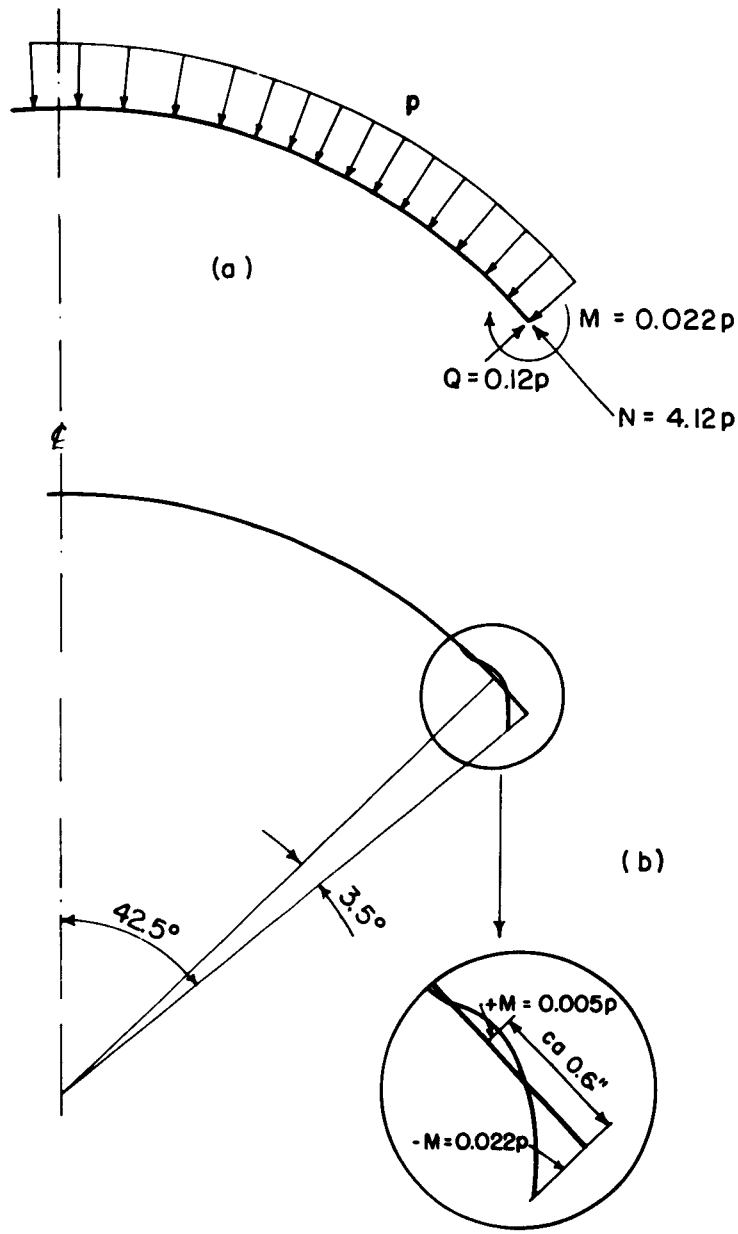

See section E. 5. 3

FIGURE E-38 COMPUTATIONS FOR PREDICTION OF FAILURE PRESSURE

COMPUTATION OF STRESSES IN DOME IN TEST 7

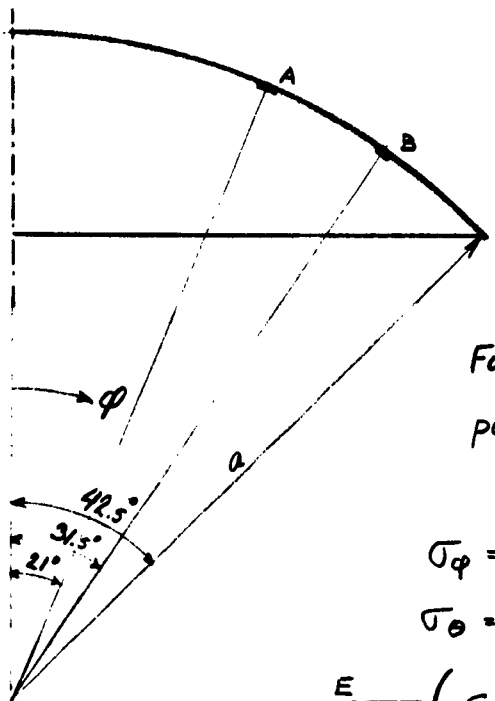

For magnitudes of strains at points A and B, see TABLE E.2

σ_φ = meridional stress

σ_θ = latitudinal stress

$$\sigma_\varphi = \frac{E}{1-\nu^2}\left(\varepsilon_\varphi + \nu\varepsilon_\theta\right)$$

$$\sigma_\theta = \frac{E}{1-\nu^2}\left(\varepsilon_\theta + \nu\varepsilon_\varphi\right)$$

For aluminum : $E = 10 \times 10^6 \frac{lbs}{in^2}$ (initially) $\quad \nu = \frac{1}{3}$

Theoretical values of stresses in the dome:

For a 'snow' load type distribution of contact pressure, membrane solution :

$$\sigma_\varphi = -\frac{pa}{2t} \qquad \sigma_\theta = \frac{pa}{2t}\cos 2\varphi$$

at $\varphi = 21°$; $\frac{\sigma_\theta}{\sigma_\varphi} = 0.74$ at $\varphi = 31.5°$; $\frac{\sigma_\theta}{\sigma_\varphi} = 0.45$

FIGURE E-39

Computed values of stress based on recorded strains:

At a surface pressure of 19 $\frac{lbs}{in^2}$:

$$\sigma_{\varphi_{21^\circ}} = \frac{10\times10^6}{0.89}\left(158 + \tfrac{1}{3}82\right)10^{-6}\ \frac{lbs}{in^2} = 2080\ \frac{lbs}{in^2}$$

$$\sigma_{\theta_{21^\circ}} = \frac{10\times10^6}{0.89}\left(82 + \tfrac{1}{3}158\right)10^{-6}\ \frac{lbs}{in^2} = 1520\ \frac{lbs}{in^2}$$

hence at $\varphi = 21^\circ$; $\frac{\sigma_\theta}{\sigma_\varphi} = \frac{1520}{2080} = 0.74$

No latitudinal strains were recorded at $\varphi = 31.5^\circ$. Assuming that the theoretical value of the ratio $\frac{\sigma_\theta}{\sigma_\varphi}$ also holds at this point, the meridional stress is computed at $\varphi = 31.5^\circ$:

$$\sigma_{31.5^\circ} = \frac{10\times10^6}{0.89}\left(168 + \tfrac{1}{3}(0.45)168\right)10^{-6}\ \frac{lbs}{in^2} = 2160\ \frac{lbs}{in^2}$$

hence, $\sigma_{\varphi_{21^\circ}} \approx \sigma_{\varphi_{31.5^\circ}}$

At a surface pressure of 48 $\frac{lbs}{in^2}$:

$$\sigma_{\varphi_{21^\circ}} = \frac{10\times10^6}{0.89}\left(341 + \tfrac{1}{3}179\right)10^{-6}\ \frac{lbs}{in^2} = 4520\ \frac{lbs}{in^2}$$

$$\sigma_{\theta_{21^\circ}} = \frac{10\times10^6}{0.89}\left(179 + \tfrac{1}{3}341\right)10^{-6}\ \frac{lbs}{in^2} = 3300\ \frac{lbs}{in^2}$$

hence at $\varphi = 21^\circ$; $\frac{\sigma_\theta}{\sigma_\varphi} = \frac{3300}{4520} = 0.73$

FIGURE E-39 (cont'd)

Computing $\sigma_{\varphi\ 31.5°}$, using same assumption as above;

$$\sigma_{\varphi\ 31.5°} = \frac{10 \times 10^6}{0.89}\left(364 + \tfrac{1}{3}(0.45)\,364\right)10^{-6}\ \frac{lbs}{in^2} = 4700\ \frac{lbs}{in^2}$$

hence $\sigma_{\varphi\ 21°} \approx \sigma_{\varphi\ 31.5°}$

Magnitude of contact pressure between sand and dome, back-figured from the strain recordings.

Now assuming that a "snow" load type distribution of pressure took place;

$$\sigma_\varphi = \frac{pa}{2t}$$

At a surface pressure of 14 $\frac{lbs}{in^2}$:

σ_φ was computed on the preceding page,

$\sigma_\varphi = 2080\ \frac{lbs}{in^2}$

giving: $p = \frac{\sigma_\varphi\, 2t}{a} = 10.5\ \frac{lbs}{in^2}$

compared to $p = 9.5\ \frac{lbs}{in^2}$ as recorded by load cell.

At a surface pressure of 48 $\frac{lbs}{in^2}$:

$\sigma_\varphi = 4520\ \frac{lbs}{in^2}$

giving: $p = \frac{\sigma_\varphi\, 2t}{a} = 24\ \frac{lbs}{in^2}$

compared to $p = 18\ \frac{lbs}{in^2}$ as recorded by load cell.

Since the modulus of elasticity for aluminum remains

FIGURE E-39 (cont'd)

constant only over the very initial portion of the stress - strain diagram, no computation of stresses have been made for higher surface pressures.

FIGURE E-39 (cont'd)

DISTRIBUTION LIST

Addresses	No. of Copies
Bureau of Mines, Washington, D. C., Attn: J. E. Crawford	1
Chief, Bureau of Yards and Docks, ND, Washington 25, D. C. Attn: D-440	1
Chief, Defense Atomic Support Agency, Washington 25, D. C. Attn: Document Library Attn: Major Vickery	12 1
Chief of Engineers, Department of the Army, Washington 25, D. C. Attn: ENGTE-E Attn: ENGMC-EB	 1 2
Chief of Naval Operations, ND, Washington, D. C. Attn: Op-75	1
Chief of Research and Development, DA, Washington 25, D.C. Attn: Atomic Division	1
Commander, Air Force Ballistic Missile Division, Air Research and Development Command, Attn: WDFN, P. O. Box 262, Inglewood 49, California	1
Commander, Armed Services Technical Information Agency (ASTIA), Arlington Hall Station, Arlington 12, Va.	20
Commander, Air Force Special Weapons Center, Kirtland Air Force Base, Albuquerque, N. M., Attn: SWRS	4
Commander, Wright Air Development Center, Wright-Patterson Air Force Base, Ohio, Attn: WCOSI	1
Command General, U. S. Army Materiel Command, Attn: AMCRD-RS-ES, Room 2507, Building T-7, Washington 25, D. C.	3
Commanding Officer and Director, U. S. Naval Civil Engineering Laboratory, Port Hueneme, Calif.	1
Director, Weapons Systems Evaluation Group OSD, Room 1E880, The Pentagon, Washington 25, D. C.	1

Director, U. S. Army Engineer Waterways Experiment Station, P. O. Box 631, Vicksburg, Miss. 25

Director of Civil Engineering, Headquarters, U. S. Air Force, Washington 25, D. C., Attn: AFOCE

Director of Defense Research and Engineering, Washington 25, D. C., Attn: Technical Library 1

Headquarters, U. S. Air Force, Washington 25, D. C., Attn: AFTAC, C. F. Romney 2

Space Technology Laboratory, Inglewood, Calif., Attn: B. Sussholz 1

U. S. Coast and Geodetic Survey, Washington, D. C. Attn: D. S. Gardner 1

U. S. Coast and Geodetic Survey, San Francisco, Calif. Attn: W. K. Cloud 1

U. S. Geological Survey, Washington, D. C., Attn: J. R. Balsley 1

California Institute of Technology, Pasadena, Calif.
Attn: F. Press 1
Attn: R. Benioff 1

Columbia University, New York, N.Y., Attn: J. E. Oliver 1

Pennsylvania State College, Atomic Defense Engineering Dept., State College, Pa., Attn: Prof. Albright 1

Stanford Research Institute, Physical Sciences Division Menlo Park, Calif., Attn: Dr. R. B. Vaille, Jr. 2

American Machine and Foundry, 7501 North Natchez Avenue, Niles 48, Ill., Attn: Mr. Tom Morrison 1

Barry Wright Corporation, 700 Pleasant St., Watertown 72, Mass., Attn: Mr. Cavanaugh 1

Holmes and Narvey, Los Angeles, Calif., Attn: S. B. Smith 1

Dr. Harold Brode, RAND Corporation, 1700 Main Street, Santa Monica, Calif. 1

Dr. N. M. Newmark, Civil Engineering Hall, University of Illinois, Urbana, Illinois 1

Dr. T. H. Schiffman, Armour Research Foundation, Illinois Institute of Technology, Technology Center, Chicago 16, Ill. 1

Prof. F. E. Richart, Jr., Dept. of Civil Engineering, University of Michigan, Ann Arbor, Michigan 1

Prof. Robert L. Kondner, The Technological Institute, Northwestern University, Evanston, Ill. 1

Prof. Gerald A. Leonards, School of Civil Engineering Purdue University, Lafayette, Indiana 1

Prof. H. Bolton Seed, Dept. of Civil Engineering, University of California, Berkeley, Calif. 1

Prof. H. Neils Thompson, Civil Engineering Dept., University of Texas, Austin 12, Texas 1

Mr. Kenneth Kaplan, United Research Services 1811 Trousdale Drive, Burlingame, Calif. 1

Mr. W. R. Perret, 5112, Sandia Corporation, Sandia Base, Albuquerque, N. M. 1

Mr. Fred Sauer, Physics Department, Stanford Research Institute, Menlo Park, Calif. 1

Mr. A. A. Thompson, Terminal Ballistics Laboratory, Aberdeen Proving Ground, Aberdeen, Md. 1

Mr. C. J. Nuttall of Wilson, Nuttall, Raimond Engineers, Inc., Chestertown, Md. 1

Dr. Grover L. Rogers, Recon, Inc., Box 3622 MSS, Tallahassee, Florida 1

ABSTRACT

Thin-walled domes were buried within a sand mass which was 5 feet in diameter. A uniform static pressure was applied to the top surface of the sand mass. Instrumentation measured the total vertical force reaching the dome, vertical movements of the dome, strains within the dome, and movements within the sand mass. Relatively little negative arching was observed when the dome had a stiff support, but considerable positive arching did appear when the support for the dome was "soft". The buried domes did not develop a "snap-through" buckling under an average vertical pressure almost three times the pressure that buckled the dome when unburied; rather the buried domes yielded as the result of bending stresses near the support. It was generally possible to increase the surface pressure considerably even after the domes failed near the support, and under certain conditions the additional deformation in the dome was quite small.

CONTENTS

FIGURES FOR MAIN BODY

TABLES FOR MAIN BODY

(a list of figures and tables appears at the beginning of each appendix)

PREFACE

The problem of designing buried structures to resist nuclear attack has been one of the prime motivations for studying the dynamic properties of soils. Hence it was rather inevitable that the soil dynamics research effort should have become involved in laboratory-scale tests upon buried structures. As stated early in the main body of this report, it would appear that many of the dynamic design problems regarding buried structures would be relatively easy if only the corresponding static problems were really understood. Because of this belief, and because static tests are so much less demanding of time and money than dynamic tests, it was decided that the initial effort should be confined to static loadings. The effort described in this report had two goals: to develop techniques for carrying out meaningful small-scale tests, and to begin identification and study of the important aspects of the behavior of soil-structure systems. This work was carried out over a two year period, ending in the summer of 1962.

This is the twelfth in a series of reports issued by M.I.T. under its present contract with the U. S. Army Engineers Waterways Experiment Station. A list of the earlier reports follows this preface. The work has been carried out by the Soils Division (headed by Dr. T. W. Lambe) of the Department of Civil Engineering. The dynamics research has been under the immediate supervision of Dr. Robert V. Whitman, Associate Professor of Civil Engineering. Professor Getzler was a Visiting Assistant Professor of Civil Engineering, and Mr. Hoeg served as a Research Assistant. Professor Getzler has since returned to his faculty duties at Technion in Israel.

Many of the authors' colleagues have made valuable suggestions concerning the conduct of this research and the interpretation of the results. The authors are especially grateful for the assistance of Professors Myle J. Holley, Jr. and Frank J. Heger.

PREVIOUS REPORTS

1. "Scope of Test Program and Equipment Specifications," November 1957
2. "Test Equipment for High Speed Triaxial Tests," January 1959
3. "First Interim Report on Dynamic Soil Tests," October 1959
4. "One-Dimensional Compression and Wave Velocity Tests," August 1960
5. "Pore Pressure Measurements During Transient Loadings," November 1960
6. "Effects of Rate-of-Strain on Stress-Strain Behavior of Saturated Soils," April 1961
7. "Adaptation and Use of the Boynton Device for Rapid One-Dimensional Compression Tests," June 1961
8. "Laboratory Measurement of Dilatational Wave Propagation Velocity," July 1961
9. "Shearing Resistance of Sands During Rapid Loading," May 1962
10. "Strength of Saturated Fat Clay," June 1962
11. "Triaxial Tests upon Saturated Fine Sand," September 1962

INTRODUCTION

The nation's protective construction effort during the past decade has kindled anew the civil engineer's interest concerning the behavior of structures buried in earth. Whereas above-ground structures are readily destroyed by the air blast from a large explosion, it is possible to construct economical underground facilities which are quite resistant to blast loadings. Moreover, earth cover provides an effective shield against the radiation and heat generated by a nuclear explosion.

The transient nature of the loading from a blast wave has, of course, given rise to new design problems. In the broad view, however, the design of underground protective construction facilities is a direct extension of quite conventional problems with which the civil engineer has long wrestled: the design of tunnels, of culverts, of retaining walls, and even of grain storage bins. One conclusion is reached quickly by engineers in the protective construction field: the dynamic structural design problems would be relatively easy if only the corresponding static problems were understood clearly.

It has been somewhat surprising to discover the limitations of present knowledge regarding the response of soil-structure systems to static loading conditions. It is true that useful procedures have been developed for specific design problems, such as proportioning certain types of flexible culverts. It is also true that some important basic principles have been established, at least in a qualitative sense. However, the store of quantitative data regarding fundamental phenomena is inadequate for analyzing new types of design situations. Moreover, even the culvert problem gives difficulties if the parameters of the problem are changed beyond their usual limits.*

*Newmark and his associates at the University of Illinois have recently put together an excellent review of knowledge concerning soil-structure interaction. This review is distributed in very limited quantities by the Defense Atomic Support Agency as Part V of "Nuclear Geoplosics:

Present knowledge is especially scant when it comes to predicting the collapse loading for a soil-structure system involving a flexible tube, arch or dome. Not only can the earth "arch" around the structure, but the earth inhibits the usual patterns of structural deformation. While the general principles have been outlined by Marston and his associates (SPANGLER: 1948, 1956), there are still such important questions as: if the structure yields suddenly, can an "arch" immediately form in the surrounding earth, or what strength and stiffness are necessary in the surrounding soil to ensure that a thin arch will fail by compressive yielding rather than by buckling or bending? Such problems are difficult enough when the soil mass and structure are both cylindrical and the loading is a uniform radial pressure (WHITMAN and LUSCHER: 1962); they become very difficult when the loading is other than uniform and the structure becomes an arch or a dome.

As a step toward closing some of these gaps in the knowledge concerning soil-structure interaction, the M.I.T. Department of Civil Engineering has initiated a program of small-scale tests using static loadings. Although horizontal tubes and arches are simple forms in the structural sense, the problem of end effects always arise when testing such structures. Hence, it was decided that the program should involve structures having a vertical axis of symmetry, and a thin-walled dome was selected for the initial tests. So as to simplify the placement of soil around the structure in these initial tests, a coarse dry sand has been employed.

This report discusses the development of testing systems and procedures, and presents the first of the experimental results.

TEST BIN AND LOADING FRAME

The testing system, shown in Figure 1, involves a soil container 5 feet in diameter, a rubber bag through which a uniform static pressure is applied to the top surface of the sand mass, and a self-contained loading

A Sourcebook of Underground Phenomena and Effects of Nuclear Explosions". SPANGLER (1948, 1956) has provided excellent surveys of knowledge concerning the conduit and culvert problem. Tunnel lining behavior is discussed in the symposium by LANE and BURKE (1960).

frame.

The soil container consists of a set of rings and upper and lower cover plates, with all parts 3/8 inch in thickness. Each ring is 10 inches high (the prime limitation being that two men must be able to handle the ring). Adjacent rings are separated by a thin piece of rubber so that the container wall is flexible in the vertical direction, and thus the side-friction problem is minimized. A maximum of four rings can be fitted into the loading frame, and the maximum possible depth of sand is about 42 inches.

The rubber bag was fabricated from 1/16 inch black neoprene, by vulcanizing together two circular disks and a long strip. The resulting bag was 4 inches thick, and fitted snugly within the upper cover plate. It was necessary to provide 1/2 inch thick rubber padding around the edge of the bag, to prevent the bag from blowing out through the inadvertent cracks between the cover plate and the topmost ring of the bin. Pressure was supplied to the bag from nitrogen bottles.

The loading frame is made up of four complete rectangular bents in parallel planes with templates at the lower corners to tie the bents together. Each bent involves two 14 WF 68 beams and two tension plates of 1 inch thickness connected by 8 high strength bolts at each corner. The maximum working pressure within the rubber bag is 300 lb/in^2, giving a maximum total force of 850,000 pounds. This huge force is carried internally by the frame, and only the dead weight (about 7.5 tons) of the testing system and sand reaches the floor of the building.

Obviously, many compromises had to be made when selecting the dimensions for the testing system. On the one hand, a large system means that the details of full-scale situations can be more fully reproduced in the small-scale tests, and the results of small scale tests can in turn be applied to full-scale problems with but a minimum of interpretation and extrapolation. On the other hand, a large system requires the expenditures of considerable money, effort and time in order to accomplish a single test.

Since the experiments were to be somewhat exploratory in nature, and aimed at basic research rather

than the modelling of full-scale situations, it was appropriate to select the minimum possible dimensions. The minimum size for the structure itself was set by the requirement of observing adequately the deformation of the structure; on this basis, a 12 inch diameter at the base of the dome was chosen. Then the clearance between structure and bin required to minimize boundary effects established the bin dimensions. By analogy to the footing problem, and by inspection of some photoelasticity results (for example, see ARMOUR RESEARCH FOUNDATION, 1962), it was decided that the bin diameter should be at least 5 times the span length of the small-scale structure and the bin depth should be at least 3 times this span length. The bin dimensions thus obtained were already at or close to those set by space limitations. A complete description and structural details of the test bin facilities are contained in Appendix A to this report.

PLACEMENT OF SAND

A sand-blasting sand, readily available and inexpensive, was used for these tests. As shown in Figure 2, this sand was of relatively uniform grain size and free from dust. Individual grains of sands were quite angular. There are unfortunately, no standard tests for determining the maximum and minimum unit weight for a sand, and hence a number of the commonly recommended tests were used. The minimum unit weight, for the sand in the air-dry state, proved to be about 90 lb/ft^3. The maximum unit weight was more elusive, but a representative value of 108 lb/ft^3 was finally selected. The friction angle of the sand ranges between 30° and 38°, depending upon the relative density.

After some experimentation, and much to our surprise, it was found that a very dense sand mass could be obtained by "showering" the sand, using a flexible hose muzzled with 1/4 inch mesh wire screen: see Figure 3. When showering into small containers (about 5 inch diameter) at a rate of about 0.2 $ft^3/min.$, a unit weight of 107.5 lb/ft^3 (97% relative density) was obtained consistently. As indicated by earlier studies (KOLBUSZEWSKI and JONES: 1961), the unit weight so obtained was a function of the height of free-fall, and especially of the rate-of-flow of the sand. Apparently, when sand particles arrive more-or-less individually at an existing sand surface, it is possible for these particles to nestle

down into the "holes" between existing sand particles, in such a way as to give nearly optimum packing and maximum unit weight. As the rate of delivery of the sand is increased, there is more-and-more likelihood that two or more particles will try simultaneously to fall into the same "hole," thus leading to arch-like arrangements and a looser sand mass. The earlier studies would not have suggested that essentially 100% relative density would be obtained by showering, and it seems likely that such a result can be obtained only for coarse, uniform sands.

When placing "dense" sand in the test bin, a quantity of the sand was supported overhead in a box, and showered through a 2 inch diameter radiator hose. It was essential to keep moving the end of the hose back-and-forth over the sand surface, so as to keep this surface free from hills and valleys. A rate of placement of 0.16 ft^3/min., well above the optimum rate of placement, was used to speed up the testing schedule.*

A simple penetrometer, using a flat disk 1.25 inches in diameter as a tip, was first calibrated vs. unit weight by tests in small containers, and then used to check the in-place unit weight of the large sand mass. In this way, it was found that the average unit weight of the sand involved in the buried dome tests was 102 lb/ft^3 (70% relative density).** Thus the increased rate of showering caused quite a marked decrease in the resultant unit weight.

The in-place unit weight of the "dense" sand, as measured by the penetrometer ranged from 101.5 to 104.0 lb/ft^3 (relative densities of 68% to 81%). A number of plate bearing tests (12 inch diameter plate) were carried out to check upon the uniformity of the dense sand mass, and it was found that the standard deviation from the mean was only 4%. It was concluded

*Approximately 7 hours were usually needed to fill the bin to 30 inch depth, of which about 5 hours were spent in actually showering the sand.

**Relative density $= \frac{e_{max} - e}{e_{max} - e_{min}} = \frac{\gamma - \gamma_{min}}{\gamma_{max} - \gamma_{min}} \times \frac{\gamma_{max}}{\gamma}$

that the as-placed sand masses were indeed quite uniform.

To create a loose sand mass, sand was poured rapidly into the center of the bin from the box supported overhead. The sand of course formed a cone, and finally the sand in the top portion of the cone was pushed carefully to the sides of the bin so as to give a level surface. Tests with the penetrometer revealed that the average unit weight was reasonably uniform throughout the mass, at the minimum unit weight of 90 lb/ft^3.

Descriptions of techniques used in placing the sand and measuring the sand density are given in detail in Appendix B to this report. Descriptions of preliminary plate bearing tests conducted primarily to develop methods of placing sand and the various instrumentation systems in the bin are presented in Appendix C to this report.

LOAD CAPACITY OF UNBURIED DOMES

A cross-section through the dome selected for these experiments is shown in Figure 4. Preliminary considerations concerning the selection of a dome suitable for use in this series of tests are given in Appendix D. This dome is a segment of a sphere with a radius of 9 inches, and the central angle for the dome is 85°. The domes were formed by pushing and spinning a flat sheet, and were then heat-treated to relieve worked-in stresses. Aluminum 6061 0, with a yield point (based on 0.2% strain) of about 8000 lb/in^2, was used.

A fixed-edge support condition was provided, as shown in Figure 4, by gluing the dome to a base plate with an epoxy adhesive. Calculations indicated that bending stresses arising from this support condition would persist only through an angle of approximately 10° from the support. Thus a membrane stress condition existed over the major portion of the dome.

According to the classical linear theory for the buckling of spheres, (see TIMOSHENKO and GERE, 1961), such a dome should be able to withstand a uniform radial pressure of 90 lb/in^2 before buckling.* However, recent

*Computed for the hypothetical case where the modulus of elasticity for aluminum remains constant.

research (for an up-to-date review, see GJELSVIK and BODNER, 1962) has indicated that a "snap-through" will occur at a much lower pressure, owing to nonlinear effects. The buckling pressure for the domes of this test program was determined by subjecting the dome, already mounted on its base plate, to a water pressure. Buckling occurred at a pressure of 25 ±2 lb/in^2, a result which is in satisfactory agreement with those obtained by KLOPPEL and JUNGBLUTH (1953). Figure 5 shows a picture of a buckled dome.

INSTRUMENTATION FOR TESTS WITH BURIED DOMES

The extent of the instrumentation used in the test program is shown in Figure 6. A load cell was placed under the base plate of the dome, so as to measure the total vertical force reaching the dome; strain gages were placed on the inside surface of the dome; deflection was recorded at various elevations of the dome-load cell system; vertical movements within the sand mass were measured; and finally the movement of the bottom of the test bin was monitored.

The load cell employed SR-4 strain gages affixed to a thin cylinder which carried the total load in axial compression. The strain gages and bridge circuit were arranged so as to provide compensation for bending strains and temperature effects. As indicated in Figure 6, this cylinder was provided with bearing plates at both ends. A pipe kept sand away from the load cell, and a piece of tape covered the gap between the pipe and the base plate of the dome.

A typical arrangement of strain gages mounted on the dome is shown in Figure 7. While it would have been desirable to have gages on the outside surface as well, it was feared that such gages might affect the soil-structure interaction patterns.

Vertical movement of the crown of the dome and of lower flange of the load cell were measured using Ames dials. Rods from the Ames dials extended up through a hole in the bottom of the bin, through the load cell, and through another hole in the base plate of the dome. Because of seating imperfections, the dome-load cell system proved to be slightly flexible. In some tests, a layer of cork was introduced below the load cell so as to give even more flexibility.

Figure 8 shows the system used to measure vertical movements within the sand. The anchor disks (1 inch in diameter and 1/16 inch thick) moved with the sand, and as a result squeezed colored water from the hydraulic cylinders resting on the bottom of the bin. The volume of water squeezed from the cylinders was measured in capillary tubes located outside of the bin.

Because the lower beams of the loading frame seated imperfectly against the floor, and because of bending under load, the bottom of the bin moved during a test. Since the dome movements were measured with respect to the floor, while the sand movements were referenced to the bottom of the bin, it was necessary to measure the bin deflections and to use this data to put all movement measurements on a common basis.

RESULTS AND ANALYSES

The test program is summarized in Table I. There were three preliminary tests that served to perfect the testing techniques. The depth of cover, relative density of the sand, and flexibility of dome support were varied from test to test as indicated. A test involving a rigid dome (a standard dome filled with gypsum) was included. Tests 6 and 10 were duplicate tests. In Test 7, the gas bag ruptured before failure developed in the dome. The applied surface pressure was generally increased in increments of 10 lb/in^2, although smaller increments were used as the point of structural yielding was approached. All instrumentation systems were read after each increment.

An initial failure developed along the spring line of the dome when the average vertical stress against the dome reached about 70 lb/in^2. At this point, the crown deflection suddenly increased, the average soil pressure against the dome suddenly decreased, and the strains within the sand alongside the dome suddenly increased. The surface pressure required to cause 70 lb/in^2 against the dome varied with the density of the sand and the flexibility of support for the dome. Following development of the yield condition, it was generally possible to increase the surface load further, without causing the structure to collapse.

The test results are summarized in the following subsections; detailed test results appear in Appendix E.

Compressibility of sand: From the measured movement of disks embedded within the sand mass, it was possible to determine the vertical strains caused within the sand by the applied surface pressure. Assuming that the vertical stresses within the sand were equal to the applied pressures, the virgin stress-strain curves shown in Figure 9 have been developed. The data used to construct these curves came from a zone which lay from 8 inches to 14 inches from the bottom of the bin (average depth below surface from 6.5 inches to 19 inches, depending upon test conditions), and from 6 to 14 inches to the side of the edge of the dome. It is believed that the actual stresses within this zone were affected only slightly by arching around the dome.

As suggested by CHAPLIN (1961), the strains within the sand were found to increase as the square root of the applied pressure; i.e. the compressibility of the sand decreased with increasing stress. The tangent modulus at a stress level of 30 lb/in^2 was 27,000 lb/in^2 for the "dense" sand and 4,000 lb/in^2 for the loose sand. From the former of these values, it is clear that the "dense" sand was indeed in a very compact state. The sand masses were essentially in a state of one-dimensional strain, and the stress-strain ratio represents a constrained modulus.

"Arching" before yield: The average vertical pressures reaching the domes are shown by the curves in Figure 10. The ratio of the pressure reaching the dome to the applied surface pressue is indicative of the "arching" or stress redistribution around the dome.

The curves of pressure ratio generally have a characteristic shape. (1) First, these curves move upward to a peak at a relatively low value of surface pressure. No satisfactory explanation has been found for this rather surprising behavior. It was suspected that the support for the dome might initially be "soft" as the result of poor seating between the various portions of the dome-load cell bin system. While the data showed that seating errors were indeed present, there was, however, no evidence that the system was unusually "soft" during the first application of pressure. (2) Following the peak, the pressure ratio decreased. The decreasing compressibility of the sand presumably accounted for this trend. In addition, the compressibility of the cork also decreased with increasing stress, and this

fact accounts for the flattening of the pressure ratio curves from Tests 6, 7 and 10. (3) The sudden drop in all curves, except those for Tests 7 (failure not reached) and 11 (rigid dome), signified yielding within the dome.

In all tests with a rigid foundation, and in the one test with both loose sand and a flexibile support, the maximum value of the pressure ratio ranged from 0.95 to 1.20. In all other tests with a flexible support, the peak value of this ratio was in the range from 0.5 to 0.6. Qualitatively, these results are as would be expected on the basis of arching theory. However, when the actual magnitudes of the pressure ratio were studied in the light of the relative movements between dome and sand, the results were rather surprising.

Figure 11(a) shows these movements for the case of dense sand and rigid support. Although the peak pressure ratios in these tests were 1.0 and 1.1, the crown moved down more than the sand located some 2 to 14 inches off to the side of the dome. Figure 11(b) shows the relative movements for the case of dense sand and flexible foundation. Here the pattern of relative movement and pressure ratio is as would be expected. Finally, results for the tests involving loose sand are shown in Figure 11(c). Although the sand has moved much more than the crown of the dome, the pressure ratio values were not far from unity; i.e. there apparently was little negative arching.

In preparing these curves, it was necessary to correct the measured crown movements for the relative movement between the bin bottom and the floor of the laboratory room; while the exact magnitude of the correction was in doubt, it is believed that the relative position of these curves is correct. Even with the so-called rigid foundation, most of the crown movement prior to yield was the result of compressions within the load cell and seating errors. The dome itself was relatively incompressible; i.e. the elastic deflection of the crown relative to its base plate was computed to be 0.004 inch at a pressure against the dome of 30 lb/in^2.

It would of course be dangerous to draw quantitative conclusions from these tests concerning the arching phenomena around buried domes. The preceding analysis has to some extent accounted for the presence of the load cell under the dome; however, there must be other effects

of this unusual structural arrangement. The results would, in general, appear to support the conclusion that it is relatively easy to induce positive arching (pressure ratio less than unity) but that negative arching (pressure ratio greater than unity) may be relatively insignificant even when the soil is extremely compressible. Such a conclusion is in line with the suggestions outlined by TAYLOR (1947).

Stress required to cause yield: It is, of course, quite significant that the buried domes sustained an average vertical pressure much larger than the pressure which would cause snap buckling of this dome if unburied. Moreover, the buried domes yielded by development of excessive bending strains at the support and in all tests save one, the only deformation was a bend along the spring line. The compressive strains measured near the crown reached values at least three times those existing just before snap buckling in the unburied dome. From all of these facts, it is clear that the sand surrounding the dome was extremely effective in inhibiting the development of elastic snap buckling, even when the sand was in a loose condition.

By analysis of the bending stresses expected near the support, it had been predicted that a pair of plastic hinges, as shown in Figure 12, should develop at the support when the average vertical pressure on the dome reached about 65 lb/in^2. Once these hinges develop, local plastic buckling should follow almost immediately. This prediction is in good agreement with the observed results, both as to magnitude and as to the nature of the observed yield: see Figure 13(a).

Starting from the recorded strain data, an attempt was made to determine the distribution of the pressure acting against the dome. Despite the difficulties inherent in such a procedure, it appeared that the loading in Tests 6, 7 and 10 resembled a snow loading (i.e. a uniform stress per unit horizontal area) while in the remaining tests there was a greater concentration of pressure near the support of the dome. Thus, comparing the strains near the crown at the dome when failure developed near the support, these strains were much greater in Tests 6 and 10 than in Tests 4, 5, 8 and 9.

Finally, it should be noted that the pressure ratio at yield was unaffected by the change in the depth of burial, for the case of dense sand and a rigid support. Even though the dome in Test 7 did not yield, the trend of the curves in Figure 10(b) suggests that this same conclusion applies to the case of dense sand and a flexible support.

Behavior following yield: When failure by local plastic buckling developed near the support (Figure 12), the crown of the dome suddenly moved downward, generally while the surface load remained constant. The magnitude of this sudden deflection varied widely from test to test, as indicated in Table II. The dome in Test 6 collapsed completely, as shown by the photograph in Figure 13(b).

The ratio between average pressure on dome and surface pressure dropped suddenly at this point of yield, and there was a transfer of stress to the surrounding sand. The amount of stress transfer was least in the cases where the pressure ratio prior to collapse was least. When the surface pressure was increased further following yield, the dome picked up some portion of the additional surface load. The ratio of additional pressure on dome to additional surface pressure seemed to be related to the magnitude of the dome's deformation during failure near the support.

These various observations might be explained by the following hypotheses. In each test, a soil "arch" (or rather a "dome") had formed to a greater or lesser degree prior to yield. (Even in tests where the pressure ratio was near unity, there was a concentration of stress near the support line of the dome.) When the structure failed near the support, the "arch" had to adjust quickly to the new conditions. Where the "arch" was relatively unimportant before yield, and where the depth of burial was large, the "arch" remained intact and effectively accomplished the redistribution of stress both at and subsequent to yield. But where the depth of burial was shallow, or where the "arch" was well developed before yield, the "arch" was not able to adjust immediately and collapsed partially. In these latter cases, the deformations at yield were large, and there was less arching subsequent to yield.

In Test 4, the burial depth was large compared to the span of the dome, and the combination of dense sand and rigid foundation meant that there was little arching prior to yield. Thus all conditions were favorable for development of "arching" as the dome yielded, and the dome in this test deformed relatively little at and subsequent to failure at the support. In fact, the crown movements in Tests 4 and 7 (same as 4 except flexible foundation) were essentially identical at a surface pressure of 220 lb/in^2, even though the dome in Test 4 had long since yielded and the dome in Test 7 had not yet yielded.

On the other hand, the worst combination of circumstances was present in Test 6: the burial was relatively shallow and there was considerable arching prior to yield. The dome in this test collapsed immediately upon failure near the support, and a depression formed in the surface of the sand. These test conditions were duplicated in Test 10. This time there was no collapse, but the deflection was quite large when failure occurred near the support.

While the foregoing hypotheses are in general supported by the results, the behavior of the dome at and following yield undoubtedly was affected by a complex interaction between a number of factors, including the pattern and magnitude of stresses within the dome just prior to yield and possible slight differences between the properties, dimensions and support conditions for the individual domes. Moreover, the amount by which the dome deflects at yield must in turn influence the ability of the sand to form and/or sustain an "arch". While the data suggest, for example, that burial depth will by itself have a significant influence upon the deformations at and following yield (compare Tests 4 and 5), it would be dangerous to draw general conclusions concerning this complex problem on the basis of such limited data.

CONCLUSIONS

It appears certain that the type of small-scale test described in this report can be of great use in studying the fundamental aspects of the soil-structure interaction problem. The tests discussed herein, even though preliminary in nature and rather crudely instrumented,

have revealed the following patterns of behavior:

(a) While comparison of structure flexibility with the compressibility of the surrounding sand did not indicate any simple relationship between these parameters and the amount of surface pressure transferred to the dome, it was notable that there was little tendency toward significant negative arching even when the sand was very loose.

(b) The domes, when buried to a depth greater than their radius, could withstand pressures several times the elastic snap-buckling pressure for the unburied dome. When the domes did yield, it was as the result of bending failure near the support, and not the result of elastic buckling.

(c) The overpressure at the sand surface, required to cause failure in the domes, was essentially the same for burial depths of 0.4 and 1.5 times the span of the dome.

(d) A sand "arch" will generally form when the structure yields. This "arch" will assume some of the pressure which had been acting upon the dome, thus preventing total collapse. "Arching" action will continue if the surface pressure is increased still further. However, unless the burial depth is great, there may be large structural deflections at and subsequent to yield.

(e) Beneficial "arching" action in the sand can be developed prior to yield by introducing foundation flexibility, even for a burial depth of approximately one-half the span. In such a case, however, the dome may deform excessively when failure occurs at the support.

These results will serve as the starting point for more detailed research concerning interaction between soil and buried structure.

REFERENCES

ARMOUR RESEARCH FOUNDATION, 1962: "A Study of Stress-Wave Interaction with Buried Structures," Report to Air Force Special Weapons Center, SWC TDR 62-47

BURKE, H., and LANE, K. S., 1960: "Garrison Dam Test Tunnel," Transactions ASCE, Vol. 125, pp 228-307

CHAPLIN, T. K., 1961: "Some Mechanical Properties of Granular Materials at Low Strains," Proc. Midland Soil Mechanics and Foundation Engineering Society, Vol. 4, pp 19-35

GJELSVIK, A. and BODNER, S. R., 1962: "Nonsymmetrical Snap Buckling of Spherical Caps," Proc. ASCE, Vol. 88, No. EM5, pp 135-165. Also see paper by same authors "The Energy Criterion and Snap Buckling of Arches," pp 87-134 of same issue.

KOLBUSZEWSKI, J., and JONES, R. H., 1961: "The Preparation of Sand Samples for Laboratory Testing," Proc. Midland Soil Mechanics and Found. Eng. Soc., Vol. 4, pp 107-124

KLOPPEL, K. and JUNGBLUTH, O., 1953: Beitrag zum Durchschlagproblem dunnwandiger Kugelschalen," der Stahlbau, Vol. 22

TAYLOR, D. W., 1947: "Review of Pressure Distribution Theories, Earth Pressure Cell Investigations and Pressure Distribution Data," U. S. Army Engineer Waterways Experiment Station, Vicksburg, Mississippi

TIMOSHENKO, S. and GERE, J., 1961: "Theory of Elastic Stability," McGraw-Hill Book Co., New York

SPANGLER, M. G., 1948: "Underground Conduits - An Apraisal of Modern Research," Trans. ASCE, Vol. 113, pp 316-374

SPANGLER, M. G., 1956: "Stresses in Pressure Pipelines and Protective Casing Pipes," Proc. ASCE, Vol. 82, No. ST5

WHITMAN, R. V. and LUSCHER, U., 1962: "Basic Experiment into Soil-Structure Interaction," Proc. ASCE, Vol. 88, No. SM6

Table I

SUMMARY OF TEST PROGRAM

Test No.	Sand	Burial	Support	Dome
4	Dense	17.5 in.	Rigid	Standard
5	Dense	5.0 in.	Rigid	Standard
6	Dense	5.0 in.	Flexible	Standard
7	Dense	17.5 in.	Flexible	Standard
8	Loose	17.5 in.	Flexible	Standard
9	Loose	17.5 in.	Rigid	Standard
10	Dense	5.0 in.	Flexible	Standard
11	Dense	5.0 in.	Rigid	Rigid

Notes: (a) Dense sand mass averaged 102 lb/ft^3 (70% relative density); loose sand mass averaged 90 lb/ft^3 (0% relative density).

(b) Depth of burial measured to crown of dome.

(c) "Rigid" support provided by load cell; "flexible" support achieved by introducing cork layer below load cell.

(d) Rigid dome is standard dome filled with gypsum.

Table II

CROWN DEFLECTION AT YIELD

Test No.	Deflection (1% of height of dome)
4	1.5
5	3.5
6	Total collapse
8	5.0
9	4.0
10	9.0

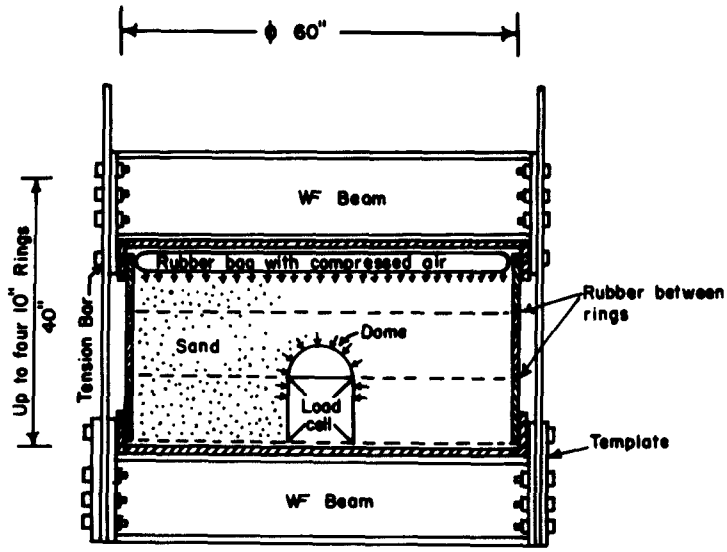

FIGURE 1 LOADING FRAME AND SOIL CONTAINER

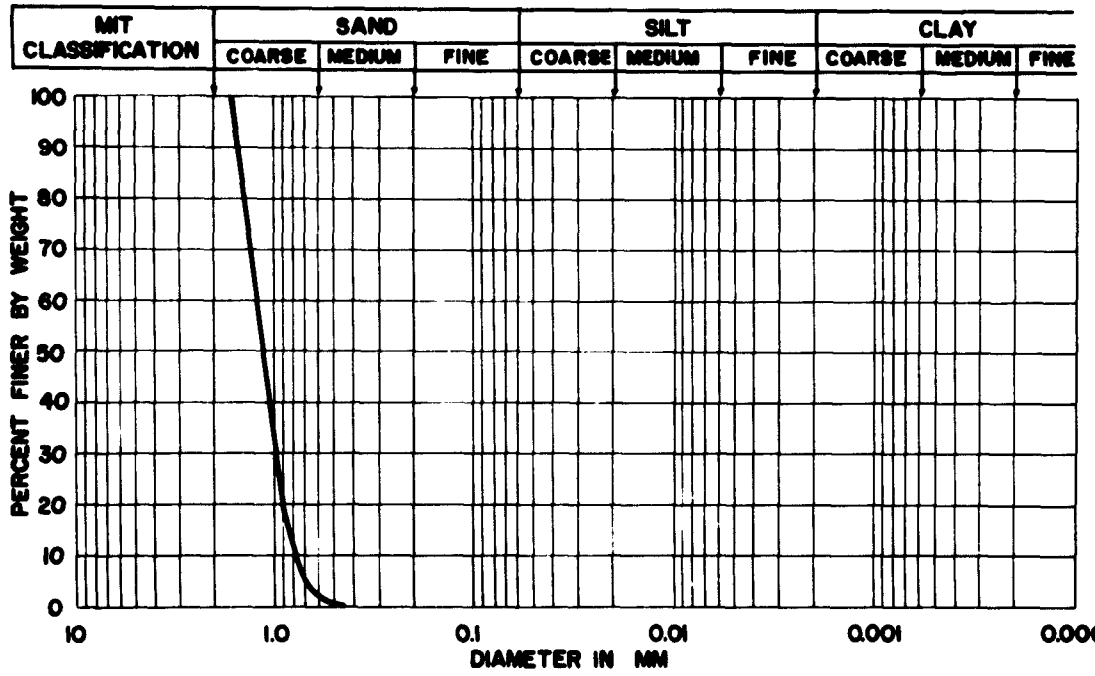

FIGURE 2 GRAIN SIZE DISTRIBUTION

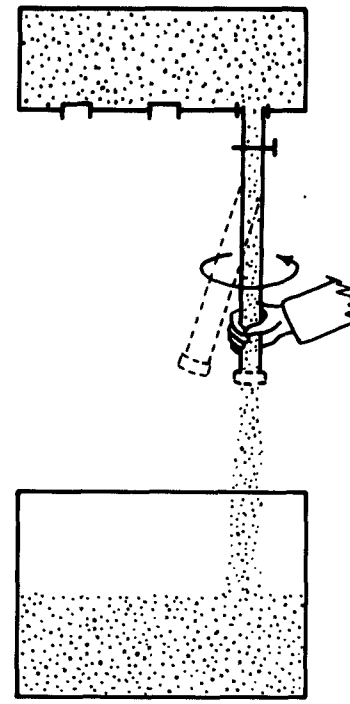

FIGURE 3 PLACING SAND BY SHOWERING

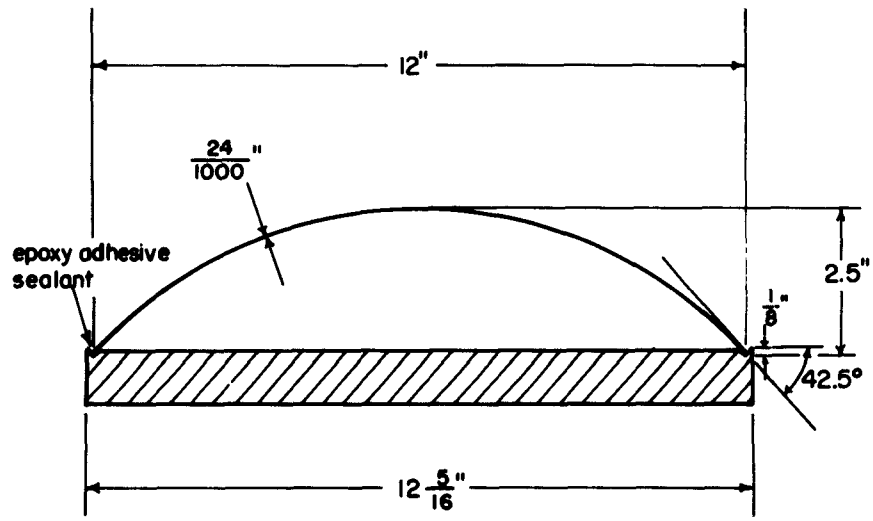

FIGURE 4 DOME AND BASE PLATE

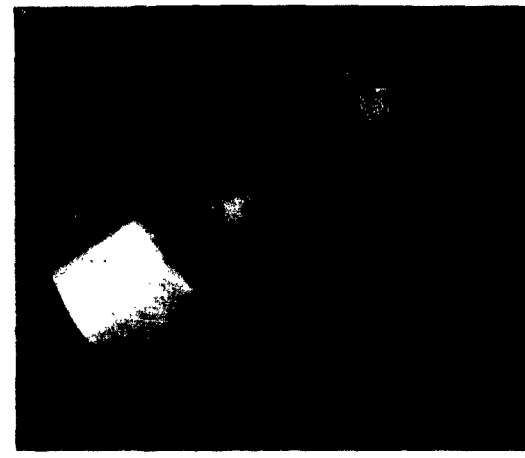

FIGURE 5 DOME BUCKLED BY HYDROSTATIC PRESSURE

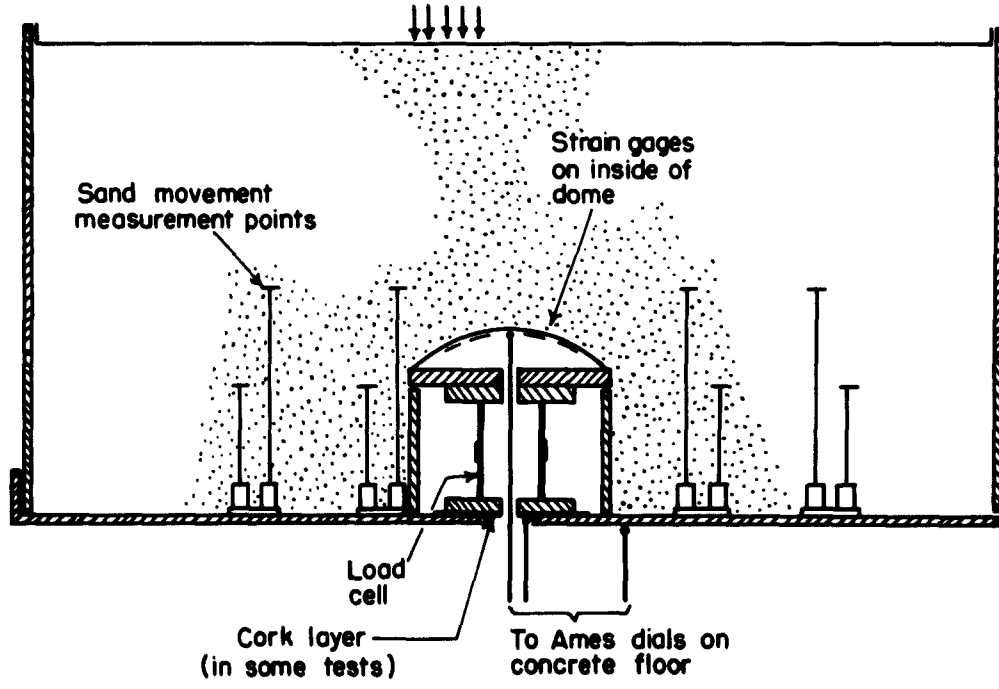

FIGURE 6 DOME SUPPORT AND INSTRUMENTATION

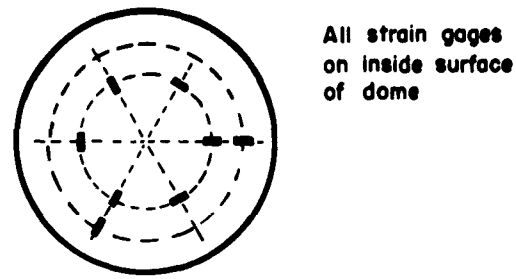

FIGURE 7 TYPICAL PATTERN OF STRAIN GAGES

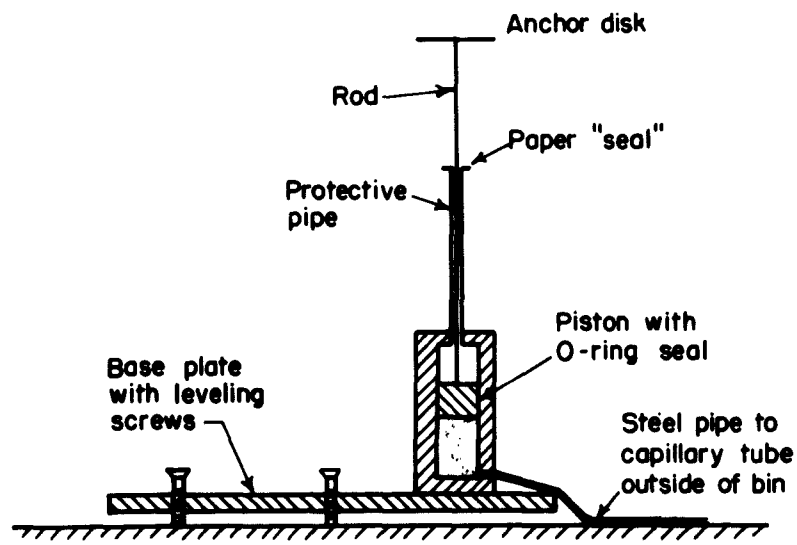

FIGURE 8 DEVICE FOR MEASURING SAND MOVEMENT

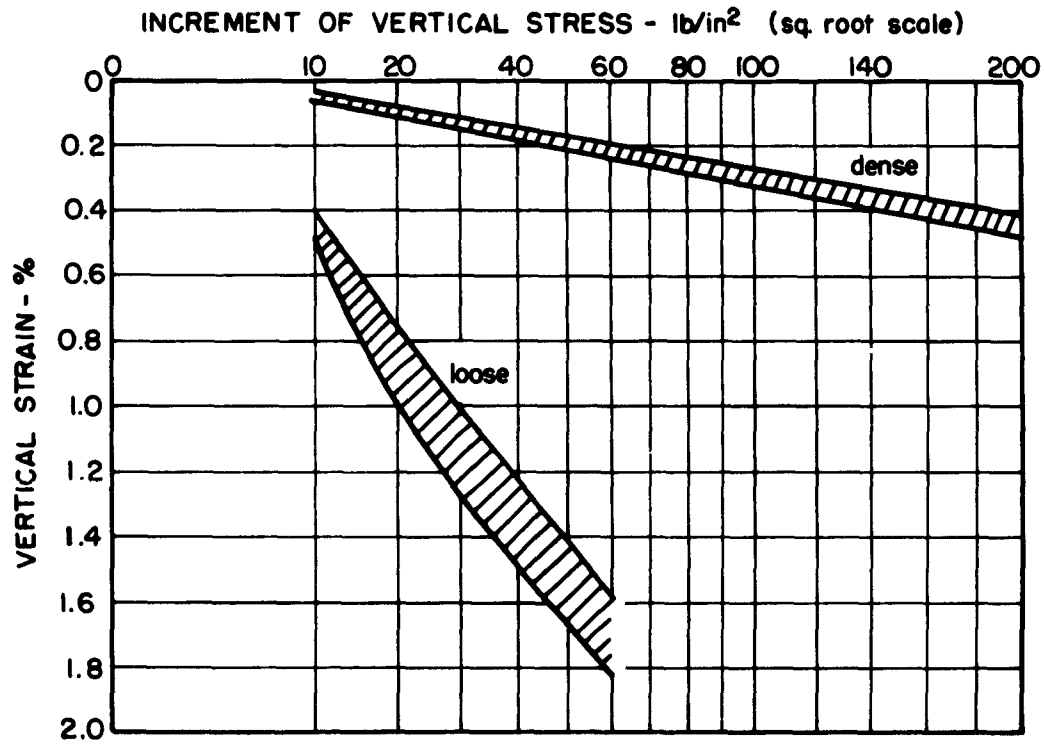

FIGURE 9 STRESS-STRAIN CURVES FOR SAND

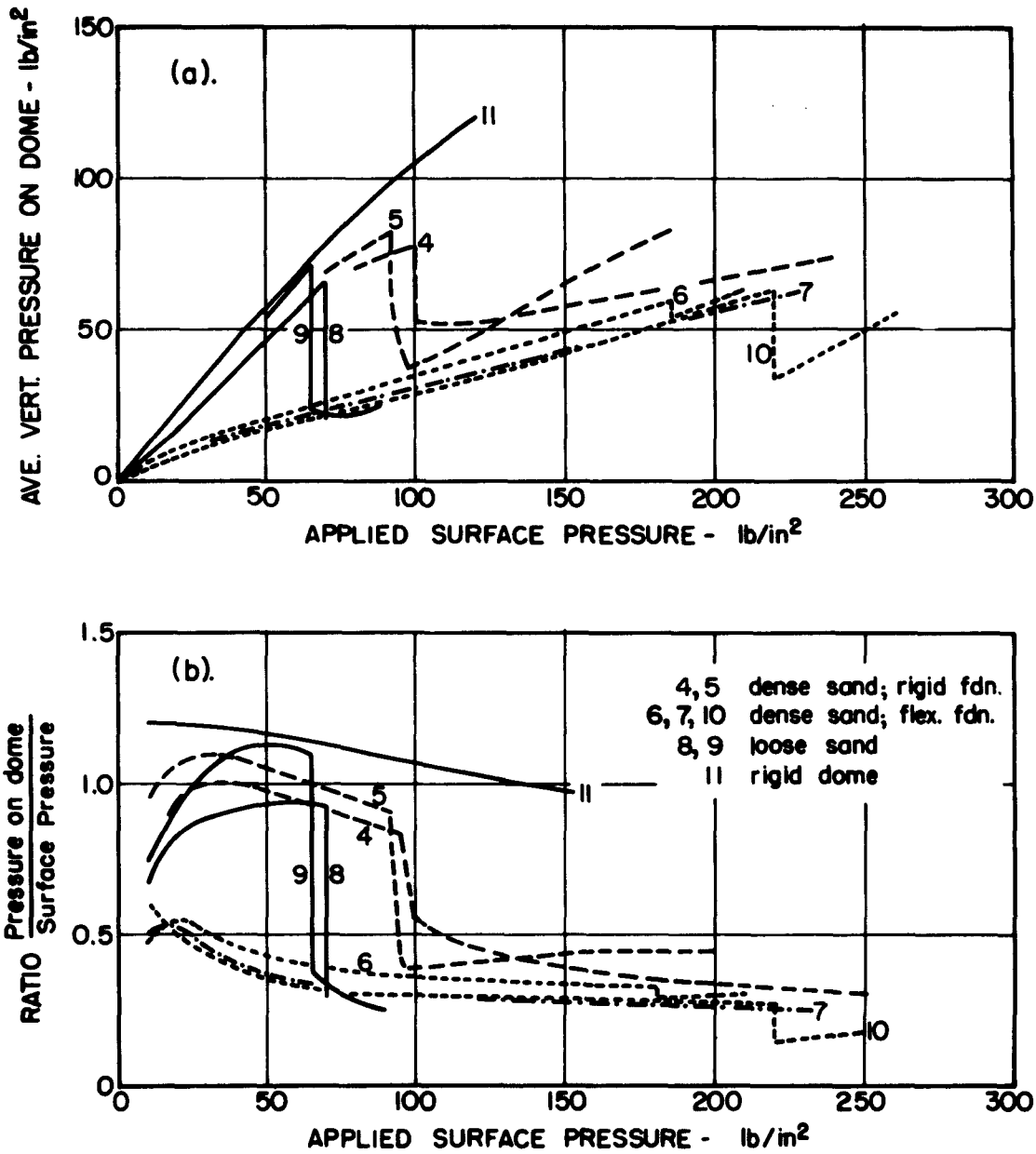

FIGURE 10 PRESSURE ON DOME vs. APPLIED SURFACE PRESSURE

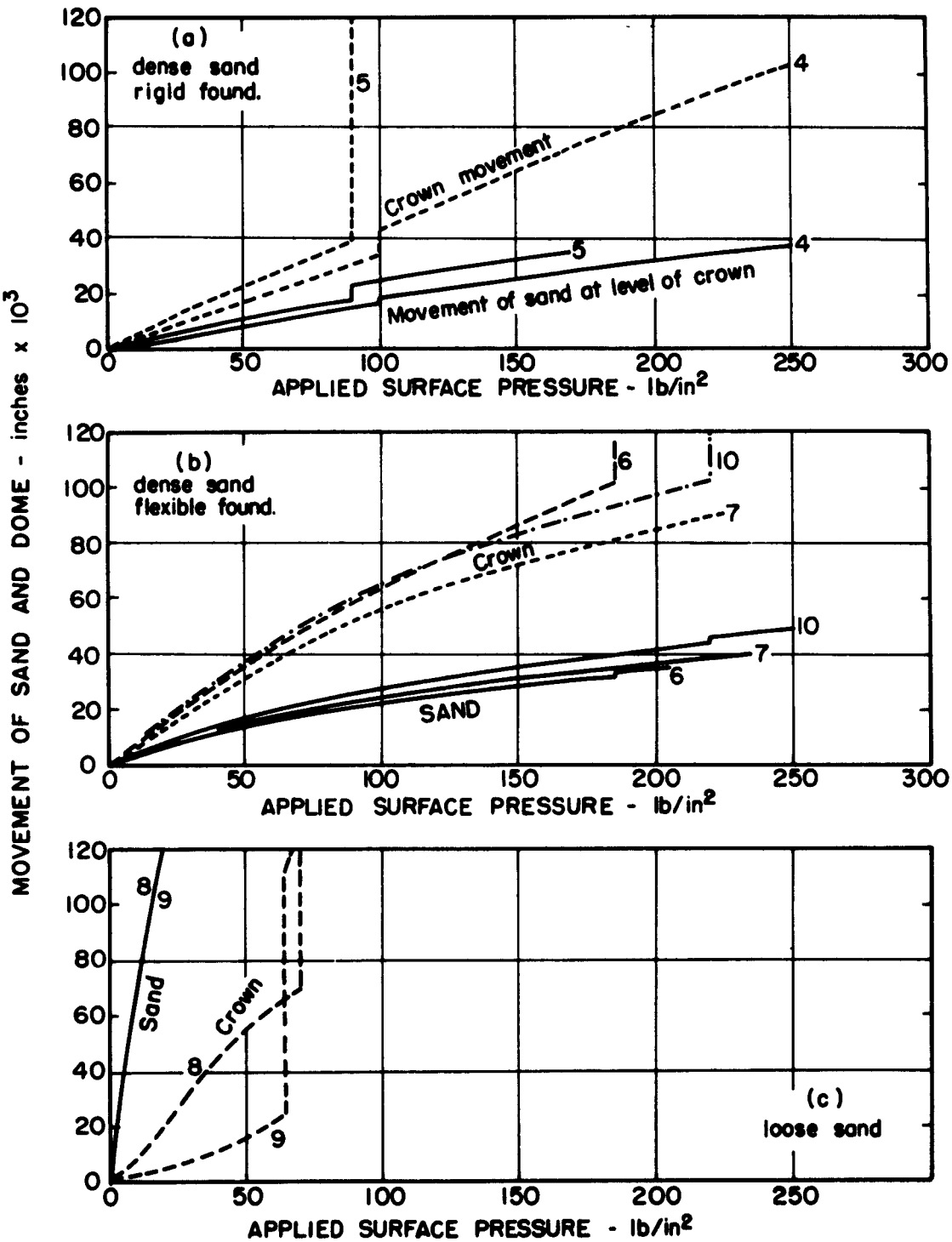

FIGURE 11 RELATIVE MOVEMENT OF SAND AND DOME

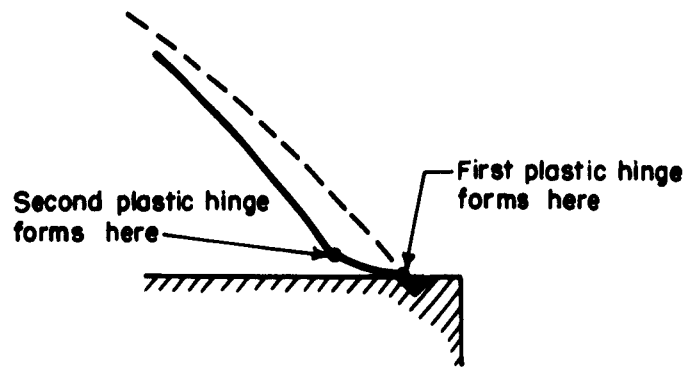

FIGURE 12 DEVELOPMENT OF FAILURE AT SUPPORT

(a) Failure at support

(b) Complete collapse

FIGURE 13 YIELDING AND COLLAPSE OF BURIED DOMES

Appendix A

TEST BIN AND LOADING FRAME

CONTENTS

LIST OF FIGURES

A.1 General Considerations

Two conflicting sets of considerations govern the selection of dimensions for a test bin. On the one hand, a large testing system means that the details of full-scale situations can be more fully reproduced in the small-scale tests, and the results of small-scale tests can in turn be applied to full-scale problems with but a minimum of interpretation and extrapolation. Considerations such as these lead to the desire for as large a testing system as possible, and set a minimum possible size for the system. On the other hand, a large testing system requires the expenditure of considerable money, effort and time in order to accomplish a single test. This type of consideration leads to the demand for relatively small testing systems, and sets an upper limit for the size of the system.

Since the program of experiments to be conducted with this test system was to be somewhat exploratory in nature, and aimed at basic research rather than the modelling of specific full-scale situations, it was deemed appropriate to utilize close to the minimum possible dimensions for the system. These minimum dimensions were determined first by the minimum dimensions for the small-scale structure, and secondly by the clearances required between structure and the boundaries of the test bin. These clearances had to be such that the boundaries would not interfere with the interaction phenomena under study.

The minimum dimensions for the small-scale structure are controlled primarily by the problem of observing adequately the response of this structure. This statement is especially true whenever deformable structures are to be tested. The patterns of movement of the structure itself, and those within the surrounding soil as well, must be recorded in some detail. The limitations of transducing element size then become the controlling factors. Preliminary studies (WHITMAN, LUSCHER and PHILIPPE, 1961) have indicated a minimum feasible span length of 9 inches (if one-half inch long strain gages can be used). This dimension appears to be sufficiently large to ensure that the essential features of full-scale situations are reproduced, since, for example, small-scale footing studies have used much smaller dimensions (see ROBERTS, 1961). Moreover, a one-foot diameter is considered satisfactory for plate bearing tests used to establish the compressibility characteristics of soils in the field.

There is very little information to guide the choice of the structure-bin dimension ratio. The footing loading case is a soil-structure interaction problem with some similarities to the buried structure case. Conduct of a satisfactory footing loading test requires a soil mass whose horizontal dimensions are at least five times the minimum width of the footing, although a smaller dimension ratio might be used in tests where the footing is not to be loaded all the way to an ultimate bearing capacity failure. The vertical dimension of the soil mass should be at least 1.5 times the footing width. Examination of some information from photoelastic studies indicated that a 1:3 ratio for structure and bin dimensions would be adequate for most buried structure problems. Taking the sum total of this scanty information, it was concluded that the test bin diameter should be at least 5 times the span length of the small-scale structure, and the test bin depth should be at least 3 times this span length.

Combining the minimum structure size with the required structure to bin ratio led to a minimum bin diameter of 4 feet, and to a minimum thickness of soil mass of 2.5 feet.

The second set of considerations, those involving the limitations of money, effort and time, included such thoughts as the following: (1) assuming that the forces to be applied in the test are to be resisted primarily by bending moments within the loading frame, the cost of the container and its associated loading frame increases in proportion to the square of the test bin diameter; (2) the quantity of sand which would have to be handled for each test increases in proportion to the cube of the test bin diameter; (3) the dimensions of the equipment had to be such that two persons could manage the task of assembling this equipment for each test; and (4) the space available for the apparatus was approximately 8 feet wide and 9 feet high, and adequate work space around the test bins had to be included within these dimensions.

Taking the maximum and minimum considerations together, it was decided that the test bin should have a diameter of 5 feet. By the same token, the minimum height for the soil mass should be 3 feet. Once the details of the bin and loading frame were worked out in detail, it was found possible to increase this thickness slightly.

There is very little information to guide the choice of the structure-bin dimension ratio. The footing loading case is a soil-structure interaction problem with some similarities to the buried structure case. Conduct of a satisfactory footing loading test requires a soil mass whose horizontal dimensions are at least five times the minimum width of the footing, although a smaller dimension ratio might be used in tests where the footing is not to be loaded all the way to an ultimate bearing capacity failure. The vertical dimension of the soil mass should be at least 1.5 times the footing width. Examination of some information from photoelastic studies indicated that a 1:3 ratio for structure and bin dimensions would be adequate for most buried structure problems. Taking the sum total of this scanty information, it was concluded that the test bin diameter should be at least 5 times the span length of the small-scale structure, and the test bin depth should be at least 3 times this span length.

Combining the minimum structure size with the required structure to bin ratio led to a minimum bin diameter of 4 feet, and to a minimum thickness of soil mass of 2.5 feet.

The second set of considerations, those involving the limitations of money, effort and time, included such thoughts as the following: (1) assuming that the forces to be applied in the test are to be resisted primarily by bending moments within the loading frame, the cost of the container and its associated loading frame increases in proportion to the square of the test bin diameter; (2) the quantity of sand which would have to be handled for each test increases in proportion to the cube of the test bin diameter; (3) the dimensions of the equipment had to be such that two persons could manage the task of assembling this equipment for each test; and (4) the space available for the apparatus was approximately 8 feet wide and 9 feet high, and adequate work space around the test bins had to be included within these dimensions.

Taking the maximum and minimum considerations together, it was decided that the test bin should have a diameter of 5 feet. By the same token, the minimum height for the soil mass should be 3 feet. Once the details of the bin and loading frame were worked out in detail, it was found possible to increase this thickness slightly.

Selection of a working pressure also represented a compromise between many considerations; e.g. it was desirable to have this pressure as high as the overpressure levels being considered in present day protective construction design practice; this pressure is related to the size of the structural members in the loading frame, and hence to the over-all dimensions for the bin and loading frame; and this pressure had to be large enough to induce failure in small scale structures of practical stiffness. In connection with the latter point, it should be noted that it is no simple matter to fail small flexible structures imbedded within a soil mass (see WHITMAN, LUSCHER and PHILLIPE, 1961). A working pressure of 300 lbs/in^2 was finally selected. It may be noted that this pressure, when applied over an area 5 feet in diameter, produces a total thrust of 850,000 pounds.

A.2 General Arrangement

The general nature of the soil bin and loading frame can be seen in Figures A.1 through A.5.

The bin is composed of a series of rings, with bottom and top cover plates. Use of a series of rings had several main advantages in the way of adaptability and flexibility of operation: different bin heights could be readily achieved, and the individual rings could be handled easily. In addition, it was anticipated that the tension strains within the individual rings might be measured so as to provide a measure of the horizontal stress within the soil mass. Finally, but by no means of least importance, the ring arrangement made it possible to obtain a container which was "soft" in the vertical direction. That is, by putting thin rings of rubber between the stiff metal rings, one can reduce the likelihood of significant side friction forces between the soil mass and the container. The cover plates, which were flanged to fit over the top and bottom rings, served to transfer load into the beams of the load frame. The top cover plate also served to contain the rubber bag used to apply a uniform load to the soil mass.

The loading frame consists of a series of beams above and below the soil bin, tension plates which connect the two series of beams together, and templates which run horizontally along the two ends of the lower set of beams and which served to position these beams and, if necessary, to transfer shear forces between the beams. Bolts were used to connect these various elements together.

The tension plates were provided with a continuous series of bolt holes, so that the spacing between the beams could be adjusted to accommodate the desired bin height.

The test bin and loading frame could be assembled in two ways, depending upon whether a uniform or a concentrated load was to be applied to the soil mass. Figures A.1 and A.4 show the arrangement for the case of a uniform load. There were, in this case, four complete frames to resist the developed forces. If but a single concentrated load were to be used, only one upper beam (and generally three lower beams) would be utilized, as shown in Figures A.2 and A.5. Here the templates were used to transfer the forces developed in the several lower beams to the single pair of tension plates.

The arrangements called for two bins, located side-by-side: see Figure A.6. The use of two bins was convenient from the standpoint of handling the soil. It was envisioned that, once a carefully planned testing effort could be set in motion, the bin to be used for the upcoming test could be filled directly from the bin used for the test just completed. In the least efficient case, the second bin would serve as a storage reservior between tests.

One complete loading frame (8 beams, 8 tension plates, 2 templates) plus two extra templates were ordered, together with two complete sets of rings, two regular cover plates and one light-weight cover plate. Thus, if a uniform load were being used, there would be one complete test system with an extra bin for the storage of soil. If, on the other hand, concentrated loads were being used in the current tests, two complete testing systems could be assembled. The components for the frames and bins were fabricated and test-assembled by a local steel fabricator, following drawings prepared by the M.I.T. staff. Subsequent disassembly and reassembly to suit the needs of each particular test was done by project personnel. An overhead, travelling hoist beam of one ton capacity was provided to assist in the movement of the frame and bin parts and of the soil.

A.3 Details of Test Bins

The height of the rings was chosen on the basis of the weight which could be handled by two men (200 lbs.). A height of 10 inches was selected, a dimension which also was convenient as an increment for changes in the

total depth of the bin. Subsequently one ring was split in half along its circumference, so that the total depth of the bin could be changed by a five inch increment.

The rings were each 3/8 inch thick, giving a suitable stiffness from the standpoint of handling. Assuming a 300 lb/in^2 pressure against the inside of a ring a hoop stress of 24,000 lb/in^2 and a strain of 0.08% would result. Such a high pressure could result only if the lateral earth pressure coefficient were to be unity (certainly an unlikely condition).

Each ring was provided with four handles, as shown in Figures A.8 and A.10. These handles also served as steps for climbing into the assembled bin. Adjuster lugs were provided for aligning the successive rings. The inside surface of the rings was untreated except for the protective red lead paint.

The details of the regular cover plates are shown in Figure A.9. The thickness of the plate was determined by the bending stresses induced by a uniform pressure of 300 lbs/in^2 acting over the 5-1/2 inch clear span between the flanges of the beams of the loading frame. Assuming that the plate would be fully restrained against rotation at the ends of this span, it was calculated that the 3/8 inch thick plate gave a safety factor of 2.2 against excessive bending deformation. The flange of the cover plate is also 3/8 inch thick, as in the case of the individual rings of the bin. The cover plates were provided with handles, and with holes through the flange for the passage of instrumentation cables. After some experience with testing procedures, a hole for instrumentation cables was also cut through the center of one cover plate (that used for the bottom plate).

One light cover plate, 3/16 inch thick, was also provided, to be employed as a base when one bin was being used simply for storage of sand.

A.4 Details of Loading Frame

Standard 14 WF 68 sections were used for the beams of the loading frame. Steel plates were welded to the ends of each beam, as shown in Figure A.11, to provide for bolting the beams to the tension plates. The maximum total load per beam was estimated as 270,000 lbs. Eight 1-1/4 inch high strength bolts were used at each end, with a calculated stress in single shear of about 19,000 lbs/in^2.

The maximum bending stress in the beams was calculated as about 20,000 lb/in^2.

The details of the tension plates appear in Figure A.12. The maximum tension stress, disregarding stress concentrations around the bolt holes, was calculated to be 18,000 lb/in^2.

It was difficult to estimate during design just how much stress would come upon the templates. For the case of a uniform loading through the gas-filled bag, there theoretically would be no stress in these members. However, some such stress must actually appear, owing to redistribution of stress by side friction between sand and bin, the action of the buried structure, and the rigidity relations between the various elements of the bin and loading frame. The templates shown in Figure A.12 were provided. It was estimated that each template could transfer a shear force of 70,000 lbs between adjacent frames, thus providing considerable rigidity. Observations during actual tests has indicated that these templates were adequate.

A.5 Systems for Applying Loads

Provisions were made for applying either a concentrated load over a small portion of the surface of the sand in the bin, or a uniform pressure over the entire surface.

The concentrated load was applied through a hydraulic jack acting against a plate one foot in diameter: see Figures A.13 and A.14. Two hydraulic jacks were provided: Blackhawk model R-159, with 10 ton capacity and an effective area of 2.234 square inches; and Blackhawk model R-540, with a 4 ton capacity and an effective area of 0.994 square inches. Pressures were developed by a manual pump, Blackhawk model P-76, with 10,000 lb/in^2 capacity. A Blackhawk model Z-721 pressure gage was provided. The force from the hydraulic jack is transferred to the loading plate through a hard steel ball 3/8 inch in diameter. The steel loading plate was 1 inch thick.

A uniform pressure was developed by air pressure acting within a rubber bag placed atop the soil. This bag, in an uninflated condition, is shown in Figure A.15. The bag is 5 feet in diameter, 4 inches high when inflated, and has a 1/16 inch wall thickness of black neoprene. It was produced, by a local rubber fabricator, from two circular

rubber sheets and a 4 inch wide strip which formed the side ring. The circular sheets were "pinked" along their circumference, so as to provide "teeth" which provided the connection to the ring. This connection was accomplished by vulcanization. An air inlet was provided at mid-height of the ring. Compressed gas was supplied from a nitrogen bottle, as shown in Figure A.16.

The rubber bag was retained within the top cover plate of the bin, and thus theoretically there should be no danger of rupturing the bag. In several of the early tests, however, the bag ruptured when it penetrated into cracks between the cover plate and the uppermost ring of the bin. Consequently a protective rubber strip (visible in Figure A.15) was placed around the circumference of the bag before the cover plate was set in place. No bag failures occurred once a 1/2 inch thick protective strip was employed, although there were failures with thinner protective strips.

References

WHITMAN, R. V., LUSCHER, U., and PHILIPPE, A. R., 1961: "Preliminary Design Study for a Dynamic Soil Testing Laboratory: Appendices K, L, M and N," Report by M.I.T. to Air Force Special Weapons Center, AFSWC-TR-61-58.

ROBERTS, J. E., 1961: "Small-Scale Footing Studies: A Review of the Literature," Report by M.I.T. to Air Force Special Weapons center, AFSWC-TR-61-48.

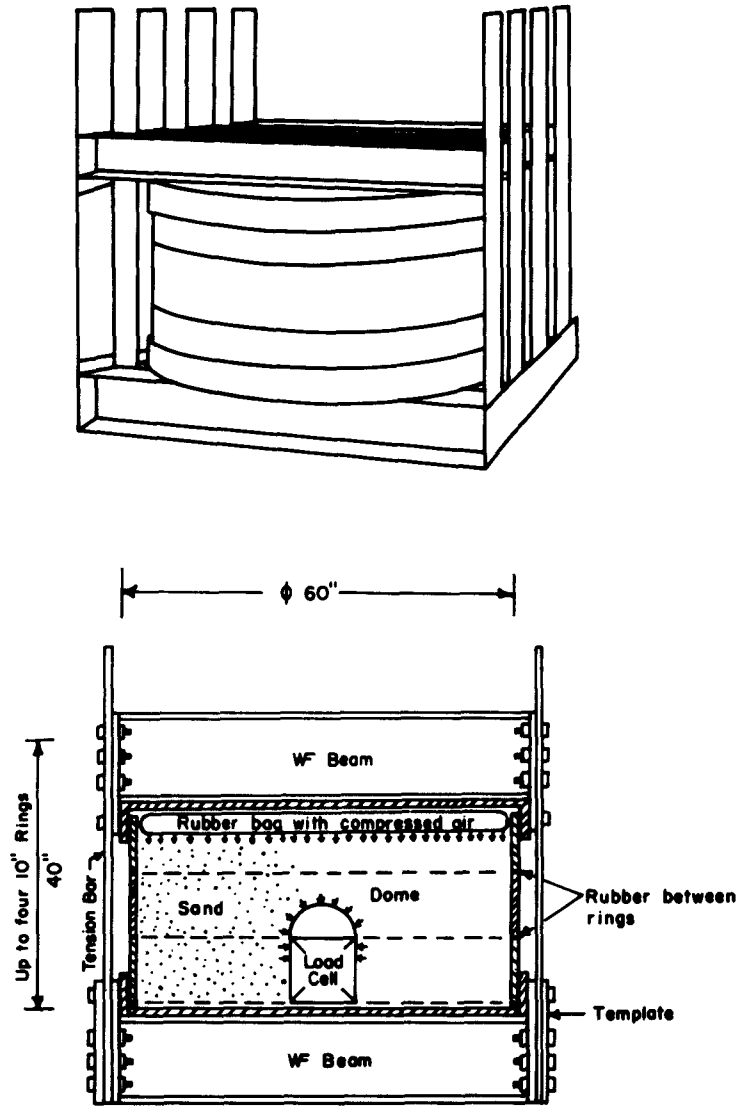

FIGURE A-1 LOADING FRAME ARRANGEMENT FOR UNIFORM LOADING

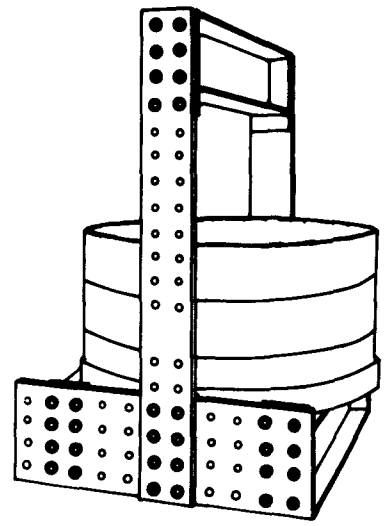

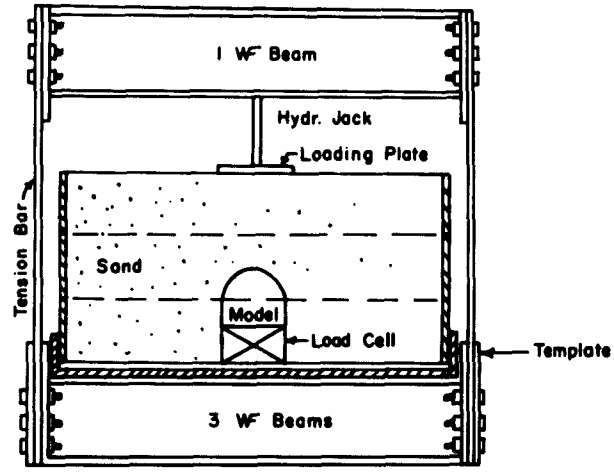

FIGURE A-2 LOADING FRAME ARRANGEMENT FOR PLATE LOADING

FIGURE A-3

BIN AND LOADING FRAME ASSEMBLY

From left to right:

1. 4 Bin Rings
2. 4 Bin Rings
3. Whole loading frame arranged for transportation
4. 3 base and cover plates

FIGURE A-4

BIN AND LOADING FRAME ARRANGED FOR UNIFORM PRESSURE

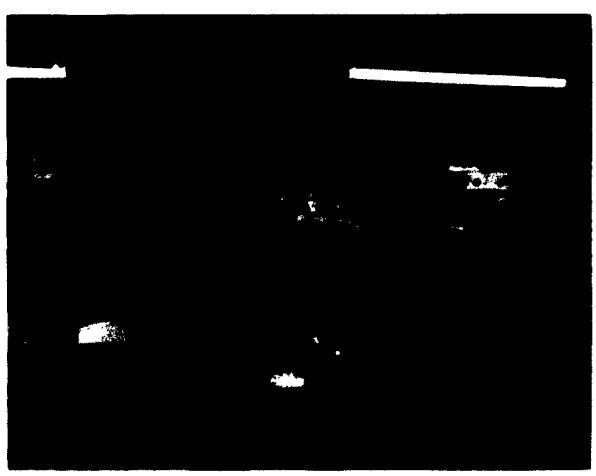

FIGURE A-5

TWO BINS AND LOADING FRAME ARRANGED FOR PLATE LOADING

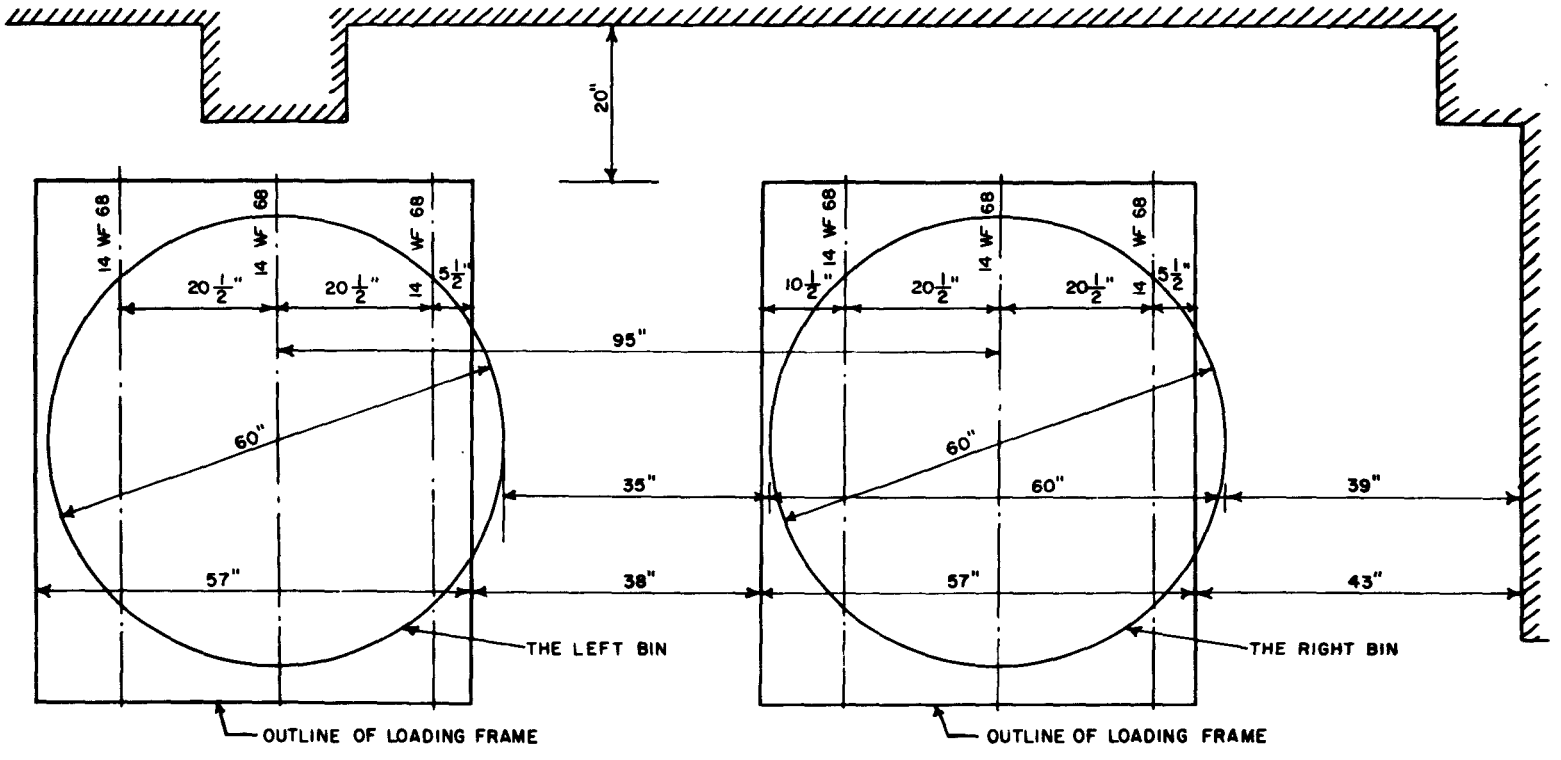

NOTE: TEMPLATE PROJECTS TO LEFT OF BIN IF ONLY THREE WF BEAMS USED

FIGURE A-6 ROOM ARRANGEMENT, PLAN

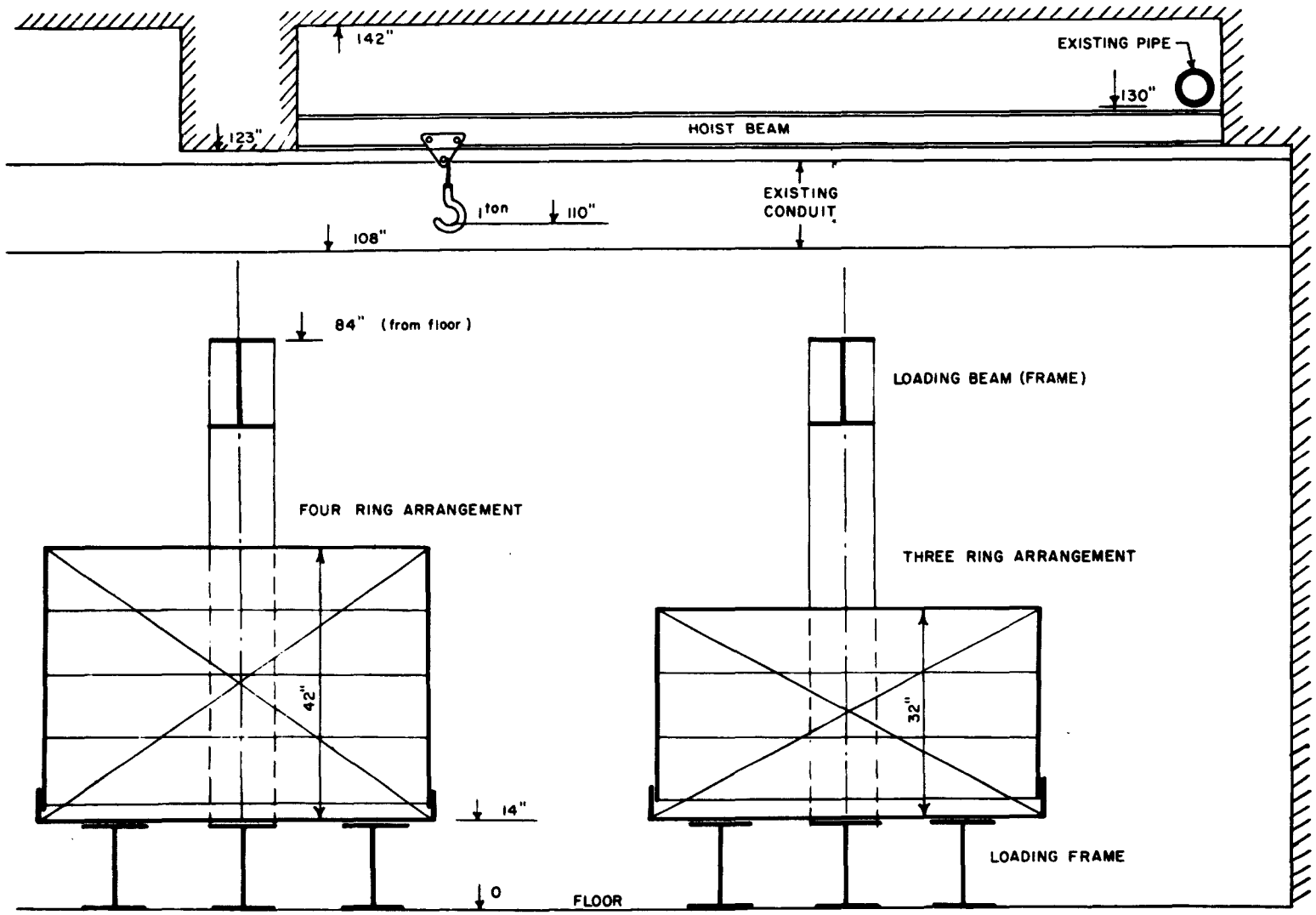

FIGURE A-7 ROOM ARRANGEMENT, ELEVATION

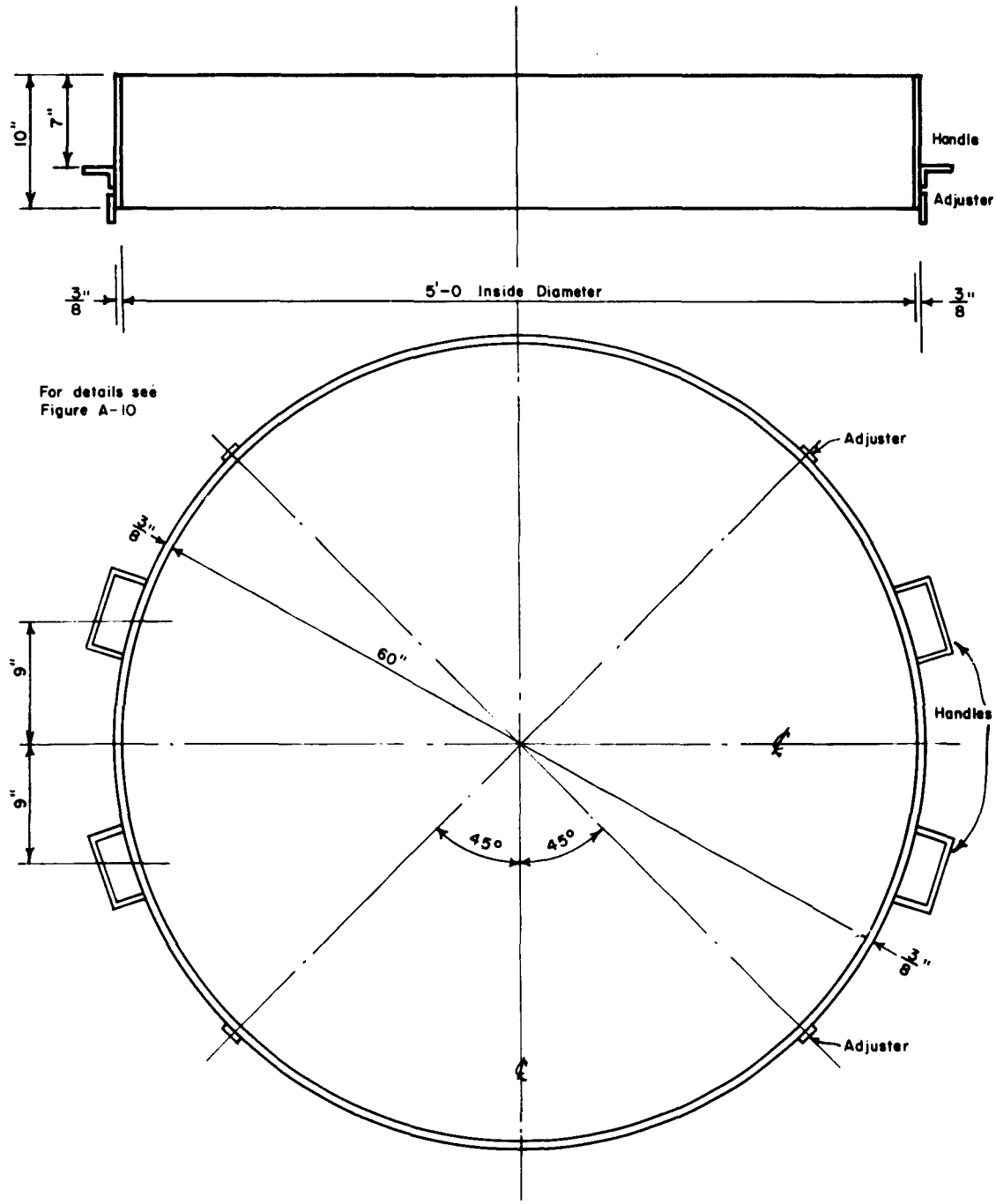

FIGURE A-8 STEEL BIN: RING DETAILS

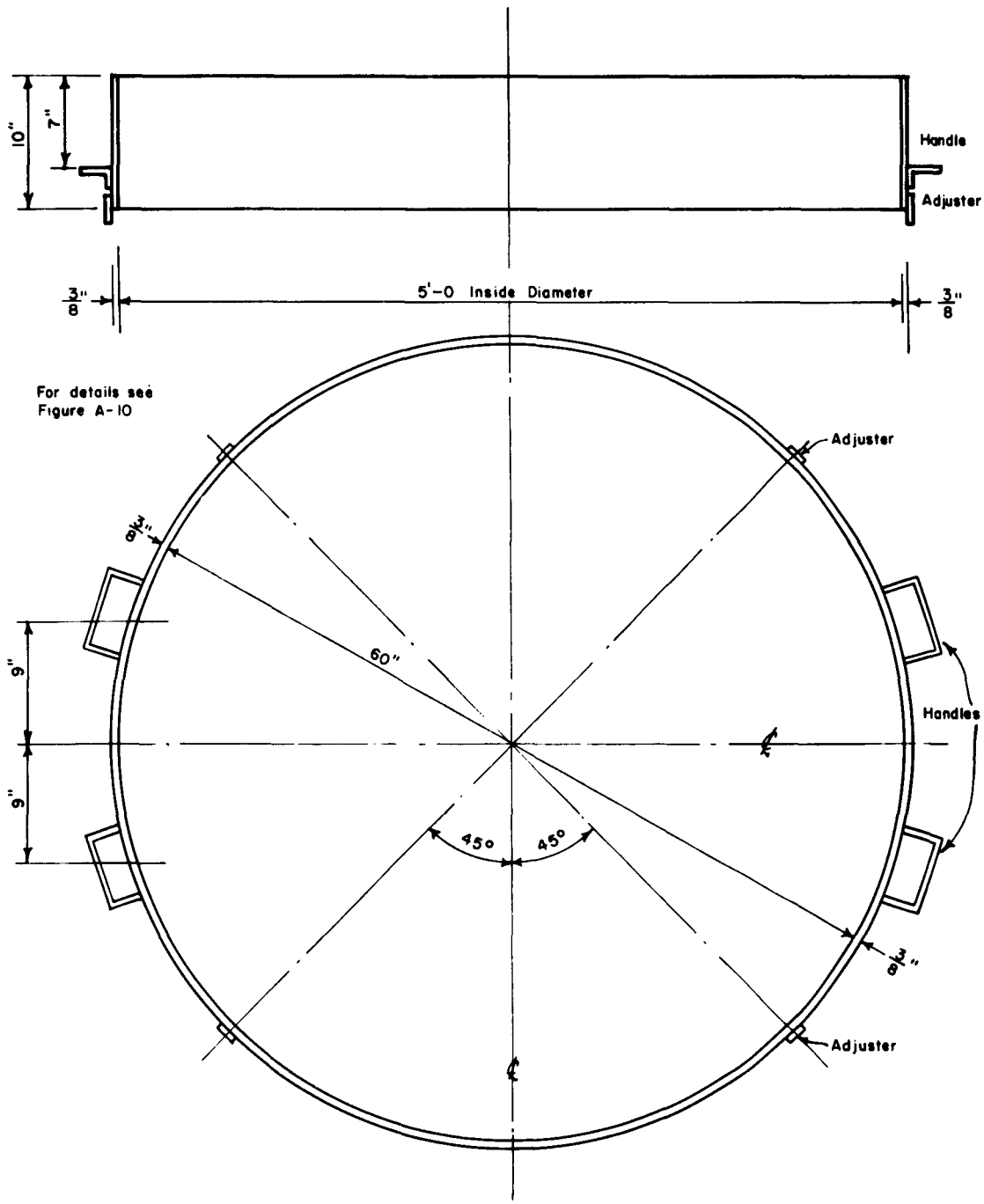

FIGURE A-8 STEEL BIN: RING DETAILS

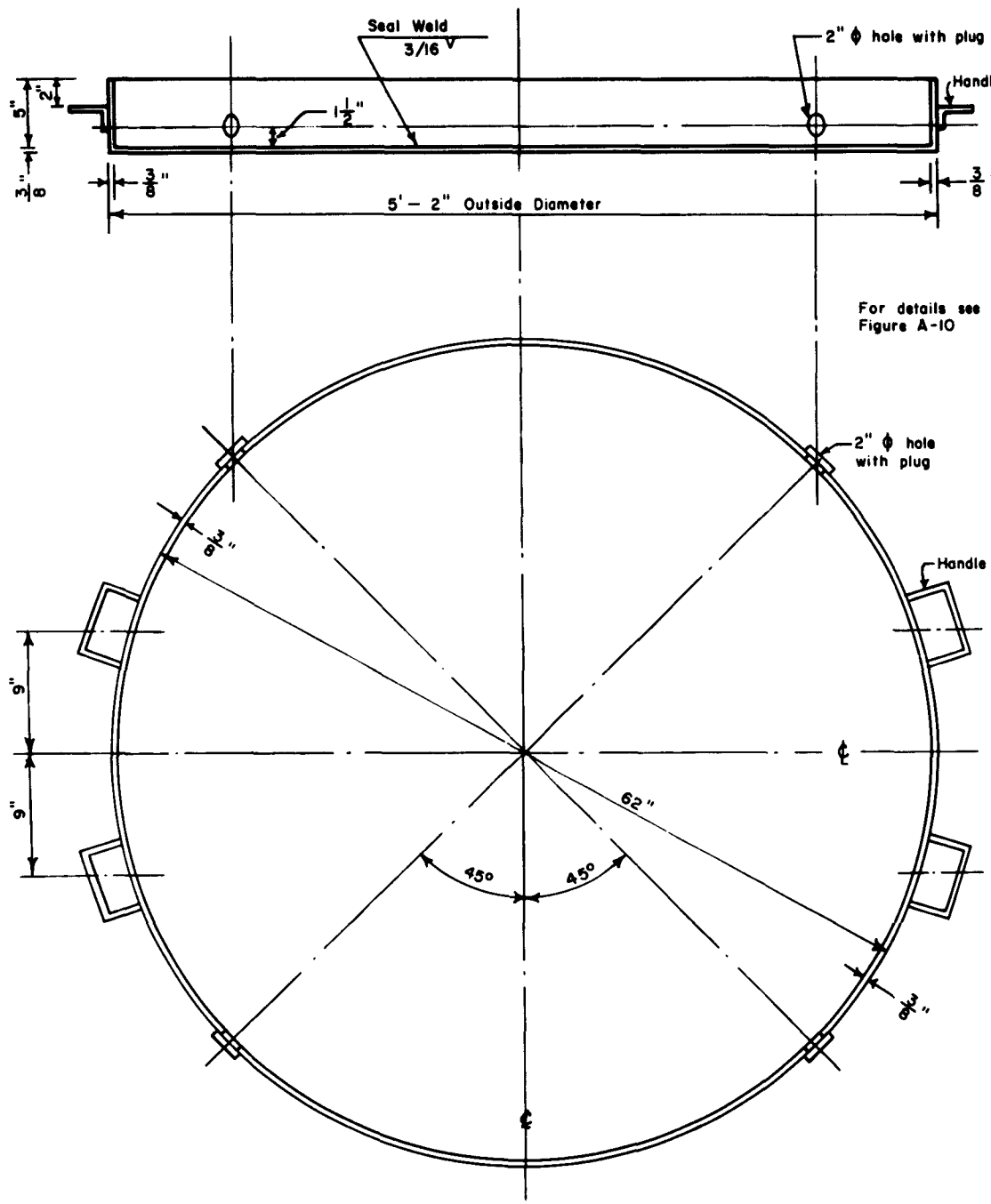

FIGURE A-9 STEEL BIN: TOP AND BOTTOM PLATES

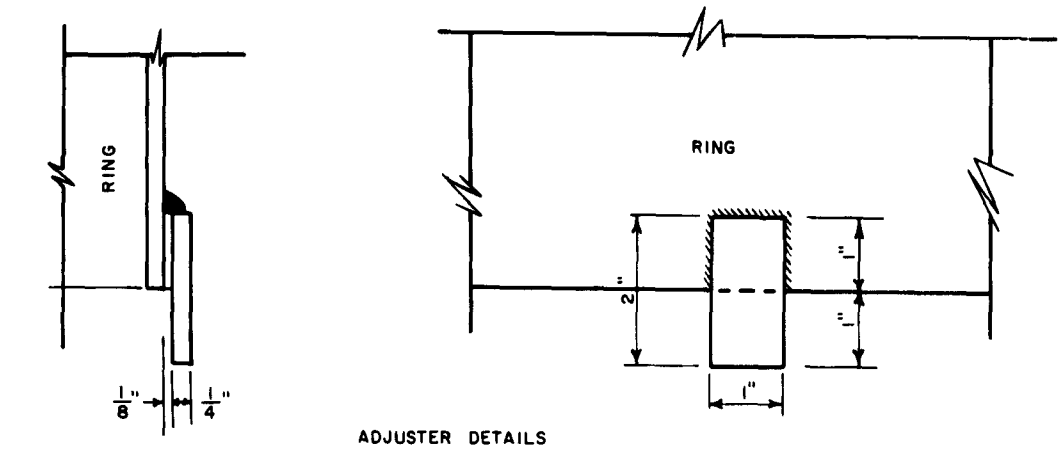

ADJUSTER DETAILS

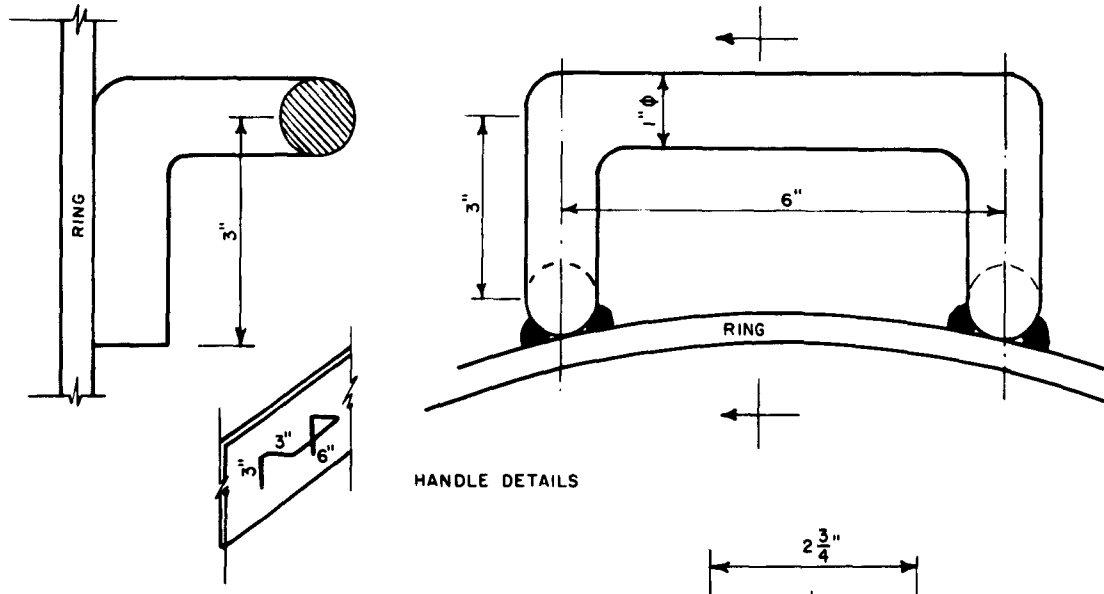

HANDLE DETAILS

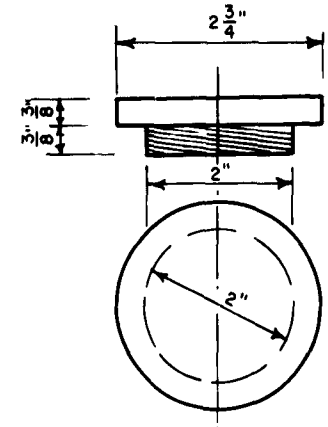

PLUG DETAILS

FIGURE A-10 STEEL BIN: ADJUSTERS, HANDLES & PLUG DETAILS

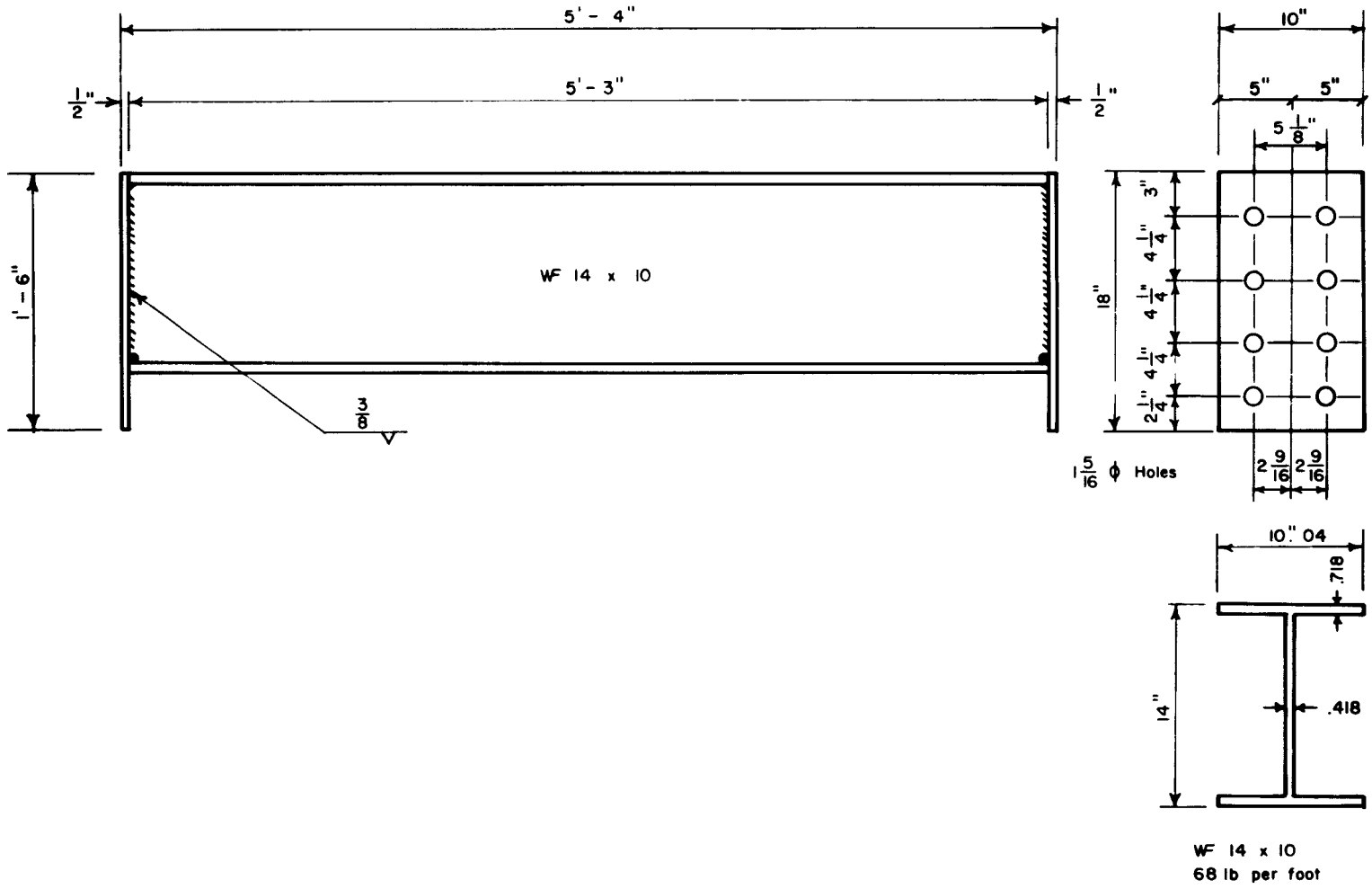

FIGURE A-11 LOADING BEAM WITH CONNECTION PLATES

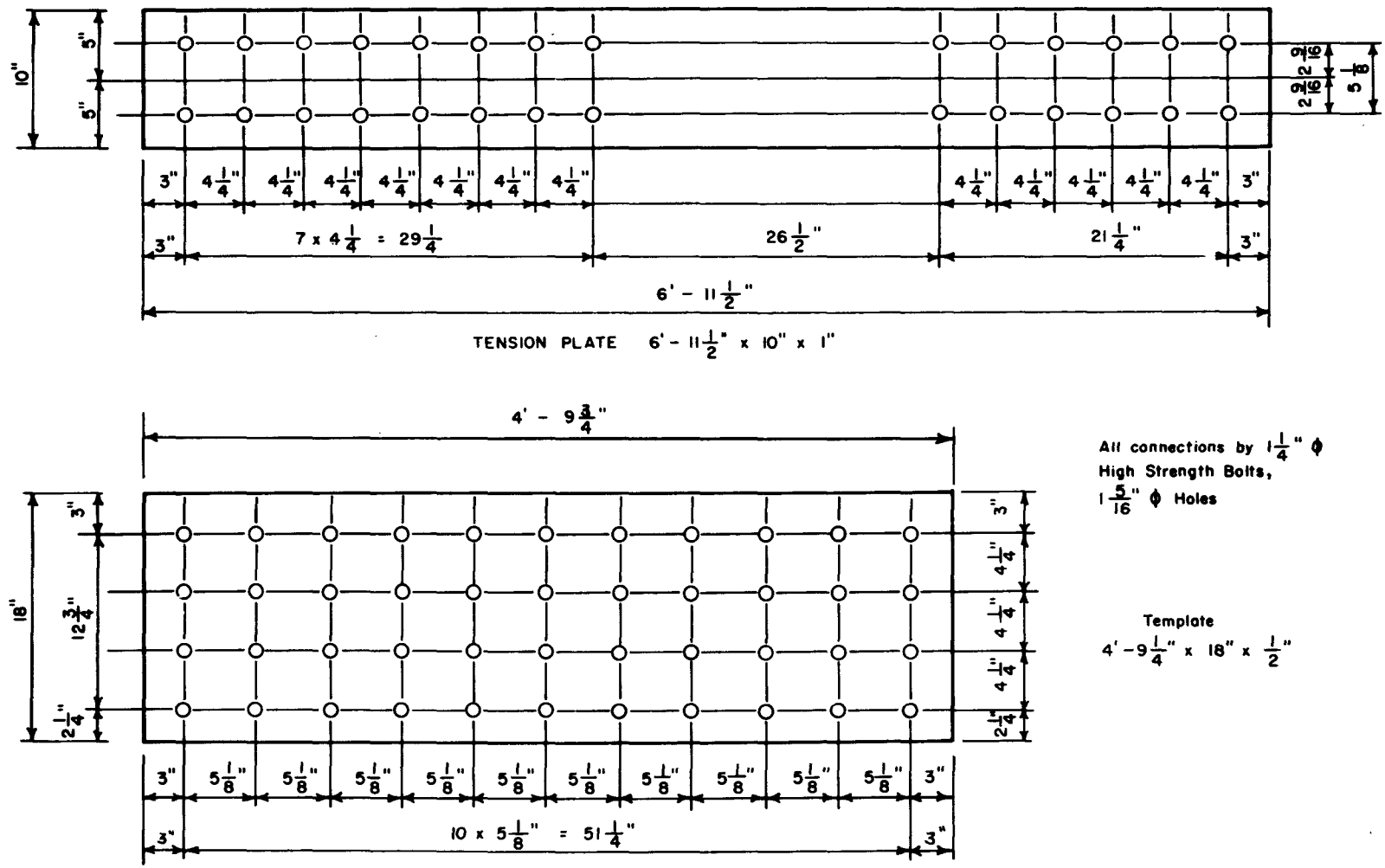

FIGURE A-12 TENSION PLATE AND TEMPLATE FOR LOADING FRAME

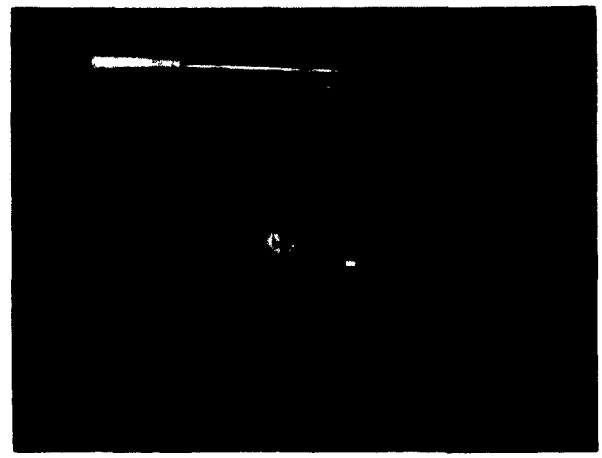

FIGURE A-13 HYDRAULIC JACK

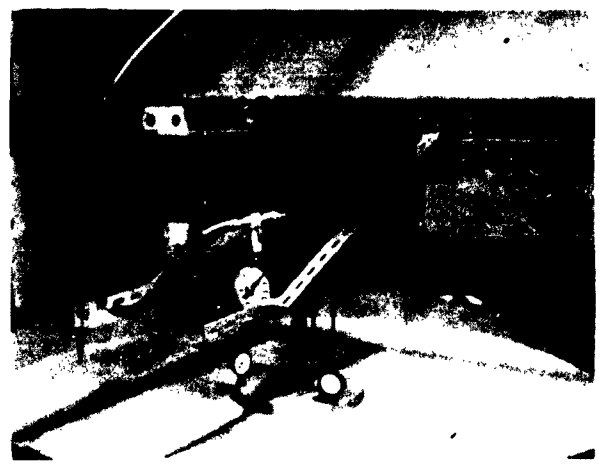

FIGURE A-14 PLATE LOADING ARRANGEMENT

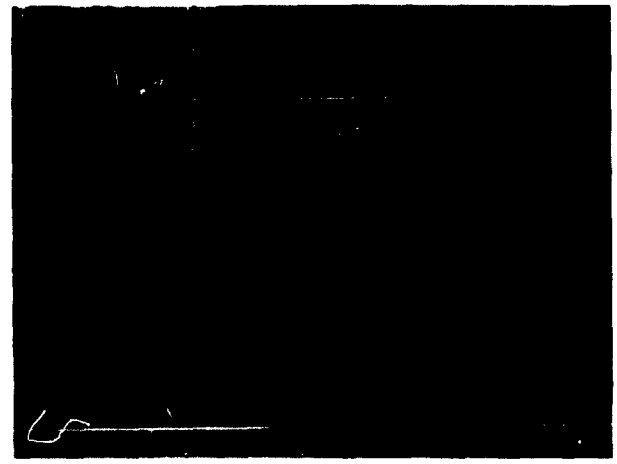

FIGURE A-15 RUBBER BAG FOR UNIFORM LOADING

FIGURE A-16 GAS SUPPLY TO RUBBER BAG

Appendix B

TECHNIQUES FOR PLACING SAND AND MEASURING DENSITY

CONTENTS

LIST OF TABLES

LIST OF FIGURES

Appendix B

TECHNIQUES FOR PLACING SAND AND MEASURING DENSITY

B.1 Nature of the Sand

Since the tests discussed in this report were to be exploratory in nature, it clearly was desirable, when selecting the soil to be used in the tests, to emphasize ease of handling and placing. The choice was further limited, since the working space was to be shared with other projects. Thus there should be no generation of dust during handling of the soil, and the use of vibratory or pneumatic compaction devices should be avoided if possible. Hence it was decided to use a sand which could be poured or sprinkled into place. Use of sprinkling and pouring techniques would, furthermore, minimize the chances of damaging the structures and instrumentation which were to be buried in the sand. A medium to coarse uniform sand appeared as the most likely candidate for meeting these criteria: both dust and segregation problems would thus be avoided.

Fortunately, just such a sand could be obtained readily and cheaply. A commercial blasting sand was available in 100 pound bags, at a cost of 75 cents per bag delivered to our working area. This sand is composed of quartz and feldspar particles, and has a specific gravity of 2.67. The grain size distribution, as determined in our laboratory, is shown in Figure B.1.* The friction angle of the dry sand in a dense state,** measured by direct shear tests, is on the order of 40°, as shown in Figure B.2. A friction angle of about 30° was measured in torsional tests (described in subsequent report) upon specimens with an initial unit weight of 98 lb/ft^3.

B.2 Unit Weight vs. Placement Techniques

Several series of tests were carried out to determine the maximum and minimum unit weight*** for this sand,

* This sand also proved to be convenient for experiments conducted in a small glass-walled container. The individual grains showed clearly on photographs taken with a Polaroid-Land camera.

**Unit weight not recorded; probably about 108 lb/ft^3.

as well as to aid in the development of suitable placement techniques. The early tests in the 5 foot bins were in themselves experiments in sand placement. Many other tests were carried out in small containers of various sizes. These tests with small containers occurred before, during, and even after the experiences with filling of the large bins, since each new experience raised new questions.

B.2.1 "Standard" density determinations

Despite numerous efforts to define standard tests for determination of the maximum and minimum unit weight of a sand, there are in reality, no generally accepted "standard" tests. Hence, a number of the various proposed tests were utilized.

Minimum unit weight: The minimum unit weight for the sand has been determined by four different methods, with the results shown in Table B.1. Each entry in this table represents a single test. Unless otherwise specified, the sand was in an air-dry condition.

Method I follows the suggestion of BURMISTER (1948). He recommended use of a funnel with at least a 1 inch diameter opening to spread sand in 1/2 inch thick layers evenly over the area of a suitable container. Two different funnels were employed: Funnel I with a 1.35 inch diameter opening, and Funnel II with an opening 0.5 inch in diameter. The container used was 5 inches in diameter by 2 inches high, and thus had a volume of 0.023 cubic feet. This same container was used for the other method as well.

Method II follows the suggestion of KITAGO and KOZAKI (1960). Sand is spread evenly and carefully from an evaporating dish, keeping the lip of the dish very close to the surface of the sand. In Method III, the tilting test due to KOLBUSZEWSKI (1948), a known weight of sand is placed in a liter hydrometer jar filled with water. The jar is turned upside down and back. When the sand settles, the volume is read and the unit weight calculated. The bulking

***Soil engineers usually speak of maximum and minimum "density," relative "density," etc. In scientific literature, the word "density" usually refers to mass density. Since we will here be speaking of weight density, the phrase "unit weight" will be used whenever units of lb/ft^3 are used. Of course, relative density and relative unit weight are equal numerically.

test (Method IV), also described by Kitago and Kozaki, is accomplished by pouring damp sand into a container of known volume. Different water contents are tried until the lowest unit weight is found.

Since the remainder of this chapter will be concerned with the relative efficiency of various techniques for placing air-dry sand, 90 lb/ft^3 has been adopted as the minimum unit weight.

Maximum unit weight: The maximum unit weight for the sand has also been determined by a variety of techniques: see Table B.2.

Method I employed a standard Proctor mold (4 inch diameter by 4.6 inch height) and a 10 pound hammer with a free fall of 18 inches. The sand (air-dry) was placed in 5 layers, each layer receiving 25 blows. Three tests gave unit weights ranging from 103.2 to 103.8 lb/ft^3.

In Method II, the air-dry sand compacted by placing the standard Proctor mold on a vibrating table, with a frequency of vibration of 294 cycles per second. In Method IIa, the sand was placed in 5 layers, with a surcharge of 47.4 lbs/ft^2 applied by weights after each layer was in place and the mold vibrated for approximately one minute. Three tests using this method yielded unit weights between 105.3 and 106.8 lb/ft^3. For Method IIb, the sand was placed in a single layer, a surcharge of 206 lb/ft^2 applied, and the mold vibrated for approximately 1.5 minutes. The resulting unit weights ranged from 100.5 to 102 lb/ft^3. Finally, in Method IIc, the mold, containing sand placed in a single layer and surcharged with 206 lb/ft^2, was submerged in a pail of water and then vibrated. The resultant dry unit weights ranged from 96.9 to 99.6 lb/ft^3.

Rodding with a steel rod approximately 1/2 inch in diameter was also attempted (Method III), using a standard Proctor mold and placing the sand in 5 layers. Three tests gave identical results: 97.8 lb/ft^3.

Some attempts were made to add small amounts of moisture to the sand prior to compaction, but this coarse sand could not retain moisture. The data as to the effect of this moisture upon the compacted dry unit weight were inconclusive.

It seems likely that a somewhat greater unit weight could have been obtained if a larger surcharge had been used together with vibratory compaction. Hence, a value of 108 lb/ft^3 was selected for the maximum unit weight.

B.2.2 Small-scale tests to evaluate placement methods

For the reasons stated at the outset of this appendix, it would be desirable to employ, in the large bins, placement methods involving sprinkling or pouring of the sand. Hence the three procedures sketched in Figure B.3 were investigated in small scale tests.

Dense sand mass: The first tests were carried out in a plexiglas container with an inside diameter of 9.23 inches. Two depths were used: 5.7 inches and 11.9 inches.

Figure B.4(a) shows placement in this container by the combined funnel approach (Method B). The upper funnel had a top diameter of 8 inches, with a 3/4 inch diameter opening. The stem of the inverted funnel had an outside diameter of 1/2 inches, an inside diameter of 3/8 inches, and a lip diameter of of 2 inches. The funnel assembly was held at a constant height above the container. Approximately 12 minutes were required to fill the 5.7 inch deep container in this fashion, or a filling rate of 0.02 ft^3/min. The measured unit weights are indicated in Table B.3, the average being 102.8 lb/ft^3.

The higher container (11.9 inches deep) was made in sections. Following determination of the average unit weight in this container, the upper part was removed and an independent check made of the unit weight of the sand in the lower part of the container.* The unit weight in the lower part was perhaps 1/2% greater than the average unit weight.

In the first tests to evaluate Method C, sand was dropped through a 10 inch length of automobile radiator hose. The hose was 2 inches in diameter, and its end was covered with a muzzle made of wire screen with 1/4 inch openings: see Figure B.5. The pipe was held at a constant

*Done in separate tests in which penetration resistance was not measured.

height (12 inches) above the container, but its end was moved horizontally to give a uniform filling of the container, avoiding at all times the formation of hills and valleys.

The container (always 5.7 inches deep in these tests) was filled in about 4 minutes, at a rate of about 0.06 ft^3/min. The average unit weight in these tests was 104.8 lb/ft^3: see Table B.3.

These tests were repeated using the small container mentioned in Section B.2.1 (5 inch diameter; 2 inch depth). The same combined funnel arrangement was used for investigating Method B. The funnel arrangement was held at various distances above the sand surface, so as to test the effect of the height-of-fall upon the unit weight. It was found that any height-of-fall between 10 and 24 inches gave the same result: 107 lb/ft^3.

For investigating Method C, a large metal funnel (Funnel III) was fitted into an automobile radiator pipe hose of 2 inch diameter, and the bottom of the hose was muzzled with wire having 1/4" openings. As in the case of Method B, any free height of fall between 10 and 24 inches produced the same result: 104.5 lb/ft^3. In other tests, a rubber stopper was used to restrict the rate of flow from the funnel: see Figure B.4(b). With this decreased intensity of flow, the unit weight increased to 107.5 lb/ft^3. Method C with the restricted flow was also checked by filling a box 2 feet by 1.6 feet in plan, and 0.8 feet deep (2.476 cubic feet). Again a density of 107.5 lb/ft^3 was obtained. With the restricted flow, the filling time was about 1 minute (0.02 cubic feet per minute), whereas with the unrestricted flow this rate was 0.06 cubic feet per minute.

The results of the various tests are summarized in Table B.4. It is evident that both Methods B and C, if used properly, will produce quite a dense sand mass: from 75% to 98% relative density. Method C was the easier technique, and after validating its use by tests in the large bin, this approach was adopted for creating "dense" sand.

Loose sand mass: With Method A (Figure B.3), the sand is poured at one spot only, thus creating a cone. Sand continuously rolls and slides down the slopes of this cone. It was not apparent at the outset that a loose sand would be created in this way, but tests proved this to be

height (12 inches) above the container, but its end was moved horizontally to give a uniform filling of the container, avoiding at all times the formation of hills and valleys.

The container (always 5.7 inches deep in these tests) was filled in about 4 minutes, at a rate of about 0.06 ft^3/min. The average unit weight in these tests was 104.8 lb/ft^3: see Table B.3.

These tests were repeated using the small container mentioned in Section B.2.1 (5 inch diameter; 2 inch depth). The same combined funnel arrangement was used for investigating Method B. The funnel arrangement was held at various distances above the sand surface, so as to test the effect of the height-of-fall upon the unit weight. It was found that any height-of-fall between 10 and 24 inches gave the same result: 107 lb/ft^3.

For investigating Method C, a large metal funnel (Funnel III) was fitted into an automobile radiator pipe hose of 2 inch diameter, and the bottom of the hose was muzzled with wire having 1/4" openings. As in the case of Method B, any free height of fall between 10 and 24 inches produced the same result: 104.5 lb/ft^3. In other tests, a rubber stopper was used to restrict the rate of flow from the funnel: see Figure B.4(b). With this decreased intensity of flow, the unit weight increased to 107.5 lb/ft^3. Method C with the restricted flow was also checked by filling a box 2 feet by 1.6 feet in plan, and 0.8 feet deep (2.476 cubic feet). Again a density of 107.5 lb/ft^3 was obtained. With the restricted flow, the filling time was about 1 minute (0.02 cubic feet per minute), whereas with the unrestricted flow this rate was 0.06 cubic feet per minute.

The results of the various tests are summarized in Table B.4. It is evident that both Methods B and C, if used properly, will produce quite a dense sand mass: from 75% to 98% relative density. Method C was the easier technique, and after validating its use by tests in the large bin, this approach was adopted for creating "dense" sand.

Loose sand mass: With Method A (Figure B.3), the sand is poured at one spot only, thus creating a cone. Sand continuously rolls and slides down the slopes of this cone. It was not apparent at the outset that a loose sand would be created in this way, but tests proved this to be

the case.

Figure B.4(b) shows this procedure being tested using the plexiglas container of 9.23 inch diameter. Height-of-drop of 5, 10 and 15 inches were used, with a very small increase in unit weight with increasing height-of-drop. The container was overfilled, as shown by the sketch in Figure B.6(a), and the excess sand carefully scraped away. Unit weights ranging from 89.2 to 91.6 lb/ft^3 (average 90.3) were obtained in this fashion, with no distinction as to whether the container was 5.7 or 11.9 inches in depth: see Table B.3.

Another scheme for creating a loose sand mass with a level top is sketched in Figure B.6(b). A few tests were run in the 9.23 inch diameter container to check the average unit weight obtained by this procedure, and it was found to be perhaps 0.5 lb/ft^3 larger than the average unit weight obtained as described above.

The unit weight created by this "hill" procedure was also checked using the very small container (5 inches in diameter by 2 inches high) and in the large rectangular box (19 inches by 24 inches by 9.5 inches deep). The sand was always mounded above the top of the container, and the excess sand then scraped away carefully. Funnels I, II and III were used, Funnel III being fitted to an unmuzzled radiator hose. The resultant unit weight was 90 lb/ft^3 in all cases.

The mounding-up procedure described here evidently will give a sand mass at the minimum unit weight for this sand; i.e. at zero relative density.

B.2.3 Hypotheses for sand behavior

Other workers have already established that the unit weight obtained by pouring sand into a container is affected especially by the rate-of-flow of the sand, and also by the height of free-fall: see KOLBUSZEWSKI and JONES (1961); also WATERWAYS EXPERIMENT STATION (1962). This earlier work would not have suggested, however, that the unit weight obtained by Methods B and C could be so close to 100% relative density.*

*A similar result for 20-30 mesh Ottawa sand has been obtained by Mr. Ulrich Luscher of the M.I.T. staff, during summer work at the Air Force Shock Tube Facility

of the University of New Mexico. Using a container with a volume of 0.564 cubic feet, he obtained a unit weight of 113.5 to 110 lb/ft^3 by various versions of Method C; 110 lb/ft^3 by placing the sand in 1.5 inch thick layers and vibrating on the surface of each layer; and 107 lb/ft^3 by bouncing the full container on the floor and/or vibrating the full container with a concrete vibrator. Method C worked best when using a funnel with 7/16 inch diameter opening, a 2 inch radiator hose with No. 5 wire mesh as a muzzle, and from 6 to 12 inch free height of drop below the mesh. The rate of filling for these conditions was 0.047 ft^3/minute.

When sand particles arrive more-or-less individually at an existing sand surface, it is possible for these particles to nestle down into the "holes" between existing sand particles in such a way as to give nearly optimum packing and maximum unit weight. The momentum of the particles is important in this process; with a large velocity-of-fall the arriving particles keep the existing surface in a state of slight agitation. It is important that the level of the sand be kept horizontal, with no hills and slopes, so that the sand grains do not roll.

As the rate at which sand is delivered increases, there is more and more likelihood that two or more particles will try simultaneously to fall into the same "hole" in the existing surface. As they come together at the "hole", these new particles form an arch-like assembly, and a loose rather than a dense packing is obtained. A small fall velocity adds to the likelihood that an open type of packing will develop.

While the experiments reported herein have established the efficiency of Methods B and C in the case of a uniform sand, the experimental program has not been extensive enough to establish the optimum placement conditions; i.e. optimum rate-of-placement, optimum free-fall height, etc. Ideally the height of the placement system should always be held at the optimum height above the sand surface; such an approach is difficult in practice, especially with a system like that in Method B. If a fixed location is accepted for the placement system, then it would be expected that the unit weight of the sand would decrease somewhat as the position of the sand surface rises. Tests in the smaller containers (see Tests Pn-9 through Pn-12, Table B.3) give some evidence concerning this problem. Some compromise will always be required when filling a large container; for example, the optimum rate-of-placement may be unacceptably low.

B.3 Handling and Placing Sand in Large Bins

B.3.1 Moving the sand

The first plan with regard to handling of the sand was to use large canvas bags with 6 to 7 ft^3 capacity: see Figure B.7. These bags were shaped so that it would be easy to fill them through a big opening at the top. They could be emptied through a hopper-shaped bottom outlet. It was hoped that it might be possible to fill the

bags by letting sand run into them through openings near the base of the bins. The bags could also be used to store sand. Ten of these bags were procured, but for one reason or another, mainly their size relative to the clear space around the bins, their use proved to be inconvenient.

The handling of sand during placement was mainly through use of the metal box shown in Figure B.8. This box was 2 feet by 3 feet by 1 foot deep, and had three openings in its bottom to which a 2 inch radiator hose could be coupled. Metal disks, with an attached rod extending up through the sand, were used to block the holes and to restrict flow of sand through the holes. The box was filled by shovel from the reserve bin, and hoisted into position over the test bin. To empty the test bin, sand was shovelled back into the reserve bin.

Some thought was given to more sophisticated systems of handling sand: screw conveyors and the like. However, as long as the rate-of-placement must be slow so as to obtain maximum density, such systems lose much of their advantage.

B.3.2 Dense sand mass

Various schemes for placing sand were evaluated by tests in the big bin, as indicated in Table C.1 of the next appendix.* The approach using combined funnels was tried; it proved to be very cumbersome and the density of the resulting sand varied with depth. The muzzled pipe approach of Method C was finally adopted for obtaining a "dense" sand. A radiator hose of 2 inch diameter was used, attached to one of three holes in the metal box suspended overhead. The hose was made up from standard lengths, as shown in Figure B.9, with connecting couplers. Thus the length of the hose could be changed as the sand surface was raised, so as to keep the free-fall height at something like an optimum value. Two men were required to operate the system: one holding and moving the end of the pipe, the other ensuring a flow of sand to the pipe. Figure B.9 shows the muzzled pipe in use, with sand pouring out of it.

*Air-dry sand was used in all of this work.

About 7 hours were ususally needed to fill the bin to a 30 inch depth. Perhaps 75% of this time was spent in spreading the sand, and thus 49 cubic feet were spread in about 5 hours--a rate of 0.16 ft^3/min. This rate was considerably above the optimum rate as suggested by the small-scale tests, and hence it is not surprising that less than the maximum density was obtained (see Section B.5). That the rate of spreading was excessive was readily apparent just from watching the spreading operation. From 20 to 30 hours would have been required for filling at the optimum rate.

B.3.3 Loose sand mass

To create the loose sand mass, sand was poured from the handling box through an unmuzzled radiator pipe held directly over the center of the bin. Following formation of a large cone, the excess sand was shoved carefully toward the edges to give a flat surface.

B.4 Penetrometer for Checking Density

A penetrometer was assembled and calibrated for checking the density of the sand as placed in the large 5 foot diameter bins. This penetrometer had a flat disk, 1.25 inches in diameter, as a tip. The area of this tip was such that the tip would support the weight of the device on top of the sand surface without penetration. The tip was connected by a 3/8 inch diameter rod to a proving ring. Force was developed by turning the disk on a threaded extension above the proving ring. The device is shown in Figure B.10.

The penetration device was calibrated against unit weight in the 9.23 inch diameter plexiglas container described above. The data are recorded in Table B.3, and the data are plotted in Figure B.11. Resistance at certain depths of penetration have been taken from these data and plotted vs. unit weight in Figure B.12. The unit weight vs. penetration relation for 3 inch penetration can be represented by a straight line, whose equation is

$$\gamma = 86 + \text{pen. resist.}/3.7$$

where γ is in lb/ft^3 and the penetration resistance is in pounds.

A few observations were made regarding the possible effect of container dimensions upon penetration

resistance. The resistance at 3 inch penetration in Test Pn-8 was notably higher than indicated by the preceding equation (78.3 lbs. vs. 52 lbs). The tests with the 11.9 inch container height tended to give somewhat lower penetration resistance (by at most 5%) than was found at comparable unit weights in the shorter container. These possible effects, especially that of container diameter, need to be checked further.

B.5 Density and Uniformity of Sand in 5 Foot Bins

Table B.5 summarizes the penetration data taken as the sand was placed in the large bins. The reference point for all recorded penetration depths was the surface of the sand mass at the time of the test. Some of the data penetrations were performed when the sand surface stood below its final elevation. The actual data for Test PB-5 are shown in Figure B.13.

It appears that the average unit weight of the "dense" sand as placed in the large bins was about 102 lb/ft^3, or a relative density of about 70%, and that the local relative density ranged at most to 68% and 81%.

References

BURMISTER, D. M., 1948: "The Importance and Practical Use of Relative Density in Soil Mechanics," Proc. of Am. Soc. of Testing Materials, Vol. 48.

KITAGO, S. and KOZAKI, F., 1960: "The Measurement of Relative Density of Sand," Am. Soc. of Testing Materials, Bul. No. 248, pp 36-40.

KOLBUSZEWSKI, J., 1948: "An Experimental Study of Maximum and Minimum Porosity of Sands," Proc. 2nd Int. Conf. on Soil Mech. and Found. Eng., Vol. I, pp 158-165.

KOLBUSZEWSKI, J., and JONES, R. H., 1961: "The Preparation of Sand Samples for Laboratory Testing," Proc. Midland Soil Mech. and Found. Eng. Society, Vol. 4, pp 107-124.

WATERWAYS EXPERIMENT STATION, 1962: "Rotary Cone Penetrometer Investigations," U. S. Army Engineer Waterways Experiment Station, Potamology Investigations, Report 18-1

Table B.1

DETERMINATIONS OF MINIMUM UNIT WEIGHT

	Method	Unit Weight lb/ft^3
Ia	Pouring through funnel: Funnel I	91
Ib	Pouring through funnel: Funnel II	91
II	Pouring from dish	90
III	Tilting water-filled container	86
IV	Pouring moist sand (bulking test)	70

Table B.2

DETERMINATIONS OF MAXIMUM UNIT WEIGHT

	Method	Unit Weight lb/ft^3
I	Dynamic compaction test	103.5
IIa	Vibration (5 layers) with 47.4 lb/ft^2 surcharge	106.3
IIb	Vibration (1 layer) with 206 lb/ft^2 surcharge	101.3
IIc	Vibration under water: 206 lb/ft^2 surcharge	98.8
III	Rodding	97.8

Penetr.	Container		Sand		Penetration Resistance at (in lb.)								
No.	Diam.	Height	Filling	Unit Weight lb/ft^3	0	$\frac{1}{2}$"	1"	1$\frac{1}{2}$"	2"	2$\frac{1}{2}$"	3"	3$\frac{1}{2}$"	4"
Pn-1	9.23"	5.7"	A	91.5	2.3	4·6	6.6	10.0	14.5	17.5	21.0	24.7	—
2	"	"	A	89.2	2.3	3.9	5.3	6.8	8.5	10.7	13.4	16.3	—
3	"	"	A	91.6	2.3	4.8	7.5	9.8	12.7	15.5	17.4	20.8	—
4	"	"	B	101.4	2.3	7.4	13.3	21.0	32.3	47.1	63.1	78.1	—
5	"	"	C	103.6	2.3	9.5	15.5	29.1	40.8	55.3	—	—	—
6	"	"	C	102.0	2.3	6.9	16.2	24.2	39.7	51.5	61.9	81.3	—
7	"	"	C	103.0	2.3	8.5	13.9	23.2	35.5	50.3	67.4	—	—
8	5"	6.25"	C	100.0	2.3	8.5	18.8	25.1	38.5	46.5	78.3	88.8	—
9	9.23"	11.93"	C	103.1 x	2.1	7.6	13.0	20.8	32.9	46.1	56.6	69.4	—
10	"	"	C	104.1 x	2.1	7.9	14.4	22.9	33.3	46.2	58.6	76.5	96.5
11	"	"	A	90.2 x	2.1	3.4	5.6	6.4	8.5	10.8	13.4	15.4	17.0
12	"	"	A	90.0 x	2.1	3.1	4.5	6.0	7.5	9.3	11.0	12.6	14.5
13	"	5.7	C	103.5	2.0	7.5	14.2	22.7	34.0	47.4	62.0	73.5	84.5
14	"	"	A	89.4	2.0	3.3	4.7	6.3	7.9	9.6	11.7	14.7	17.7
15	"	"	A	89.8	2.0	3.2	4.7	6.2	7.7	9.9	12.1	14.5	19.2
16	"	"	C	104.8	2.6	7.7	14.3	24.5	36.4	49.8	66.8	79.1	94.6
17	"	"	D	105.5	2.6	13.3	21.8	31.0	45.0	64.9	85.1	—	—
18	"	"	D	104.6	2.6	8.0	18.3	28.8	43.2	58.6	71.6	90.1	>100
19	"	"	D	104.3	2.6	10.5	17.7	30.3	41.5	60.6	84.6	99.0	—

For filling methods (A, B, C) – see text

x Average density. Surface density about 1 % less than average

TABLE B-3 UNIT WEIGHT AND PENETRATION TESTS IN SMALL CONTAINER

Table B.4

UNIT WEIGHTS IN SHOWERING TESTS

Method	Volume of Container, ft^3	Approx. filling rate, $ft^3/min.$	Unit Weight lb/ft^3	Relative Density
B	0.22 to 0.46	0.02	102.8	75%
C	0.22 to 0.46	0.06	104.8	85%
B	0.023	0.02	107.0	95%
C	0.023	0.06	104.5	83%
C	0.023	0.02	107.5	98%
C	0.023	0.02	107.5	98%

Table B.5

PENETRATION TESTS IN LARGE BIN

Test	No. of Penetrations	Resistance (lbs) @ 3 inch Penetration	Apparant Unit Weight, lb/ft^3	Depth** Inches
PB-3	3	46 ± 2	98.3 ± 0.5	0
	4	61 ± 7	102.4 ± 1.9	20
PB-5	2	60 ± 4	102.4 ± 1.1	0
	2	57.5 ± 1.5	101.5 ± 0.4	12
	3	$57.6 \begin{smallmatrix}+7.4\\-3.6\end{smallmatrix}$	$101.6 \begin{smallmatrix}+2.0\\-1.0\end{smallmatrix}$	18
PB-6	5	10 ± 2	89.6 ± 0.5	0
PB-7	1	53.5	100.5	0
PB-8	1	58*	101.7	0

*Penetration after load test, at point 20 inches away from center-line.

**Distance of surface below eventual surface.

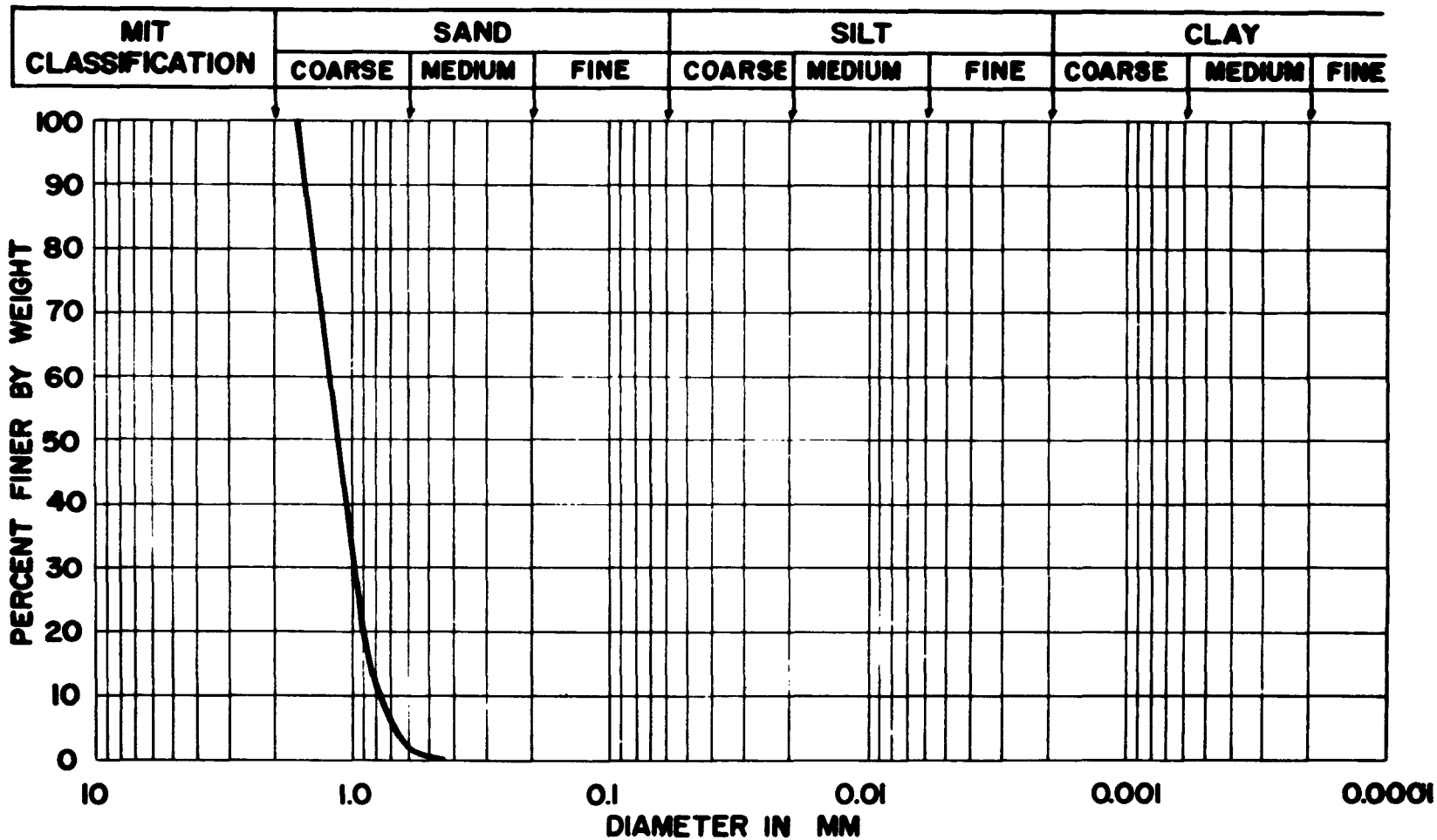

FIGURE B-1 GRAIN SIZE DISTRIBUTION

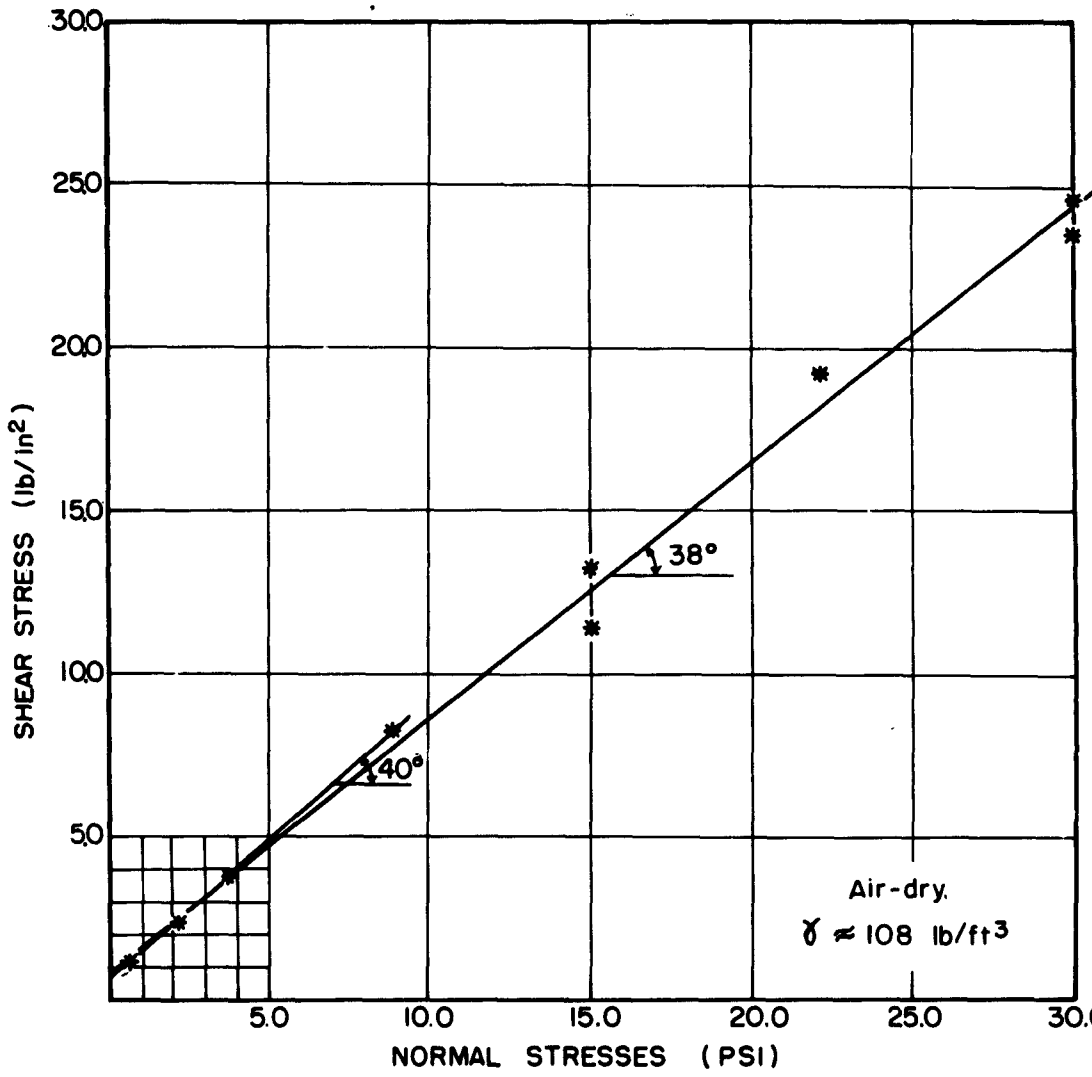

FIGURE B-2 DIRECT SHEAR TESTS

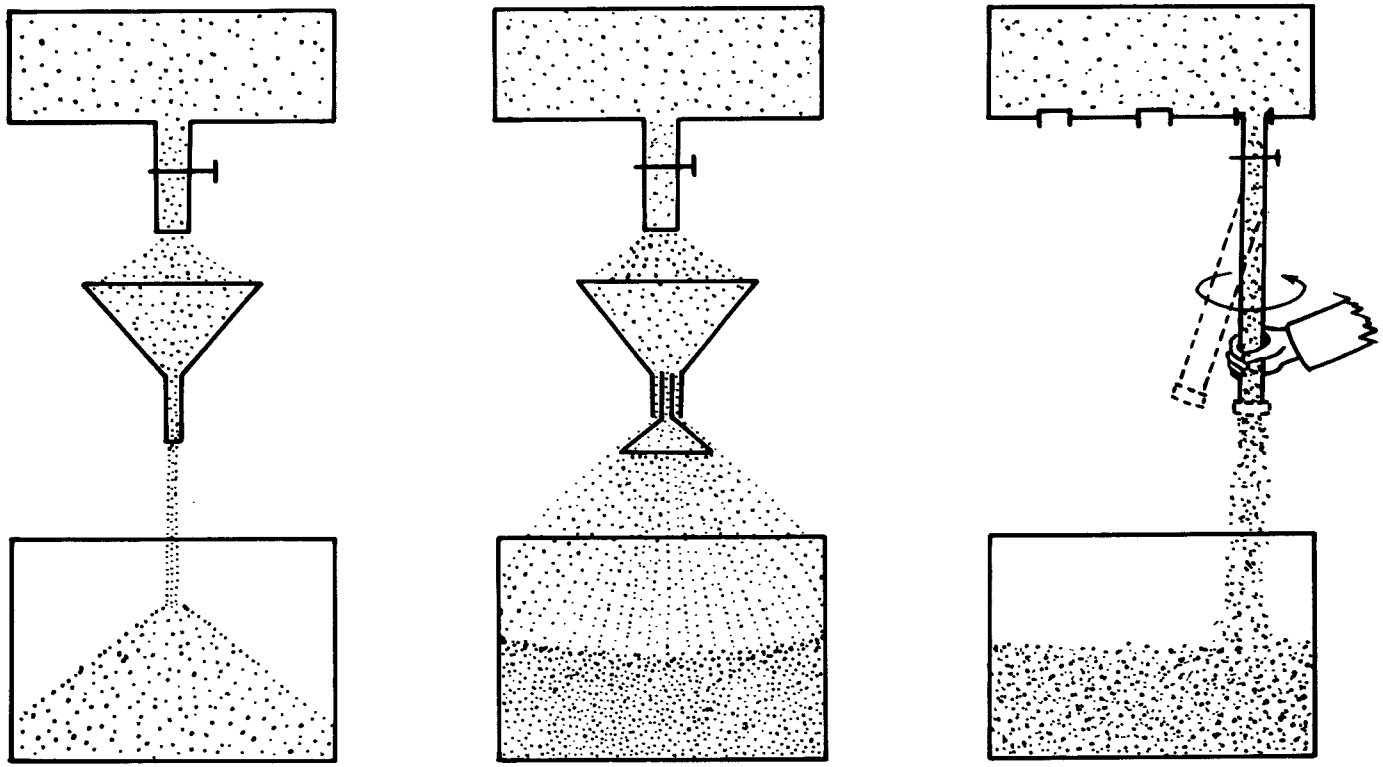

METHOD A

Central pouring, creating sloped surface (loose sand)

METHOD B

"Combined funnels" pouring, creating a flat surface (dense sand)

METHOD C

Pouring through muzzle-pipe, creating a flat surface (dense sand)

FIGURE B-3 METHODS FOR SHOWERING SAND

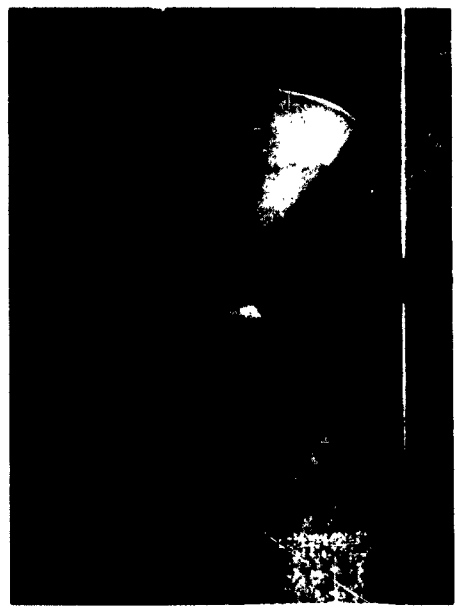

(a) Showering sand through "combined funnels"

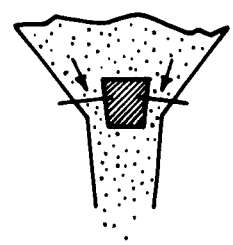

Rubber stopper used to restrict flow in some tests

(b) "Free-pouring through single funnel

FIGURE B-4 PHOTOGRAPHS OF SAND SHOWERING

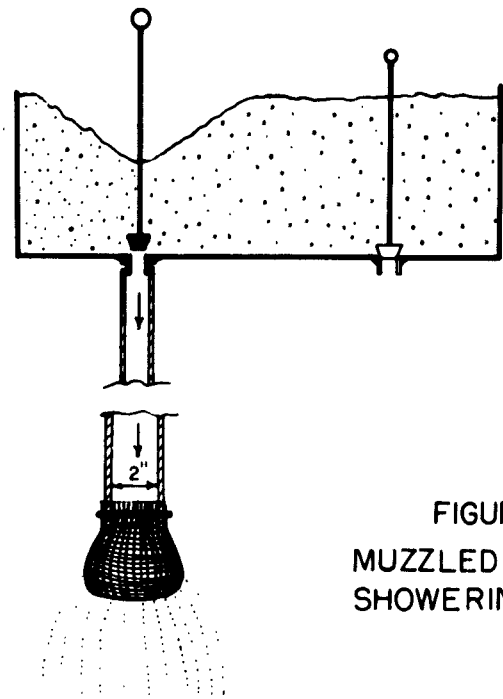

FIGURE B-5
MUZZLED PIPE FOR
SHOWERING SAND

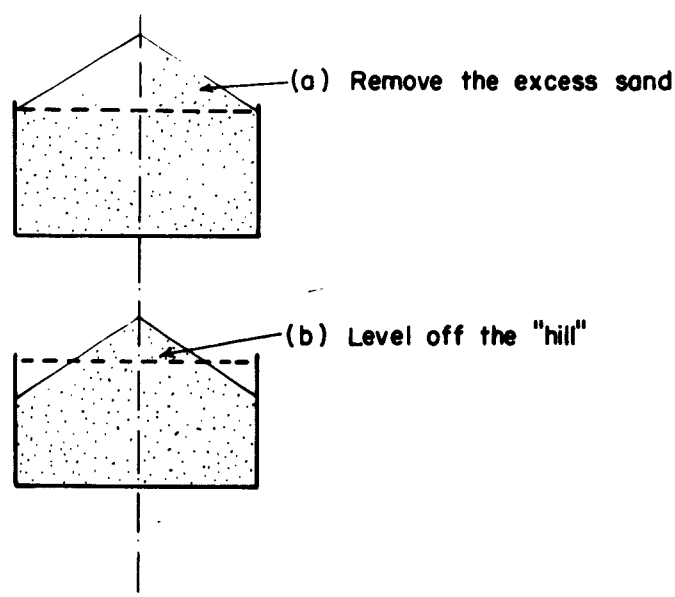

FIGURE B-6 METHODS FOR OBTAINING
LOOSE SAND

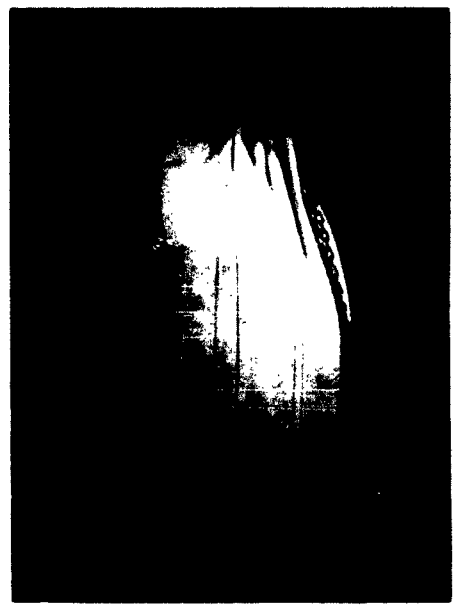

FIGURE B-7 BAG FOR MOVING AND STORING SAND

FIGURE B-8 METAL BOX FOR MOVING SAND

FIGURE B-9

PLACING SAND IN LARGE BINS

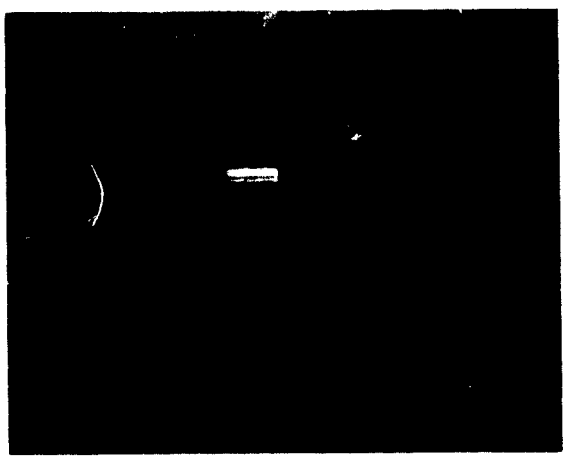

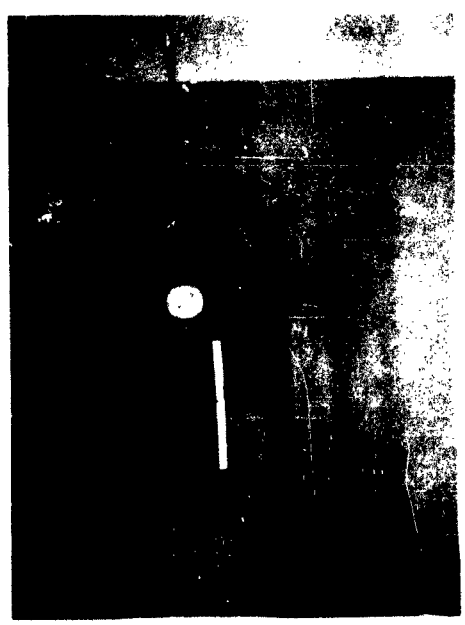

FIGURE B-10

PENETRATION TEST IN SMALL CONTAINER

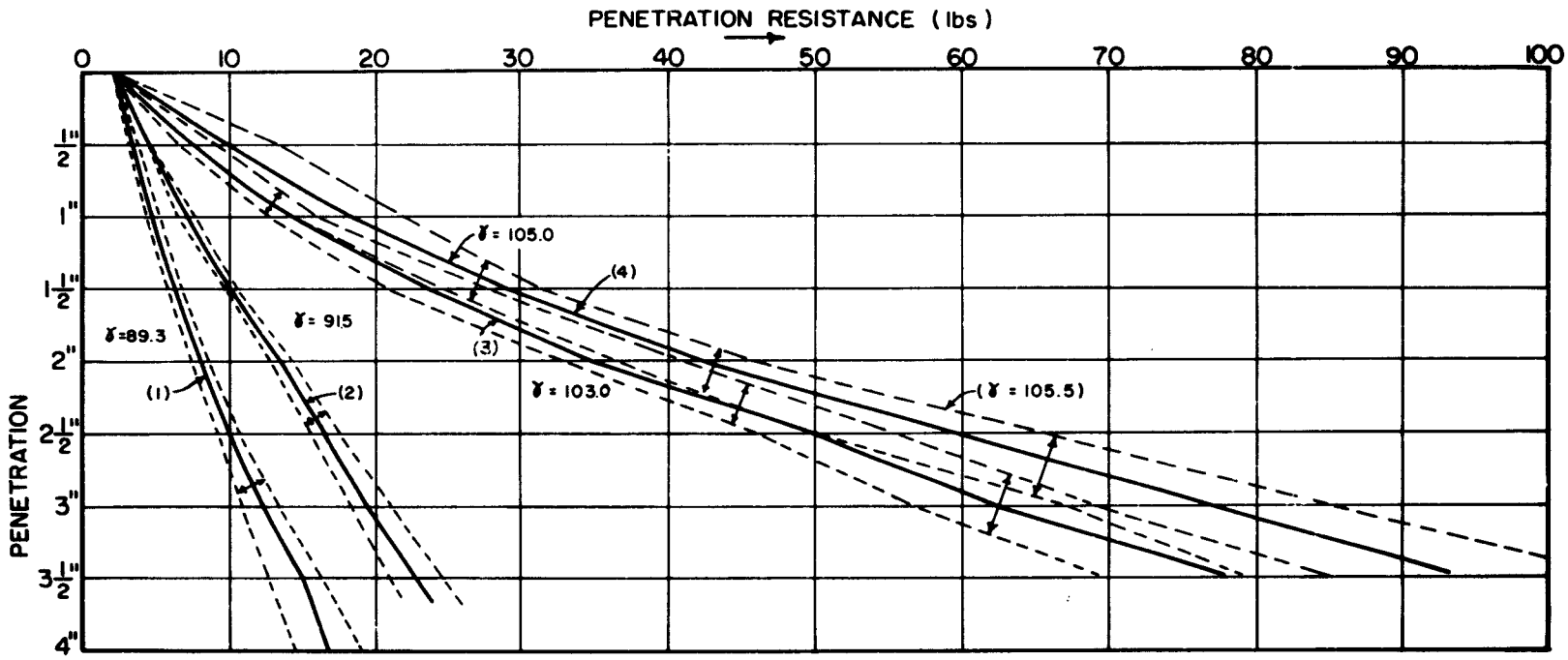

(1) AVERAGE CURVE FOR γ = 89.3 lb/c.f. FROM 5 TESTS (Pn-2, 11, 12, 14, 15) (γ = 89.1 to 89.8)

(2) AVERAGE CURVE FOR γ = 91.5 lb/c.f. FROM 2 TESTS (Pn-1 & 3) (γ = 91.5 to 91.6)

(3) AVERAGE CURVE FOR γ = 103.0 lb/c.f. FROM 5 TESTS (Pn-5, 7, 9, 10, 13) (γ = 102.0 to 103.6)

(4) AVERAGE CURVE FOR γ = 105.0 lb/c.f. FROM 4 TESTS (Pn-16, 17, 18, 19.) (γ = 104.3 to 105.5)

THE SOLID LINES SHOW THE AVERAGE; THE DASHED LINES SHOW THE SCATTERING ZONES.

FIGURE B-11 TESTS TO CALIBRATE PENETROMETER

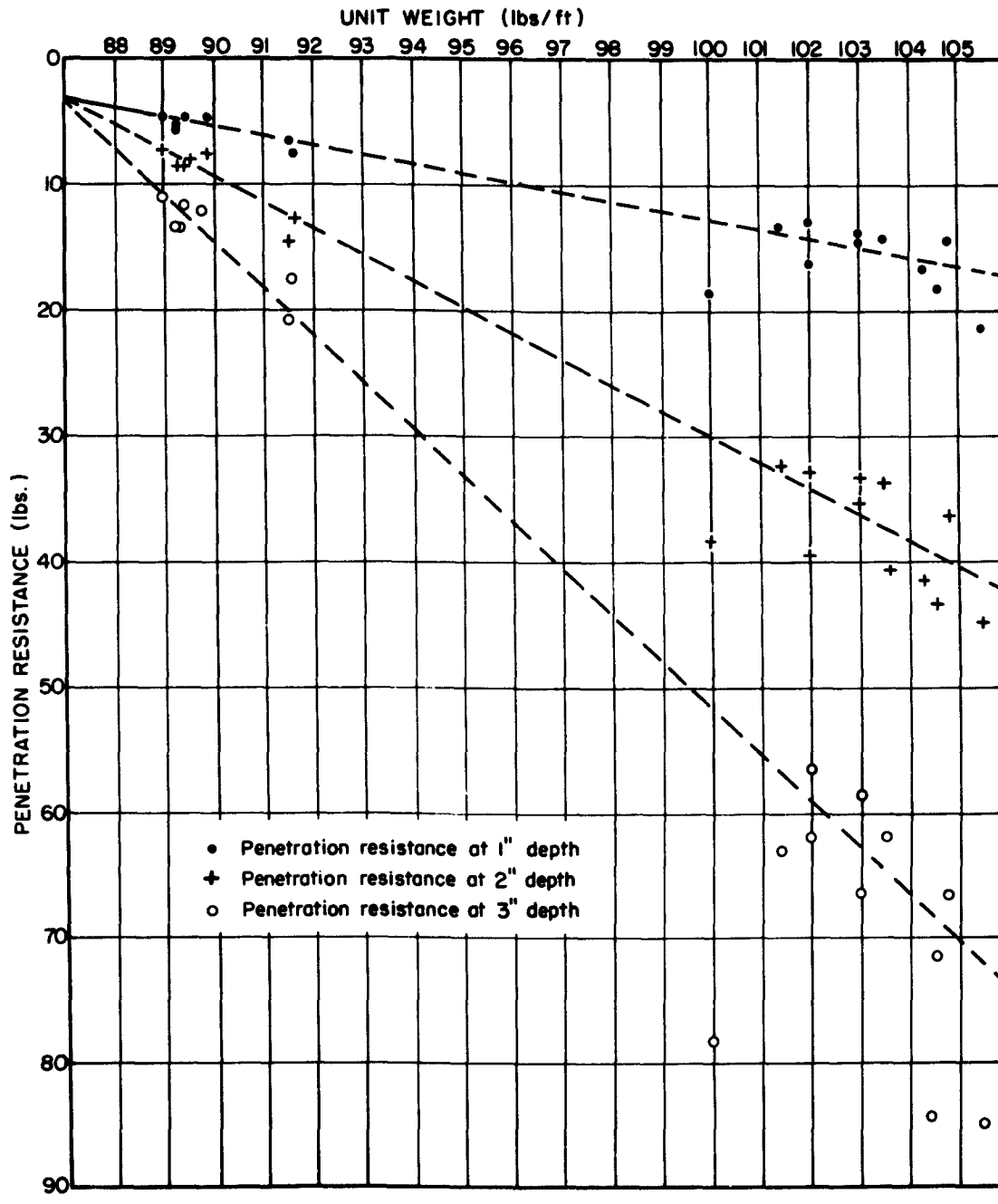

FIGURE B-12 CALIBRATION CURVES FOR PENETROMETER

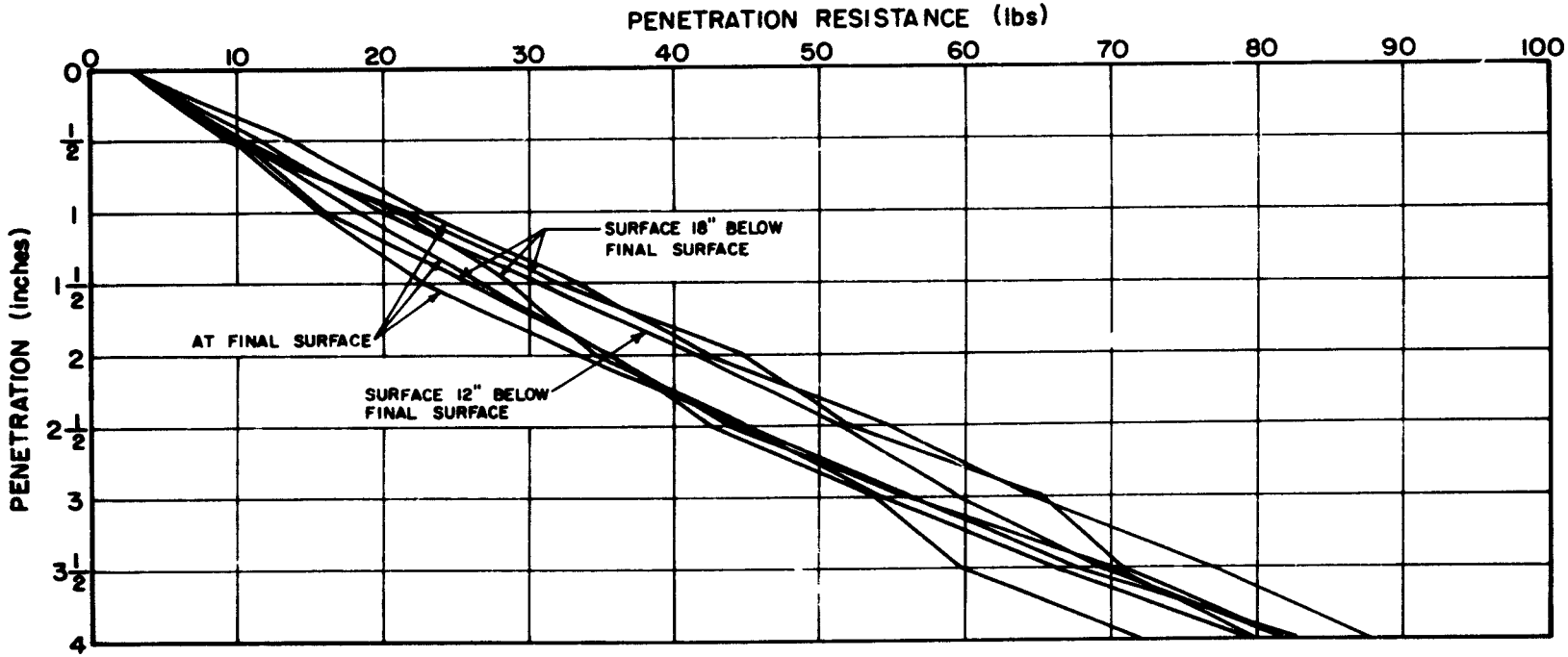

FIGURE B-13 PENETRATION TESTS DURING TEST PB-5